Neural Plasticity

Stress Induced Neuroplasticity and Mental Disorders 2018

Lead Guest Editor: Fushun Wang
Guest Editors: Fang Pan, Lee Shapiro, and Jason H. Huang

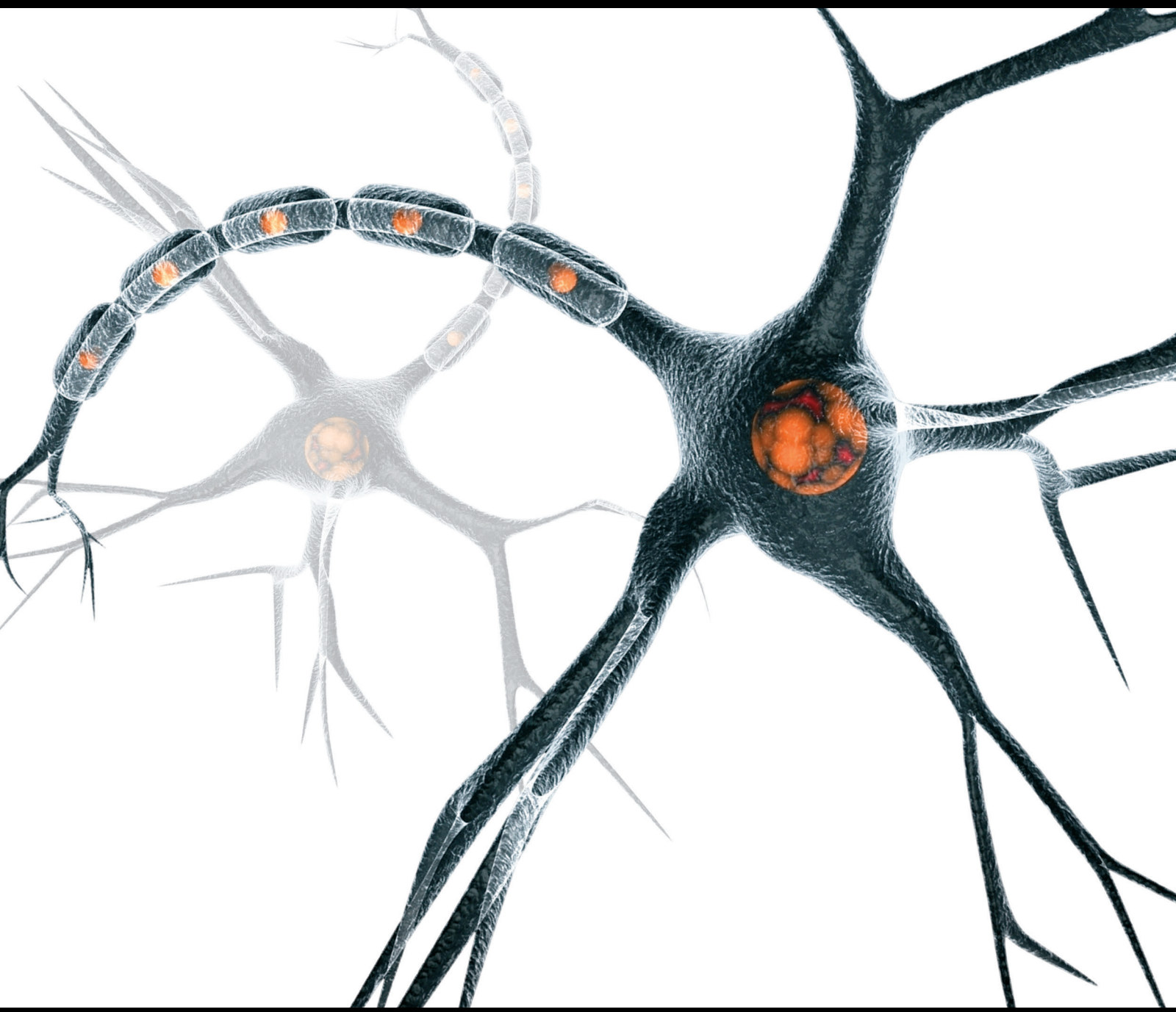

Stress Induced Neuroplasticity and Mental Disorders 2018

Neural Plasticity

Stress Induced Neuroplasticity and Mental Disorders 2018

Lead Guest Editor: Fushun Wang
Guest Editors: Fang Pan, Lee Shapiro, and Jason H. Huang

Editorial Board

Contents

Hindawi
Neural Plasticity
Volume 2018, Article ID 5382537, 3 pages
https://doi.org/10.1155/2018/5382537

Editorial

Stress Induced Neuroplasticity and Mental Disorders 2018

Fushun Wang,[1,2] **Fang Pan**,[3] **Lee A. Shapiro**,[4] **and Jason H. Huang**[2,5]

[1]*Institute of Emotional Studies, School of Psychology, Nanjing University of Chinese Medicine, Nanjing 210023, China*
[2]*Department of Neurosurgery, Baylor Scott & White Health, Temple, TX 76508, USA*
[3]*Department of Medical Psychology, School of Basic Medical Sciences, Shandong University, Jinan 250012, China*
[4]*Department of Surgery, Texas A&M College of Medicine, Temple, TX 76504, USA*
[5]*Texas A&M University College of Medicine, Temple, TX 76508, USA*

Correspondence should be addressed to Fushun Wang; 13814541138@163.com and Jason H. Huang; jason.huang@bswhealth.org

Received 19 June 2018; Accepted 21 June 2018; Published 16 August 2018

Stress was first named as the general adaptation syndrome to define a process when the body confronts noxious agents. Nearly a century has passed since Hans Selye first introduced the word stress in 1936, and this brilliant idea about stress has helped an entirely new field to be forged and attracted thousands of researchers to work on the biological mechanism of stress. Now stress is extended to the field of psychology and redefined as the presence of acute or persistent physiological or psychological threats to the organism that result in significant strain on the body's compensatory systems.

In face of stress, the first reaction of the body is an alarm reaction, preparing the body to "fight or flight," as was motivated by the emotional changes, such as fear (flight) and anger (fight) [1, 2]. Nowadays, it is found that emotional stress affects the organism even more seriously, and most of the mental diseases are due to stress-induced emotional changes, which can induce significant strains to the body. Folkman et al. proposed that there are two kinds of emotional changes [3]: the first is related to threat and fearful emotion, which motivates withdrawal and flight behavior; and the second is related to coping with the situation, when the organism activates energy in the body to cope with the situation and show angry emotions. Thus, *fear and anger are two basic emotions at stressful events*: fear is the scariness at the threat, while anger is trying to cope with the stressful situation [4]. Lazarus proposed that stress depends on cognitive appraisals of situation [5]. He distinguished two kinds of appraisals: the first appraisal is unconscious and fast activating, which is related to harm and threat and induces fearful emotion to motivate avoidance and withdrawal; the second is conscious and concerned with coping with the uncontrolled situation. In the face of threat, the organism was scared at first and showed fearful emotions; then to cope with the threats, the organism collects energy in the body to "fight or flight". Therefore, fear and anger usually come in a tandem at the stressful events [6]. Fear and anger are hard to be detached and are two sides of the same coin [5].

Lazarus suggested another stage of appraisal after coping with the situation (called reappraisal). At this stage, an individual employs two kinds of reappraisals: problem-focused (cognition), and emotion-focused. If the organism can cope successfully with the stressful situation, the organism will get positive emotions and be happy. If the organism failed to cope with the situation, the organism would get negative emotions and be sad. Therefore, a stressful event-induced emotion will go through "fear-anger-joy or sadness" *emotion flow*. If the organism cannot overcome the stressful events, like the chronic stresses, some mental disorders will appear. The relations of the process with the emotional changes and some mental disorders were shown in our previous editorial. Therefore, when something happens, people will first evaluate whether it is dangerous (fear/anger) or not (calm) and next evaluate if they fit into our need (happy/sad) [7]. This hypothesis is exactly consistent with Lazarus' reappraisal theory about happiness or sadness [5]: the happy

and sad emotion are related to the success or failure to cope with stressful situations.

The mechanisms whereby external stressors affecting brain function have been the subject of extensive study over the past half a century. It is well known that the major function of NE is "fight (anger) or flight (fear)" [8, 9]. The stress-induced neural plasticity undoubtedly affects the brain function and may prompt functional alternations in mental disorders. Indeed, stress-induced neuroplasticity plays a critical role in almost all of the mental disorders, and stress has become a synonym for diverse terms of negative emotions, such as depression, anxiety.

In previous special issues, we already collected 9 papers on stress-induced neural plasticity and some neurological diseases. Because of its popularity, we were invited to hold this issue as the annual topic in 2018, and we are glad to get 31 submissions, and 11 of which are accepted for publication. These reviews and experimental papers present more evidence about stress.

In the experimental paper "The Neural Basis of Fear Promotes Anger and Sadness Counteracts Anger," J. Zhan et al. probed into the relationships about basic emotions and reported that fear leads to anger. They tested this hypothesis with MRI and found that the selective involvement of different brain regions in different basic emotions might be the reason for the relationship between the basic emotions. For example, they found that the posterior insula (PI) is involved in sadness, while the anterior insula (AI) is involved in fear. Their interesting data helped explain the relationship between the basic emotions: fear-anger-sadness.

In the review paper "Persistent Stress-Induced Neuroplastic Changes in the Locus Coeruleus/Norepinephrine System," O. Borodovitsyna et al. reviewed papers about neural mechanisms underlying stress, especially locus coeruleus/norepinephrine system. In this paper, they reported how stress changes the structure and function of LC from a genetic, cellular, and neuronal circuitry/transmission perspective. They further linked stress to altered LC function and pathogenesis of posttraumatic stress disorder.

Chronic stress often induces neural plasticity in the brain at molecular, cellular level. In the experimental paper "Recovery of Chronic Stress-Triggered Changes of Hippocampal Glutamatergic Transmission," M. Lin et al. probed into the dynamic changes in excitatory transmission in the hippocampus and investigated the spontaneous recovery of spatial memory function and glutamatergic transmission in the hippocampus after chronic stress. They found that chronic unpredicted mild stress transiently increased AMPA receptor GluA2/3 subunit expression, together with elevated PICK-1 protein expression. They further probed into the spontaneous recovery after the stress is removed.

In the experimental paper "Metabolic Changes Associated with a Rat Model of Diabetic Depression Detected by Ex Vivo 1H Nuclear Magnetic Resonance Spectroscopy in the Prefrontal Cortex, Hippocampus, and Hypothalamus," K. Liu et al. reported stress-induced depression in diabetic depression. They used magnetic resonance spectroscopy and immunohistochemistry to investigate the metabolic and pathological changes in the rat brain and found that the levels of glutamate decrease at depression, which are possibly due to dysfunction of neurons and astrocytes.

In the experimental paper "Context and Time Matter: Effects of Emotion and Motivation on Episodic Memory Overtime," Q. Sun et al. compared the reaction times about reward stimuli, punishment stimuli, and stressful stimuli in human subjects and found that stressful stimuli are highly arousing and can trigger more efficient memory consolidation.

In the experimental paper "Direct Electrophysiological Mapping of Shape-Induced Affective Perception," Y. Li et al. reported a very interesting behavior and ERP study about emotional arousal of pleasant and unpleasant stimuli. Consistent with Lazarus's theory of two processing pathways of the brain about stressful stimuli and hedonic stimuli, they found that stressful stimuli, such as angry face, can induce faster and larger response in the earlier ERP responses, particular P1, N1.

In the experimental paper "TLR4-NF-κB Signal Involved in Depressive-Like Behaviors and Cytokine Expression of Frontal Cortex and Hippocampus in Stressed C57BL/6 and ob/ob Mice," Y. Wang et al. reported that elevated levels of cytokines such as interleukin- (IL-) 1β, IL-6, and tumor necrosis factor-α (TNF-α) are closely associated with pathology of depression in obesity mice during stress processing.

In the experimental paper "Danshen-Honghua Ameliorates Stress-Induced Menopausal Depression in Rats," S. Gu et al. reported neurotransmitter and sex hormone changes in an animal model of menopause depression. In addition, they found that a kind of Chinese herb can help treat menopause depression. This paper will help understand the pathogenesis of perimenstrual depression.

In the experimental paper "Language and Sensory Neural Plasticity in the Superior Temporal Cortex of the Deaf," M. Que et al. showed plausible neural pathways for auditory reorganization for deaf patients. They probed into the correlations of activations of the reorganized cortical areas with developmental factors and provided unique evidence towards the understanding of neural circuits involved in cross-modal plasticity.

In the experimental paper "Examination Stress Results in Attentional Bias and Altered Neural Reactivity in Test-Anxious Individuals," X. Zhang et al. studied the test stress in college students, using ERP (event-related potentials). They found that test stress can induce functional perturbations of brain circuitry that reacts rapidly to test threat.

In the experimental paper "Relationship between Insulin Levels and Nonpsychotic Dementia: A Systematic Review and Meta-Analysis," Q. Pan et al. reported a special relationship about stress with dementia in human subjects. They found that dementia is related with insulin, which can induce a variety of neural plasticities, such as apoptosis in neurons, thus cognitive functions, such as learning and memory.

Collectively, these studies demonstrate that stress can induce many critical changes in many mental disorders. We hope that this special issue will stimulate interests in the field of the mechanism of stress inducing the neural plasticity and

will help achieve a deeper understanding of the molecular mechanism of stress-induced mental disorders.

Fushun Wang
Fang Pan
Lee A. Shapiro
Jason H. Huang

References

[1] M. E. Fox, R. I. Studebaker, N. J. Swofford, and R. M. Wightman, "Stress and drug dependence differentially modulate norepinephrine signaling in animals with varied HPA axis function," *Neuropsychopharmacology*, vol. 40, no. 7, pp. 1752–1761, 2015.

[2] G. P. Chrousos, "Stress and disorders of the stress system," *Nature Reviews Endocrinology*, vol. 5, no. 7, pp. 374–381, 2009.

[3] S. Folkman, R. S. Lazarus, R. J. Gruen, and A. DeLongis, "Appraisal, coping, health status, and psychological symptoms," *Journal of Personality and Social Psychology*, vol. 50, no. 3, pp. 571–579, 1986.

[4] Z. Zheng, S. Gu, Y. Lei et al., "Safety needs mediate stressful events induced mental disorders," *Neural Plasticity*, vol. 2016, Article ID 8058093, 6 pages, 2016.

[5] R. S. Lazarus, *Stress and Emotion: A New Synthesis*, Springer Pub. Co, New York, NY, USA, 1999.

[6] S. Gu, W. Wang, F. Wang, and J. H. Huang, "Neuromodulator and emotion biomarker for stress induced mental disorders," *Neural Plasticity*, vol. 2016, Article ID 2609128, 6 pages, 2016.

[7] S. Gu, F. Wang, T. Yuan, B. Guo, J. H Huang, and Department of Psychology, Nanjing University of Chinese Medicine, Nanjing, 210023 China, "Differentiation of primary emotions through neuromodulators: review of literature," *International Journal of Neurology Research*, vol. 1, no. 2, pp. 43–50, 2015.

[8] L. H. Miner, H. P. Jedema, F. W. Moore, R. D. Blakely, A. A. Grace, and S. R. Sesack, "Chronic stress increases the plasmalemmal distribution of the norepinephrine transporter and the coexpression of tyrosine hydroxylase in norepinephrine axons in the prefrontal cortex," *Journal of Neuroscience*, vol. 26, no. 5, pp. 1571–1578, 2006.

[9] S. Sandrini, F. Alghofaili, P. Freestone, and H. Yesilkaya, "Host stress hormone norepinephrine stimulates pneumococcal growth, biofilm formation and virulence gene expression," *BMC Microbiology*, vol. 14, no. 1, p. 180, 2014.

Hindawi
Neural Plasticity
Volume 2018, Article ID 9795013, 8 pages
https://doi.org/10.1155/2018/9795013

Research Article

Direct Electrophysiological Mapping of Shape-Induced Affective Perception

Yingli Li,[1,2] Qingguo Ding,[1,3] Yuancun Zhao,[1,2] Yanan Bu,[1,2] Xiaoyan Tang,[1] Peiguo Wang,[1] Genhua Zhang,[1] Mengling Chen ,[1] and Pei Liang [1]

[1]*Sensory Cognition and Design Institute, Changshu Institute of Technology, Changshu, China*
[2]*The School of Education, Soochow University, Soochow, China*
[3]*The No. 2 Peoples' Hospital of Changshu, Changshu, China*

Correspondence should be addressed to Mengling Chen; cml198010003@qq.com and Pei Liang; liangpei0108@126.com

Received 10 January 2018; Revised 17 May 2018; Accepted 4 June 2018; Published 2 August 2018

Academic Editor: Jason H. Huang

Visual information may convey different affective valences and induce our brain into different affective perceptions. Many studies have found that unpleasant stimuli could produce stronger emotional effects than pleasant stimuli could. Although there has been a notion that triangle is perceived as negative and circle as positive, there has been no systematic study to map the degrees of valence of shapes with different affective perceptions. Here, we employed four shapes (ellipse, triangle, and line-drawn happy and angry faces) to investigate the behavior and electrophysiological responses, in order to systematically study shape-induced affective perception. The reaction time delay and the event-related potential (ERP), particularly the early ERP component, were applied to find the associations with different affective perceptions. Our behavioral results showed that reaction time for angry face was significantly shorter than those for the other three types of stimuli ($p < 0.05$). In the ERP results, P1, N1, P2, and N2 amplitudes for angry face were significantly larger than those for happy face. Similarly, P1, N1, P2, and N2 amplitudes for triangle were significantly larger than those for ellipse. Particularly, P1 amplitude in the parietal lobe for angry face was the strongest, followed by happy face, triangle, and ellipse. Hence, this work found distinct electrophysiological evidence to map the shape-induced affective perception. It supports the hypothesis that affective strain would induce larger amplitude than affective ease does and strong affective stimuli induce larger amplitude than mild affective stimuli do.

1. Introduction

Threat detection from visual perception has been developed for our survival over the time span of the biological evolution. From conscious to subconscious levels, our brain has been tuned to be sensitive to all kinds of affective information with different degrees of positive and negative values. For instance, facial expressions such as a happy face and an angry face are consciously perceived as positive and negative in social interaction [1]. Some isolated schematic facial expressions such as V-shaped downward eyebrow configuration have been rated to be more negative and arousing than upside-down patterns [2]. Even a simple shape, which is similar to the geometric configuration of the face in angry expression, is perceived as threatening. In 2006, Aronoff reviewed how humans recognize angry and happy emotions in people, places, and objects. He demonstrated that it is the geometrical patterns, such as diagonal and angular configurations, rather than actual facial features that conveyed the message of threats, while round and curved shapes were linked to warmth [3]. Growing evidence suggests that the underlying geometry of a visual image might serve as an effective vehicle for conveying the affective meaning of a scene or of an object. A recent study has demonstrated that downward triangle is perceived as negative and circle as positive, and their emotional meanings can be activated automatically, as shown at both behavioral and electrophysiological levels [4]. Hence, the questions arise: From complex faces to simple geometric shapes, is there any shared cognitive processing? What is the perception advantage of shapes developed in our brain?

Kahneman hypothesized that information in the human brain may be processed in different psychological statuses,

such as cognitive "ease" and cognitive "strain" [5]. In each status, the information flow might be mediated by different networks of the brain. Motivated from Kahneman's theory, we further proposed that visual information might induce *affective ease* or *affective strain* in our brain. Such affective status might modify the brain's processing of information flow and thereby influence our perception of the environment. For instance, it has been observed that detecting an angry face among happy faces is faster and more accurate in contrast to a happy amid angry ones [6]. A similar effect has been found not only in faces but also in shapes. Triangles are more easily detected among circles than the reverse [7]. Negative things elicit a more rapid and more prominent response than nonnegative events do [8]. Moreover, the emotional valences of the geometrical figures have been demonstrated to impact even cross-sensory perceptions such as taste. For instance, a circular shape may enhance sweetness sensitivity [9], and this effect is invariant across different cultures [10]. All these findings support that different affective states may influence the neural information processing and the behavior pattern. Few fMRI studies have elucidated that downward-pointing triangles activated the same neural circuitry known to facilitate the processing of realistic, contextual threatening stimuli [11]. Bilateral amygdales were more strongly activated by angular objects than by curved ones [12]. However, the neural basis of such subtle impact of geometrical figures on perception remains unclear still. Hence, our present study is aimed at exploring the human brain's reaction to "positive" and "negative" geometrical figures and finding the evidence of electrophysiological mapping of shape-induced affective ease and affective strain.

The ERP is a powerful electrophysiological technique for measuring brain activation signals, with a time resolution accurate down to milliseconds [13]. The literature suggests that early ERP components are sensitive to emotional stimuli, and the right hemisphere plays a critical role in emotion processing. Some local brain regions such as the frontal lobe and the parietal lobe are especially sensitive to emotional pressure [14]. Recent studies find that the target detection sensitivity for a negative emotional stimulus was higher than that for a neutral stimulus. ERP revealed that high-intensity anger expressions elicited larger P3a and late positive potential amplitudes relative to prototypical anger expressions for power-motivated individuals [15]. N170 response to facial expressions is modulated by the affective congruency between the emotional expression and preceding affective pictures [16]. Positive emotions evoke N170 significantly earlier than negative emotions do, and the amplitude evoked by fearful faces was larger than that evoked by neutral or surprised faces [17]. The greater the affective distance of a target, the larger the late potential. In the present study, we chose six early ERP components (N1, P1, N2, P2, N3, and P3) to investigate the electrophysiological correlates of cognitive status.

In the present study, we hypothesized that the two groups of stimuli (positive versus negative) would be differentiable in early ERP components, despite that facial stimuli might elicit stronger brain activation than geometrical stimuli might. To compare directly the perception of simple geometric shapes and faces, which are with different degrees of affective values, a comparison of two target shapes (i.e., an ellipse and a triangle) and two emotional shapes (i.e., a line-drawn happy face and an angry face) was carried out. Moreover, the present study deals with a particular process within the emotion reaction: attention to affective stimuli. Since shapes provide very abstract information, it may influence our behavior subconsciously. We hypothesize that the angry face and triangle may lead the brain into a similar perception of affective strain, while the happy face and ellipse will take the brain to a perception of affective ease. The present study is to test this hypothesis that simple geometric forms convey emotion and that this perception does not require explicit judgment. In this study, the following questions will be addressed: (1) Do brain EEG signals elicit different patterns for affective ease and affective strain? (2) If so, what is the difference between these two groups? (3) Does the brain EEG signal behave similarly for the stimulus from the same group? (4) Can we generalize the stimulation types and predict our brain response? All these questions will be answered and discussed in the end.

2. Methods

2.1. Participants. Twenty randomly selected college students (10 males and 10 females, averaged age = 23.11, SD = 1.53) participated in the present study. All participants were right-handed, with normal or normal-after-correction vision. They were well explained about the details of their performance. They have all agreed and signed on the written informed consent declaration to volunteer as subjects in these experiments. The study was approved by the Ethics Committee of Changshu Institute of Technology, according to the National Ethics Guidelines.

2.2. Materials. Two target shapes (i.e., ellipse and triangle) and two emotional shapes (i.e., smile and angry faces) for comparison were designed (see Figure 1). The four shapes (with a diameter of about 20 cm) were programmed via E-Prime 2.0 to present on a computer screen in a random sequence, with each shape repeated for 100 times, resulting in 400 trials in total. Each shape lasted for 1.5 s, interpolated by a 2 s interval. A practice section consisting of 12 trials (3 trials for each shape) was also programmed in the same way. Participants were required to identify each shape and press the corresponding key on a keyboard by using the index and middle fingers of both hands ("D" represents ellipse, "F" represents triangle, "J" represents happy face, and "K" represents angry face) as quickly and as accurately as possible.

2.3. EEG Recording. After signing a consent form, participants were seated in front of a computer screen in a sound-proof chamber and fitted with a 32-channel Neuroscan electrode cap. All electrodes were positioned in accordance to the International 10-20 System (Binnie, Dekker, Smit, and Van der Linden, 1982) and referenced to CZ (central cortex) during recording. An EOG (electrooculogram) was also recorded from electrodes placed above and below each eye. Electrode

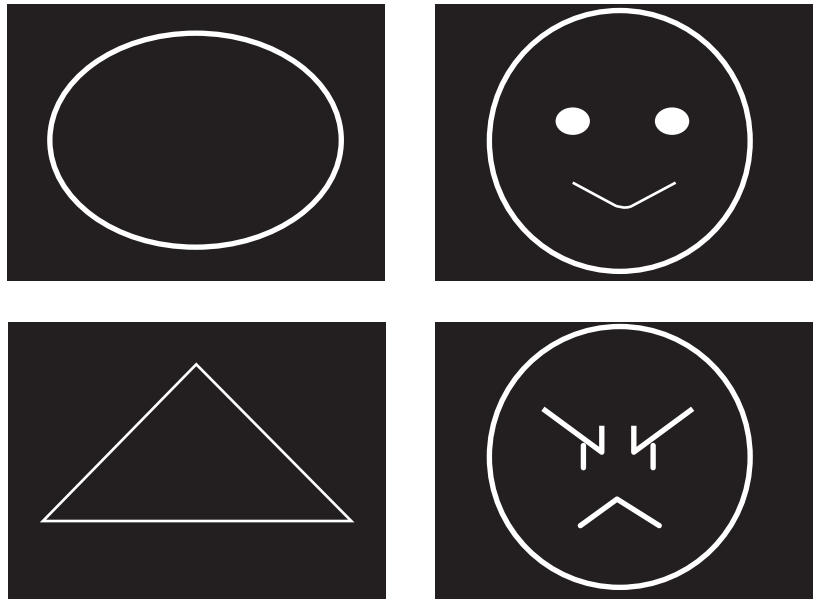

Figure 1: The left side illustrates ellipse and triangle as the target stimuli, and the right side shows a line-drawn happy face and an angry face as stronger emotional stimuli.

impendence was maintained below 5 kΩ with a sampling rate of 500 Hz and a 0.15–50 Hz band-pass filter.

Participants were trained during the practice section as long as they needed to be familiarized with the key-pressing pattern before the formal test. They were required to keep their body as still as possible during the formal test, in which the EEG signals were concurrently recorded.

2.4. EEG Data Analysis. EEG data were analyzed using standard off-line procedures in BrainVision Analyzer software (Brain Products GmbH, Germany). After eye blink correction, other artifacts (i.e., epochs with EEG power exceeding ±100 microvolts) were removed from the EEG data, and 96.6% of the original EEG data were retained. Subsequently, these artifact-free data were segmented into 1000 ms epochs, baseline-corrected with a 100 ms prestimulus interval, and averaged, respectively, for the four types of stimuli. Based on the literature suggesting that early ERP components are sensitive to emotional processing [18, 19], peak amplitudes were computed for N1 (50 ms–150 ms), P1 (50 ms–150 ms), N2 (150 ms–250 ms), P2 (150 ms–250 ms), N3 (250 ms–350 ms), and P3 (250 ms–350 ms). For our research interest, peak amplitudes of the abovementioned six ERP components in eight selected electrodes (F3, F4, P3, P4, T7, T8, O1, and O2) were computed to represent frontal, parietal, temporal, and occipital lobes in both left and right hemispheres.

3. Results

3.1. Behavioral Data. A single-factor repeated-measures ANOVA with type as the independent variable and accuracy as the dependent variable showed no significant result. The reaction time of the stimuli for triangle, ellipse, angry face, and smiling face is 376 ± 102, 380 ± 108, 366 ± 104, and 379 ± 100 milliseconds, respectively. The same ANOVA with reaction time as the dependent variable showed a significant main effect for type: $F(3, 54) = 3.62$, $p < 0.05$. Post hoc analysis revealed that reaction time for angry face was significantly shorter than those for the other three types of stimuli ($p < 0.05$). Although the average reaction time for triangle is shorter than that for ellipse, we did not find significance of difference in behavior level.

3.2. ERP Data. 2 (hemisphere: left versus right hemisphere) × 4 (lobe: frontal, parietal, temporal, and occipital) × 4 (type: ellipse, triangle, smiling face, and angry face) within-group repeated-measures ANOVAs were done separately for the six early ERP components (N1, P1, N2, P2, N3, and P3). Figure 2 depicts the examples of average waveform of the ERP induced with different stimuli from the frontal, parietal, occipital, and temporal lobes, respectively. The averaged response amplitudes for the four early components of the four lobes are illustrated in Figure 3.

3.2.1. N1. A significant main effect was found for type ($F(3, 54) = 5.85$, $p < 0.01$). Post hoc analysis showed that N1 amplitude for angry face was significantly larger than that for happy face ($p < 0.05$), and N1 amplitude for triangle was significantly larger than that for ellipse ($p < 0.05$). These results suggested that the "cognitive strain" group (i.e., angry face and triangle) induced larger response amplitude than the "cognitive ease" group did (i.e., happy face and ellipse). Lobe responses vary significantly ($F(3, 54) = 10.22$, $p < 0.001$). N1 amplitude in the temporal lobe was significantly smaller than that in the parietal lobe (post hoc, $p < 0.01$) and that in the occipital lobe (post hoc, $p < 0.01$). The right hemisphere responded significantly stronger than the left hemisphere did ($F(1, 18) = 14.03$, $p < 0.01$).

Significant interaction effects for type × lobe ($F(9, 162) = 3.28$, $p < 0.01$), type × hemisphere ($F(3, 54) = 2.94$, $p < 0.05$),

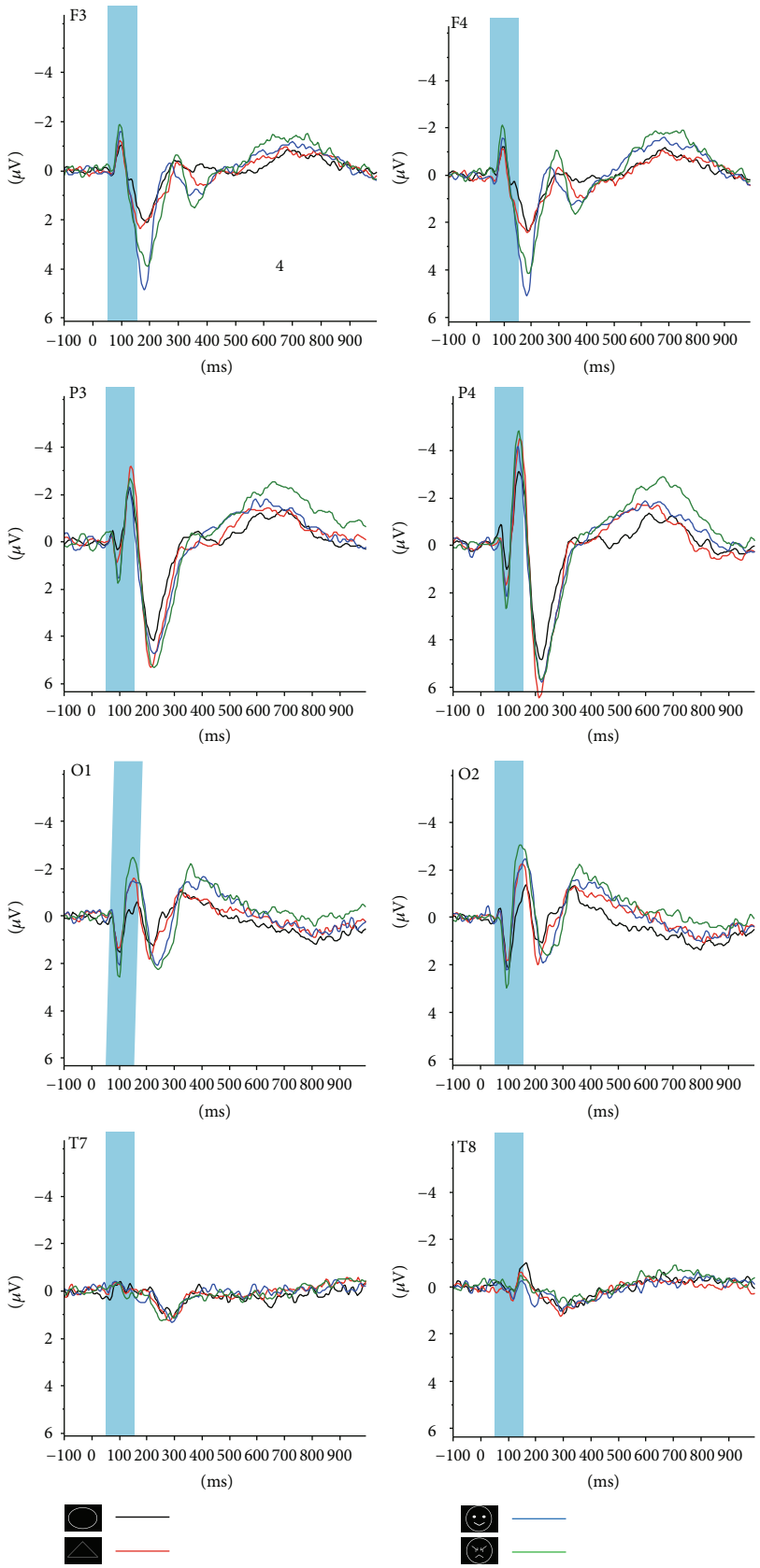

Figure 2: F3, F4, P3, P4, O1, O2, T7, and T8 are the examples of grand averaged waveforms of the left and right frontal, parietal, occipital, and temporal lobes, respectively. Black and red and blue and green lines represent the responses of the ellipse and triangle and smiling and angry faces as stimuli, respectively. The blue bars represent the time windows for ERP N1 component analysis.

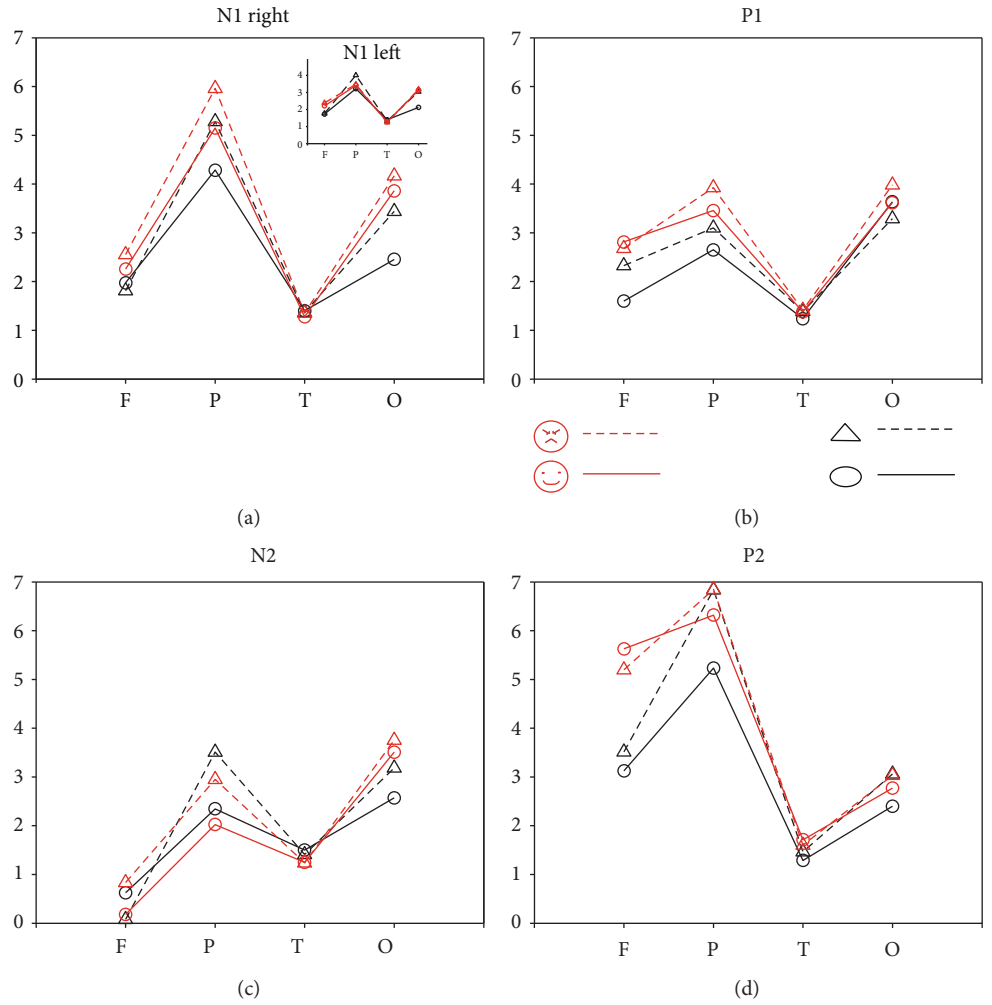

Figure 3: (a) N1 amplitude differences among the four types of stimuli; (b) P1 amplitude differences among the four types of stimuli; (c) N2 amplitude differences among the four types of stimuli; (d) P2 amplitude differences among the four types of stimuli. Note: LF = left frontal; RF = right frontal; LP = left parietal; RP = right parietal; LT = left temporal; RT = right temporal; LO = left occipital; RO = right occipital.

lobe × hemisphere ($F(3, 54) = 7.69$, $p < 0.001$), and type × lobe × hemisphere ($F(9, 162) = 2.66$, $p < 0.01$) were found as well. Follow-up Bonferroni-corrected paired t-tests for the three-way interaction effect showed that N1 amplitude for happy face was significantly larger than that for ellipse ($p < 0.05$) in the left frontal lobe; N1 amplitude for angry face was significantly larger than that for triangle ($p < 0.05$) in the right frontal lobe; N1 amplitude for ellipse was significantly smaller than that for triangle ($p < 0.05$) and that for happy face ($p < 0.05$), as well as that for angry face ($p < 0.01$) in the right parietal lobe; N1 amplitude for ellipse was significantly smaller than that for triangle ($p < 0.05$) and that for happy face ($p < 0.5$) in the left occipital lobe; and N1 amplitude for ellipse was significantly smaller than that for happy face ($p < 0.01$) and angry face ($p < 0.05$) in the right occipital lobe.

3.2.2. P1. Significant main effects were found for type ($F(3, 54) = 7.73$, $p < 0.001$; post hoc analysis showed that P1 amplitude for angry face was significantly larger than that for ellipse ($p < 0.05$) and that for triangle ($p < 0.05$)), lobe ($F(3, 54) = 6.44$, $p < 0.01$; post hoc analysis showed that P1 amplitude in the temporal lobe was significantly smaller than those in the other lobes ($p < 0.05$)), and hemisphere ($F(1, 18) = 9.62$, $p < 0.001$; P1 amplitude in the right hemisphere was significantly larger than that in the left hemisphere ($p < 0.01$)).

A significant interaction effect for type × lobe was also found ($F(9, 162) = 3.07$, $p < 0.01$). Follow-up Bonferroni-corrected paired t-tests showed that P1 amplitude for ellipse was significantly smaller than that for happy face ($p < 0.5$) and that for angry face ($p < 0.5$) over the frontal lobe; P1 amplitude for angry face was significantly larger than that for ellipse ($p < 0.01$) and triangle ($p > 0.05$) over the parietal lobe.

3.2.3. N2. Significant main effects were found for lobe ($F(3, 54) = 10.66$, $p < 0.001$; N2 amplitudes in the occipital lobe and the parietal lobe were significantly larger than those in the frontal lobe ($p < 0.01$) and temporal lobe ($p < 0.05$)) and hemisphere ($F(1, 18) = 5.50$, $p < 0.001$; N2 amplitude in the right hemisphere was significantly larger than that in the left hemisphere).

A significant interaction effect for type × lobe ($F(9, 162) = 8.27$, $p < 0.001$) was also found. Follow-up Bonferroni-corrected paired t-tests for this interaction effect showed that N2 amplitude for angry face was significantly smaller than that for ellipse ($p < 0.01$) and that for triangle ($p < 0.05$), as well as that for happy face ($p < 0.01$) in the frontal lobe; N2 amplitude for angry face was significantly larger than that for happy face ($p < 0.05$) and N2 amplitude for triangle was significantly larger than that for ellipse ($p < 0.01$) in the parietal lobe; N2 amplitude for angry face was significantly larger than that for happy face ($p < 0.05$) in the occipital lobe.

3.2.4. P2. Significant main effects were found for type ($F(3, 54) = 12.69$, $p < 0.001$; P2 amplitude for ellipse was significantly smaller than those for other figures ($p < 0.01$)) and lobe ($F(3, 54) = 26.61$, $p < 0.001$; P2 amplitude in the temporal lobe was significantly smaller than that in the frontal lobe ($p < 0.05$) and that in the parietal lobe ($p < 0.001$), as well as that in the occipital lobe ($p < 0.001$)).

A significant interaction effect for type × lobe ($F(9, 162) = 6.27$, $p < 0.001$) was also found. Follow-up Bonferroni-corrected paired t-tests for this interaction effect showed that P2 amplitudes for happy and angry face were significantly larger than those for ellipse and triangle ($p < 0.001$) in the frontal lobe; P2 amplitude for triangle was significantly larger than that for ellipse ($p < 0.01$) in the parietal lobe.

3.2.5. N3. A significant main effect for lobe was found: $F(3, 54) = 8.75$, $p < 0.001$. N3 amplitude in the occipital lobe was significantly larger than those in other lobes ($p < 0.01$).

3.2.6. P3. A significant main effect for lobe was found: $F(3, 54) = 4.38$, $p < 0.01$. P3 amplitude in the parietal lobe was significantly larger than that in the occipital lobe ($p < 0.01$).

4. Discussion

The aim of this study was to investigate the neural responses to different line-drawn configurations, which may induce the brain into different affective perceptions. Our hypothesis is that the circular shape leads the brain into mild "affective ease," which means the subject feels relaxed and comfortable subconsciously, whereas the angular shape induces mild "affective strain." Likewise, the happy and angry faces make the subject feel more relaxed or stressed consciously. The results obtained here support our hypothesis. We observed that the reaction time with the angry face is significantly shorter than that with the happy face, and the response amplitudes of P1, N1, P2, and N2 with angry face are significantly larger than those with happy face ($p < 0.05$). On the other hand, subjects respond to triangle with significantly larger amplitudes than to ellipse ($p < 0.05$). However, the reaction time for triangle is not significantly shorter than that for ellipse. Among the four types of stimuli, the early component P1 amplitude in the parietal lobe for angry face is the strongest, followed by happy face, triangle, and ellipse. The overall response of the right hemisphere is stronger than that of the left one.

For the behavior findings, our observation is consistent with the previous literature reports [3, 12, 20, 21]. The negative stimuli (affective strain group) elicit a faster and stronger response than the positive stimuli do (affective ease group). It is worthy of mentioning that negative stimuli evoked a stronger response in early EPR components than did positive stimuli, which was mostly mediated by the parietal and occipital lobes, as shown in N1, P1, and N2 components. It is known that the parietal and occipital lobes play critical roles in visual information processing, with the occipital lobe mediating the primary coding of visual configuration and the parietal lobe further supporting detailed analysis of spatial organization of visual stimuli. Early sensitivity of the two lobes to affective stimuli suggests that the emotional meaning of visual stimuli can be aroused in a very early stage of information processing. This early processing of emotional signals (i.e., identifying "threat" or "nonthreat") is likely to help humans survive in a complex environment. Moreover, the timescale of the early response of visual affective stimuli also matches with previously published research results [22].

In general, the faces have more complex information and strong affective expression and could induce strong arousal and affective values [23]. The simple geometric shapes are usually treated as much less affective or almost neutral stimuli. However, it has been shown that angular shapes may activate fear and be crucial to processing the threat cues and negative emotion and thus modulate the behavior and performance in real life [11]. Even at the peripheral level, research has demonstrated that triangle and circle could modulate the skin conductance resistance and the startle reflex differently [24]. Here, we could expect that the four types of stimuli applied in our experiments may induce the brain into different degrees of affective strain and affective ease. Our data here matches our expectation. The affective strain group induces a stronger response amplitude than the ease group does (N1, P1, N2, and P2). Within the strain group, angry face induces a larger amplitude than triangle does (N1 right frontal lobe, P1 parietal lobe, and N2 frontal lobe). Within the ease group, happy face induces a stronger response than ellipse does (N1 left frontal, right parietal, left and right occipital, and P1 and N2 frontal lobes). These results indicate that at the early stage, the brain responds to the variant affective visual stimuli differently. The prominent activities of N1, P1, N2, and P2 have significant main effects of different shape-induced degrees of cognitive ease and cognitive strain.

Interestingly, the frontal lobe was more sensitive to facial figures than to geometrical figures (i.e., as shown in N1, P1, and P2 components). This result is consistent with the literature showing that the frontal lobe, especially the lateral inferior prefrontal lobe, is the "social part" of the human brain, which deals with social relationships and functions critically in empathy. A recent review of ERP studies has demonstrated that affective stimulus factors primarily modulate ERP component amplitude [8]. Affective ERPs have been linked to attention orientation for unpleasant pictures at earlier components. Many face ERP studies have shown that emotion facial expressions elicit an early fronto-central positive shift, ranging from 120 to 180 ms poststimulus [25].

Another recent EEG study has shown that emotional facial expression evokes faster attention orientation, but weaker affective neural activity and behavioral responses, compared to that when exposed to emotional scenes [26]. Our data are different from this study, as we did not use the real human face and real scene as stimuli, but simple lines and curves. Thus, our stimuli are much simpler, abstract, and mild compared with the real face pictures. This point is consistent with the finding from Rossi et al. that photographic but not line-drawn faces show early perceptual neural sensitivity [27]. Moreover, Salgado-Montejo et al. found that facial gestures that are associated with specific emotions can be captured by simple shapes and lines [28]. Hence, different types and different intensities of visually elicited emotions may be mapped with different patterns of early responses. For instance, positive emotional faces evoked N170 significantly earlier than did negative emotional faces and the amplitude of fearful faces was larger than that of neutral or surprised faces [17]. Within the same type of emotion, different intensities of angry facial expression lead to different response patterns; higher intensity induces larger P3 and late positive potential [15]. Consistent along the above lines, in our study, different degrees of affective states evoke different response patterns. Affective strain induces larger amplitude of early ERP than affective ease does, and higher intensity of affective states evokes larger amplitude of early ERP than lower intensity of affective states does.

Studies on simple geometric shapes have received more attention recently in behavior and neural physiological research. Using circle and downward triangle as affective priming, Wang and Zhang found a typical effect of affective congruency in the task of face and word analysis [4]. Consistent with previous studies, here we show that triangle is perceived as "affective strain" and evokes larger amplitudes than ellipse does which is perceived as "affective ease." Therefore, our study has extended previous studies and has shown directly the event-related brain potentials with simple line-drawn shapes and faces. It may suggest that the perception advantage of shapes might be activated from conscious to subconscious levels.

Regarding the neural network of emotion processing, the amygdala, nucleus accumbens, hypothalamus, hippocampus, insula, cingulate cortex, and orbitofrontal cortex have been suggested to be involved [29]. Due to the vague spatial information of EEG, the signals from parietal and occipital channels are most reliable for visually elicited human emotion encoding and classification [14]. In our study, we observed that significant effects of angry and happy faces are registered in frontal, parietal, and occipital lobes. The other significant effects of triangle and ellipse are found in the parietal lobe. Hence, our data support the hypothesis that different degrees of affective states could be mapped with different patterns of neural activities.

Earlier studies showed that basic facial expressions can be processed very rapidly which also includes emotional information processing [17]. Neutral and positive emotions like happiness and pleasant surprise evoked N170 more rapidly than did negative emotions like fear, sadness, and disgust. It has been proposed that a subcortical pathway conveys information more rapidly to various ventral pathways than does the N170 latency. For the negative emotion, the subcortical feedback loop activates a larger underlying neuronal network. In the literature, no subcortical sources have been shown to be active before 140 ms (early processing periods) most likely due to the insensitivity of ERP methods to deep and transient sources. Later activation of subcortical sources (after 320 ms) has been attributed to the extensive spatial and temporal activation at such later time periods. It has also been shown earlier that middle and superior temporal regions are activated in the intermediate time periods (140–400 ms). These areas are particularly sensitive for processing of human and facial expressions. Earlier ERP and clinical studies further suggest the activation of the right lentiform nucleus along with basal ganglia for angry, sad, and neutral faces. Moreover, amygdala activation is invisible to ERP methods. Clinical studies on patients with cerebral injuries have proposed inferior frontal and ventral areas to process recognition in humans. It has been suggested elsewhere that separate recognition of fear, anger, and disgust involves separate neural systems altogether. To localize the accurate areas in the brain for processing of shapes, we need to apply fMRI studies as the next step of investigation in the future.

In short, this study has shown directly the electrophysiological mapping of the brain with different degrees of affective perception induced by visual shapes. It would be interesting to add more parameters to the shapes, such as asymmetry and complexity, to systematically study the influence of shape on inducing different cognitive perceptions. Since shapes are in general more abstract and context-free, this study will help to understand the configuration-induced affective cognition and the related cross-modal sensory integration.

5. Conclusions

To conclude, our results provide the first neurophysiological evidence that two geometrical figures which are opposite in emotional valence can be identified as "threat' and "non-threat" in the human mind. Consistent with our hypothesis, happy and angry faces, as commonly perceived strong emotional signals in social interaction, aroused stronger ERP amplitudes than the two target geometrical figures did (i.e., ellipse and triangle). Importantly, ellipse and triangle were found to arouse similar ERP responses to happy and angry faces (i.e., as shown in N1 and N2 components), respectively. Our ERP data showed that the right hemisphere was more sensitive to emotional stimuli than the left hemisphere, which is consistent with the emotional role associated with the right hemisphere, as reported in previous studies.

Data Availability

The data used to support the findings of this study are available from the corresponding author upon request.

Disclosure

Yingli Li and Qingguo Ding are the co-first authors.

Conflicts of Interest

The authors declare that they have no conflicts of interest.

Authors' Contributions

Yingli Li and Qingguo Ding contributed equally to this work.

Acknowledgments

This work has been supported by the National Natural Science Foundation of China (no. 61703058), the Social Science Foundation of Jiangsu Educational Department (nos. 14YSB003 and 2017SJB1396), and the Natural Science Foundation of Jiangsu Educational Department (no. 16KJB510001).

References

[1] J. Aronoff, A. M. Barclay, and L. A. Stevenson, "The recognition of threatening facial stimuli," *Journal of Personality and Social Psychology*, vol. 54, no. 4, pp. 647–655, 1988.

[2] D. Lundqvist, F. Esteves, and A. Öhman, "The face of wrath: the role of features and configurations in conveying social threat," *Cognition and Emotion*, vol. 18, no. 2, pp. 161–182, 2004.

[3] J. Aronoff, "How we recognize angry and happy emotion in people, places, and things," *Cross-Cultural Research*, vol. 40, no. 1, pp. 83–105, 2006.

[4] Y. Wang and Q. Zhang, "Affective priming by simple geometric shapes: evidence from event-related brain potentials," *Frontiers in Psychology*, vol. 7, p. 917, 2016.

[5] D. Kahneman, *Thinking, Fast and Slow*, Macmillan, 2011.

[6] C. H. Hansen and R. D. Hansen, "Finding the face in the crowd: an anger superiority effect," *Journal of Personality and Social Psychology*, vol. 54, no. 6, pp. 917–924, 1988.

[7] C. L. Larson, J. Aronoff, and J. J. Stearns, "The shape of threat: simple geometric forms evoke rapid and sustained capture of attention," *Emotion*, vol. 7, no. 3, pp. 526–534, 2007.

[8] J. K. Olofsson, S. Nordin, H. Sequeira, and J. Polich, "Affective picture processing: an integrative review of ERP findings," *Biological Psychology*, vol. 77, no. 3, pp. 247–265, 2008.

[9] P. Liang, S. Roy, M. L. Chen, and G. H. Zhang, "Visual influence of shapes and semantic familiarity on human sweet sensitivity," *Behavioural Brain Research*, vol. 253, pp. 42–47, 2013.

[10] P. Liang, P. Biswas, S. Vinnakota et al., "Invariant effect of vision on taste across two Asian cultures: India and China," *Journal of Sensory Studies*, vol. 31, no. 5, pp. 416–422, 2016.

[11] C. L. Larson, J. Aronoff, I. C. Sarinopoulos, and D. C. Zhu, "Recognizing threat: a simple geometric shape activates neural circuitry for threat detection," *Journal of Cognitive Neuroscience*, vol. 21, no. 8, pp. 1523–1535, 2009.

[12] M. Bar and M. Neta, "Visual elements of subjective preference modulate amygdala activation," *Neuropsychologia*, vol. 45, no. 10, pp. 2191–2200, 2007.

[13] T. W. Picton and M. J. Taylor, "Electrophysiological evaluation of human brain development," *Developmental Neuropsychology*, vol. 31, no. 3, pp. 249–278, 2007.

[14] L. Bozhkov, P. Georgieva, I. Santos, A. Pereira, and C. Silva, "EEG-based subject independent affective computing models," *Procedia Computer Science*, vol. 53, pp. 375–382, 2015.

[15] J. Wang, L. Liu, and J. H. Yan, "Implicit power motive effects on the ERP processing of emotional intensity in anger faces," *Journal of Research in Personality*, vol. 50, pp. 90–97, 2014.

[16] J. K. Hietanen and P. Astikainen, "N170 response to facial expressions is modulated by the affective congruency between the emotional expression and preceding affective picture," *Biological Psychology*, vol. 92, no. 2, pp. 114–124, 2013.

[17] M. Batty and M. J. Taylor, "Early processing of the six basic facial emotional expressions," *Cognitive Brain Research*, vol. 17, no. 3, pp. 613–620, 2003.

[18] V. Ferrari, M. Codispoti, and M. M. Bradley, "Repetition and ERPs during emotional scene processing: a selective review," *International Journal of Psychophysiology*, vol. 111, pp. 170–177, 2017.

[19] H. T. Schupp, J. Markus, A. I. Weike, and A. O. Hamm, "Emotional facilitation of sensory processing in the visual cortex," *Psychological Science*, vol. 14, no. 1, pp. 7–13, 2003.

[20] G. Horstmann, K. Borgstedt, and M. Heumann, "Flanker effects with faces may depend on perceptual as well as emotional differences," *Emotion*, vol. 6, no. 1, pp. 28–39, 2006.

[21] S.-L. Huang, Y.-C. Chang, and Y.-J. Chen, "Task-irrelevant angry faces capture attention in visual search while modulated by resources," *Emotion*, vol. 11, no. 3, pp. 544–552, 2011.

[22] R. Ratcliff, "Methods for dealing with reaction time outliers," *Psychological Bulletin*, vol. 114, no. 3, pp. 510–532, 1993.

[23] R. Adolphs, "Recognizing emotion from facial expressions: psychological and neurological mechanisms," *Behavioral and Cognitive Neuroscience Reviews*, vol. 1, no. 1, pp. 21–62, 2002.

[24] D. Armbruster, V. Suchert, A. Gärtner, and A. Strobel, "Threatening shapes: the impact of simple geometric configurations on peripheral physiological markers," *Physiology & Behavior*, vol. 135, pp. 215–221, 2014.

[25] M. Eimer and A. Holmes, "Event-related brain potential correlates of emotional face processing," *Neuropsychologia*, vol. 45, no. 1, pp. 15–31, 2007.

[26] A. Mavratzakis, C. Herbert, and P. Walla, "Emotional facial expressions evoke faster orienting responses, but weaker emotional responses at neural and behavioural levels compared to scenes: a simultaneous EEG and facial EMG study," *NeuroImage*, vol. 124, Part A, pp. 931–946, 2016.

[27] A. Rossi, F. J. Parada, M. Latinus, and A. Puce, "Photographic but not line-drawn faces show early perceptual neural sensitivity to eye gaze direction," *Frontiers in Human Neuroscience*, vol. 9, p. 185, 2015.

[28] A. Salgado-Montejo, C. J. Salgado, J. Alvarado, and C. Spence, "Simple lines and shapes are associated with, and communicate, distinct emotions," *Cognition and Emotion*, vol. 31, no. 3, pp. 511–525, 2017.

[29] S. Koelsch, "Brain correlates of music-evoked emotions," *Nature Reviews Neuroscience*, vol. 15, no. 3, pp. 170–180, 2014.

Hindawi
Neural Plasticity
Volume 2018, Article ID 3479059, 13 pages
https://doi.org/10.1155/2018/3479059

Research Article

The Neural Basis of Fear Promotes Anger and Sadness Counteracts Anger

Jun Zhan,[1,2] **Jingyuan Ren**,[1] **Pei Sun**,[3] **Jin Fan**,[4] **Chang Liu**,[5] **and Jing Luo**[1]

[1]*School of Psychology, Capital Normal University, Beijing, China*
[2]*School of Marxism, Fujian Agriculture and Forestry University, Fuzhou, China*
[3]*Department of Psychology, Tsinghua University, Beijing, China*
[4]*Department of Psychology, The City University of New York, New York City, NY, USA*
[5]*School of Psychology, Nanjing Normal University, Nanjing, China*

Correspondence should be addressed to Chang Liu; cglew@163.com and Jing Luo; luoj@psych.ac.cn

Received 26 January 2018; Revised 21 April 2018; Accepted 7 May 2018; Published 14 June 2018

Academic Editor: Fushun Wang

In contrast to cognitive emotion regulation theories that emphasize top-down control of prefrontal-mediated regulation of emotion, in traditional Chinese philosophy and medicine, different emotions are considered to have mutual promotion and counteraction relationships. Our previous studies have provided behavioral evidence supporting the hypotheses that "fear promotes anger" and "sadness counteracts anger"; this study further investigated the corresponding neural correlates. A basic hypothesis we made is the "internal versus external orientation" assumption proposing that fear could promote anger as its external orientation associated with motivated action, whereas sadness could counteract anger as its internal or homeostatic orientation to somatic or visceral experience. A way to test this assumption is to examine the selective involvement of the posterior insula (PI) and the anterior insula (AI) in sadness and fear because the posterior-to-anterior progression theory of insular function suggests that the role of the PI is to encode primary body feeling and that of the AI is to represent the integrative feeling that incorporates the internal and external input together. The results showed increased activation in the AI, parahippocampal gyrus (PHG), posterior cingulate (PCC), and precuneus during the fear induction phase, and the activation level in these areas could positively predict subsequent aggressive behavior; meanwhile, the PI, superior temporal gyrus (STG), superior frontal gyrus (SFG), and medial prefrontal cortex (mPFC) were more significantly activated during the sadness induction phase, and the activation level in these areas could negatively predict subsequent feelings of subjective anger in a provocation situation. These results revealed a possible cognitive brain mechanism underlying "fear promotes anger" and "sadness counteracts anger." In particular, the finding that the AI and PI selectively participated in fear and sadness emotions was consistent with our "internal versus external orientation" assumption about the different regulatory effects of fear and sadness on anger and aggressive behavior.

1. Introduction

Western psychology generally advocates the use of cognitive methods, such as rational or cognitive reappraisal, to down-regulate negative emotions. However, hormones released in response to stress can impair the advanced function of the prefrontal cortex (PFC), leading to a failure of cognitive reappraisal in regulating conditioned fear under stress [1, 2]; thus, emotion regulation strategies that are less reliant on the PFC could be more suitable for changing negative responses to emotional arousal under stress than normal downregulating strategies [3]. In contrast to cognitive emotion regulation theories, traditional Chinese philosophy and medicine consider different types of emotions to have mutual promotion and mutual counteraction (MPMC) relationships (Figure 1) involving a down-up process that depends less on the PFC

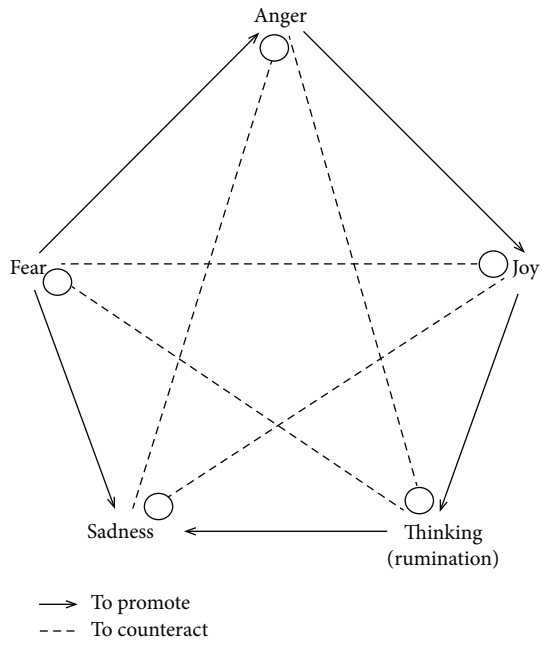

Figure 1: Relationships of mutual promotion and mutual restraint and the emotions of joy, thinking/anxiety (The original word for "thinking" in the Chinese literature is 思 [read as si]; 思 may indicate either the pure cognitive thinking and reasoning process that is nonpathogenic or the maladaptive repetitive thinking or ruminative thinking that is typically associated with negative emotion and has pathogenic potential. Thus, 思 may have different meanings in different contexts of the MPMC theory. The implication of maladaptive "thinking" in the MPMC theory of emotionality includes not only ruminative thought per se but also the negative, depression-like emotion associated with it. Therefore, in specific contexts, particularly the context discussed in this study, 思 indicates the ruminative or repetitive thinking that is closely related to rumination in modern psychology, which is defined as a pattern of repetitive self-focus and recursive thinking focused on negative cases or problems (e.g., unfulfilled goals or unemployment) that is always associated with the aggravation of negative mood states (e.g., sadness, tension, and self-focus) and has been shown to increase one's vulnerability to developing or exacerbating depression [4].), sadness, fear, and anger. The promotion relationships include the following: joy promotes thinking/anxiety, thinking/anxiety promotes sadness, sadness promotes fear, fear promotes anger, and anger promotes joy. The restraint relationships include the following: joy counteracts sadness, sadness counteracts anger, anger counteracts thinking/anxiety, thinking/anxiety counteracts fear, and fear counteracts joy.

[4], thereby suggesting a novel approach for emotion regulation that may overcome the shortcomings of traditional cognitive regulation strategies.

In our recent study, aggressive behavior associated with anger was found to be effectively reduced by inducing sadness, while the induction of fear significantly increased self-reported anger; these findings provided behavioral evidence supporting the hypotheses proposed by the MPMC theory of emotionality that suggest "sadness counteracts anger" and "fear promotes anger" [3, 4]. In that experiment, anger was first induced by asking the participants to read an extremely negative comment regarding their viewpoints (the mutual article evaluation paradigm) or watch standardized anger-inducing movie clips; then, fear, sadness, or a neutral mood was induced. The participants who were provoked exhibited less aggressive behavior if sadness was subsequently induced; however, the participants became increasingly angry if fear was subsequently induced.

More importantly, the principle of "sadness counteracts anger" may have application value because the induction of sadness (e.g., passively watching a clip from a sad movie or listening to sad music) requires obviously fewer cognitive control resources mediated by the PFC and may regulate negative emotion; therefore, this principle could have some advantages in regulating emotion relative to cognitive-regulation strategies that may fail to work under stress. To test this hypothesis, in our recent study, we directly compared the effects of cognitive reappraisal and sadness induction on reducing anger or anger-related aggression in nonstressful and stressful situations [3]. Expectedly, cognitive reappraisal was unable to effectively relieve the subjective feeling of anger under the stress condition; however, the stressful condition did not influence the efficiency of sadness induction in reducing aggressive behavior. First, all the participants were assigned to a nonstressful or stressful condition and were provoked using the mutual article evaluation paradigm; then, the participants were asked to make a cognitive reappraisal or watch sad movie clips. The cognitive reappraisal effectively reduced self-reported anger under the nonstress condition but failed to have such an effect under the stress condition; meanwhile, high cortisol levels were found to be maintained in and after the reappraisal. It is possible that cortisol activation triggered by the arousal of the hypothalamic-pituitary-adrenal (HPA) axis disrupted the PFC function and further impaired the efficiency of cognitive regulation, while stress did not influence the effects of sadness induction on aggressive behavior and related skin conductance, suggesting that the emotion regulation strategy is relatively immune to stress.

However, the cognitive brain processes underlying the phenomenon of "sadness counteracts anger" and "fear promotes anger" are still unknown. A general perspective for understanding these mechanisms is to consider the ways in which different types of emotions interact, that is, how an antecedent or subsequent emotion (such as sadness or fear) could interact with the targeted emotion (such as anger). This investigation of the process and neural mechanism of the interactions among different emotions could increase our understanding of the effective principle of the "sadness counteracts anger" strategy. For example, if an individual is aroused by sadness or fear before or after being provoked, a certain pattern of neuropsychological components activated by the sadness or fear could affect the expression of anger or aggressive behavior.

More specifically, according to a meta-analysis of the neural activation patterns associated with different types of basic emotions, the anger and fear categories both prioritized cortical processes that support an "external orientation/object-focused" schema, which is characterized by goal-driven responses in which objects and events in the world are in the foreground [5]. In contrast, the cortical patterns

associated with sadness support an internal orientation/homeostatic-focused schema characterized by an orientation toward immediate somatic or visceral experiences, which prioritizes the processing of interoceptive and homeostatic events [5]. Thus, the neural circuits mediating anger and related aggression may be more easily triggered by the neural activity underlying fear but more efficiently eliminated by the neural activity underlying sadness [4].

To test this hypothesis, this study investigated the regulatory effects of antecedently induced sadness or fear on the subsequent anger and related aggressive behavior in a provoking situation and analyzed the accompanying brain mechanisms using functional magnetic resonance imaging (fMRI). Specifically, we explored and verified the possibility that following antecedent-induced sadness, individuals are less likely to become angry or aggressive ("sadness counteracts anger") in a provoking situation, while following antecedent-induced fear, individuals are more likely to become angry or display more aggression ("fear promotes anger") in a provoking situation. We identified the key brain regions activated by sadness or fear inducing and further analyzed the correlation between the activations of these regions and the subsequent anger-related responses in subsequent provocation.

In particular, we made an "internal versus external orientation" assumption proposing that fear could promote anger because of its external orientation associated with motivated action, whereas sadness could counteract anger because of its internal or homeostatic orientation to somatic or visceral experience. This assumption could be examined by detecting the selective involvement of the posterior insula (PI) and the anterior insula (AI) in sadness and fear. According to the theory of the posterior-to-anterior progression of insular function in re-representing human feeling and emotion, the PI represents more primary quantities, whereas the AI integrates more contextual information in its representation of emotion [6, 7]. Therefore, we propose that fear could be more intensively represented in the AI by its external encoding or contextual integrating orientation and that this orientation, because of its similarities with anger, will promote anger-related feeling and behavior, whereas sadness could be more intensively represented in the PI by its internal orientation or homeostatic-focused schema and that this orientation, because of its dissimilarities with anger, will counteract with anger-related feeling and behavior.

2. Materials and Methods

2.1. Participants. The sample size was 24, which was calculated with the G*Power software 3.1.9.2 (input parameter: α: 0.05; power $(1 - \beta)$: 0.8). In addition, to minimize the potential impact of age differences, twenty-six college students (17 females and 9 males, aged 19–25 years, mean age = 22 years, all native Chinese speakers) at universities in Beijing were recruited to participate in this study as paid volunteers. All the participants were right-handed, had normal or corrected-to-normal vision, and had no history of neurological or psychiatric problems. Prior to the scanning session, the participants signed informed consent forms, and the study was approved by the Institutional Review Board of the Center for Biomedical Imaging Research of Tsinghua University. After the experiment, each participant was compensated with 120 RMB for participating in the study. Two participants (1 male and 1 female) were excluded from the analysis due to excessive head motion during the scanning.

2.2. Experimental Design and Procedures

2.2.1. Overview of the Experimental Procedure. In contrast to the experimental procedure used in our previous study, which examined the regulatory effects of subsequently evoked sadness or fear on the anger emotion that had already been evoked [3, 4], in this study, we adopted a modified experimental procedure to examine the interaction between anger and sadness or fear, which could be more suitable for within-subject design. We examined the inhibitory or facilitatory effects of the antecedently evoked sadness or fear on anger or aggressive behavior in an offensive situation subsequently experienced by the participants. A single-factor (mood induction: fear versus sadness versus neutral mood) within-subject design was adopted in this study in which the participants experienced three episodes of fear, sadness, or neutral emotion induction, and each emotion induction was followed by a modified competitive reaction time task to provoke the participants; the level of subjective anger was measured at baseline and after the competitive reaction time task. Using this paradigm, a within-subject design that is more suitable for an fMRI investigation could be applied.

2.2.2. Evaluation of Subjective Anger. The subjective feeling of anger was measured using the hostility subscale of the revised Multiple Affect Adjective Checklist (MAACL) [8, 9]. In the Chinese version of the MAACL [10], the hostility subscale contains 22 adjectives, including 11 words that are positively associated with anger (i.e., irritable, cruel, jealous, disgruntled, indignant, impatient, hostile, irritated, violent, furious, and exasperated) and 11 words that are negatively associated with anger (i.e., gracious, easy-going, good-natured, helpful, friendly, courteous, gentle, pleasantly agreeable, kind, affable, and cooperative). All the participants were required to assess these 22 adjectives according to their current feelings and to select each positive anger word (press the "1" button) or to unselect each negative anger word (press the "2" button). Each selection accumulated one point, and the final scores were the sum of the total points of the selected positive anger words and unselected negative anger words. A high total score indicated a high level of anger.

2.2.3. Fear/Sadness/Neutral Mood Induction. In this study, 3 video clips were used to induce fear (duration, 2 min 20 sec; from the movie "Help"; intensity, M = 3.33, SD = 2.1), sadness (duration, 2 min 20 sec; from the movie "Mom Love Me Once Again"; intensity, M = 3.17, SD = 1.56), and a neutral emotion (duration, 2 min 20 sec; from the movie "Computer Repair"; intensity, M = 1.0625, SD = 0.25). The movie clips were extracted from the Chinese Emotional Visual Stimulus (CEVS) database [11]. While watching the clips, the participants were asked to be as attentive to the clips as possible, to express their natural feelings, and to avoid suppressing any emotion.

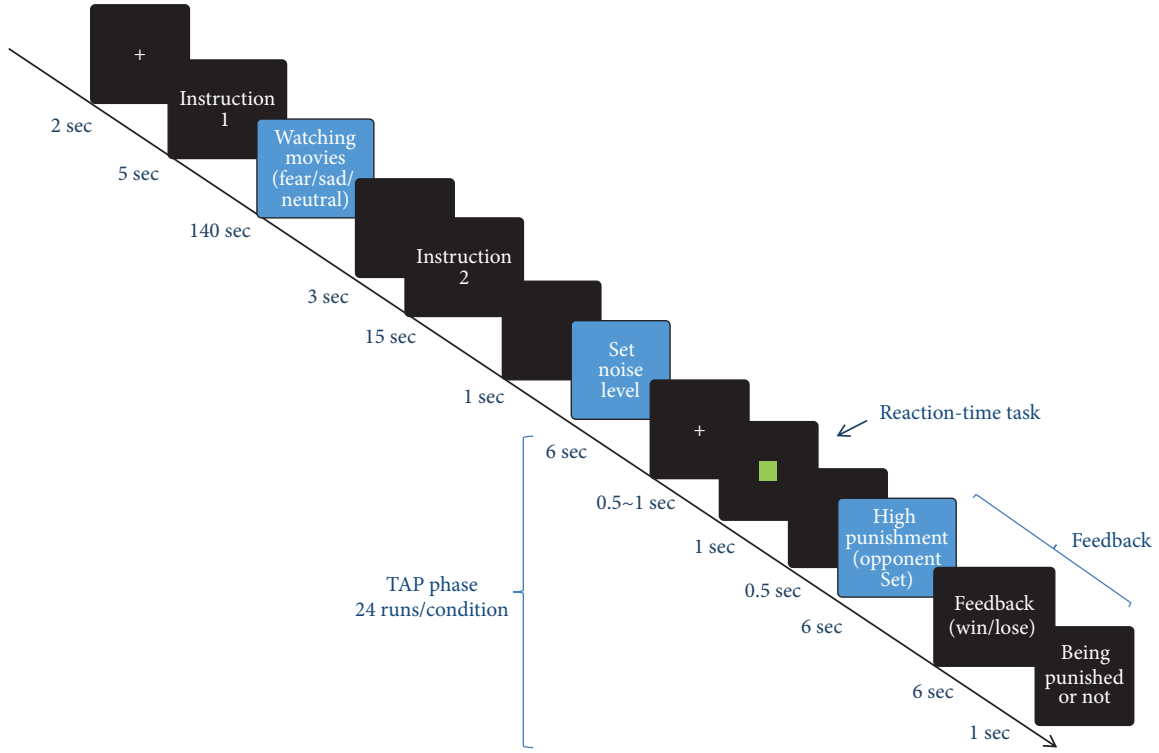

Figure 2: Overview of the presentations experienced by each subject over the course of the experiment. The entire experiment consisted of three runs (i.e., fear/sadness/neutral mood conditions) of the procedure.

2.2.4. Anger Induction and Aggressive Behavior Measure. The Taylor Aggression Paradigm (TAP) was used to induce anger and measure aggressive behaviors [12–15]. The modified version of the TAP was used in this study, and the task paradigm was adopted from a previous study [16]. In this task, the participants were informed that they would be playing 24 successive competitive reaction-time trials against an opponent. However, there was no opponent, and the entire program was established in advance. At the beginning of each trial, the participant was shown the opponent number for the upcoming competition (each of the three runs was supposedly played against a different opponent to avoid the possible influence of the competition experience with the opponent against whom they had competed in the previous run). Each participant was allowed to determine the intensity of the noise, that is, between 65 decibels (1—very weak) and 95 decibels (4—very strong), his/her opponent would hear if the opponent lost; each noise had a 2-second duration. Participants were instructed to select the noise intensity from 1 to 4 before each competition trial, and the average noise intensity selected by the participants over 24 rounds was used to indicate participants' aggression levels. After the participants selected the noise intensity, they were provoked by being shown the high-punishment selection (level 3 or 4, each 50%) of their opponents. Finally, feedback was provided regarding whether the participant won or lost. In the losing trials, the participants were exposed to aversive noise; in the winning trials, the participants did not receive a punishment. However, all win and fail trials were secretly controlled by the experimenter, and the participants won 12 of the 24 trials of the competition game.

2.3. Imaging Procedure. The scanning was divided into three runs according to the mood induction (fear, sadness, or neutral mood), and the run sequence was balanced across all participants. The interval between two runs was 3 min to allow the participants' mood to return to the baseline level and minimize any carryover effect [17]. The duration of each run was 12 min and 54 sec, and the total time of the functional imaging was 38 min and 42 sec. Each run consisted of two sessions (Figure 2). The first session included the phases of "introduction 1" and "watching movies." During "introduction 1," the participant was required to pay attention to watching movies, and in the phase of "watching movies," the participant was assigned to watch one of three different emotional movie clips to induce sadness, fear, or neutral emotions, with a clip duration of 140 sec. During the second session, "instruction 2" was used to introduce the rules of the TAP, which consisted of 24 trials and was used to elicit and assess aggression [16]. Each trial included the phase of "set noise level" (duration: 6 sec), in which the participant set the noise intensity for the opponent; the phase of "reaction-time task" (duration: 1 sec), in which the participant played against an opponent; and the phase of "feedback" (duration: 13 sec), in which the participant was provoked by being shown the opponent's high-punishment selection.

2.4. Image Acquisition. The data were acquired from the Center for Biomedical Imaging Research of Tsinghua University.

Table 1: Illustration of the eighteen events defined in the image analysis.

Number	Run—condition	Session	Event	Onset time (sec)	Duration (sec)
1	Run 1—fear	Fear induction	Instruction 1	20	5
2			Watching fear movie clip	25	140
3			Instruction 2	168	15
4			Determining noise level	186	6
5		TAP (first trial)	Reaction time task	192	1
6			Provocation	193	13
7	Run 2—sadness	Sadness induction	Instruction 1	20	5
8			Watching sad movie clip	25	140
9			Instruction 2	168	15
10			Determining noise level	186	6
11		TAP (first trial)	Reaction time task	192	1
12			Provocation	193	13
13	Run 3—neutral	Neutral induction	Instruction 1	20	5
14			Watching neutral movie clip	25	140
15			Instruction 2	168	15
16			Determining noise level	186	6
17		TAP (first trial)	Reaction time task	192	1
18			Provocation	193	13

The fMRI scanning was performed using a 3 T magnetic resonance scanner (Philips, Netherlands) with a 32-channel frequency head coil. To restrict head movements, the participants' heads were fixed with plastic braces and foam pads during the entire experiment. To perform the functional imaging, we used an echo-planar sequence based on blood oxygenation level-dependent (BOLD) contrast with the following parameters: time (TR) = 2000 ms, echo time (TE) = 35 ms, flip angle (FA) = 90°, field of view (FOV) = 200 mm × 200 mm, 64 × 64 matrix, voxel size = 2.5 × 2.5 × 4 mm^3, 30 slices, and 4 mm thickness. T2*-weighted function images parallel to the anterior commissure-posterior commissure (AC-PC) were obtained. To obtain structural images, high-resolution structural T1*-weighted anatomical scanning was performed using a 3D gradient-echo pulse sequence (TR = 7.65, TE = 3.73, flip = 90°, FOV = 230 mm × 230 mm, and voxel size = 0.96 mm × 0.96 mm × 1 mm).

2.5. Image Analysis. The imaging data were analyzed using SPM 8 (Statistical Parametric Mapping, Wellcome Department of Cognitive Neurology, London, UK). During preprocessing, the images of each participant were corrected with slice-timing, realigned to correct for head motion, spatially normalized into a standard echo planar imaging (EPI) template in the Montreal Neurological Institute (MNI) space, and smoothed using an 8 mm Gaussian kernel full width at half maximum (FWHM).

For each participant, a general linear model with eighteen events was defined. Specifically, each run consisted of six events, including "instruction 1," "watching movies," "instruction 2," "set noise level," "reaction-time task," and "feedback" (merged with "the presentation of a high punishment by the opponent," "feedback regarding winning or losing," and "being punished or not punished"). Because each run included one experimental condition (fearful, sad, or neutral), the three runs had eighteen (3 runs × 6 events/run) events (Figure 2 and Table 1). All the events were modeled with a canonical hemodynamic response function using the standard SPM8 settings. Six covariates (i.e., three rigid-body translations and three rotations resulting from the realignment) were also included to account for movement-related variability. Regionally specific condition effects were tested with performing linear contrasts for each key event relative to the baseline and each participant.

During the mood-induction phase, we were primarily interested in the differences in the cognitive brain responses among the different mood inductions (i.e., fear versus neutral mood induction, fear versus sadness induction, sadness versus neutral mood induction, and sadness versus fear induction). We additionally performed conjunction analyses of "fear induction > neutral mood induction," "fear induction > sadness induction," "sadness induction > neutral mood induction," and "sadness induction > fear induction" to identify the selective effects of the fear and sadness inductions.

The threshold of the whole-brain analyses was generally set at the threshold of $p < 0.001$ (uncorrected for multiple comparisons). All ROIs were created by superimposing the activated clusters obtained from the given contrast (e.g., the parahippocampal activation obtained in the conjunction analysis of "fear induction > neutral mood induction" and "fear induction > sadness induction") on the mask defined in the WFU PickAtlas (Version 3.0, http://fmri.wfubmc.edu/software/PickAtlas), and the percentage signal changes were extracted from MarsBar (http://marsbar.sourceforge.net). The percentage signal changes within each ROI were extracted separately for each participant under each condition.

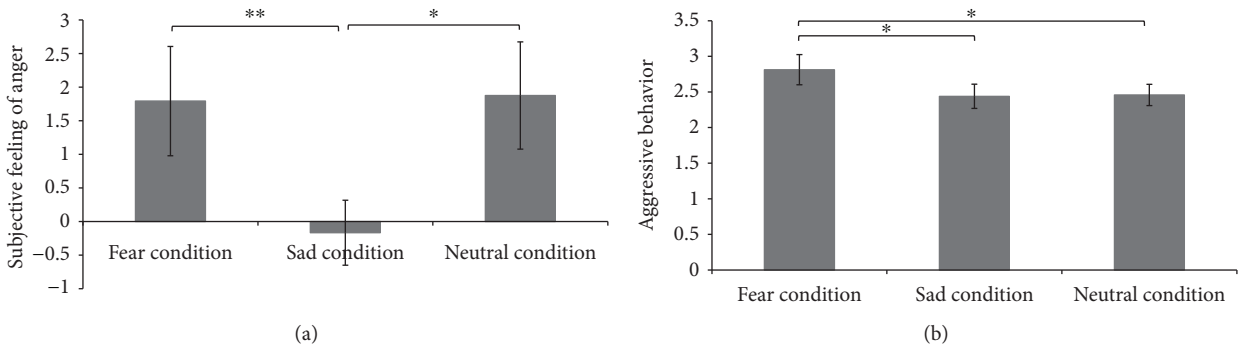

Figure 3: Comparison of the subjective feeling of anger and aggressive behavior under the fear, sad, and neutral conditions. The difference between the subjective anger feeling in each condition and that at baseline is shown in (a). The aggressive behavior under the three conditions is shown in (b). The error bars (capped vertical bars) represent (−1)/(+1)SE. ** indicates a significant difference at $p < 0.01$; * indicates a significant difference at $p < 0.05$.

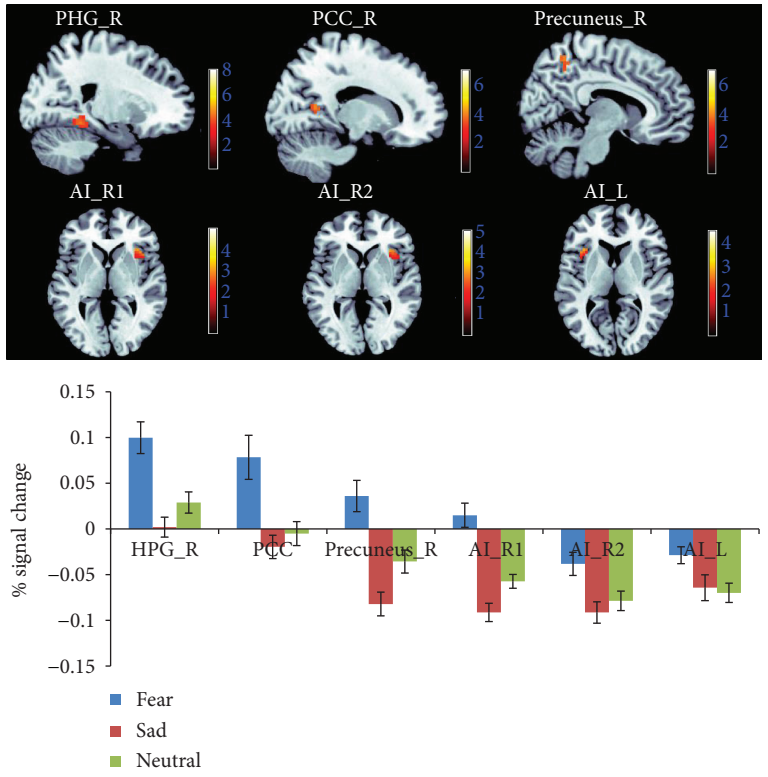

Figure 4: Neuroimaging results showing brain activation associated with fear induction (i.e., watching movies). The activation of the PHG_R, PCC_R, and precuneus_R result was taken from the conjunction analysis of "fear > neutral" and "fear > sadness" (depicted at threshold of $p < 0.001$), the activation of AI_R1 was taken from the contrast of "fear > sadness" (depicted at threshold of $p < 0.05$), and the activation of AI_R2 and AI_L was taken from the contrast of "fear > neutral" (depicted at $p < 0.05$). The graphs show the mean percent signal changes for the PHG_R, PCC_R, precuneus_R, AI_R1, AI_R2, and AI_L across the three experimental conditions.

3. Results

3.1. Behavioral Results. The change in subjective anger (the difference between subjective anger after the TAP session and at baseline) was significantly lower under the sadness condition than under the fear $[t(23) = -2.964, p < 0.05, d = 0.526]$ and neutral mood $[t(23) = -2.553, p < 0.05, d = 0.470]$ conditions, and no significant differences were observed between the fear and neutral mood conditions (Figure 3(a)). In addition, aggressive behavior, as determined with the average noise intensity set by the participant to punish his/her opponent over 24 rounds of the competition, under the fear condition was significantly higher than under the sadness $[t(23) = 2.382, p < 0.05, d = 0.445]$

Table 2: Brain regions associated with the effects of fear induction.

Brain regions	Hemisphere	Brodmann's area	MNI coordinates			$t(24)$	k
			x	y	z		
(fear > neutral) ∩ (fear > sadness) (conjunction)							
Parahippocampal gyrus	Right	19	24	−46	−5	4.46	48
Culmen	Left		−18	−46	−8	4.42	58
Posterior cingulate	Right	30	18	−55	13	4.02	19
Precuneus	Right	7	9	−49	55	3.96	27
Precuneus	Right	7	9	−52	46	3.37	
Cingulate gyrus	Left	31	−15	−37	43	3.82	7
Uvula	Left		0	−70	−29	3.77	6
Claustrum	Right		30	29	1	3.69	9
fear > sadness							
Parahippocampal gyrus	Right	36	30	−46	−11	7.35	214
Parahippocampal gyrus	Left	36	−30	−40	−11	7.14	290
Fusiform gyrus	Left	37	−30	−52	−11	6.95	
Declive	Left		−30	−67	−14	3.33	
Cingulate gyrus	Left	31	−15	−37	43	6.8	1270
Middle occipital gyrus	Right	19	42	−79	19	5.8	
Precuneus	Right	7	9	−52	55	5.78	
Middle temporal gyrus	Left	19	−36	−82	28	5.06	89
Middle occipital gyrus	Left	19	−48	−79	13	4.48	
Middle occipital gyrus	Left	19	−36	−85	19	4.4	
Superior frontal gyrus	Right	8	30	41	43	4.51	9
Middle frontal gyrus	Right	8	42	35	37	3.61	
Middle frontal gyrus	Right	6	30	8	64	4.4	11
Pyramis	Right		6	−76	−26	4.31	88
Pyramis	Left		−6	−73	−26	4.16	
Posterior cingulate	Right	30	18	−55	13	4.16	26
Posterior cingulate	Right	30	24	−58	22	3.6	
Inferior parietal lobule	Right	40	57	−40	40	4.04	40
Insula	Right	13	33	29	4	3.8	19
Middle frontal gyrus	Right	9	39	47	25	3.7	11
Inferior frontal gyrus	Left	46	−45	44	7	3.64	5
fear > neutral							
Parahippocampal gyrus	Right	30	21	−43	−5	4.68	95
Insula	Right	13	36	14	−14	4.52	104
Inferior frontal gyrus	Right	45	48	23	−2	4.29	
Insula	Right	13	33	29	−2	3.82	
Culmen	Left		−18	−46	−8	4.42	90
Culmen	Right		3	−40	−2	3.84	
Culmen	Left		−18	−37	−17	3.54	
Uvula	Right		0	−67	−29	4.11	17
Thalamus (medial dorsal nucleus)	Right		6	−10	13	4.1	36
Posterior cingulate	Right	30	18	−55	13	4.02	28
Posterior cingulate	Right	31	24	−61	22	3.38	
Precuneus	Right	7	9	−49	55	3.96	27
Precuneus	Right	7	9	−52	46	3.37	
Thalamus	Left		0	−31	7	3.92	30

Table 2: Continued.

Brain regions	Hemisphere	Brodmann's area	MNI coordinates			$t(24)$	k
			x	y	z		
Cingulate gyrus	Left	31	−15	−37	43	3.82	7
Precuneus	Left	7	−9	−52	58	3.54	9
Insula	Left	13	−39	23	1	3.54	11
Supramarginal gyrus	Right	40	63	−49	31	3.53	9

Note: threshold was set at $p < 0.001$ (uncorrected). Cluster size is represented by k. MNI = Montreal Neurological Institute.

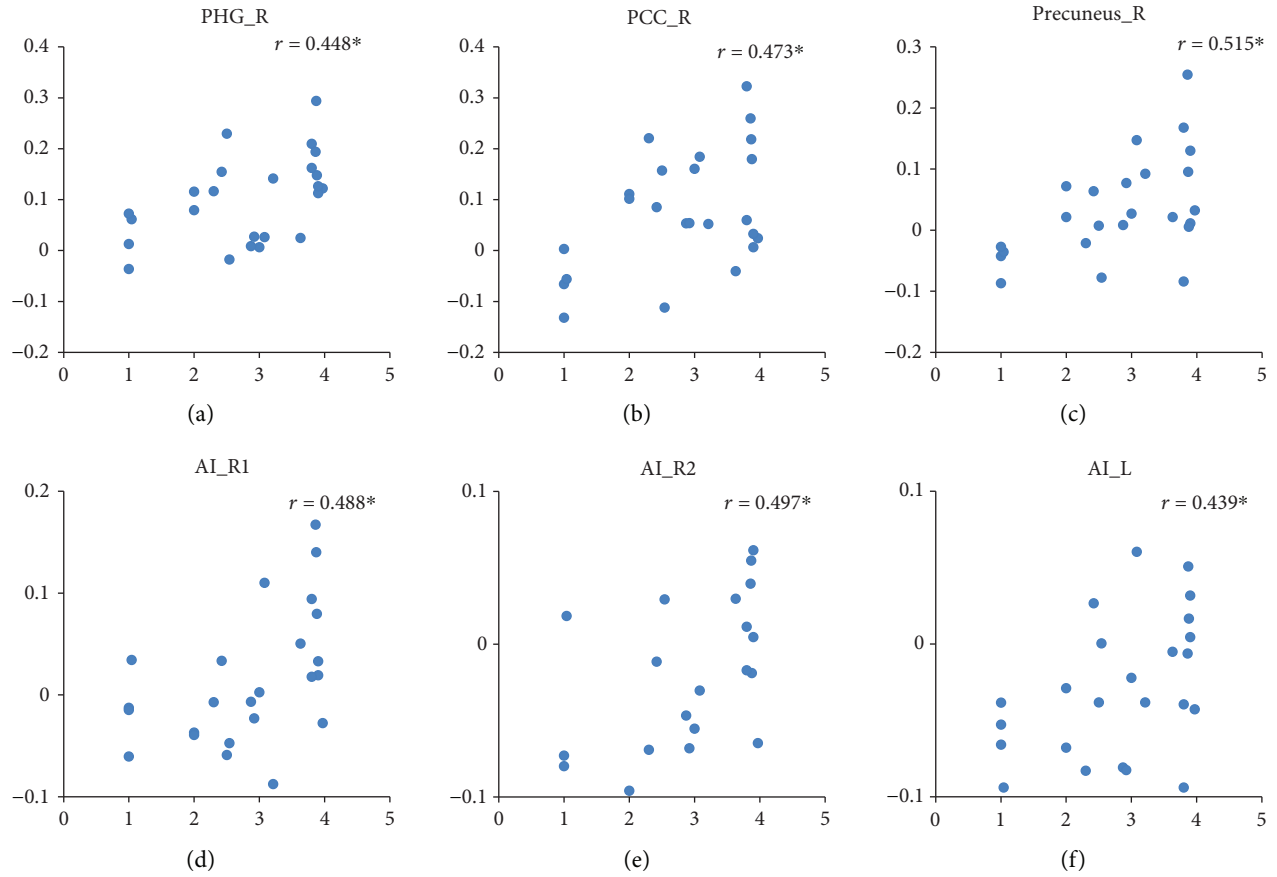

Figure 5: Relationships between brain activation associated with fear induction and aggressive behavior under the fear condition. r represents the correlation coefficient. * indicates a significant difference at $p < 0.05$.

and neutral mood [$t(23) = 2.384$, $p < 0.05$, $d = 0.445$] conditions, and no significant differences were observed between the sadness and neutral mood conditions (Figure 3(b)).

3.2. Imaging Results. The effect of fear induction was examined using the contrasts of "fear induction > sadness induction" and "fear induction > neutral mood induction" (both sampled during the emotional movie-clip-viewing) and with the conjunction analyses of these two contrasts. Increased neural activity selectively associated with fear was identified in the right parahippocampal gyrus (PHG_R, BA19), right posterior cingulate cortex (PCC_R, BA30), and right precuneus (precuneus_R, BA7) by the conjunction analyses of "fear induction > sadness induction" and "fear induction > neutral mood induction." Right anterior insula (AI_R, BA13) and left anterior insula (AI_L, BA13) activation was detected in both contrasts of "fear induction > sadness induction" and "fear induction > neutral mood induction" but was located in different AI regions in these two contrasts. Thus, the conjunction analysis did not identify AI activation (Figure 4 and Table 2). In addition, under the fear condition, the BOLD responses in the ROIs of the PHG, PCC, precuneus, and AI positively predicted the subsequent aggressive behavior levels (i.e., noise intensity determined by the participants to punish their opponents) [$r_{\text{PHG\_R}} = 0.488$, $p < 0.05$; $r_{\text{PCC\_R}} = 0.473$, $p < 0.05$; $r_{\text{precuneus\_R}} = 0.515$, $p < 0.05$; $r_{\text{AI\_R(fear>sadness)}} = 0.488$, $p < 0.05$; $r_{\text{AI\_R(fear>neutral)}} = 0.497$, $p < 0.05$; and $r_{\text{AI\_L(fear>neutral)}} = 0.439$, $p < 0.05$] (Figure 5).

The effects of the sadness induction were examined by the contrasts of "sadness induction > fear induction" and

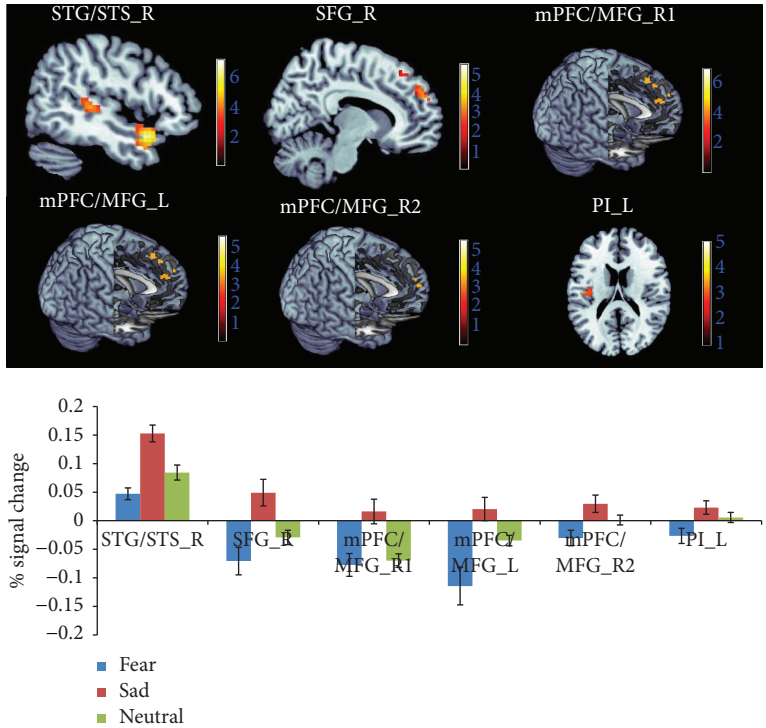

Figure 6: Neuroimaging results showing brain activation associated with sadness induction (i.e., watching movies). The activation of the STG/STS_R and SFG_R was taken from the conjunction analysis of "sadness > neutral" and "sadness > fear" (depicted at $p < 0.001$), the activation of the mPFC/MFG_R1 and mPFC/MFG_L was taken from the contrast of "sadness > fear", the activation of the mPFC/MFG_R2 was taken from the contrast of "sadness > neutral" (depicted at $p < 0.05$), and the activation of PI was taken from the contrast of "sadness > fear" (depicted at $p < 0.005$). The graphs show the mean percent signal changes separately for the STG/STS_R, SFG_R, mPFC/MFG_L, mPFC/MFG_R2, and PI_L across the three experimental conditions.

"sadness induction > neutral mood induction" (both sampled during the emotional movie-clip-viewing) and by the conjunction analyses of these two contrasts. Increased neural activity selectively associated with sadness induction was identified in the right superior temporal gyrus/sulcus (STG/STS_R, BA 22/38/41) and right superior frontal gyrus (SFG_R, BA9) by the conjunction analysis. Left and right medial prefrontal cortex/medial frontal gyrus (mPFC/MFG_L, mPFC/MFG_R) activation was detected in both contrasts of "sadness induction > fear induction" and "sadness induction > neutral mood induction," but the exact location in the mPFC/MFG differed between these two contrasts (Figure 6 and Table 3), and left posterior insula (PI_L) activation was only detected in the contrast of "sadness induction > fear induction." Under the sadness condition, the BOLD responses in the ROIs of the STG/STS, SFG, mPFC/MFG, and PI were negatively correlated with the subjective anger feeling [$r_{\text{STG/STS\_R}} = -0.661$, $p < 0.001$; $r_{\text{SFG\_R}} = -0.519$, $p < 0.01$; $r_{\text{mPFC/MFG\_R (sadness>fear)}} = -0.471$, $p < 0.05$; $r_{\text{mPFC/MFG\_L (sadness>fear)}} = -0.560$, $p < 0.01$; $r_{\text{mPFC/MFG\_R (sadness>neutral)}} = -0.517$, $p < 0.01$; and $r_{\text{PI\_L(sadness>fear)}} = -0.564$, $p < 0.01$] (Figure 7).

4. Discussion

In the current study, the participants showed more aggressive behavior after they were induced with fear and a lower level of anger after they were induced with sadness, thus supporting the hypotheses of the MPMC theory of emotionality that "sadness counteracts anger" and "fear promotes anger" from a "proactive interference perspective" that is different from the "retroactive interference perspective" in our previous studies [3, 4]. In our previous study, participants were first provoked, and we found that afterward-induced sadness could reduce the subsequent aggressiveness level, whereas afterward-induced fear promoted angry feelings [3, 4]. Therefore, the MPMC theory principle of "sadness counteracts anger" may refer to the following two different situations: the subsequently induced sadness could help to control anger-related aggressive behavior (the retroactive regulatory effects) and the antecedently induced sadness could help to reduce angry feelings (the proactive regulatory effects). Similarly, the principle of "fear promotes anger" also involves the following two situations: feelings of anger could increase if fear is subsequently experienced, indicating that fear promotes existing anger (the retroactive regulatory effects), and an individual may express more aggressive behavior during an aggravating situation if he/she is antecedently evoked by fear, indicating that existing fear could foster aggressive behavior (the proactive regulatory effects). Interestingly, the principles of "sadness counteracts anger" and "fear promotes anger" have different effects on subjectively reported anger and aggressive behavior in their retroactive or proactive regulation form. In the retroactive regulation form, "sadness

Table 3: Brain regions associated with the effects of the sadness induction.

Brain regions	Hemisphere	Brodmann's area	MNI coordinates			$t(24)$	k
			x	y	z		
(sadness > neutral) ∩ (sadness > fear) (conjunction)							
Superior temporal gyrus/superior temporal sulcus	Right	38	51	11	−20	7.11	127
Superior temporal gyrus/superior temporal sulcus	Right	41	51	−31	4	4.41	57
Superior temporal gyrus/superior temporal sulcus	Right	22	60	−37	10	3.41	
Superior temporal gyrus/superior temporal sulcus	Left	38	−48	11	−17	4.12	36
Superior temporal gyrus/superior temporal sulcus	Left	38	−48	8	−26	4.02	
Superior frontal gyrus	Right	9	12	53	28	3.53	17
sadness > fear							
Superior temporal gyrus/superior temporal sulcus	Right	38	54	11	−17	7.74	449
Superior temporal gyrus/superior temporal sulcus	Right	22	66	−10	−2	6.27	
Superior temporal gyrus/superior temporal sulcus	Right	41	54	−31	7	6.26	
Superior temporal gyrus/superior temporal sulcus	Left	22	−60	−4	1	5.3	287
Superior temporal gyrus/superior temporal sulcus	Left	38	−48	11	−17	5.02	
Middle temporal gyrus	Left	22	−51	−37	1	4.92	
Superior frontal gyrus	Right	9	15	53	25	4.66	279
Superior frontal gyrus	Right	6	15	23	52	3.72	
Medial prefrontal cortex/medial frontal gyrus	Right	32	21	20	43	3.66	
Parahippocampal gyrus	Left	27	−27	−28	−5	4.27	30
Superior frontal gyrus	Left	9	−15	50	25	4.14	143
Medial prefrontal cortex/medial frontal gyrus	Left	8	−15	38	37	3.59	
Medial prefrontal cortex/medial frontal gyrus	Left	9	−24	50	7	3.56	
Postcentral gyrus	Left	3	−51	−16	55	4.05	11
Insula	Left	13	−48	−16	22	3.77	46
Insula	Left	13	−39	−16	25	3.72	
sadness > neutral							
Superior temporal gyrus/superior temporal sulcus	Right	38	51	11	−20	7.11	209
Parahippocampal gyrus (amygdala)	Left		−18	−7	−14	4.84	29
Insula	Right	13	39	14	−14	4.7	
Superior temporal gyrus/superior temporal sulcus	Right	41	51	−31	4	4.41	58
Superior temporal gyrus/superior temporal sulcus	Right	22	63	−37	10	3.42	
Superior temporal gyrus/Superior temporal sulcus	Left	38	−48	11	−17	4.12	36
Superior temporal gyrus/superior temporal sulcus	Left	38	−48	8	−26	4.02	
Inferior frontal gyrus	Right	47	48	32	−8	3.73	15
Inferior frontal gyrus	Right	45	51	23	−2	3.42	
Medial prefrontal cortex/medial frontal gyrus	Right	6	9	53	31	3.63	28
Medial prefrontal cortex/medial frontal gyrus	Right	9	6	59	16	3.48	

Note: threshold was set at $p < 0.001$ (uncorrected). Cluster size is represented by k. MNI = Montreal Neurological Institute.

counteracts anger" significantly reduces aggressive behavior, whereas in the proactive regulation form, "sadness counteracts anger" significantly reduces anger. Similarly, in the retroactive regulation form, "fear promotes anger" significantly promotes anger, whereas in the proactive regulation form, "fear promotes anger" significantly promotes aggressive behavior. Thus, aggressive behavior, despite its close relationship with anger [12, 18], may be selectively regulated in different ways depending on the context. Further studies should investigate the difference between anger and aggressive behavior in terms of their regulatory approaches and context.

The main goal of this study was to explore the cognitive brain mechanism underlying the principles of "fear promotes anger" and "sadness counteracts anger." Compared with the sadness and neutral mood induction, the fear mood induction was associated with more activation in the AI, PHG, PCC, and precuneus, and activation in these regions could positively predict the individuals' anger feelings in a subsequent provocation situation. However, compared with the fear and neutral mood inductions, the sadness mood induction was associated with more activation in the PI, STG/STS, and SFG, and the activation in these regions

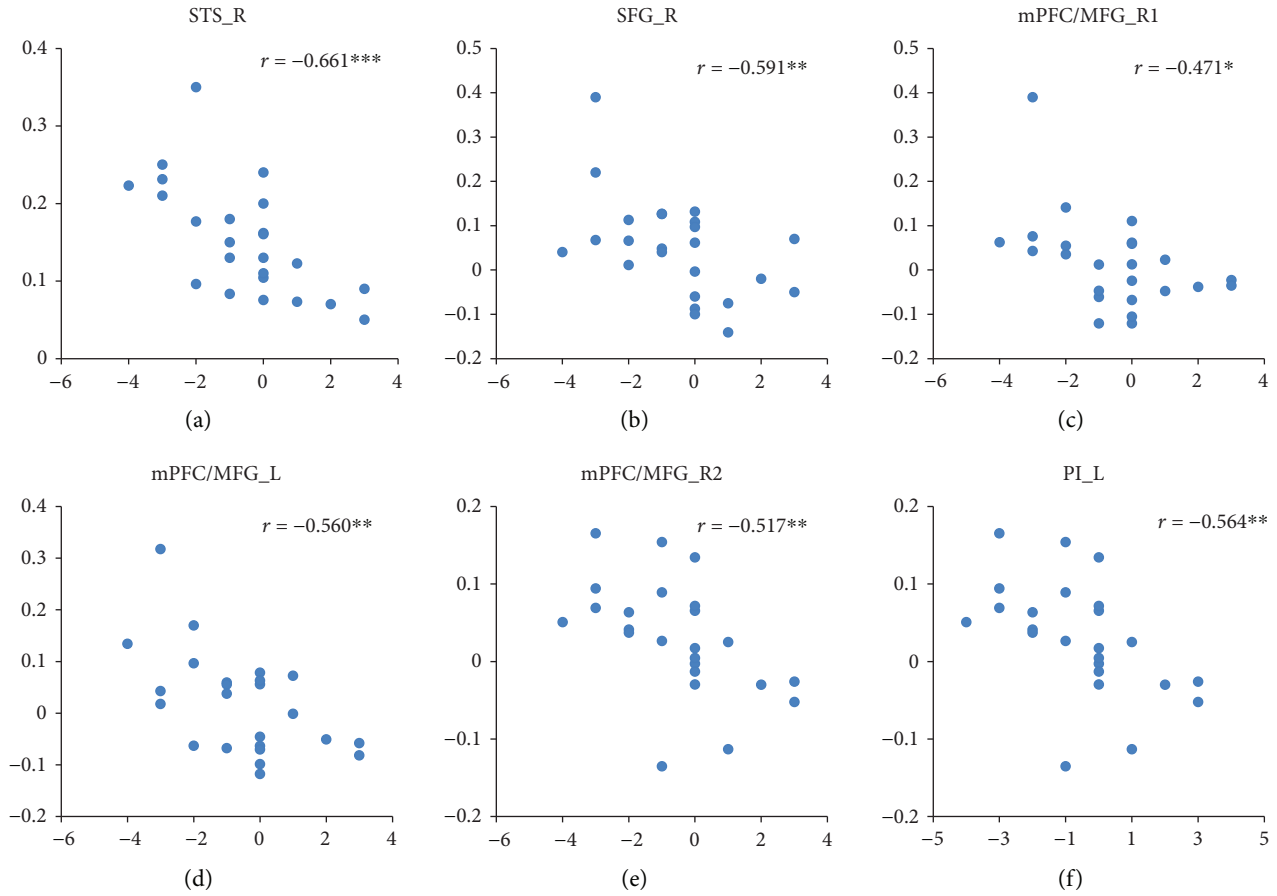

Figure 7: Relationships between brain activation associated with sadness induction and subjective anger feelings under the sadness condition. r represents the correlation coefficient. *** indicates a significant difference at $p < 0.001$, ** indicates a significant difference at $p < 0.01$, * indicates a significant difference at $p < 0.05$.

could negatively predict the individuals' aggressive behavior in subsequent provocation situations.

First, the AI, PHG, PCC, and precuneus activation was associated with the processing of the fear-inducing movie clip, which is consistent with previous neuroscience studies showing that fearful or threatening stimuli elicit activity in the AI, hippocampus, PCC, and precuneus, and this activation is mainly characterized by wakefulness and goal-driven responses [5, 19]. Second, areas in the PI, frontal lobe (e.g., superior frontal gyrus and medial frontal gyrus) and superior temporal gyrus were selectively activated during the processing of the sadness-inducing movie clip, which is also consistent with previous studies investigating the neural correlates of sadness [20–23]. These findings, together with the significant correlation between the brain activation and subsequent anger or aggressive behavior, may imply the possible neural mechanism of "fear promotes anger" and "sadness counteracts anger."

Most importantly, our results demonstrate a clear functional dissociation between the AI and PI in which the AI is more involved in fear induction, and this AI activation positively predicted later anger, whereas the PI was more involved in sadness induction, and this PI activation negatively predicted later aggressive behavior. This result not only proved that sadness and fear could be different in their representation location in the posterior-to-anterior progression of insular structure but also implied that the mechanism mediating the different inducing effects of sadness and fear on anger and aggressive behavior could be related to this difference. The AI is generally considered a part of the neural loop that notices, evaluates, and adapts to threat signals [7, 24]; the AI also reflects negative emotions, such as anxiety, aversion and alertness, arising from individual conflicts in the face of unfair events [25]. The AI activation in fear, together with the activation in the PHG, PCC, and precuneus, which could be related to conscious information processing such as attentive focusing and awakening [26–29], implied that the reason fear enhanced aggressive behavior could be attributed to an externally oriented threat-driven arousal state. Different from fear, sadness tended to be selectively represented in the PI and was associated with the representation of feeling oriented toward one's internal feeling and experience. The PI has been shown to connect reciprocally with the secondary somatosensory cortex and is highly specialized to convey homeostatic information such as pain, temperature, itch, and sensual touch [6, 30, 31], and a number of studies indicate that a subsection of the PI both anatomically and functionally serves a primary and fundamental role in pain processing [30, 32–34]. In addition, the induction of sadness was also accompanied by the empathy-

or sympathy-related neural processing process embodied by the activation of STG/STS and mPFC [35, 36]. Previous studies suggested that STS was engaged in tasks that required one to infer and share in another individual's mental [37, 38] and emotional state [39, 40]. For example, Zelinková and colleagues found that videos depicting dangerous behavior in a traffic campaign ending with tragic consequences activated the STS and that this activation was directly related to the participants' empathy and sympathy [41]. Thus, the possible neurological basis of "sadness counteracts anger" is that sadness induced internally oriented feeling represented in the PI, while eliciting empathy and sympathy processes mediated by STS/STG and mPFC, and finally producing less of a tendency to feel anger when provoked by others.

The current findings and conclusions must be considered in light of our study's limitations. First, as discussed above, the self-reported anger and aggressive behavior were inconsistent because the sadness induction successfully decreased the self-reported anger but not aggressive behavior; thus, whether the target of "fear promotes anger" or "sadness counteracts anger" occurs at the cognition or behavior level or both requires further confirmation in future studies. Second, we only examined 24 healthy, young Chinese college students. Thus, our findings cannot be generalized to larger populations, a nationality-unspecific context, or any clinical population. Finally, the mood (fear, sadness, or anger) inductions in this study were almost controlled in a moderate intensity. Regulating different intensities of emotional stimuli, however, may involve different neural mechanisms [42]; thus, studies should investigate the influence of the inducing mood intensity on the neural responses of "fear promotes anger" and "sadness counteracts anger."

5. Conclusions

In summary, our findings suggest a clear functional dissociation between the anterior and posterior parts of insula in which the AI is more involved in the processing of "fear promotes anger" than the PI and the PI is more involved in the processing of "sadness counteracts anger" than the AI. Specifically, fear-induced AI activity is associated with negative feelings (e.g., disgust and cognitive conflict) and neural responses are related to arousal (PHG, PCC, and precuneus), further promoting more aggression to external irritation. In contrast, sadness elicited the activation of the PI, which is involved in the processing of primary feeling and neural regions that may be related to empathy/sympathy (STG/STS, SFG, and mPFC), further producing less of a tendency to feel anger when provoked by others. These findings provide compelling neurological evidence supporting the "fear promotes anger" and "sadness counteracts anger" hypotheses of the MPMC theory of emotionality, which is based on traditional Chinese medicine.

Data Availability

The datasets generated during and/or analyzed during the current study are available from the corresponding author Jing Luo (luoj@psych.ac.cn) on reasonable request.

Conflicts of Interest

The authors declare that this study was conducted in the absence of any commercial or financial relationships that could be construed as potential conflicts of interest.

Acknowledgments

This work was supported by the Fundamental Research Funds from CNU's special construction project on supporting capacity for scientific and technological innovation (025-185305000), the National Natural Science Foundation of China (31671124 and 31471000), and the Beijing Municipal Commission of Education (TJSH20161002801).

References

[1] C. M. Raio, T. A. Orederu, L. Palazzolo, A. A. Shurick, and E. A. Phelps, "Cognitive emotion regulation fails the stress test," *Proceedings of the National Academy of Sciences of the United States of America*, vol. 110, no. 37, pp. 15139–15144, 2013.

[2] C. M. Raio and E. A. Phelps, "The influence of acute stress on the regulation of conditioned fear," *Neurobiology of Stress*, vol. 1, pp. 134–146, 2015.

[3] J. Zhan, X. Wu, J. Fan et al., "Regulating anger under stress via cognitive reappraisal and sadness," *Frontiers in Psychology*, vol. 8, p. 1372, 2017.

[4] J. Zhan, J. Ren, J. Fan, and J. Luo, "Distinctive effects of fear and sadness induction on anger and aggressive behavior," *Frontiers in Psychology*, vol. 6, p. 725, 2015.

[5] T. D. Wager, J. Kang, T. D. Johnson, T. E. Nichols, A. B. Satpute, and L. F. Barrett, "A Bayesian model of category-specific emotional brain responses," *PLoS Computational Biology*, vol. 11, no. 4, article e1004066, 2015.

[6] A. D. Craig, "How do you feel? Interoception: the sense of the physiological condition of the body," *Nature Reviews Neuroscience*, vol. 3, no. 8, pp. 655–666, 2002.

[7] A. D. Craig, "How do you feel — now? The anterior insula and human awareness," *Nature Reviews Neuroscience*, vol. 10, no. 1, pp. 59–70, 2009.

[8] B. J. Bushman, R. F. Baumeister, and C. M. Phillips, "Do people aggress to improve their mood? Catharsis beliefs, affect regulation opportunity, and aggressive responding," *Journal of Personality and Social Psychology*, vol. 81, no. 1, pp. 17–32, 2001.

[9] M. Zuckerman and B. Lubin, *Manual for the MAACL-R: The Multiple Affect Adjetive Check List Revised*, Educational and Industrial Testing Service, 1985.

[10] Y. Zhang, "The measurement of experimentally induced affects," *Acta Psychologica Sinica*, vol. 23, no. 1, pp. 101–108, 1991.

[11] P. Xu, Y. Huang, and Y. Luo, "Establishment and assessment of native Chinese affective video system," *Chinese Mental Health Journal*, vol. 24, no. 7, pp. 551–554, 2010.

[12] B. J. Bushman, R. F. Baumeister, and A. D. Stack, "Catharsis, aggression, and persuasive influence: self-fulfilling or self-defeating prophecies?," *Journal of Personality and Social Psychology*, vol. 76, no. 3, pp. 367–376, 1999.

[13] F. Dambacher, A. T. Sack, J. Lobbestael, A. Arntz, S. Brugman, and T. Schuhmann, "Out of control: evidence for anterior

insula involvement in motor impulsivity and reactive aggression," *Social Cognitive and Affective Neuroscience*, vol. 10, no. 4, pp. 508–516, 2015.

[14] P. R. Giancola and D. J. Parrott, "Further evidence for the validity of the Taylor aggression paradigm," *Aggressive Behavior*, vol. 34, no. 2, pp. 214–229, 2008.

[15] S. P. Taylor, "Aggressive behavior and physiological arousal as a function of provocation and the tendency to inhibit aggression," *Journal of Personality*, vol. 35, no. 2, pp. 297–310, 1967.

[16] U. M. Krämer, H. Jansma, C. Tempelmann, and T. F. Münte, "Tit-for-tat: the neural basis of reactive aggression," *NeuroImage*, vol. 38, no. 1, pp. 203–211, 2007.

[17] C. Fernández, J. C. Pascual, J. Soler, M. Elices, M. J. Portella, and E. Fernández-Abascal, "Physiological responses induced by emotion-eliciting films," *Applied Psychophysiology and Biofeedback*, vol. 37, no. 2, pp. 73–79, 2012.

[18] D. J. Parrott and P. R. Giancola, "Addressing "the criterion problem" in the assessment of aggressive behavior: development of a new taxonomic system," *Aggression and Violent Behavior*, vol. 12, no. 3, pp. 280–299, 2007.

[19] N. Kirlic, R. Aupperle, J. Rhudy, and R. Alvarez, "122. pain-related negative affect relates to anxious reactivity and anterior insula activity during unpredictable threat of shock," *Biological Psychiatry*, vol. 81, no. 10, article S51, 2017.

[20] M. E. Sachs, A. Damasio, and A. Habibi, "The pleasures of sad music: a systematic review," *Frontiers in Human Neuroscience*, vol. 9, p. 404, 2015.

[21] E. Brattico, B. Bogert, V. Alluri, M. Tervaniemi, T. Eerola, and T. Jacobsen, "It's sad but I like it: the neural dissociation between musical emotions and liking in experts and laypersons," *Frontiers in Human Neuroscience*, vol. 9, p. 676, 2016.

[22] H. S. Mayberg, M. Liotti, S. K. Brannan et al., "Reciprocal limbic-cortical function and negative mood: converging PET findings in depression and normal sadness," *The American Journal of Psychiatry*, vol. 156, no. 5, pp. 675–682, 1999.

[23] K. Vytal and S. Hamann, "Neuroimaging support for discrete neural correlates of basic emotions: a voxel-based meta-analysis," *Journal of Cognitive Neuroscience*, vol. 22, no. 12, pp. 2864–2885, 2010.

[24] R. Kalisch and A. M. V. Gerlicher, "Making a mountain out of a molehill: on the role of the rostral dorsal anterior cingulate and dorsomedial prefrontal cortex in conscious threat appraisal, catastrophizing, and worrying," *Neuroscience & Biobehavioral Reviews*, vol. 42, pp. 1–8, 2014.

[25] C. Corradi-Dell'Acqua, C. Civai, R. I. Rumiati, and G. R. Fink, "Disentangling self- and fairness-related neural mechanisms involved in the ultimatum game: an fMRI study," *Social Cognitive and Affective Neuroscience*, vol. 8, no. 4, pp. 424–431, 2013.

[26] R. Leech and D. J. Sharp, "The role of the posterior cingulate cortex in cognition and disease," *Brain*, vol. 137, no. 1, pp. 12–32, 2014.

[27] P. Qin, Y. Liu, J. Shi et al., "Dissociation between anterior and posterior cortical regions during self-specificity and familiarity: a combined fMRI–meta-analytic study," *Human Brain Mapping*, vol. 33, no. 1, pp. 154–164, 2012.

[28] X. Xu, H. Yuan, and X. Lei, "Activation and connectivity within the default mode network contribute independently to future-oriented thought," *Scientific Reports*, vol. 6, no. 1, article 21001, 2016.

[29] B. A. Vogt and S. Laureys, "Posterior cingulate, precuneal and retrosplenial cortices: cytology and components of the neural network correlates of consciousness," *Progress in Brain Research*, vol. 150, pp. 205–217, 2005.

[30] A. R. Segerdahl, M. Mezue, T. W. Okell, J. T. Farrar, and I. Tracey, "The dorsal posterior insula subserves a fundamental role in human pain," *Nature Neuroscience*, vol. 18, no. 4, pp. 499-500, 2015.

[31] A. D. Craig, K. Chen, D. Bandy, and E. M. Reiman, "Thermosensory activation of insular cortex," *Nature Neuroscience*, vol. 3, no. 2, pp. 184–190, 2000.

[32] L. Mazzola, J. Isnard, R. Peyron, M. Guénot, and F. Mauguière, "Somatotopic organization of pain responses to direct electrical stimulation of the human insular cortex," *Pain*, vol. 146, no. 1, pp. 99–104, 2009.

[33] J. D. Greenspan, R. R. Lee, and F. A. Lenz, "Pain sensitivity alterations as a function of lesion location in the parasylvian cortex," *Pain*, vol. 81, no. 3, pp. 273–282, 1999.

[34] L. Garcia-Larrea and R. Peyron, "Pain matrices and neuropathic pain matrices: a review," *Pain*, vol. 154, pp. S29–S43, 2013.

[35] J. Decety and T. Chaminade, "Neural correlates of feeling sympathy," *Neuropsychologia*, vol. 41, no. 2, pp. 127–138, 2003.

[36] S. Nichols, "Mindreading and the cognitive architecture underlying altruistic motivation," *Mind & Language*, vol. 16, no. 4, pp. 425–455, 2001.

[37] H. L. Gallagher and C. D. Frith, "Functional imaging of 'theory of mind'," *Trends in Cognitive Sciences*, vol. 7, no. 2, pp. 77–83, 2003.

[38] U. M. Krämer, B. Mohammadi, N. Doñamayor, A. Samii, and T. F. Münte, "Emotional and cognitive aspects of empathy and their relation to social cognition—an fMRI-study," *Brain Research*, vol. 1311, pp. 110–120, 2010.

[39] C. Lamm, J. Decety, and T. Singer, "Meta-analytic evidence for common and distinct neural networks associated with directly experienced pain and empathy for pain," *NeuroImage*, vol. 54, no. 3, pp. 2492–2502, 2011.

[40] I. Dziobek, S. Preißler, Z. Grozdanovic, I. Heuser, H. R. Heekeren, and S. Roepke, "Neuronal correlates of altered empathy and social cognition in borderline personality disorder," *NeuroImage*, vol. 57, no. 2, pp. 539–548, 2011.

[41] J. Zelinková, D. J. Shaw, R. Mareček et al., "An evaluation of traffic-awareness campaign videos: empathy induction is associated with brain function within superior temporal sulcus," *Behavioral and Brain Functions*, vol. 10, no. 1, p. 27, 2014.

[42] J. A. Silvers, J. Weber, T. D. Wager, and K. N. Ochsner, "Bad and worse: neural systems underlying reappraisal of high- and low-intensity negative emotions," *Social Cognitive and Affective Neuroscience*, vol. 10, no. 2, pp. 172–179, 2015.

Hindawi
Neural Plasticity
Volume 2018, Article ID 1892570, 14 pages
https://doi.org/10.1155/2018/1892570

Review Article

Persistent Stress-Induced Neuroplastic Changes in the Locus Coeruleus/Norepinephrine System

Olga Borodovitsyna, Neal Joshi, and Daniel Chandler

Department of Cell Biology and Neuroscience, Rowan University School of Osteopathic Medicine, Stratford, NJ 08084, USA

Correspondence should be addressed to Daniel Chandler; chandlerd@rowan.edu

Received 26 January 2018; Revised 9 May 2018; Accepted 27 May 2018; Published 13 June 2018

Academic Editor: Jason H. Huang

Neural plasticity plays a critical role in mediating short- and long-term brain responses to environmental stimuli. A major effector of plasticity throughout many regions of the brain is stress. Activation of the locus coeruleus (LC) is a critical step in mediating the neuroendocrine and behavioral limbs of the stress response. During stressor exposure, activation of the hypothalamic-pituitary-adrenal axis promotes release of corticotropin-releasing factor in LC, where its signaling promotes a number of physiological and cellular changes. While the acute effects of stress on LC physiology have been described, its long-term effects are less clear. This review will describe how stress changes LC neuronal physiology, function, and morphology from a genetic, cellular, and neuronal circuitry/transmission perspective. Specifically, we describe morphological changes of LC neurons in response to stressful stimuli and signal transduction pathways underlying them. Also, we will review changes in excitatory glutamatergic synaptic transmission in LC neurons and possible stress-induced modifications of AMPA receptors. This review will also address stress-related behavioral adaptations and specific noradrenergic receptors responsible for them. Finally, we summarize the results of several human studies which suggest a link between stress, altered LC function, and pathogenesis of posttraumatic stress disorder.

1. Introduction

Stressful stimuli and events engage a number of brain circuits that ultimately activate the hypothalamic-pituitary-adrenal (HPA) axis. During periods of stress, the paraventricular nucleus of the hypothalamus (PVN) releases the stress peptide corticotropin-releasing factor (CRF), which stimulates both direct central and indirect peripheral effects, activating signal transduction pathways that enhance catabolism of energy stores and mobilize physiological and psychological resources of the organism to permit an appropriate behavioral response to the stressor. These pathways become dysregulated following chronic or traumatic stress, which leads to destabilization of homeostasis and impaired immune, cardiovascular, and gastrointestinal functions, and promoting central nervous system (CNS) changes associated with depressive and anxiety-like behaviors that contribute to the diagnosis of stress-associated disorders [1–10]. The ability to mobilize CNS function to respond to stressful stimuli and ensure survival is explained in part by changes in neuroplastic adaptations. Several CNS structures have been demonstrated to undergo neuroplastic changes following stress [2, 11–24] which may contribute to stress-associated anxiety and mood disorders [12, 14, 19, 25, 26]. Chronically altered noradrenergic transmission is a characteristic of many neuropsychiatric and neurodegenerative disorders [12, 27–34], and therefore, short- and long-term stress-induced adaptations in norepinephrine- (NE-) containing cell bodies may contribute to these conditions. For the purposes of this review, we consider short-term effects to refer to the immediate and primary action CRF signaling during stressor exposure and the stress response on electrophysiological properties such as membrane depolarization and action potential generation that result from the opening of channels already inserted in the membrane. Long-term effects on the other hand include persistent changes that continue long after the stress response and CRF signaling have ceased and resulted from intracellular signaling cascades that promote

receptor and channel trafficking, altered gene expression, and neurite outgrowth.

A major node in the stress response that promotes noradrenergic signaling in the CNS is the brain stem nucleus locus coeruleus (LC). The LC and other smaller noradrenergic brainstem nuclei, such as A1/C2 region in the solitary tract, are activated by CRF and reciprocally communicate with the HPA axis. Activation of A1/C2 promotes a positive feedback loop in stress circuitry by releasing NE in the PVN which stimulates CRF production and release by engaging α_1-adrenoreceptors (α_1AR) [35, 36]. The LC is the primary source of NE to the forebrain [37–45], where its actions affect sleep/wake cycles, sensory signal discrimination and detection, and cognition [2, 37, 46, 47]. It is innervated by a number of stress-responsive CRF-containing brain regions which when released, acts on CRF receptor 1 (CRFR1) receptor to produce acute changes in LC physiology and responsiveness to synaptically released transmitters [48–51]. Additionally, activation of CRFR1 stimulates Gs proteins and cAMP production [48, 52], which promotes numerous genetic and cellular effects [28, 50, 53–57]. These observations suggest that LC neurons may undergo many long-lasting stress-induced adaptations (Figure 1). These changes include receptor trafficking [58–60], altered expression of genes necessary for transmitter synthesis and release [28, 54–56, 61], protein kinases that activate transcription factors [57] and growth factors [18], electrophysiological properties [53, 62], and morphological changes [50, 53, 63], all of which would directly impact LC function at both immediate and chronic time point poststress.

While most investigations have focused on the transient effects of stress and CRF on LC function [48, 49, 51, 64–66], some have examined their lasting impact [28, 50, 52–54, 56, 57, 62]. This review will summarize how stress and CRF signaling persistently modify morphological and physiological features of the locus coeruleus/norepinephrine (LC/NE) system and its associated behaviors from a genetic, cellular, and neuronal circuitry/transmission perspective. While the stress-induced plastic changes that occur in LC and other brain regions during disease pathogenesis are not entirely clear, identifying how stress can chronically alter the function of this broadly projecting brainstem nucleus across multiple levels of regulation represents an important step forward in clarifying the mechanisms of conditions characterized by hyperactive noradrenergic transmission.

2. LC/NE Synaptic Plasticity Changes during Stress

2.1. Adaptive Functional and Anatomical Changes of LC after Stress. HPA axis activation is pivotal for mediating the central stress response. Through the release of peripheral and central neurohormones, it mobilizes various body tissues and brain areas to orchestrate an appropriate physiological and behavioral response. Importantly, during stressor exposure, CRF is released onto the LC by the PVN and other CRF-containing stress-responsive structures, such as the bed nucleus of the stria terminalis, Barrington's nucleus, and the central nucleus of the amygdala [67–73] which increase its tonic discharge [51, 62, 65, 66]. LC activity correlates highly with an animal's behavioral state: during quiet rest, LC discharges slowly in a highly regular fashion. During periods of focused attention, a phasic mode of operation dominates such that LC responds to salient stimuli with high-frequency bursts of action potentials that facilitate orientation and sustained attention towards behaviorally relevant stimuli [74]. During stress, CRF causes increased tonic discharge which compromises the ability of LC to respond to salient sensory stimuli with phasic bursts. This leads to impairments in sensory signal discrimination, several aspects of cognition, and a generally anxious state [2, 37, 74–77]. While this might seem generally maladaptive, a consequence of short-term stress-induced LC activation is to promote behaviors that increase the likelihood of survival in a threatening situation [2, 66]. By increasing LC discharge [51, 62, 65, 66] and therefore forebrain NE release [78–82], prefrontal cortical operations are inhibited [3, 78], promoting a behavioral phenotype characterized by broad scanning attention and vigilance [2, 66, 81, 83], which facilitates escape from a threatening situation.

The role of LC in stress has been the subject of study since 1970, when karyometric studies of sleep-resistant rabbits demonstrated an increase in nuclear size during stress [84]. Subsequently, an extensive body of literature has shown that LC is critical for mediating stress-induced behavioral and neuroendocrine responses. The electrophysiological effects of stress and CRF on LC have been well characterized in a number of *in vivo* and ex vivo studies [48, 49, 51, 53, 62, 65, 85]. *In vivo*, CRF increases tonic/spontaneous LC discharge [65, 86, 87] through a cyclic AMP (cAMP)/protein kinase A-dependent mechanism that depolarizes the membrane by decreasing potassium conductance [48]. Additionally, CRF has been demonstrated to decrease sensory-evoked phasic responses by LC [65, 86]. This effect could partially be explained by recent findings from our laboratory that show that a high concentration of bath-applied CRF [49] and preexposure to acute stress [62] both diminish excitatory glutamatergic synaptic transmission in LC. We found that these electrophysiological effects persist for at least a week poststress in adolescent rats. Moreover, electrophysiological changes which were absent immediately after stressor exposure develop over seven days, including increased intrinsic excitability and a hyperpolarized threshold for action potential generation [62]. These findings suggest that LC cells in adolescent rat brain undergo long-lasting changes following even short-term acute stressor exposure and lead to chronically increased forebrain NE concentration and behavioral changes.

2.2. CRF and Morphological Changes. CRF orchestrates a series of neuroplastic changes in LC neurons and LC-derived cell cultures [50, 52, 53, 58, 63]. Specifically, CRF triggers morphological changes in immortalized catecholaminergic neurons, such as the formation of long neurites with prominent growth cones [52]. Similarly, another study demonstrated the ability of CRF to promote neuronal outgrowth in organotypic slice cultures of rat LC [50]. In this study, it was found that 12 hours of CRF exposure increased

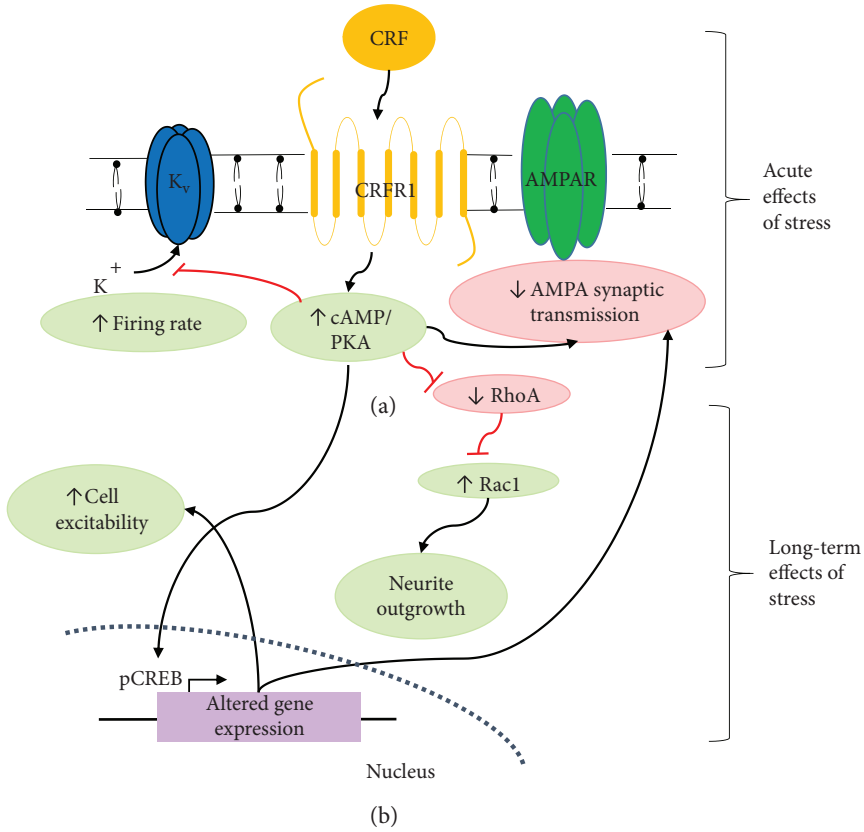

Figure 1: Model of signal transduction pathways induced by stress in LC neurons. (a) Pathways which mediate short-term effects of stressor exposure. CRF interacts with CRFR1, which through Gs-coupled receptor mechanisms increases intracellular cAMP levels, reducing potassium conductance resulting in cell depolarization. Through unknown mechanisms, CRF decreases glutamatergic synaptic transmission through AMPARs. (b) Pathways which mediate long-term effects of stressor. Initial CRF activation of Gs-coupled CRFR1 increases PKA activity, which phosphorylates CREB to initiate expression of stress-induced genes. These could potentially include genes regulating AMPAR and voltage-gated ion channel expression. Inactivation of RhoA by PKA phosphorylation disinhibits Rac1 to increase neurite outgrowth via actin remodeling and microtubule stabilization.

the number of primary processes and branching pattern of neurites. Mechanisms of dendritic growth regulation by CRF have been proposed to occur through Rac and RhoA GTPases (Figure 1), which regulate intracellular actin dynamics and spine length [88]. Elsewhere in the brain, inhibition of Rac1 has been shown to promote strong effects on dendritic spines from apical and basal dendrites on pyramidal neurons with relative absence of branching effects [89].

Additional unpublished observations from our laboratory also suggest that in animals subjected to acute intense stressor exposure, LC cells might undergo morphological changes. We have previously shown that fifteen minutes of combined physical restraint and exposure to predator odor induces a number of long-lasting changes in LC function that are accompanied by chronically increased anxiety-like behavior [62]. During whole-cell patch clamp electrophysiological recordings, some neurons were filled with biocytin so their morphology could be recovered. Preliminary findings show that LC cells from stressed animals have larger and more complex dendritic arbors than those from control rats. Additionally, using RNA-Seq, we identified that expression of Ntf3, the gene for neurotrophin 3, which promotes neuronal survival, differentiation, and neurite outgrowth [18, 90], was approximately twice as high in rats one week after stressor exposure than in their control counterparts (Figure 2). These observations, in combination with earlier reports of stress-induced morphological alterations in LC neurons [50, 52, 53, 75, 91–93], suggest that stress may cause long-lasting changes in noradrenergic transmission throughout the CNS in response to even acute stressor exposure. Such an effect on CNS noradrenergic transmission might be achieved through morphological plasticity because as LC dendrites and axons proliferate, there would be more sites of afferent input to excite LC neurons and a greater density of release points from which NE efflux could occur upon this enhanced excitation, respectively. Such findings could have important implications for posttraumatic stress disorder (PTSD), a condition in which evidence suggests that NE transmission is impaired [12, 31, 79, 94].

It is interesting to note that rodent LC neurons are sexually dimorphic with respect to their morphological characteristics and response to stress/CRF exposure. Female LC dendritic arbors have been reported to extend further into the peri-LC region where synaptic contacts with CRF-positive afferents are made [71, 95, 96] and are larger with more branching points than those of males [68, 97]. This

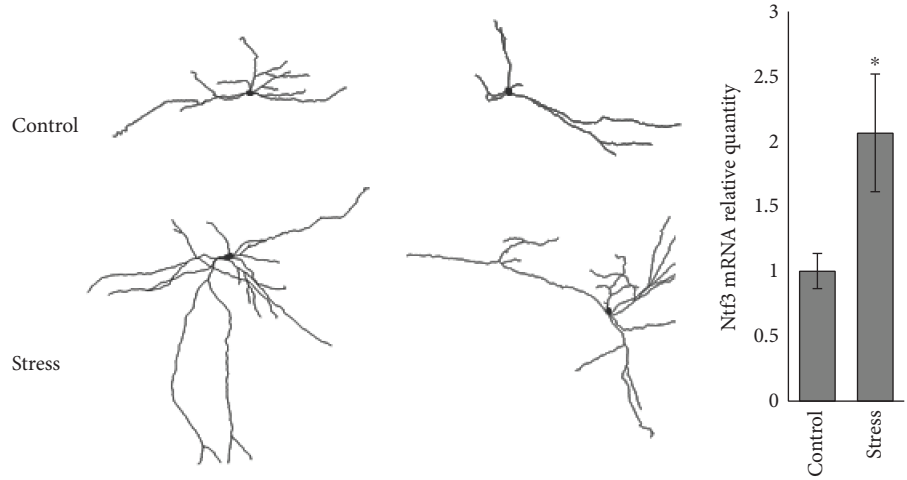

Figure 2: LC neurons from stressor-exposed animals show a trend for increased dendritic complexity. Representative traced neurons from control (top) and stressor exposed (bottom) animals filled with biocytin reveal a tendency for LC cells from stressed rats to possess larger and more complex dendritic arbors a week after stressor exposure. Additionally, neurotrophin 3, which promotes neurite outgrowth and dendritic proliferation, is upregulated in LC one week after stressor exposure. $^{*}p < 0.05$ versus control.

suggests that the female LC might be subjected to greater afferent regulation by CRF and therefore more stress-responsive. This sexual dimorphism might provide a structural basis for differences in emotional arousal between sexes and the greater increased susceptibility of females to anxiety disorders [98]. Interestingly, in mice that genetically overexpress CRF, the complexity of male dendritic morphology increases to resemble the morphology of wild-type and CRF-overexpressing females. This further suggests that enhanced CRF signaling produces neurite proliferation and extension in LC [58]. Such observations provide further evidence for stress and CRF-induced central noradrenergic reorganization.

2.3. CRF and Modified AMPA Receptor-Dependent Synaptic Transmission. Plasticity is highly dependent on the AMPA receptor (AMPAR), an ionotropic glutamate receptor, permeable to Na^{+} and Ca^{2+} ions. It is composed of four subunits: GluA1, GluA2, GluA3, and GluA4, which form a heterotetramer. [99–103]. We have previously shown that both stressor exposure *in vivo* [62] and CRF exposure ex vivo [49] alter LC AMPAR signaling. Given that stress and CRF can alter AMPAR-dependent transmission, this receptor might play a critical role in stress-induced neural plasticity. Several mechanisms could account for altered AMPAR functioning in LC following CRF exposure. CRF signaling in LC causes internalization of its own receptor [59, 60, 63], and thus, if CRF and AMPARs are in close apposition to one another on postsynaptic LC membranes, CRF receptor trafficking might inadvertently induce AMPAR internalization as well. This is particularly important with respect to some of the intracellular proteins that AMPARs interact with. AMPARs interact directly and indirectly with kinases and GTPases that regulate actin cytoskeletal dynamics [50, 53, 99–101, 104, 105]. In particular, Rho GTPase activity is modulated by guanine nucleotide exchange factors (GEFs), which are known to interact with *surface-expressed* AMPARs and promote synaptic plasticity [104]. Thus, if CRF causes shuttling of vesicular AMPARs to the cell membrane, which, based on our prior observations, might occur during high concentrations of CRF exposure [49], their association with GEFs could promote structural plasticity in LC neurons through interaction with Rho GTPases and modulation of cytoskeletal structure. Identifying the mechanisms that link CRF and AMPA receptor function and trafficking could be informative of how LC cells adapt morphologically following stress, thus providing insights to a number of disease states in which LC plasticity is perturbed [29, 50, 53, 106, 107]. In addition to receptor trafficking and altered gene expression, there are other posttranslational modifications that can be made to the AMPAR and its subunits which could promote plastic changes to LC neurons. Using data from both LC and non-LC studies of AMPAR function and modification, we will review possible mechanisms for AMPAR regulation.

There are multiple mechanisms of posttranslational regulation of AMPAR function, which include reversible phosphorylation, ubiquitination, and palmitoylation [108–110]. CRF stimulates cAMP synthesis and PKA activity [48, 50, 52], and therefore, stress could potentially alter AMPAR phosphorylation states. The GluA1 subunit is phosphorylated at different positions at the C-terminal end. For example, phosphorylation at Ser-845 by PKA [101] and Ser-831 by PKC and CaMKII [111, 112] increase single channel conductance. Phosphorylation of Ser-818 and Thr–840 by PKC increases the mean channel conductance [113]. Importantly, mechanisms that increase channel conductance have been shown to promote activity-dependent plasticity [99, 114]. PKCλ was found to phosphorylate Ser-818 on the GluA1 subunit which mediates PI3K-induced AMPAR insertion [115]. GluR2 can also regulate synaptic plasticity through Ser-880 phosphorylation-dependent interactions with PDZ domain-containing proteins, which regulate receptor internalization in the hippocampus [116] and cerebellum [117].

Thus, due to the actions of CRF on cAMP production and PKA activity, stress could potentially impact LC plasticity through modulation of AMPAR function which we have demonstrated in the past [49, 62].

Another modification of AMPARs is ubiquitination, which promotes endocytosis and degradation [108, 109, 118–120] and can occur at multiple places across the subunits. One effect of stress on AMPAR ubiquitination is to decrease glutamatergic synaptic transmission in the prefrontal cortex (PFC), which requires specific ubiquitin ligases Nedd4-1 and Fbx2, an effect which can be blocked by a proteasome inhibitor [121]. Identification of LC-specific ubiquitin ligases would help to find a precise target for stress response control and intervention. In contrast to ubiquitination, AMPAR C-terminal cysteine residue palmitoylation protects from degradation [122] and regulates its internalization [123]. Palmitoylation of the transmembrane domain promotes accumulation of AMPAR in the Golgi, possibly performing a quality control step for proper folding, while depalmitoylation stimulates membrane insertion of AMPAR [123–125]. Identifying any potential mechanisms linking CRF signaling to AMPAR ubiquitination in LC or elsewhere would be informative of means of promoting or inhibiting stress-induced plasticity within the nucleus.

2.4. CRF and Intracellular Signal Transduction. CRF mediates its action through CRFR1, which through Gs-coupled mechanisms increases the concentration of cAMP that phosphorylates PKA [52]. However, there is another mechanism caused by CRFR1 activation which acts through a MAPK cascade, in which a Gq-coupled mechanism increases concentration of phospholipase C (PLC), which activates metabolites which phosphorylate PKC, which in turn phosphorylates ERK1/2 [50, 126]. CRF has been shown to cause an increase in LC neurite length, an effect that is abolished by specific inhibition of PKA or MAPK, but not PKC [50]. PKC appears to also trigger a RhoA-activating cascade through downstream Rho-associated protein kinase (ROCK), which subsequently phosphorylates the collapsin response mediator protein 2 (CRMP-2) and causes growth cone collapse [127] (Figure 2).

Such receptor-mediated acute cellular changes could occur through the aforementioned mechanisms, but long-term changes could also potentially occur through regulation of gene expression. A study of single and repeated restraint stress demonstrated an increase in immunoreactivity of c-Fos, pERK, pCaMKII, and pCREB in the LC two hours following the stressor [128]. The same study also showed that pERK and pCREB had the same expression pattern and were colocalized to the same neurons, suggesting that activation of the MAPK/ERK pathways with CREB phosphorylation promote changes in gene expression. The exact mechanism of transcriptional changes following CRF expression in the LC is not clear. However, another study demonstrated increased c-Fos expression and CREB phosphorylation after acute immobilization stress, while repeated stress increased phosphorylation of p38, cJun N-teminal kinase (JNK 1/2/3), and ERK1/2 [129]. CREB is a transcriptional factor which regulates transcription of multiple downstream genes including c-Fos, brain-derived neurotrophic factor (BDNF), tyrosine hydroxylase (TH), and neuropeptides [130, 131]. These observations corroborate other studies that have shown altered expression of trophic factors and NE synthetic enzymes [18, 28, 54–57, 61].

BDNF stimulates dendritic outgrowth and increased synaptic connectivity. Mice genetically overexpressing the receptor for neurotrophin 3, TrkC, show increased anxiety-like behavior, as well as increased LC neuronal density [132], suggesting that some degree of positive feedback might exist between stress, neurotrophin 3 signaling, and LC plasticity. This is particularly interesting in light of preliminary observations by our laboratory that show that one week after acute stressor exposure, neurotrophin mRNA is increased, an effect accompanied by a trend for increased LC dendritic length and complexity (Figure 2). Others have also reported increased neurotrophin 3 expression in LC following stress, which can be normalized with antidepressant treatment [18]. Interestingly, in addition to sexual dimorphism of LC morphology and stress responsiveness, there are also sex differences in LC intracellular signaling induced by CRF: specifically, CRFR1 is more strongly coupled to β-arrestin in males, promoting receptor internalization and potentially blunted responsiveness to CRF in the future. In females, however, CRFR1 is more strongly coupled to Gs signaling pathways, which promotes increased LC discharge and dendritic proliferation, potentially increasing future sensitivity to stress by providing more space for synaptic contacts with CRF-positive afferents [63, 133]. In this way, the male and female LC may be differentially aligned to respond to stress with specific neuroplastic adaptations that promote disease.

3. CNS Neural Plasticity Changes in Response to NE Volume Transmission Changes

LC contributes to major CNS functions such as waking, arousal, attention, sensory discrimination, and cognition. Because stress promotes both short- and long-term functional and neuroplastic changes in LC, some of these functions might also be impacted by stressor exposure, either directly or indirectly. Through modulation of intrinsic and synaptic features of LC neurons, stress likely modifies noradrenergic volume transmission in target brain areas such as the amygdala, hippocampus, and PFC, where it potently modulates neural plasticity [134–138]. Because stress acutely and chronically alters LC discharge [53, 62, 66, 86] and NE release [78–82], different adrenergic receptors might become engaged during and after stressor exposure. The adrenergic receptors vary in their affinity for NE [3, 78, 139, 140], and different receptors promote different forms of plasticity and learning [134, 135, 137, 141]. Low concentrations of NE engage the high-affinity α_1 receptor, particularly in the prefrontal cortex, which promotes working memory, sustained attention, and other cognitive functions [3, 142, 143].

Conversely, high NE concentration which occurs in response to stress causes engagement of the α_1 and β adrenergic receptors. The α_1 receptor promotes LTD of prefrontal synapses [137] and inhibition of prefrontal-dependent cognitive functions such as working memory and sustained

attention [2, 83]. Indeed, enhanced α_1 signaling in PFC is associated with increased behavioral flexibility [144]. Furthermore, stressor exposure has been shown to increase tonic LC discharge and promote scanning attention and behavioral flexibility [65, 66]. It has been proposed that such a change would permit lower-order sensorimotor regions to guide behavior with little modulation by prefrontal circuitry, allowing disengagement from specific stimuli and goal-oriented behaviors to instead promote rapid impulsive responses [2]. Such a stress-induced shift might be beneficial when an animal is faced with a threatening stimulus and a quick escape must be made. Additionally, engagement of the β receptor promotes hippocampal plasticity and encoding and recall of contextual fear memory [141, 145, 146]. Therefore, persistent stress-induced changes in LC function would elevate NE concentration in prefrontal cortex and hippocampus enhancing plasticity in both areas through signaling at α_1 and β receptors to synergistically promote encoding and recall of fear memories, impaired cognition, hypervigilance, and behaviors that allow an appropriate behavioral response to be generated. Therefore, an inverted U relationship between LC firing and arousal/behavioral performance model has been proposed [2, 37, 139], with maximal cognitive function corresponding to "ideal" levels of LC tonic firing [147] and hyperarousal and vigilance corresponding with excessive levels of discharge. During stress, increased tonic LC firing is enhanced, which leads to increased levels of NE in LC projection fields, promoting broad scanning attention, hyperarousal, hypervigilance, and other anxiety-like behavioral symptoms in stressed subjects.

4. Role of Stress-Induced LC/NE Changes in PTSD

Chronic stress-induced alterations in LC structure and function that lead to behavioral impairments might contribute to disease pathogenesis and symptomatology. Many studies show the involvement or potential involvement of the LC in stress-related disease states, particularly PTSD. Both peripheral and central measures of NE activity are increased in PTSD patient populations, including enhanced sympathetic nervous system function [148–151], and increased functional connectivity between LC and the basolateral amygdala during conscious processing of threatening stimuli [152]. This enhanced connectivity is particularly important because of the role that the basolateral amygdala and its noradrenergic inputs in particular [153–157] play in fear conditioning. Furthermore, PTSD patients frequently show disturbances in sleep patterns [158–160], which may be related to chronically elevated LC discharge due to its well-established role in mediating arousal and a forebrain EEG associated with waking [161]. Such an effect could potentially be related to dysregulation of other stress-sensitive systems, such as the HPA axis which releases CRF. LC is potently activated by CRF, and increased levels of the peptide have been found in the cerebrospinal fluid of combat veterans afflicted with PTSD [162, 163], providing a potential means for maintaining LC hyperactivity even in the absence of a stressor. More recently, an fMRI study showed that PTSD patients showed exaggerated behavioral and autonomic responses to loud sounds, suggesting sensitized phasic responses of LC neurons [34]. Evidence for LC as a central mediator of PTSD-like symptoms comes from observations that yohimbine, an α_{2A} receptor antagonist which disinhibits LC neurons, produces panic attacks in up to 70% of PTSD patients and in 89% of patients with comorbid PTSD and panic disorder, but not in control subjects. Additionally, plasma levels of a NE metabolite postyohimbine administration were twice as high in PTSD patients [163]. These findings suggest that NE release is altered presynaptically at the level of the LC in PTSD patients, which may affect many downstream targets [164].

In contrast to the actions of yohimbine, clonidine, a presynaptic α_{2A} receptor agonist which limits noradrenergic transmission in the forebrain, has been shown to have beneficial effects on hyperarousal, hypervigilance, sleep disruption, exaggerated startle responses, and nightmares in veterans with PTSD [31]. The notion that increased NE release promotes some behaviors associated with PTSD and anxiety is further supported by observations that the β-receptor antagonist propranolol attenuates PTSD symptoms, possibly due to the actions that the β receptor plays in fear memory consolidation and emotion [31, 134, 135, 165–167]. Prazosin, an α_1-adrenergic antagonist, has also been shown to be beneficial for alleviating nightmares and sleep disturbances in both veteran [168] and children PTSD patients [169], as well as for improving symptoms of hyperarousal, avoidance/numbing, and traumatic recall of past events [170]. It is also interesting to note that an *in vivo* PET study that the availability of the NE transporter in the LC is decreased in PTSD patients [171]. This could be indicative of elevated extracellular NE concentration and would be consistent with other reports of LC hyperactivity in this population. Thus, due to the well-documented ability of stress to promote forebrain NE release through short-term physiological activation and enduring molecular and cellular changes in the LC, stress-induced neuroplastic adaptations in the LC likely contribute to disease pathogenesis. This could occur at the level of the LC as a primary site of stress-induced plasticity or in downstream targets of the LC due to the well-established role of NE in mediating neuroplastic changes throughout the brain: fMRI studies have also shown changes in hippocampal volume and altered function in the amygdala, hippocampus, mPFC, orbitofrontal cortex, anterior cingulate, and insular cortex in PTSD patients [172], all of which may be related to maladaptive plastic changes in the LC or the plastic changes promoted by it [134, 135, 137, 165].

Based on these clinical reports, there is clear evidence that LC hyperfunction is at least characteristic of, if not causal to, PTSD symptomatology. However, some clinical observations suggest a more complicated relationship that exists between LC function and PTSD disease progression and treatment. As mentioned above, there is clinical evidence for decreased NE transporter availability in the LC of PTSD patients. This could be explained by elevated extracellular NE concentration; another potential explanation could be LC neuronal loss. Indeed, a postmortem neuromorphometric analysis of veterans with probable or possible war-related PTSD showed

a lower LC cell count compared to controls [173], suggesting that the LC plays in the role in the pathophysiology of PTSD, or that a lower LC cell count may predispose individuals to PTSD. While decreased LC cell numbers would suggest reduced forebrain NE levels, in other pathologies in which LC cell counts are decreased such as Alzheimer's disease, the surviving neurons show evidence for hyperactivity [174] and dendritic sprouting and remodeling [107]. Additionally, recent clinical trials using 3,4-methylenedioxymethamphetamine (MDMA) have shown promising results in reduction or remission of PTSD symptoms: specifically, six phase II clinical trials have shown that combined MDMA and psychotherapy are safe and efficacious such that 52.7% of patients receiving active drug no longer meet PTSD criteria [175]. Despite a wealth of evidence showing that enhanced noradrenergic transmission contributes to PTSD etiology, MDMA increases release of catecholamines, including NE. One potential explanation for MDMA's somewhat paradoxical efficacy is that memory reconsolidation is enhanced via plastic changes in the hippocampus due to elevated NE levels [141, 145]. MDMA also facilitates fear extinction learning [176], and thus, enhanced NE efflux following MDMA administration might also promote plastic changes within the amygdala [12]. Additionally, because NE is generally increased in PTSD patients, the benefits of MDMA on symptom improvement are likely due to the drug complex polypharmacological interactions and its effects on brainwide neurotransmission. It is hypothesized that in addition to enhanced plasticity and memory reconsolidation, heightened monoaminergic neurotransmission following MDMA administration promotes a number of subjective psychological effects such as increased introspection and receptiveness for psychotherapy that lead to improved outcomes in PTSD patients [175]. Collectively, however, many clinical observations strongly suggest that hyperactive noradrenergic transmission contributes to PTSD symptomology and anxiety-like behavior.

5. Conclusions

Stressor exposure induces a series of neuroendocrine, physiological, and behavioral adaptations that promote an appropriate response to the stressor. Central to these diverse functions is CRF signaling which in a number of brain regions promotes a number of immediate [48, 49, 51, 177–184] and persistent [50, 52, 60, 121, 185–187] cellular changes. These effects are of particular interest in LC, where the interaction of CRF with its receptor CRFR1 activates cAMP-dependent intracellular signaling cascades, increasing tonic discharge and promoting anxiety-like behavior [64, 77, 188, 189]. Evidence suggests that chronic stressor exposure is able to alter LC gene expression [18, 28, 54–57, 61], promote long-term changes in synaptic transmission and excitability [53, 62] and receptor trafficking [58–60, 185], and, importantly, induce morphological changes and dendritic remodeling (Figure 1) [50, 52, 53, 57, 190]. These actions appear to be dependent on a number of kinases and GTPases and their associated signaling pathways [50, 52, 57] and potentially on AMPAR function [191, 192] which is modulated by CRF in the short term [49] and stressor exposure in the long term [62]. Through its complex signaling cascades, CRFR1 activation in LC induces a number of long-lasting cellular effects which ultimately impact the function of the nucleus itself as well as other target brain regions which are heavily innervated by LC and modulated by noradrenergic transmission. Critically, the LC promotes plasticity in other structures including the PFC, amygdala, and hippocampus by promoting noradrenergic transmission at α_1 and β receptors [137, 141, 145, 146]. Therefore, stress and CRF can induce neuroplastic changes in LC, which can lead to subsequent neuroplastic changes elsewhere, ultimately promoting causing chronic anxiety-like behavior. Specifically, increased tonic discharge in the short term will drive an animal to display such behavior [62, 64, 77]. Maintenance of increased LC discharge in the long term [62] along with enhanced expression of genes necessary for NE synthesis and release [54–56] will lead to chronically elevated forebrain NE levels. This promotes network adaptations and plasticity in target regions which facilitate fear memory encoding and drive an animal towards a behavioral state characterized by vigilance, impulsivity, and impaired cognition [3, 78, 83, 193]. Meanwhile, morphological plasticity and dendritic outgrowth into the peri-LC area [50, 52, 53, 68, 194] will make LC subject to greater afferent regulation by stress-responsive structures such as PVN and CeA [58, 63, 194]. Through these mechanisms, chronic or traumatic stress could permanently alter forebrain noradrenergic transmission to promote long-lasting changes in behavior, manifesting in humans as mood and anxiety disorders such as depression and posttraumatic stress disorder. Thus, identifying how stress and CRF promote synaptic and morphological plasticity in LC to chronically elevate forebrain NE concentration represents an important step in understanding disease pathogenesis and symptomatology for mood, anxiety, and other neuropsychiatric disorders.

Conflicts of Interest

The authors declare that there is no conflict of interest regarding the publication of this paper.

Acknowledgments

The authors wish to acknowledge Mr. Matthew Flamini for his assistance in reviewing and editing the manuscript.

References

[1] P. E. Greenberg, T. Sisitsky, R. C. Kessler et al., "The economic burden of anxiety disorders in the 1990s," *The Journal of Clinical Psychiatry*, vol. 60, no. 7, pp. 427–435, 1999.

[2] A. F. T. Arnsten, "Through the looking glass: differential noradenergic modulation of prefrontal cortical function," *Neural Plasticity*, vol. 7, no. 1-2, 146 pages, 2000.

[3] A. F. T. Arnsten, "Prefrontal cortical network connections: key site of vulnerability in stress and schizophrenia," *International Journal of Developmental Neuroscience*, vol. 29, no. 3, pp. 215–223, 2011.

[4] R. Crupi, A. Marino, and S. Cuzzocrea, "New therapeutic strategy for mood disorders," *Current Medicinal Chemistry*, vol. 18, no. 28, pp. 4284–4298, 2011.

[5] G. C. Curtis, J. L. Abelson, and P. W. Gold, "Adrenocorticotropic hormone and cortisol responses to corticotropin-releasing hormone: changes in panic disorder and effects of alprazolam treatment," *Biological Psychiatry*, vol. 41, no. 1, pp. 76–85, 1997.

[6] J. F. W. Deakin, "Depression and 5HT," *International Clinical Psychopharmacology*, vol. 6, pp. 23–32, 1991.

[7] J. Ho, S. P. C. Ngai, W. K. K. Wu, and W. K. Hou, "Association between daily life experience and psychological well-being in people living with nonpsychotic mental disorders: protocol for a systematic review and meta-analysis," *Medicine*, vol. 97, no. 4, article e9733, 2018.

[8] T. L. Tay, C. Béchade, I. D'Andrea et al., "Microglia gone rogue: impacts on psychiatric disorders across the lifespan," *Frontiers in Molecular Neuroscience*, vol. 10, p. 421, 2018.

[9] S. K. Wood, H. E. Walker, R. J. Valentino, and S. Bhatnagar, "Individual differences in reactivity to social stress predict susceptibility and resilience to a depressive phenotype: role of corticotropin-releasing factor," *Endocrinology*, vol. 151, no. 4, pp. 1795–1805, 2010.

[10] C. S. Wood, R. J. Valentino, and S. K. Wood, "Individual differences in the locus coeruleus-norepinephrine system: relevance to stress-induced cardiovascular vulnerability," *Physiology & Behavior*, vol. 172, pp. 40–48, 2017.

[11] O. Berton, C. McClung, R. J. Dileone et al., "Essential role of BDNF in the mesolimbic dopamine pathway in social defeat stress," *Science*, vol. 311, no. 5762, pp. 864–868, 2006.

[12] J. D. Bremner, B. Elzinga, C. Schmahl, and E. Vermetten, "Structural and functional plasticity of the human brain in posttraumatic stress disorder," *Progress in Brain Research*, vol. 167, pp. 171–186, 2008.

[13] A. C. Campos, F. R. Ferreira, W. A. da Silva Jr, and F. S. Guimarães, "Predator threat stress promotes long lasting anxiety-like behaviors and modulates synaptophysin and CB1 receptors expression in brain areas associated with PTSD symptoms," *Neuroscience Letters*, vol. 533, pp. 34–38, 2013.

[14] C. Challis, J. Boulden, A. Veerakumar et al., "Raphe GABAergic neurons mediate the acquisition of avoidance after social defeat," *Journal of Neuroscience*, vol. 33, no. 35, pp. 13978–13988, 2013.

[15] A. Chocyk, B. Bobula, D. Dudys et al., "Early-life stress affects the structural and functional plasticity of the medial prefrontal cortex in adolescent rats," *European Journal of Neuroscience*, vol. 38, no. 1, pp. 2089–2107, 2013.

[16] V. Krishnan, M. H. Han, D. L. Graham et al., "Molecular adaptations underlying susceptibility and resistance to social defeat in brain reward regions," *Cell*, vol. 131, no. 2, pp. 391–404, 2007.

[17] S. D. Kuipers, A. Trentani, J. A. den Boer, and G. J. ter Horst, "Molecular correlates of impaired prefrontal plasticity in response to chronic stress," *Journal of Neurochemistry*, vol. 85, no. 5, pp. 1312–1323, 2003.

[18] M. A. Smith, S. Makino, M. Altemus et al., "Stress and antidepressants differentially regulate neurotrophin 3 mRNA expression in the locus coeruleus," *Proceedings of the National Academy of Sciences of the United States of America*, vol. 92, no. 19, pp. 8788–8792, 1995.

[19] A. Veerakumar, C. Challis, P. Gupta et al., "Antidepressant-like effects of cortical deep brain stimulation coincide with pro-neuroplastic adaptations of serotonin systems," *Biological Psychiatry*, vol. 76, no. 3, pp. 203–212, 2014.

[20] P. R. Zoladz, C. R. Park, J. D. Halonen et al., "Differential expression of molecular markers of synaptic plasticity in the hippocampus, prefrontal cortex, and amygdala in response to spatial learning, predator exposure, and stress-induced amnesia," *Hippocampus*, vol. 22, no. 3, pp. 577–589, 2012.

[21] F. Jeanneteau, C. Barrère, M. Vos et al., "The stress-induced transcription factor NR4A1 adjusts mitochondrial function and synapse number in prefrontal cortex," *The Journal of Neuroscience*, vol. 38, no. 6, pp. 1335–1350, 2018.

[22] F. F. Scarante, C. Vila-Verde, V. L. Detoni, N. C. Ferreira-Junior, F. S. Guimarães, and A. C. Campos, "Cannabinoid modulation of the stressed hippocampus," *Frontiers in Molecular Neuroscience*, vol. 10, p. 411, 2017.

[23] K. G. Bath, S. J. Russo, K. E. Pleil, E. S. Wohleb, R. S. Duman, and J. J. Radley, "Circuit and synaptic mechanisms of repeated stress: perspectives from differing contexts, duration, and development," *Neurobiology of Stress*, vol. 7, pp. 137–151, 2017.

[24] Y. S. Nikolova, K. A. Misquitta, B. R. Rocco et al., "Shifting priorities: highly conserved behavioral and brain network adaptations to chronic stress across species," *Translational Psychiatry*, vol. 8, no. 1, p. 26, 2018.

[25] I. A. Paul and P. Skolnick, "Glutamate and depression: clinical and preclinical studies," *Annals of the New York Academy of Sciences*, vol. 1003, no. 1, pp. 250–272, 2003.

[26] P. J. Lucassen, J. Pruessner, N. Sousa et al., "Neuropathology of stress," *Acta Neuropathologica*, vol. 127, no. 1, pp. 109–135, 2014.

[27] B. E. Leonard, "Psychopathology of depression," *Drugs of Today*, vol. 43, no. 10, pp. 705–716, 2007.

[28] E. Mamalaki, R. Kvetnansky, L. S. Brady, P. W. Gold, and M. Herkenham, "Repeated immobilization stress alters tyrosine hydroxylase, corticotropin-releasing hormone and corticosteroid receptor messenger ribonucleic acid levels in rat brain," *Journal of Neuroendocrinology*, vol. 4, no. 6, pp. 689–699, 1992.

[29] D. Weinshenker, "Functional consequences of locus coeruleus degeneration in Alzheimer's disease," *Current Alzheimer Research*, vol. 5, no. 3, pp. 342–345, 2008.

[30] J. D. Bremner, "Traumatic stress: effects on the brain," *Dialogues in Clinical Neuroscience*, vol. 8, no. 4, pp. 445–461, 2006.

[31] J. R. Strawn and T. D. Geracioti, "Noradrenergic dysfunction and the psychopharmacology of posttraumatic stress disorder," *Depression and Anxiety*, vol. 25, no. 3, pp. 260–271, 2008.

[32] O. Borodovitsyna, M. Flamini, and D. Chandler, "Noradrenergic modulation of cognition in health and disease," *Neural Plasticity*, vol. 2017, Article ID 6031478, 14 pages, 2017.

[33] R. A. Eser, A. J. Ehrenberg, C. Petersen et al., "Selective vulnerability of brainstem nuclei in distinct tauopathies: a postmortem study," *Journal of Neuropathology and Experimental Neurology*, vol. 77, no. 2, pp. 149–161, 2018.

[34] C. Naegeli, T. Zeffiro, M. Piccirelli et al., "Locus coeruleus activity mediates hyperresponsiveness in posttraumatic stress disorder," *Biological Psychiatry*, vol. 83, no. 3, pp. 254–262, 2018.

[35] E. T. Cunningham, M. C. Bohn, and P. E. Sawchenko, "Organization of adrenergic inputs to the paraventricular and supraoptic nuclei of the hypothalamus in the rat," *The Journal of Comparative Neurology*, vol. 292, no. 4, pp. 651–667, 1990.

[36] J. P. Herman, H. Figueiredo, N. K. Mueller et al., "Central mechanisms of stress integration: hierarchical circuitry controlling hypothalamo–pituitary–adrenocortical responsiveness," *Frontiers in Neuroendocrinology*, vol. 24, no. 3, pp. 151–180, 2003.

[37] C. W. Berridge and B. D. Waterhouse, "The locus coeruleus–noradrenergic system: modulation of behavioral state and state-dependent cognitive processes," *Brain Research Reviews*, vol. 42, no. 1, pp. 33–84, 2003.

[38] D. J. Chandler, W. J. Gao, and B. D. Waterhouse, "Heterogeneous organization of the locus coeruleus projections to prefrontal and motor cortices," *Proceedings of the National Academy of Sciences of the United States of America*, vol. 111, no. 18, pp. 6816–6821, 2014.

[39] S. L. Foote, F. E. Bloom, and G. Aston-Jones, "Nucleus locus ceruleus: new evidence of anatomical and physiological specificity," *Physiological Reviews*, vol. 63, no. 3, pp. 844–914, 1983.

[40] S. E. Loughlin, S. L. Foote, and F. E. Bloom, "Efferent projections of nucleus locus coeruleus: topographic organization of cells of origin demonstrated by three-dimensional reconstruction," *Neuroscience*, vol. 18, no. 2, pp. 291–306, 1986.

[41] S. D. Robertson, N. W. Plummer, J. de Marchena, and P. Jensen, "Developmental origins of central norepinephrine neuron diversity," *Nature Neuroscience*, vol. 16, no. 8, pp. 1016–1023, 2013.

[42] D. Chandler and B. D. Waterhouse, "Evidence for broad versus segregated projections from cholinergic and noradrenergic nuclei to functionally and anatomically discrete subregions of prefrontal cortex," *Frontiers in Behavioral Neuroscience*, vol. 6, p. 20, 2012.

[43] D. J. Chandler, "Evidence for a specialized role of the locus coeruleus noradrenergic system in cortical circuitries and behavioral operations," *Brain Research*, vol. 1641, Part B, pp. 197–206, 2016.

[44] D. J. Chandler, C. S. Lamperski, and B. D. Waterhouse, "Identification and distribution of projections from monoaminergic and cholinergic nuclei to functionally differentiated subregions of prefrontal cortex," *Brain Research*, vol. 1522, pp. 38–58, 2013.

[45] D. J. Chandler, B. D. Waterhouse, and W. J. Gao, "New perspectives on catecholaminergic regulation of executive circuits: evidence for independent modulation of prefrontal functions by midbrain dopaminergic and noradrenergic neurons," *Frontiers in Neural Circuits*, vol. 8, p. 53, 2014.

[46] D. M. Devilbiss, M. E. Page, and B. D. Waterhouse, "Locus ceruleus regulates sensory encoding by neurons and networks in waking animals," *Journal of Neuroscience*, vol. 26, no. 39, pp. 9860–9872, 2006.

[47] B. D. Waterhouse, H. C. Moises, and D. J. Woodward, "Phasic activation of the locus coeruleus enhances responses of primary sensory cortical neurons to peripheral receptive field stimulation," *Brain Research*, vol. 790, no. 1-2, pp. 33–44, 1998.

[48] H. P. Jedema and A. A. Grace, "Corticotropin-releasing hormone directly activates noradrenergic neurons of the locus ceruleus recorded *in vitro*," *Journal of Neuroscience*, vol. 24, no. 43, pp. 9703–9713, 2004.

[49] E. W. Prouty, B. D. Waterhouse, and D. J. Chandler, "Corticotropin releasing factor dose-dependently modulates excitatory synaptic transmission in the noradrenergic nucleus locus coeruleus," *European Journal of Neuroscience*, vol. 45, no. 5, pp. 712–722, 2017.

[50] J. D. Swinny and R. J. Valentino, "Corticotropin-releasing factor promotes growth of brain norepinephrine neuronal processes through Rho GTPase regulators of the actin cytoskeleton in rat," *European Journal of Neuroscience*, vol. 24, no. 9, pp. 2481–2490, 2006.

[51] R. J. Valentino, S. L. Foote, and G. Aston-Jones, "Corticotropin-releasing factor activates noradrenergic neurons of the locus coeruleus," *Brain Research*, vol. 270, no. 2, pp. 363–367, 1983.

[52] G. Cibelli, P. Corsi, G. Diana, F. Vitiello, and G. Thiel, "Corticotropin-releasing factor triggers neurite outgrowth of a catecholaminergic immortalized neuron via cAMP and MAP kinase signalling pathways," *European Journal of Neuroscience*, vol. 13, no. 7, pp. 1339–1348, 2001.

[53] J. D. Swinny, E. O'Farrell, B. C. Bingham, D. A. Piel, R. J. Valentino, and S. G. Beck, "Neonatal rearing conditions distinctly shape locus coeruleus neuronal activity, dendritic arborization, and sensitivity to corticotrophin-releasing factor," *The International Journal of Neuropsychopharmacology*, vol. 13, no. 04, pp. 515–525, 2010.

[54] Y. Fan, P. Chen, Y. Li, and M. Y. Zhu, "Effects of chronic social defeat on expression of dopamine β-hydroxylase in rat brains," *Synapse*, vol. 67, no. 6, pp. 300–312, 2013.

[55] M. Rusnák, R. Kvetňanský, J. Jeloková, and M. Palkovits, "Effect of novel stressors on gene expression of tyrosine hydroxylase and monoamine transporters in brainstem noradrenergic neurons of long-term repeatedly immobilized rats," *Brain Research*, vol. 899, no. 1-2, pp. 20–35, 2001.

[56] S. A. George, D. Knox, A. L. Curtis, J. W. Aldridge, R. J. Valentino, and I. Liberzon, "Altered locus coeruleus–norepinephrine function following single prolonged stress," *European Journal of Neuroscience*, vol. 37, no. 6, pp. 901–909, 2013.

[57] S. Salim, B. Hite, and D. C. Eikenburg, "Activation of the CRF_1 receptor causes ERK1/2 mediated increase in GRK3 expression in CATH.a cells," *FEBS Letters*, vol. 581, no. 17, pp. 3204–3210, 2007.

[58] D. A. Bangasser, B. A. S. Reyes, D. Piel et al., "Increased vulnerability of the brain norepinephrine system of females to corticotropin-releasing factor overexpression," *Molecular Psychiatry*, vol. 18, no. 2, pp. 166–173, 2013.

[59] B. A. S. Reyes, D. A. Bangasser, R. J. Valentino, and E. J. Van Bockstaele, "Using high resolution imaging to determine trafficking of corticotropin-releasing factor receptors in noradrenergic neurons of the rat locus coeruleus," *Life Sciences*, vol. 112, no. 1-2, pp. 2–9, 2014.

[60] B. A. S. Reyes, R. J. Valentino, and E. J. Van Bockstaele, "Stress-induced intracellular trafficking of corticotropin-releasing factor receptors in rat locus coeruleus neurons," *Endocrinology*, vol. 149, no. 1, pp. 122–130, 2008.

[61] E. L. Sabban, L. I. Serova, E. Newman, N. Aisenberg, and I. Akirav, "Changes in gene expression in the locus coeruleus-amygdala circuitry in inhibitory avoidance PTSD model," *Cellular and Molecular Neurobiology*, vol. 38, no. 1, pp. 273–280, 2018.

[62] O. Borodovitsyna, M. D. Flamini, and D. J. Chandler, "Acute stress persistently alters locus coeruleus function and anxiety-like behavior in adolescent rats," *Neuroscience*, vol. 373, pp. 7–19, 2018.

[63] R. J. Valentino, D. Bangasser, and E. J. Van Bockstaele, "Sex-biased stress signaling: the corticotropin-releasing factor receptor as a model," *Molecular Pharmacology*, vol. 83, no. 4, pp. 737–745, 2013.

[64] J. G. McCall, R. al-Hasani, E. R. Siuda et al., "CRH engagement of the locus coeruleus noradrenergic system mediates stress-induced anxiety," *Neuron*, vol. 87, no. 3, pp. 605–620, 2015.

[65] A. L. Curtis, S. C. Leiser, K. Snyder, and R. J. Valentino, "Predator stress engages corticotropin-releasing factor and opioid systems to alter the operating mode of locus coeruleus norepinephrine neurons," *Neuropharmacology*, vol. 62, no. 4, pp. 1737–1745, 2012.

[66] K. Snyder, W. W. Wang, R. Han, K. McFadden, and R. J. Valentino, "Corticotropin-releasing factor in the norepinephrine nucleus, locus coeruleus, facilitates behavioral flexibility," *Neuropsychopharmacology*, vol. 37, no. 2, pp. 520–530, 2012.

[67] L. A. Schwarz, K. Miyamichi, X. J. Gao et al., "Viral-genetic tracing of the input–output organization of a central noradrenaline circuit," *Nature*, vol. 524, no. 7563, pp. 88–92, 2015.

[68] D. A. Bangasser, X. Zhang, V. Garachh, E. Hanhauser, and R. J. Valentino, "Sexual dimorphism in locus coeruleus dendritic morphology: a structural basis for sex differences in emotional arousal," *Physiology & Behavior*, vol. 103, no. 3-4, pp. 342–351, 2011.

[69] A. Kreibich, B. A. S. Reyes, A. L. Curtis et al., "Presynaptic inhibition of diverse afferents to the locus ceruleus by κ-opiate receptors: a novel mechanism for regulating the central norepinephrine system," *Journal of Neuroscience*, vol. 28, no. 25, pp. 6516–25, 2008.

[70] B. A. S. Reyes, R. J. Valentino, G. Xu, and E. J. Van Bockstaele, "Hypothalamic projections to locus coeruleus neurons in rat brain," *European Journal of Neuroscience*, vol. 22, no. 1, pp. 93–106, 2005.

[71] B. A. S. Reyes, G. Zitnik, C. Foster, E. J. Van Bockstaele, and R. J. Valentino, "Social stress engages neurochemically-distinct afferents to the rat locus coeruleus depending on coping strategy," *eNeuro*, vol. 2, no. 6, 2015.

[72] R. J. Valentino, C. Rudoy, A. Saunders, X. B. Liu, and E. J. van Bockstaele, "Corticotropin-releasing factor is preferentially colocalized with excitatory rather than inhibitory amino acids in axon terminals in the peri-locus coeruleus region," *Neuroscience*, vol. 106, no. 2, pp. 375–384, 2001.

[73] R. J. Valentino, M. Page, E. van Bockstaele, and G. Aston-Jones, "Corticotropin-releasing factor innervation of the locus coeruleus region: distribution of fibers and sources of input," *Neuroscience*, vol. 48, no. 3, pp. 689–705, 1992.

[74] G. Aston-Jones and J. D. Cohen, "Adaptive gain and the role of the locus coeruleus–norepinephrine system in optimal performance," *The Journal of Comparative Neurology*, vol. 493, no. 1, pp. 99–110, 2005.

[75] D. A. Bangasser and R. J. Valentino, "Sex differences in stress-related psychiatric disorders: neurobiological perspectives," *Frontiers in Neuroendocrinology*, vol. 35, no. 3, pp. 303–319, 2014.

[76] R. J. Valentino, S. L. Foote, and M. E. Page, "The locus coeruleus as a site for integrating corticotropin-releasing factor and noradrenergic mediation of stress responses," *Annals of the New York Academy of Sciences*, vol. 697, no. 1 Corticotropin, pp. 173–188, 1993.

[77] J. G. McCall, E. R. Siuda, D. L. Bhatti et al., "Locus coeruleus to basolateral amygdala noradrenergic projections promote anxiety-like behavior," *eLife*, vol. 6, 2017.

[78] A. F. T. Arnsten, "Catecholamine modulation of prefrontal cortical cognitive function," *Trends in Cognitive Sciences*, vol. 2, no. 11, pp. 436–447, 1998.

[79] A. K. Rajbhandari, B. A. Baldo, and V. P. Bakshi, "Predator stress-induced CRF release causes enduring sensitization of basolateral amygdala norepinephrine systems that promote PTSD-like startle abnormalities," *Journal of Neuroscience*, vol. 35, no. 42, pp. 14270–14285, 2015.

[80] G. Bouchez, M. J. Millan, J. M. Rivet, R. Billiras, R. Boulanger, and A. Gobert, "Quantification of extracellular levels of corticosterone in the basolateral amygdaloid complex of freely-moving rats: a dialysis study of circadian variation and stress-induced modulation," *Brain Research*, vol. 1452, pp. 47–60, 2012.

[81] G. Patki, F. Atrooz, I. Alkadhi, N. Solanki, and S. Salim, "High aggression in rats is associated with elevated stress, anxiety-like behavior, and altered catecholamine content in the brain," *Neuroscience Letters*, vol. 584, pp. 308–313, 2015.

[82] M. J. Mana and A. A. Grace, "Chronic cold stress alters the basal and evoked electrophysiological activity of rat locus coeruleus neurons," *Neuroscience*, vol. 81, no. 4, pp. 1055–1064, 1997.

[83] A. F. T. Arnsten, R. Mathew, R. Ubriani, J. R. Taylor, and B.-M. Li, "α-1 noradrenergic receptor stimulation impairs prefrontal cortical cognitive function," *Biological Psychiatry*, vol. 45, no. 1, pp. 26–31, 1999.

[84] J. Korf, G. K. Aghajanian, and R. H. Roth, "Increased turnover of norepinephrine in the rat cerebral cortex during stress: role of the locus coeruleus," *Neuropharmacology*, vol. 12, no. 10, pp. 933–938, 1973.

[85] B. Bingham, K. McFadden, X. Zhang, S. Bhatnagar, S. Beck, and R. Valentino, "Early adolescence as a critical window during which social stress distinctly alters behavior and brain norepinephrine activity," *Neuropsychopharmacology*, vol. 36, no. 4, pp. 896–909, 2011.

[86] R. J. Valentino and S. L. Foote, "Corticotropin-releasing hormone increases tonic but not sensory-evoked activity of noradrenergic locus coeruleus neurons in unanesthetized rats," *The Journal of Neuroscience*, vol. 8, no. 3, pp. 1016–1025, 1988.

[87] F. Lejeune and M. J. Millan, "The CRF_1 receptor antagonist, DMP695, abolishes activation of locus coeruleus noradrenergic neurones by CRF in anesthetized rats," *European Journal of Pharmacology*, vol. 464, no. 2-3, pp. 127–133, 2003.

[88] A. Tashiro and R. Yuste, "Regulation of dendritic spine motility and stability by Rac1 and Rho kinase: evidence for two forms of spine motility," *Molecular and Cellular Neuroscience*, vol. 26, no. 3, pp. 429–440, 2004.

[89] A. Y. Nakayama, M. B. Harms, and L. Luo, "Small GTPases Rac and Rho in the maintenance of dendritic spines and branches in hippocampal pyramidal neurons," *The Journal of Neuroscience*, vol. 20, no. 14, pp. 5329–5338, 2000.

[90] L. Van Aelst and H. T. Cline, "Rho GTPases and activity-dependent dendrite development," *Current Opinion in Neurobiology*, vol. 14, no. 3, pp. 297–304, 2004.

[91] E. J. Van Bockstaele, B. A. S. Reyes, and R. J. Valentino, "The locus coeruleus: a key nucleus where stress and opioids intersect to mediate vulnerability to opiate abuse," *Brain Research*, vol. 1314, pp. 162–174, 2010.

[92] Y. Liu and S. Nakamura, "Stress-induced plasticity of monoamine axons," *Frontiers in Bioscience*, vol. 11, no. 1, pp. 1794–1801, 2006.

[93] S. Nakamura, T. Sakaguchi, and F. Aoki, "Electrophysiological evidence for terminal sprouting of locus coeruleus neurons following repeated mild stress," *Neuroscience Letters*, vol. 100, no. 1–3, pp. 147–152, 1989.

[94] A. M. Rasmusson, R. L. Hauger, C. A. Morgan III, J. D. Bremner, D. S. Charney, and S. M. Southwick, "Low baseline and yohimbine-stimulated plasma neuropeptide Y (NPY) levels in combat-related PTSD," *Biological Psychiatry*, vol. 47, no. 6, pp. 526–539, 2000.

[95] B. A. S. Reyes, J. D. Glaser, and E. J. Van Bockstaele, "Ultrastructural evidence for co-localization of corticotropin-releasing factor receptor and μ-opioid receptor in the rat nucleus locus coeruleus," *Neuroscience Letters*, vol. 413, no. 3, pp. 216–221, 2007.

[96] E. J. Van Bockstaele, E. E. O. Colago, and R. J. Valentino, "Amygdaloid corticotropin-releasing factor targets locus coeruleus dendrites: substrate for the co-ordination of emotional and cognitive limbs of the stress response," *Journal of Neuroendocrinology*, vol. 10, no. 10, pp. 743–757, 1998.

[97] D. A. Bangasser, S. R. Eck, A. M. Telenson, and M. Salvatore, "Sex differences in stress regulation of arousal and cognition," *Physiology & Behavior*, vol. 187, pp. 42–50, 2018.

[98] R. C. Kessler, P. Berglund, O. Demler, R. Jin, K. R. Merikangas, and E. E. Walters, "Lifetime prevalence and age-of-onset distributions of DSM-IV disorders in the National Comorbidity Survey Replication," *Archives of General Psychiatry*, vol. 62, no. 6, pp. 593–602, 2005.

[99] T. G. Banke, D. Bowie, H. K. Lee, R. L. Huganir, A. Schousboe, and S. F. Traynelis, "Control of GluR1 AMPA receptor function by cAMP-dependent protein kinase," *The Journal of Neuroscience*, vol. 20, no. 1, pp. 89–102, 2000.

[100] J. A. Esteban, S. H. Shi, C. Wilson, M. Nuriya, R. L. Huganir, and R. Malinow, "PKA phosphorylation of AMPA receptor subunits controls synaptic trafficking underlying plasticity," *Nature Neuroscience*, vol. 6, no. 2, pp. 136–143, 2003.

[101] K. W. Roche, R. J. O'Brien, A. L. Mammen, J. Bernhardt, and R. L. Huganir, "Characterization of multiple phosphorylation sites on the AMPA receptor GluR1 subunit," *Neuron*, vol. 16, no. 6, pp. 1179–1188, 1996.

[102] I. H. Greger, J. F. Watson, and S. G. Cull-Candy, "Structural and functional architecture of AMPA-type glutamate receptors and their auxiliary proteins," *Neuron*, vol. 94, no. 4, pp. 713–730, 2017.

[103] A. S. Kato and J. M. Witkin, "Auxiliary subunits of AMPA receptors: the discovery of a forebrain-selective antagonist, LY3130481/CERC-611," *Biochemical Pharmacology*, vol. 147, pp. 191–200, 2018.

[104] M. G. Kang, Y. Guo, and R. L. Huganir, "AMPA receptor and GEF-H1/Lfc complex regulates dendritic spine development through RhoA signaling cascade," *Proceedings of the National Academy of Sciences of the United States of America*, vol. 106, no. 9, pp. 3549–3554, 2009.

[105] Z. Szíber, H. Liliom, C. O. O. Morales et al., "Ras and Rab interactor 1 controls neuronal plasticity by coordinating dendritic filopodial motility and AMPA receptor turnover," *Molecular Biology of the Cell*, vol. 28, no. 2, pp. 285–295, 2017.

[106] M. Gesi, P. Soldani, F. S. Giorgi, A. Santinami, I. Bonaccorsi, and F. Fornai, "The role of the locus coeruleus in the development of Parkinson's disease," *Neuroscience & Biobehavioral Reviews*, vol. 24, no. 6, pp. 655–668, 2000.

[107] P. J. McMillan, S. S. White, A. Franklin et al., "Differential response of the central noradrenergic nervous system to the loss of locus coeruleus neurons in Parkinson's disease and Alzheimer's disease," *Brain Research*, vol. 1373, pp. 240–252, 2011.

[108] W. Lu and K. W. Roche, "Posttranslational regulation of AMPA receptor trafficking and function," *Current Opinion in Neurobiology*, vol. 22, no. 3, pp. 470–479, 2012.

[109] J. Widagdo, S. Guntupalli, S. E. Jang, and V. Anggono, "Regulation of AMPA receptor trafficking by protein ubiquitination," *Frontiers in Molecular Neuroscience*, vol. 10, p. 347, 2017.

[110] M. P. Lussier, A. Sanz-Clemente, and K. W. Roche, "Dynamic regulation of *N*-methyl-d-aspartate (NMDA) and α-amino-3-hydroxy-5-methyl-4-isoxazolepropionic acid (AMPA) receptors by posttranslational modifications," *Journal of Biological Chemistry*, vol. 290, no. 48, pp. 28596–28603, 2015.

[111] A. L. Mammen, K. Kameyama, K. W. Roche, and R. L. Huganir, "Phosphorylation of the α-amino-3-hydroxy-5-methylisoxazole4-propionic acid receptor GluR1 subunit by calcium/calmodulin-dependent kinase II," *Journal of Biological Chemistry*, vol. 272, no. 51, pp. 32528–32533, 1997.

[112] M. A. Jenkins and S. F. Traynelis, "PKC phosphorylates GluA1-Ser831 to enhance AMPA receptor conductance," *Channels*, vol. 6, no. 1, pp. 60–64, 2012.

[113] M. A. Jenkins, G. Wells, J. Bachman et al., "Regulation of GluA1 α-amino-3-hydroxy-5-methyl-4-isoxazolepropionic acid receptor function by protein kinase C at serine-818 and threonine-840," *Molecular Pharmacology*, vol. 85, no. 4, pp. 618–629, 2014.

[114] V. Derkach, A. Barria, and T. R. Soderling, "Ca^{2+}/calmodulin-kinase II enhances channel conductance of α-amino-3-hydroxy-5-methyl-4-isoxazolepropionate type glutamate receptors," *Proceedings of the National Academy of Sciences of the United States of America*, vol. 96, no. 6, pp. 3269–3274, 1999.

[115] S. Q. Ren, J. Z. Yan, X. Y. Zhang et al., "PKCλ is critical in AMPA receptor phosphorylation and synaptic incorporation during LTP," *The EMBO Journal*, vol. 32, no. 10, pp. 1365–1380, 2013.

[116] C. H. Kim, H. J. Chung, H. K. Lee, and R. L. Huganir, "Interaction of the AMPA receptor subunit GluR2/3 with PDZ domains regulates hippocampal long-term depression," *Proceedings of the National Academy of Sciences of the United States of America*, vol. 98, no. 20, pp. 11725–11730, 2001.

[117] J. Xia, H. J. Chung, C. Wihler, R. L. Huganir, and D. J. Linden, "Cerebellar long-term depression requires PKC-regulated interactions between GluR2/3 and PDZ domain–containing proteins," *Neuron*, vol. 28, no. 2, pp. 499–510, 2000.

[118] A. N. Hegde, "The ubiquitin-proteasome pathway and synaptic plasticity," *Learning & Memory*, vol. 17, no. 7, pp. 314–327, 2010.

[119] M. S. Goo, S. L. Scudder, and G. N. Patrick, "Ubiquitin-dependent trafficking and turnover of ionotropic glutamate receptors," *Frontiers in Molecular Neuroscience*, vol. 8, p. 60, 2015.

[120] J. Jiang, V. Suppiramaniam, and M. W. Wooten, "Posttranslational modifications and receptor-associated proteins in AMPA receptor trafficking and synaptic plasticity," *Neurosignals*, vol. 15, no. 5, pp. 266–282, 2006.

[121] E. Y. Yuen, J. Wei, W. Liu, P. Zhong, X. Li, and Z. Yan, "Repeated stress causes cognitive impairment by suppressing glutamate receptor expression and function in prefrontal cortex," *Neuron*, vol. 73, no. 5, pp. 962–977, 2012.

[122] G. Yang, W. Xiong, L. Kojic, and M. S. Cynader, "Subunit-selective palmitoylation regulates the intracellular trafficking of AMPA receptor," *European Journal of Neuroscience*, vol. 30, no. 1, pp. 35–46, 2009.

[123] T. Hayashi, G. Rumbaugh, and R. L. Huganir, "Differential regulation of AMPA receptor subunit trafficking by palmitoylation of two distinct sites," *Neuron*, vol. 47, no. 5, pp. 709–723, 2005.

[124] D. T. Lin, Y. Makino, K. Sharma et al., "Regulation of AMPA receptor extrasynaptic insertion by 4.1N, phosphorylation and palmitoylation," *Nature Neuroscience*, vol. 12, no. 7, pp. 879–887, 2009.

[125] G. M. Thomas and R. L. Huganir, "Palmitoylation-dependent regulation of glutamate receptors and their PDZ domain-containing partners," *Biochemical Society Transactions*, vol. 41, no. 1, pp. 72–78, 2013.

[126] B. K. Brar, A. Chen, M. H. Perrin, and W. Vale, "Specificity and regulation of extracellularly regulated kinase1/2 phosphorylation through corticotropin-releasing factor (CRF) receptors 1 and 2β by the CRF/urocortin family of peptides," *Endocrinology*, vol. 145, no. 4, pp. 1718–1729, 2004.

[127] N. Arimura, C. Menager, Y. Kawano et al., "Phosphorylation by Rho kinase regulates CRMP-2 activity in growth cones," *Molecular and Cellular Biology*, vol. 25, no. 22, pp. 9973–9984, 2005.

[128] M. S. Kwon, Y. J. Seo, E. J. Shim, S. S. Choi, J. Y. Lee, and H. W. Suh, "The effect of single or repeated restraint stress on several signal molecules in paraventricular nucleus, arcuate nucleus and locus coeruleus," *Neuroscience*, vol. 142, no. 4, pp. 1281–1292, 2006.

[129] M. A. Hebert, L. I. Serova, and E. L. Sabban, "Single and repeated immobilization stress differentially trigger induction and phosphorylation of several transcription factors and mitogen-activated protein kinases in the rat locus coeruleus," *Journal of Neurochemistry*, vol. 95, no. 2, pp. 484–498, 2005.

[130] E. J. Nestler, "Chapter six—role of the brain's reward circuitry in depression: transcriptional mechanisms," *International Review of Neurobiology*, vol. 124, pp. 151–170, 2015.

[131] L. Aurelian, K. T. Warnock, I. Balan, A. Puche, and H. June, "TLR4 signaling in VTA dopaminergic neurons regulates impulsivity through tyrosine hydroxylase modulation," *Translational Psychiatry*, vol. 6, no. 5, article e815, 2016.

[132] M. Dierssen, M. Gratacòs, I. Sahún et al., "Transgenic mice overexpressing the full-length neurotrophin receptor TrkC exhibit increased catecholaminergic neuron density in specific brain areas and increased anxiety-like behavior and panic reaction," *Neurobiology of Disease*, vol. 24, no. 2, pp. 403–418, 2006.

[133] G. A. Zitnik, "Control of arousal through neuropeptide afferents of the locus coeruleus," *Brain Research*, vol. 1641, Part B, pp. 338–350, 2016.

[134] N. Hansen and D. Manahan-Vaughan, "Hippocampal long-term potentiation that is elicited by perforant path stimulation or that occurs in conjunction with spatial learning is tightly controlled by beta-adrenoreceptors and the locus coeruleus," *Hippocampus*, vol. 25, no. 11, pp. 1285–1298, 2015.

[135] N. Hansen and D. Manahan-Vaughan, "Locus coeruleus stimulation facilitates long-term depression in the dentate gyrus that requires activation of β-adrenergic receptors," *Cerebral Cortex*, vol. 25, no. 7, pp. 1889–1896, 2015.

[136] N. Lemon, S. Aydin-Abidin, K. Funke, and D. Manahan-Vaughan, "Locus coeruleus activation facilitates memory encoding and induces hippocampal LTD that depends on β-adrenergic receptor activation," *Cerebral Cortex*, vol. 19, no. 12, pp. 2827–2837, 2009.

[137] A. Marzo, J. Bai, J. Caboche, P. Vanhoutte, and S. Otani, "Cellular mechanisms of long-term depression induced by noradrenaline in rat prefrontal neurons," *Neuroscience*, vol. 169, no. 1, pp. 74–86, 2010.

[138] H. Salgado, M. Trevino, and M. Atzori, "Layer- and area-specific actions of norepinephrine on cortical synaptic transmission," *Brain Research*, vol. 1641, Part B, pp. 163–176, 2016.

[139] A. F. T. Arnsten, "Catecholamine and second messenger influences on prefrontal cortical networks of "representational knowledge": a rational bridge between genetics and the symptoms of mental illness," *Cerebral Cortex*, vol. 17, Supplement 1, pp. i6–15, 2007.

[140] M. Atzori, R. Cuevas-Olguin, E. Esquivel-Rendon et al., "Locus ceruleus norepinephrine release: a central regulator of CNS spatio-temporal activation?," *Frontiers in Synaptic Neuroscience*, vol. 8, p. 25, 2016.

[141] K. Schutsky, M. Ouyang, and S. A. Thomas, "Xamoterol impairs hippocampus-dependent emotional memory retrieval via $G_{i/o}$-coupled β_2-adrenergic signaling," *Learning & Memory*, vol. 18, no. 9, pp. 598–604, 2011.

[142] C. W. Berridge and R. C. Spencer, "Differential cognitive actions of norepinephrine a2 and a1 receptor signaling in the prefrontal cortex," *Brain Research*, vol. 1641, Part B, pp. 189–196, 2016.

[143] S. Amemiya, N. Kubota, N. Umeyama, T. Nishijima, and I. Kita, "Noradrenergic signaling in the medial prefrontal cortex and amygdala differentially regulates vicarious trial-and-error in a spatial decision-making task," *Behavioural Brain Research*, vol. 297, pp. 104–111, 2016.

[144] R. E. Nicholls, J. M. Alarcon, G. Malleret et al., "Transgenic mice lacking NMDAR-dependent LTD exhibit deficits in behavioral flexibility," *Neuron*, vol. 58, no. 1, pp. 104–117, 2008.

[145] C. F. Murchison, X. Y. Zhang, W. P. Zhang, M. Ouyang, A. Lee, and S. A. Thomas, "A distinct role for norepinephrine in memory retrieval," *Cell*, vol. 117, no. 1, pp. 131–143, 2004.

[146] M. Ouyang, M. B. Young, M. M. Lestini, K. Schutsky, and S. A. Thomas, "Redundant catecholamine signaling consolidates fear memory via phospholipase C," *Journal of Neuroscience*, vol. 32, no. 6, pp. 1932–1941, 2012.

[147] F. M. Howells, D. J. Stein, and V. A. Russell, "Synergistic tonic and phasic activity of the locus coeruleus norepinephrine

(LC-NE) arousal system is required for optimal attentional performance," *Metabolic Brain Disease*, vol. 27, no. 3, pp. 267–274, 2012.

[148] S. P. Orr, N. B. Lasko, L. J. Metzger, and R. K. Pitman, "Physiologic responses to non-startling tones in Vietnam veterans with post-traumatic stress disorder," *Psychiatry Research*, vol. 73, no. 1-2, pp. 103–107, 1997.

[149] S. P. Orr, N. B. Lasko, A. Y. Shalev, and R. K. Pitman, "Physiologic responses to loud tones in Vietnam veterans with posttraumatic stress disorder," *Journal of Abnormal Psychology*, vol. 104, no. 1, pp. 75–82, 1995.

[150] S. P. Orr, L. J. Metzger, N. B. Lasko et al., "Physiologic responses to sudden, loud tones in monozygotic twins discordant for combat exposure: association with posttraumatic stress disorder," *Archives of General Psychiatry*, vol. 60, no. 3, pp. 283–288, 2003.

[151] R. K. Pitman and S. P. Orr, "Twenty-four hour urinary cortisol and catecholamine excretion in combat-related posttraumatic stress disorder," *Biological Psychiatry*, vol. 27, no. 2, pp. 245–247, 1990.

[152] R. A. Lanius, D. Rabellino, J. E. Boyd, S. Harricharan, P. A. Frewen, and M. C. McKinnon, "The innate alarm system in PTSD: conscious and subconscious processing of threat," *Current Opinion in Psychology*, vol. 14, pp. 109–115, 2017.

[153] S. Soya, H. Shoji, E. Hasegawa et al., "Orexin receptor-1 in the locus coeruleus plays an important role in cue-dependent fear memory consolidation," *Journal of Neuroscience*, vol. 33, no. 36, pp. 14549–14557, 2013.

[154] A. Uematsu, B. Z. Tan, and J. P. Johansen, "Projection specificity in heterogeneous locus coeruleus cell populations: implications for learning and memory," *Learning & Memory*, vol. 22, no. 9, pp. 444–451, 2015.

[155] A. Uematsu, B. Z. Tan, E. A. Ycu et al., "Modular organization of the brainstem noradrenaline system coordinates opposing learning states," *Nature Neuroscience*, vol. 20, no. 11, pp. 1602–1611, 2017.

[156] T. F. Giustino, P. J. Fitzgerald, and S. Maren, "Revisiting propranolol and PTSD: memory erasure or extinction enhancement?," *Neurobiology of Learning and Memory*, vol. 130, pp. 26–33, 2016.

[157] T. F. Giustino and S. Maren, "Noradrenergic modulation of fear conditioning and extinction," *Frontiers in Behavioral Neuroscience*, vol. 12, p. 43, 2018.

[158] R. J. Ross, W. A. Ball, D. F. Dinges et al., "Rapid eye movement sleep disturbance in posttraumatic stress disorder," *Biological Psychiatry*, vol. 35, no. 3, pp. 195–202, 1994.

[159] R. J. Ross, W. A. Ball, L. D. Sanford et al., "Rapid eye movement sleep changes during the adaptation night in combat veterans with posttraumatic stress disorder," *Biological Psychiatry*, vol. 45, no. 7, pp. 938–941, 1999.

[160] T. A. Mellman, R. Kulick-Bell, L. E. Ashlock, and B. Nolan, "Sleep events among veterans with combat-related posttraumatic stress disorder," *The American Journal of Psychiatry*, vol. 152, no. 1, pp. 110–115, 1995.

[161] M. E. Page, C. W. Berridge, S. L. Foote, and R. J. Valentino, "Corticotropin-releasing factor in the locus coeruleus mediates EEG activation associated with hypotensive stress," *Neuroscience Letters*, vol. 164, no. 1-2, pp. 81–84, 1993.

[162] D. G. Baker, S. A. West, W. E. Nicholson et al., "Serial CSF corticotropin-releasing hormone levels and adrenocortical activity in combat veterans with posttraumatic stress disorder," *American Journal of Psychiatry*, vol. 156, no. 4, pp. 585–588, 1999.

[163] J. D. Bremner, R. B. Innis, C. K. Ng et al., "Positron emission tomography measurement of cerebral metabolic correlates of yohimbine administration in combat-related posttraumatic stress disorder," *Archives of General Psychiatry*, vol. 54, no. 3, pp. 246–254, 1997.

[164] C. S. Fullerton, H. B. Herberman Mash, K. N. Benevides, J. C. Morganstein, and R. J. Ursano, "Distress of routine activities and perceived safety associated with post-traumatic stress, depression, and alcohol use: 2002 Washington, DC, sniper attacks," *Disaster Medicine and Public Health Preparedness*, vol. 9, no. 5, pp. 509–515, 2015.

[165] H. Hagena, N. Hansen, and D. Manahan-Vaughan, "β-adrenergic control of hippocampal function: subserving the choreography of synaptic information storage and memory," *Cerebral Cortex*, vol. 26, no. 4, pp. 1349–1364, 2016.

[166] B. Huang, H. Zhu, Y. Zhou, X. Liu, and L. Ma, "Unconditioned- and conditioned- stimuli induce differential memory reconsolidation and β-AR-dependent CREB activation," *Frontiers in Neural Circuits*, vol. 11, p. 53, 2017.

[167] H. Villain, A. Benkahoul, P. Birmes, B. Ferry, and P. Roullet, "Influence of early stress on memory reconsolidation: implications for post-traumatic stress disorder treatment," *PLoS One*, vol. 13, no. 1, article e0191563, 2018.

[168] M. A. Raskind, D. J. Dobie, E. D. Kanter, E. C. Petrie, C. E. Thompson, and E. R. Peskind, "The α_1-adrenergic antagonist prazosin ameliorates combat trauma nightmares in veterans with posttraumatic stress disorder: a report of 4 cases," *The Journal of Clinical Psychiatry*, vol. 61, no. 2, pp. 129–134, 2000.

[169] B. R. Keeshin, Q. Ding, A. P. Presson, S. J. Berkowitz, and J. R. Strawn, "Use of prazosin for pediatric PTSD-associated nightmares and sleep disturbances: a retrospective chart review," *Neurology and Therapy*, vol. 6, no. 2, pp. 247–257, 2017.

[170] M. A. Raskind, E. R. Peskind, E. D. Kanter et al., "Reduction of nightmares and other PTSD symptoms in combat veterans by prazosin: a placebo-controlled study," *American Journal of Psychiatry*, vol. 160, no. 2, pp. 371–373, 2003.

[171] R. H. Pietrzak, J. D. Gallezot, Y. S. Ding et al., "Association of posttraumatic stress disorder with reduced in vivo norepinephrine transporter availability in the locus coeruleus," *JAMA Psychiatry*, vol. 70, no. 11, pp. 1199–1205, 2013.

[172] I. Liberzon and K. L. Phan, "Brain-imaging studies of posttraumatic stress disorder," *CNS Spectrums*, vol. 8, no. 9, pp. 641–650, 2003.

[173] H. S. Bracha, E. Garcia-Rill, R. E. Mrak, and R. Skinner, "Postmortem locus coeruleus neuron count in three American veterans with probable or possible war-related PTSD," *The Journal of Neuropsychiatry and Clinical Neurosciences*, vol. 17, no. 4, pp. 503–509, 2005.

[174] W. J. G. Hoogendijk, M. G. P. Feenstra, M. H. A. Botterblom et al., "Increased activity of surviving locus ceruleus neurons in Alzheimer's disease," *Annals of Neurology*, vol. 45, no. 1, pp. 82–91, 1999.

[175] A. A. Feduccia and M. C. Mithoefer, "MDMA-assisted psychotherapy for PTSD: are memory reconsolidation and fear extinction underlying mechanisms?," *Progress in Neuro-Psychopharmacology & Biological Psychiatry*, vol. 84, Part A, pp. 221–228, 2018.

[176] M. B. Young, R. Andero, K. J. Ressler, and L. L. Howell, "3,4-Methylenedioxymethamphetamine facilitates fear extinction learning," *Translational Psychiatry*, vol. 5, no. 9, article e634, 2015.

[177] A. L. Curtis, S. M. Lechner, L. A. Pavcovich, and R. J. Valentino, "Activation of the locus coeruleus noradrenergic system by intracoerulear microinfusion of corticotropin-releasing factor: effects on discharge rate, cortical norepinephrine levels and cortical electroencephalographic activity," *Journal of Pharmacology and Experimental Therapeutics*, vol. 281, no. 1, pp. 163–172, 1997.

[178] A. Asok, J. Schulkin, and J. B. Rosen, "Corticotropin releasing factor type-1 receptor antagonism in the dorsolateral bed nucleus of the stria terminalis disrupts contextually conditioned fear, but not unconditioned fear to a predator odor," *Psychoneuroendocrinology*, vol. 70, pp. 17–24, 2016.

[179] G. Aston-Jones, M. T. Shipley, G. Chouvet et al., "Chapter 4 - afferent regulation of locus coeruleus neurons: anatomy, physiology and pharmacology," *Progress in Brain Research*, vol. 88, pp. 47–75, 1991.

[180] G. F. Koob, S. C. Heinrichs, F. Menzaghi, E. M. Pich, and K. T. Britton, "Corticotropin releasing factor, stress and behavior," *Seminars in Neuroscience*, vol. 6, no. 4, pp. 221–229, 1994.

[181] S. Kratzer, C. Mattusch, M. W. Metzger et al., "Activation of CRH receptor type 1 expressed on glutamatergic neurons increases excitability of CA1 pyramidal neurons by the modulation of voltage-gated ion channels," *Frontiers in Cellular Neuroscience*, vol. 7, p. 91, 2013.

[182] A. R. Howerton, A. V. Roland, J. M. Fluharty et al., "Sex differences in corticotropin-releasing factor receptor-1 action within the dorsal raphe nucleus in stress responsivity," *Biological Psychiatry*, vol. 75, no. 11, pp. 873–883, 2014.

[183] L. G. Kirby, E. Freeman-Daniels, J. C. Lemos et al., "Corticotropin-releasing factor increases GABA synaptic activity and induces inward current in 5-hydroxytryptamine dorsal raphe neurons," *Journal of Neuroscience*, vol. 28, no. 48, pp. 12927–12937, 2008.

[184] C. M. Lamy and S. G. Beck, "Swim stress differentially blocks CRF receptor mediated responses in dorsal raphe nucleus," *Psychoneuroendocrinology*, vol. 35, no. 9, pp. 1321–1332, 2010.

[185] K. D. Holmes, A. V. Babwah, L. B. Dale, M. O. Poulter, and S. S. G. Ferguson, "Differential regulation of corticotropin releasing factor 1α receptor endocytosis and trafficking by β-arrestins and Rab GTPases," *Journal of Neurochemistry*, vol. 96, no. 4, pp. 934–949, 2006.

[186] R. Zhao-Shea, S. R. DeGroot, L. Liu et al., "Increased CRF signalling in a ventral tegmental area-interpeduncular nucleus-medial habenula circuit induces anxiety during nicotine withdrawal," *Nature Communications*, vol. 6, no. 1, p. 6770, 2015.

[187] N. V. Gounko, J. D. Swinny, D. Kalicharan et al., "Corticotropin-releasing factor and urocortin regulate spine and synapse formation: structural basis for stress-induced neuronal remodeling and pathology," *Molecular Psychiatry*, vol. 18, no. 1, pp. 86–92, 2013.

[188] D. A. Bangasser, "Sex differences in stress-related receptors: "micro" differences with "macro" implications for mood and anxiety disorders," *Biology of Sex Differences*, vol. 4, no. 1, p. 2, 2013.

[189] F. G. Graeff, "Neuroanatomy and neurotransmitter regulation of defensive behaviors and related emotions in mammals," *Brazilian Journal of Medical and Biological Research*, vol. 27, no. 4, pp. 811–829, 1994.

[190] K. L. Widnell, J. S. Chen, P. A. Iredale et al., "Transcriptional regulation of CREB (cyclic AMP response element-binding protein) expression in CATH.a cells," *Journal of Neurochemistry*, vol. 66, no. 4, pp. 1770–1773, 1996.

[191] M. P. Lussier, Y. Nasu-Nishimura, and K. W. Roche, "Activity-dependent ubiquitination of the AMPA receptor subunit GluA2," *Journal of Neuroscience*, vol. 31, no. 8, pp. 3077–3081, 2011.

[192] R. Malinow and R. C. Malenka, "AMPA receptor trafficking and synaptic plasticity," *Annual Review of Neuroscience*, vol. 25, no. 1, pp. 103–126, 2002.

[193] B. Aisa, R. Tordera, B. Lasheras, J. del Río, and M. J. Ramírez, "Cognitive impairment associated to HPA axis hyperactivity after maternal separation in rats," *Psychoneuroendocrinology*, vol. 32, no. 3, pp. 256–266, 2007.

[194] R. J. Valentino, B. Reyes, E. van Bockstaele, and D. Bangasser, "Molecular and cellular sex differences at the intersection of stress and arousal," *Neuropharmacology*, vol. 62, no. 1, pp. 13–20, 2012.

Hindawi
Neural Plasticity
Volume 2018, Article ID 6589608, 5 pages
https://doi.org/10.1155/2018/6589608

Research Article

Danshen-Honghua Ameliorates Stress-Induced Menopausal Depression in Rats

Simeng Gu,[1,2] **Yao Ma**,[2] **Kemin Ge**,[2] **Ruifang Nie**,[2] **Erxi Wu**,[3,4,5] **and Yang Li**[2,6]

[1]*Department of Psychology, Jiangsu University Medical School, Zhenjiang 212013, China*
[2]*School of Life Science, Nanjing University of Chinese Medicine, Nanjing 210023, China*
[3]*Department of Neurosurgery, Baylor Scott & White Health, Temple, TX 76358, USA*
[4]*Department of Surgery, College of Medicine, Texas A&M University, Temple, TX 76354, USA*
[5]*Department of Pharmaceutical Sciences, College of Pharmacy, Texas A&M University, College Station, TX 77843, USA*
[6]*School of Psychology, Nanjing Forest Police College, Nanjing 210023, China*

Correspondence should be addressed to Simeng Gu; gsm_2007@126.com

Received 29 December 2017; Revised 2 February 2018; Accepted 26 March 2018; Published 3 May 2018

Academic Editor: Fang Pan

Objective. Previously, we have shown that Danshen-Honghua (DSHH) for cognitive deficits after ischemia induced impairments of the hippocampus. Here, we investigate the effects of DSHH on stress-induced depression in menopausal rats. *Methods*. A rat model with menopausal depression was established with bilateral ovariectomies in female SD rats followed by chronic mild stress treatment for 21 days. 40 rats were randomly divided into the sham surgery group (sham surgery and no stress treatment), surgery group (surgery with no stress treatment), surgery/stress group (surgery and stress treatment), fluoxetine group ($2.4\,mg{\cdot}kg^{-1}$, with surgery and stress treatment), and DSHH group ($35\,g{\cdot}kg^{-1}$, with surgery and stress treatment). The rats in the last two groups were treated with stresses together with intragastric drug administration for three weeks after the surgery. Then open-field locomotor scores and sucrose intake were tested for behavior changes. Also, the levels of norepinephrine (NE), dopamine (DA), serotonin (5-HT), and cortisone were determined by high-performance liquid chromatography (HPLC). Serum estradiol (E_2), follicle-stimulating hormone (FSH), and luteinizing hormone (LH) were determined by radioimmunoassay. *Results*. The results of open-field locomotor scores, sucrose intake in both the fluoxetine group and DSHH group, were significantly higher than those of the surgery/stress group ($P < 0.01$). Serum LH, FSH, and cortisone levels in both the DSHH group and fluoxetine group were significantly lower than those in the surgery/stress group ($P < 0.01$). Serum E_2 levels in these groups were slightly increased in these medicine groups ($P < 0.01$). The monoamine levels in the DSHH group were much higher than those in the surgery/stress group ($P < 0.01$). *Conclusion*. DSHH can ameliorate stress-induced depressed syndromes in the surgery/stressed rats via regulating LH and FSH levels as well as monoamine levels.

1. Introduction

Major depressive disorder (MDD) is a leading health-related cause of human suffering [1, 2]. The pathological mechanisms of MDD are far from clear [2, 3] and are a hot topic for neuroscience research [4, 5]. Previous studies have pointed out that the mechanism of depression is majorly due to the monoamine neurotransmitters, including norepinephrine (NE), serotonin (5-HT), and dopamine (DA) [6, 7], because most of the first choice antidepressants affect 5-HT and NE or 5-HT reuptakes. However, even though many studies support the role of the central monoamine network, other hormones or neuromodulators are involved too, such as hormones released from the hypothalamus-pituitary axis (HPA) [8] and sex hormones [9]. Depression occurrence in female is twice as many as male patients [10] and is a well-known symptom for the menopausal period [11, 12]. In fact, one of the major symptoms of menopause is depression [12, 13]. However, the treatment methods for menopausal depression are different. A published study from our colleagues showed that a Chinese medicine, Danshen-Honghua (DSHH), is effective for cognitive deficits after

ischemia-induced impairments of the hippocampus [14]. A wealth of clinical experience has demonstrated that DSHH is very effective in the treatment of menopausal depression. Here, we tested its mechanisms in the treatment of depression by screening many hormone and neurotransmitter changes after administration with these drugs. This study will not only shed light on the mechanisms of depression but also help us find alternative ways for depression treatment.

2. Materials and Methods

2.1. Animals. 40 female Sprague-Dawley (SD) rats with body weight averaging 500 ± 20 g, at the age of 12 months, were randomly divided into 5 groups: the sham surgery group (sham surgery and no stress treatment), surgery group (surgery with no stress treatment), surgery/stress group (surgery and stress treatment), fluoxetine group, and DSHH group, with 8 rats in each group. The animals were treated as shown before: the sham surgery group rats were treated with sham surgery (only the skin was opened), the surgery group rats were treated with surgery to remove the ovaries but no stress treatment was introduced, the surgery/stress group rats were treated with surgery and stress, the fluoxetine group rats were treated with fluoxetine ($2.4\ \text{mg}\cdot\text{kg}^{-1}$) in addition to surgery and stress, and the DSHH group rats were treated with DSHH ($35\ \text{g}\cdot\text{kg}^{-1}$) in addition to surgery and stress. The rats in the last two groups were treated with stresses together with intragastric drug administration for three weeks continuously, three times a day, after the surgery recovery. DSHH included *Carthamus tinctorius* 15 g and *Salvia miltiorrhiza* Bge 20 g. These drugs were grounded into powder and mixed with 200 mL deionized water and intragastrically administrated according the $35\ \text{g}\cdot\text{kg}^{-1}$ amounts. All the procedures were approved by the Institution of Animal Care and Use Committee.

3. Instrument

US Thermo Microplate Reader and KH30R desktop high-speed refrigerated centrifuge were used in the experiments. Analytical balance, low-temperature ultracentrifuge, paraffin embedding machine, slicer, and so on are provided by the central laboratory. 3200 ATRAP high-performance liquid chromatography (HPLC) tandem mass spectrometer (ABI, USA), equipped with atmospheric pressure chemical ionization sources (LC-APCI-MS/MS).

4. Animal Surgery/Control

4.1. Ovary Removal [2]. In addition to the sham surgery group, the other four groups were given "ovariectomy." During the surgical procedure, the rats were given $100\ \text{mg}\cdot\text{kg}^{-1}$ ketamine to induce anesthesia and fixed on a hard plate in supine position. A marker was marked in the rat 2 cm outside the spine and 1 cm below the ribs; the soft tissue was sectioned separately. The peripheral blood vessels were ligated, and both sides of the ovaries were removed, and finally, the uterus was removed. The method of determining successful ovariectomy is the vaginal epithelium keratosis test: 5 days of continuous monitoring of the rat vagina did not find the estrous cycle. The animals were screened with the estrous cycle one week before the surgery, to make sure they have normal cycles.

Table 1: Effect of DSHH on body weight of rats with menopausal depression ($\bar{x} \pm s, g$).

Group	N	Before castration	After castration	After medication
Sham surgery	8	470.53 ± 5.49	474.32 ± 6.34	484.53 ± 5.63
Surgery	7	475.29 ± 6.15	466.31 ± 5.43	488.54 ± 6.84
Surgery/ stress	8	473.49 ± 4.75	$457.73 \pm 4.15^{*}$	$474.32 \pm 6.22^{\$}$
Fluoxetine	7	479.15 ± 4.94	$462.69 \pm 5.28^{*}$	$478.33 \pm 6.39^{\$}$
DSHH	8	469.64 ± 5.23	$452.74 \pm 6.36^{*}$	$488.16 \pm 5.54^{\$}$

Compared with the sham surgery group, $^{*}P < 0.01$, one way ANNOVA; $^{\$}P < 0.01$, t-test, compared with after castration.

4.2. Chronic Mild Unpredictable Stress. In addition to the sham surgery group and the surgery group, the other three groups of rats were housed in a single cage after the surgery and after 5 days of surgery, they were treated with chronic unavoidable stresses for 21 days. Stress treatment lasted for 2 h, including 36 V AC electric foot shock (stimulated 1 time every l min; each time lasted 10 s, for a total of 30 times), 4°C ice-cold water swimming (5 min), 45°C heat stress (5 min), 15 min shaking (1 times/s), 45-degree tilting of the rat cage (24 h), tail clipping (1 min), bed wetting (10 h), bottle emptying (1 h), and application of each stimulus 2 times.

5. Administration

Rats in each group, except the sham surgery group, were treated consecutively with stress for 21 days, after the surgery recovery. Rats in the fluoxetine group were given Prozac $2.4\ \text{mg}\cdot\text{kg}^{-1}$, 1 time per day. Rats in the DSHH group were given DSHH $35\ \text{g}\cdot\text{kg}^{-1}$, which was divided 2 times a day through gavage (the dosage was referred to a previous publication [14]). In the course of study, two rats died—one in the surgery/stress group and one in the fluoxetine group died during intragastric administration. Because these two rats were dead by accident (not related to the treatments from this study), they were excluded from the number of studies. On the last treatment day, all 38 rats were sacrificed (cervical dislocation). Each rat was rapidly decapitated and 5–10 mL of blood was obtained. The serum was separated by centrifuge.

6. Observation Indicators

6.1. Open-Field Test. Open-field test was done in an open box with both the length and width to be 80 cm and the height to be 40 cm, the same as those that we have reported before [15]. The bottom surface was divided into 25 large areas with white lines. The rats were placed at the center of the bottom of the box, and the vertical activity points were measured as the number of uprights, from the time the rat's feet left the

Table 2: Open-box experiment of menopausal depression rat ($\bar{x} \pm s$).

Group	N	Before castration		After surgery/stress		After medication	
		Horizontal movement	Vertical movement	Horizontal movement	Vertical movement	Horizontal movement	Vertical movement
Sham surgery	8	54.3 ± 4.5	11.1 ± 2.5	$45.2 \pm 5.5^{**}$	$10.4 \pm 3.7^{**}$	$48.4 \pm 4.9^{**}$	$10.8 \pm 2.4^{**}$
Surgery	7	55.7 ± 5.3	10.9 ± 2.2	35.1 ± 4.8	8.2 ± 2.5	$38.7 \pm 3.8^{*}$	$8.4 \pm 1.9^{*}$
Surgery/stress	8	59.2 ± 6.2	11.8 ± 1.7	28.6 ± 5.3	7.5 ± 3.2	21.8 ± 3.9	7.4 ± 2.9
Fluoxetine	7	57.3 ± 8.6	9.8 ± 3.6	$27.3 \pm 5.2^{*}$	$5.1 \pm 1.5^{*}$	$48.3 \pm 2.5^{**}$	$9.7 \pm 2.3^{**}$
DSHH	8	52.4 ± 1.9	10.5 ± 1.9	$21.3 \pm 2.1^{*}$	$6.8 \pm 2.9^{*}$	$50.2 \pm 4.2^{**}$	$9.7 \pm 2.9^{**}$

Compared with the surgery/stress group, $^{*}P < 0.01$ and $^{**}P < 0.001$.

bottom to the time their feet back to the bottom. The level of activity of rats was measured through the number of bottom blocks, through 1 grid for 1 point, such as rats walking along the line, every 10 cm considered as 1 time. Each rat walks one time for 3 min.

6.2. Sucrose Intake Test. Sucrose intake test was carried out on the 21st day after surgery recovery. Each rat was given 135 mL of 1% sucrose solution after 24 h fasting, and the amount of sucrose solution consumed by rats was calculated.

7. Sex Hormone Measurement

Estradiol (E_2), luteinizing hormone (LH), and follicle-stimulating hormone (FSH) were measured. On the last treatment day, the abdominal aorta was taken and the serum was separated as soon as possible (within 8 h). The contents of E_2, LH, and FSH were determined by radioimmunoassay. The RIA kit used was bought from the United States Depp Company. Specific operation was carried out according to the instructions.

8. Measurement of Monoamine Neurotransmitters

After the chronic stress test and the behavior test, the animals were decapitated under anesthesia with isoflurane (2%). The brain was quickly removed and the cortex and hippocampus were collected for HPLC and electron microscopy experiment. The cerebral spinal fluid was saved in a glass syringe and injected into a HPLC to measure NE, DA, and serotonin. The monoamine levels were assessed by comparing the reference standard and respective peak area and elution time of the samples using a calibration curve for each monoamine neurotransmitter.

9. Statistical Processing Method

SPSS20.0 software was used for statistical analysis, and the data were used in the form of $\bar{x} \pm s$. The data were compared with t-test; analysis of variance was used to compare the difference between groups.

10. Results

10.1. Body Weight. Table 1 shows that there was no significant difference in body weight among the five groups before ovariectomy (one-way ANOVA, $P > 0.05$). After surgery and/or stress, the body weights of the animals in each group decreased than those in the sham surgery group and the body weights of the rats in the surgery/stress group were significantly lower than those in the surgery group (one-way ANOVA, $^{*}P < 0.01$, $N = 38$; Table 1), but there was no significant difference among the surgery/stress group, fluoxetine group, and DSHH group ($P > 0.05$).

Table 3: Sucrose intake in rats with menopausal depression ($\bar{x} \pm s$, g).

Group	N	Before castration	After castration/ stress	After medication
Sham surgery	8	23.32 ± 3.53	$21.84 \pm 2.74^{*}$	$22.15 \pm 2.26^{**}$
Surgery	7	25.27 ± 3.37	$16.44 \pm 2.06^{*}$	$15.66 \pm 2.83^{**}$
Surgery/ stress	8	22.54 ± 2.43	6.34 ± 1.65	7.14 ± 1.69
Fluoxetine	7	24.84 ± 2.68	8.85 ± 2.43	$18.98 \pm 2.68^{**}$
DSHH	8	22.32 ± 3.05	7.45 ± 2.87	$19.58 \pm 2.22^{**}$

Compared with the surgery/stress group, $^{*}P < 0.01$ and $^{**}P < 0.001$.

10.2. Behavioral Assessment. The results showed that there was no significant difference in the behavior tests among the surgery groups (one-way ANOVA, $P > 0.05$, Table 2). The scores of vertical movement and horizontal movement in the surgery groups were significantly decreased than those in the sham surgery group, (one-way ANOVA, $P < 0.01$). The scores of vertical movement and horizontal movement in the fluoxetine group were significantly lower than those in the sham surgery group (one-way ANOVA, $P < 0.01$), and the scores of horizontal movement and vertical movement in the DSHH group were also significantly higher than those in the surgery group (one-way ANOVA, $P < 0.01$), but there was no significant difference between the two groups (one-way ANOVA, $P > 0.05$).

10.3. Sucrose Intake. The rats in the castration group consumed less sucrose than those in the sham surgery group (one-way ANOVA, $^{*}P < 0.01$; Table 3). But the sucrose consumption in the DSHH group was significantly higher than that in the surgery/stress group (one-way ANOVA, $^{*}P < 0.01$), and the sucrose consumption in the fluoxetine group was significantly higher than that in the surgery/stress

Table 4: Comparison of monoamine and cortisone levels in CSF ($\bar{x} \pm s$).

Group	N	NE (pg/mL)	DA (pg/mL)	5-HT (pg/mL)	Cortisone (ng/mL)
Sham surgery	8	1.98 ± 1.23	$4.98 \pm 1.45^{*}$	$6.05 \pm 1.13^{*}$	$0.36 \pm 0.26^{*}$
Surgery	7	1.88 ± 1.34	5.12 ± 1.78	5.98 ± 1.32	0.73 ± 0.53
Surgery/stress	8	1.33 ± 0.56	1.86 ± 1.48	3.56 ± 0.44	0.89 ± 0.35
Fluoxetine	7	$1.98 \pm 0.57^{*}$	$4.15 \pm 1.88^{*}$	4.47 ± 1.35	$0.53 \pm 0.26^{*}$
DSHH	8	$1.75 \pm 0.76^{*}$	$4.26 \pm 1.25^{*}$	$5.08 \pm 1.36^{*}$	$0.45 \pm 0.22^{**}$

Compared with the surgery/stress group, $^{*}P < 0.05$ and $^{**}P < 0.01$.

group (one-way ANOVA, $^{*}P < 0.01$), but there was no significant difference between the two groups ($P > 0.05$).

10.4. Monoamine Neurotransmitters and Hormones. The levels of neurotransmitters norepinephrine (NE), dopamine (DA), and serotonin (5-HT) in the CSF and cortisone in the serum were tested with high-performance liquid chromatography (HPLC). The levels of NE, DA, and 5-HT in the CSF were significantly lower in the surgery groups compared with the sham surgery group, but cortisone levels in the serum in the surgery/stress group were much higher than those in the sham surgery group. The levels of these monoamines in the two drug-treated groups were significantly higher than those in the surgery/stress group (one-way ANOVA, $P < 0.05$; Table 4). Compared with that of the surgery/stress group, the 5-HT level of the DSHH group was statistically significantly higher (one-way ANOVA, $P < 0.01$).

10.5. Sex Hormones. The levels of E_2 in the serum of the two drug-treated groups were not significantly different in the surgery group and surgery/stress group. Compared with that of the surgery/stress group, the E_2 level of the DSHH group was not statistically significant (one-way ANOVA, $P > 0.05$; Table 5). The levels of FSH in the two groups were lower than those in the surgery group and surgery/stress group. Compared with those in the surgery/stress group, the levels of FSH in the DSHH group were significantly higher ($t = 5.740$, $P < 0.05$). The level of LH in the treatment group was not significantly different from that in the sham surgery group (one-way ANOVA, $P > 0.05$), suggesting that DSHH can restore ovarian function by adjusting the E_2 and FSH.

Table 5: Comparisons of serum sex hormone levels in rats after manipulation ($\bar{x} \pm s$).

Group	N	E2 (pg/mL)	FSH (mIU/mL)	LH (mIU/mL)
Sham surgery	8	$5.39 \pm 1.88^{**}$	$12.34 \pm 1.46^{**}$	$17.54 \pm 2.55^{**}$
Surgery	7	1.87 ± 1.02	$15.65 \pm 1.44^{**}$	24.98 ± 2.67
Surgery/stress	8	1.34 ± 1.25	23.57 ± 1.56	28.43 ± 4.35
Fluoxetine	7	$2.45 \pm 1.36^{*}$	$15.32 \pm 1.22^{**}$	$18.33 \pm 2.54^{**}$
DSHH	8	$2.76 \pm 1.29^{*}$	$16.77 \pm 1.46^{**}$	$17.95 \pm 1.53^{**}$

Compared with the surgery/stress group, $^{*}P < 0.01$ and $^{**}P < 0.001$.

11. Discussion

There are tons of studies suggesting that depressions are due to monoamine neurotransmitter changes [16–19]; in addition, many other hormones are also involved, such as sex hormones [20]. In this study, we probed into the effects of sex hormone changes in the menopausal depression after treatment with medicines. We used ovariectomized female SD rats to stop the E_2 release and found that these rats were much easier to get depressed through chronic mild stress. On the contrary to decreases in E_2 release, LH and FSH levels are greatly increased, possibly due the removal of feedback inhibition of E_2. In addition, the levels of cortisone are also increased, which suggested that LH and FSH in the pituitary might affect cortisone directly. Consistent with the increase of LH and FSH after ovariectomization in the rats, this phenomenon also exists in the menopause patients. LH, FSH, and ACTH are all released from the pituitary gland, which are possibly interacted with each other. LH and FSH leading to depression might also be the reasons for women being prone to depression, especially LH, whose release surges up during ovulation in the menstrual cycle [12], and LH detection is used to detect ovulation, which occurs about 24–48 hours after the LH surge. In all, LH release increase might be the reason for depression at both the ovulaton in the menstrual cycle and menopause.

Contrary to enhancing E_2, which might have a negative feedback on LH release after menopause and thus depression, DSHH can reduce the LH release after ovary removal, increase CSF monoamine concentrations, and improve the score of horizontal movement and vertical movement effectively in the surgery rats. In addition, DSHH increased the consumption of sugar water, suggesting that DSHH can alleviate depressed syndromes in menopausal depressive rats via regulating hormone levels, especially LH. In this experiment, the activity of the rats in each group was reflected by the horizontal activity score [21]. The sensitivity of rats to the reward substance was reflected by the consumption of sugar [2]. After a period of stress, the score of exploration behavior, activity level, and sugar consumption in the surgery/stress groups significantly decreased. These data suggested that the DSHH can successfully reverse LH surge after ovary removal and also increase the monoamine neurotransmitters in the menopausal rats with the lack of interest, loss of will behavior, loss of pleasure, and so on. Ingredients of DSHH such as Danshen and Honghua support the synergistic effects on promoting blood circulation and removing blood stasis [22] and balance yin and yang. These herbs' comprehensive treatment of menopausal depression is by

tonifying the kidney, decreasing mental anxiety, harmonizing qi and blood, and so on. The antidepressant effects of DSHH on stress after ovariectomization may also be related to changes in sex hormone levels. The multitarget effects of traditional Chinese medicine therapy have a great advantage in the treatment of depression.

Conflicts of Interest

The authors declare no competing financial interests.

Acknowledgments

This work was supported, in part, by Scott & White Plummer Foundation grant, National Science Foundation in China (816280007), Jiangsu Specially Appointed Professorship Foundation, Jiangsu Nature Foundation (BK20151565), Jiangsu Traditional Chinese Medicine Foundation (ZD201351), Jiangsu Six Talent Peak project (2015YY006), University Science Research Project of Jiangsu Province (17KJD310001), and the priority academic program development of Jiangsu Higher Education Institute (Integrated Chinese and Western Medicine).

References

[1] H. Wang, J. Warner-Schmidt, S. Varela, G. Enikolopov, P. Greengard, and M. Flajolet, "Norbin ablation results in defective adult hippocampal neurogenesis and depressive-like behavior in mice," *Proceedings of the National Academy of Sciences of the United States of America*, vol. 112, no. 31, pp. 9745–9750, 2015.

[2] P. Wang, H. Li, S. Barde et al., "Depression-like behavior in rat: involvement of galanin receptor subtype 1 in the ventral periaqueductal gray," *Proceedings of the National Academy of Sciences of the United States of America*, vol. 113, no. 32, pp. E4726–E4735, 2016.

[3] R. Malinow, "Depression: ketamine steps out of the darkness," *Nature*, vol. 533, no. 7604, pp. 477-478, 2016.

[4] Y. Cui, Y. Yang, Z. Ni et al., "Astroglial Kir4.1 in the lateral habenula drives neuronal bursts in depression," *Nature*, vol. 554, no. 7692, pp. 323–327, 2018.

[5] Y. Yang, Y. Cui, K. Sang et al., "Ketamine blocks bursting in the lateral habenula to rapidly relieve depression," *Nature*, vol. 554, no. 7692, pp. 317–322, 2018.

[6] J. T. da Rocha, B. M. Gai, S. Pinton, T. B. Sampaio, C. W. Nogueira, and G. Zeni, "Effects of diphenyl diselenide on depressive-like behavior in ovariectomized mice submitted to subchronic stress: involvement of the serotonergic system," *Psychopharmacology*, vol. 222, no. 4, pp. 709–719, 2012.

[7] T. W. Robbins and A. F. T. Arnsten, "The neuropsychopharmacology of fronto-executive function: monoaminergic modulation," *Annual Review of Neuroscience*, vol. 32, no. 1, pp. 267–287, 2009.

[8] W. G. Moons, N. I. Eisenberger, and S. E. Taylor, "Anger and fear responses to stress have different biological profiles," *Brain, Behavior, and Immunity*, vol. 24, no. 2, pp. 215–219, 2010.

[9] E. W. Freeman, "Associations of depression with the transition to menopause," *Menopause*, vol. 17, no. 4, pp. 823–827, 2010.

[10] J. A. Blair, R. Palm, J. Chang et al., "Luteinizing hormone downregulation but not estrogen replacement improves ovariectomy-associated cognition and spine density loss independently of treatment onset timing," *Hormones and Behavior*, vol. 78, pp. 60–66, 2016.

[11] R. Zahn, K. E. Lythe, J. A. Gethin et al., "Negative emotions towards others are diminished in remitted major depression," *European Psychiatry*, vol. 30, no. 4, pp. 448–453, 2015.

[12] C. N. Soares, "Menopause and depression: keep your eye on the long run," *Menopause*, vol. 23, no. 12, pp. 1272–1274, 2016.

[13] E. A. Stone, D. Quartermain, Y. Lin, and M. L. Lehmann, "Central α_1-adrenergic system in behavioral activity and depression," *Biochemical Pharmacology*, vol. 73, no. 8, pp. 1063–1075, 2007.

[14] X. Zhang, W. Zheng, T. Wang et al., "Danshen-Chuanxiong-Honghua ameliorates cerebral impairment and improves spatial cognitive deficits after transient focal ischemia and identification of active compounds," *Frontiers in Pharmacology*, vol. 8, p. 452, 2017.

[15] W. Xue, W. Wang, T. Gong et al., "PKA-CREB-BDNF signaling regulated long lasting antidepressant activities of Yueju but not ketamine," *Scientific Reports*, vol. 6, no. 1, article 26331, 2016.

[16] S. Gu, W. Du, and F. Wang, "Effects of maternal deprivation at different lactation period on depression behavior and brain catecholamine of rats offsprings," *Chinese Journal of Behaviroal Medicine and Brain Science*, vol. 23, pp. 394–397, 2014.

[17] S. Gu, F. Wang, T. Yuan, B. Guo, and J. H Huang, "Differentiation of primary emotions through neuromodulators: review of literature," *International Journal of Neurology Research*, vol. 1, no. 2, pp. 43–50, 2015.

[18] S. Gu, W. Wang, F. Wang, and J. H. Huang, "Neuromodulator and emotion biomarker for stress induced mental disorders," *Neural Plasticity*, vol. 2016, Article ID 2609128, 6 pages, 2016.

[19] Z. Zheng, S. Gu, Y. Lei et al., "Safety needs mediate stressful events induced mental disorders," *Neural Plasticity*, vol. 2016, Article ID 8058093, 6 pages, 2016.

[20] N. Goel, L. Innala, and V. Viau, "Sex differences in serotonin (5-HT) 1A receptor regulation of HPA axis and dorsal raphe responses to acute restraint," *Psychoneuroendocrinology*, vol. 40, pp. 232–241, 2014.

[21] M. Fukui, R. M. Rodriguiz, J. Zhou et al., "*Vmat2* heterozygous mutant mice display a depressive-like phenotype," *The Journal of Neuroscience*, vol. 27, no. 39, pp. 10520–10529, 2007.

[22] C. Qu, Z. J. Pu, G. S. Zhou et al., "Comparative analysis of main bio-active components in the herb pair Danshen-Honghua and its single herbs by ultra-high performance liquid chromatography coupled to triple quadrupole tandem mass spectrometry," *Journal of Separation Science*, vol. 40, no. 17, pp. 3392–3401, 2017.

Hindawi
Neural Plasticity
Volume 2018, Article ID 9456891, 17 pages
https://doi.org/10.1155/2018/9456891

Research Article

Language and Sensory Neural Plasticity in the Superior Temporal Cortex of the Deaf

Mochun Que,[1,2,3] Xinjian Jiang,[1] Chunyang Yi,[1] Peng Gui,[4] Yuwei Jiang,[4] Yong-Di Zhou,[5,6] and Liping Wang[4]

[1]*Key Laboratory of Brain Functional Genomics, Institute of Cognitive Neuroscience, School of Psychology and Cognitive Science, East China Normal University, Shanghai 200062, China*
[2]*Department of Physiology and Neurobiology, Medical College of Soochow University, Suzhou 215123, China*
[3]*Institute of Medical Psychology, Medical College of Soochow University, Suzhou 215123, China*
[4]*Institute of Neuroscience, Key Laboratory of Primate Neurobiology, CAS Center for Excellence in Brain Science and Intelligence Technology, Chinese Academy of Sciences, Shanghai 200031, China*
[5]*Department of Neurosurgery, Johns Hopkins University, Baltimore, MD 21218, USA*
[6]*NYU-ECNU Institute of Brain and Cognitive Science, NYU Shanghai and Collaborative Innovation Center for Brain Science, Shanghai 200062, China*

Correspondence should be addressed to Liping Wang; lipingwng@gmail.com

Received 25 January 2018; Accepted 26 March 2018; Published 2 May 2018

Academic Editor: Fushun Wang

Visual stimuli are known to activate the auditory cortex of deaf people, presenting evidence of cross-modal plasticity. However, the mechanisms underlying such plasticity are poorly understood. In this functional MRI study, we presented two types of visual stimuli, language stimuli (words, sign language, and lip-reading) and a general stimulus (checkerboard) to investigate neural reorganization in the superior temporal cortex (STC) of deaf subjects and hearing controls. We found that only in the deaf subjects, all visual stimuli activated the STC. The cross-modal activation induced by the checkerboard was mainly due to a sensory component via a feed-forward pathway from the thalamus and primary visual cortex, positively correlated with duration of deafness, indicating a consequence of pure sensory deprivation. In contrast, the STC activity evoked by language stimuli was functionally connected to both the visual cortex and the frontotemporal areas, which were highly correlated with the learning of sign language, suggesting a strong language component via a possible feedback modulation. While the sensory component exhibited specificity to features of a visual stimulus (e.g., selective to the form of words, bodies, or faces) and the language (semantic) component appeared to recruit a common frontotemporal neural network, the two components converged to the STC and caused plasticity with different multivoxel activity patterns. In summary, the present study showed plausible neural pathways for auditory reorganization and correlations of activations of the reorganized cortical areas with developmental factors and provided unique evidence towards the understanding of neural circuits involved in cross-modal plasticity.

1. Introduction

Cortical structures that are deprived of their normal sensory input may become responsive to the stimulation of adjacent receptors, a process that is generally known as cross-modal plasticity or cross-modal reorganization [1]. In human brain imaging studies, there is growing evidence showing that, in early bilaterally deaf adults, the superior temporal cortex (STC) may experience cross-modal recruitment of different visual inputs, such as visual motion [2–8], biological motion [9–11], sign language [11–19], and silent speech reading [15, 20–23]. Animal models have also confirmed the dystrophic change that occurs when the auditory cortex fails to develop typically due to the absence of auditory input [24–28].

Visual-related responses in the STC of deaf subjects could result from long-term auditory deprivation (e.g., missing auditory sensory input) but could also be caused

by other dynamic cognitive functions (e.g., sign language learning) [1, 12, 16, 19, 29, 30]. In the previous studies, STC activity was found to positively correlate with the duration of deafness or the age at cochlear implantation [2, 18, 31–35], suggesting that functional reorganization was likely to take place in the auditory cortex over a considerable period of time. A functional magnetic resonance imaging (fMRI) study showed that STC activation was highly correlated with speech reading fluency, but not with the duration of sensory deprivation [36], indicating that functional compensation of sensory deprivation did not require slow progressive colonization of the STC by visual inputs, but instead rapidly modulated by the preexisting latent connectivity from high-level language-related cortical areas. Thus, for the reorganization of STC, potentially both bottom-up signals (e.g., from the visual cortex) and top-down modulation (e.g., from the associative frontal-temporal areas) could contribute to such cross-modal activity [30]. Meanwhile, a magnetoencephalography study showed that the left frontotemporal network, including the STG, was activated during lexicosemantic processing in the congenitally deaf individuals, but not responsive to the early sensory visual processing, suggesting a more top-down modulation from high-level language-related regions [37].

Although it is clearly known that the STC responds to various visual stimuli in deaf people, the neural mechanisms underlying this cross-modal plasticity are still not fully understood. There are questions remaining to be answered. First, how do developmental factors (e.g., the duration of deafness or the learning of sign languages) in deaf people constrain or promote the reorganized activity in the auditory cortex? Second, how do the bottom-up and top-down two neural pathways contribute to cross-modal activation? Third, does the STC integrate inputs from different pathways, or does it keep them functionally segregated?

In the present study, using fMRI, we aimed to directly compare cross-modal activity and whole-brain functional connectivity in subjects when they were viewing a general stimulus (checkerboard) representing the bottom-up input from the visual cortex and language-related stimuli (words, sign language, and lip-reading) denoting the both bottom-up from visual regions and top-down signals from associative cortical areas. Nineteen profoundly deaf (congenital) subjects, 15 residual hearing subjects with a hearing aid, and 15 hearing subjects were recruited to investigate how behavioral factors (e.g., the duration of hearing loss and age at sign language learning) affected cross-modal activity. This study also aimed to investigate possible sources of cross-modal activation by applying dynamic causal modeling (DCM) [38] and representational similarity analysis (RSA) [39]. We hypothesized that the reorganized STC activity by a checkerboard was mainly induced through a feed-forward network and that activity provoked by language-related stimuli was instigated from both feed-forward and feedback components, but relied more on the feedback regulation. Furthermore, it was considered that the STC activities responsive to the two pathways were likely to be functionally segregated.

2. Materials and Methods

2.1. Participants. Thirty-four early-deaf subjects (14 males; mean age: 20.8 years old) and 15 hearing controls (7 males; mean age: 20.3 years old) participated in the study. The deaf participants were from the Shanghai Youth Technical School for the Deaf (http://www.shlqj.net/longxiao), and their information on the history of hearing loss, hearing aid use, and sign language use was documented through an individual interview (Table 1). All participants were healthy, had a normal or corrected-to-normal vision, were not taking psychoactive medications, did not have a history of neurological or psychiatric illness, took classes at the high-school level, and had normal cognitive functions. In the residual hearing group, most participants communicated by a combination of two or three strategies, which included spoken language (13 out of 15), lip-reading (8 out of 15), and sign language (11 out of 15), while most of the profound deaf (15 out of 19) communicated only via sign language. The ethical committee at East China Normal University in China approved the experimental procedure. All participants gave their informed and written consent according to the Declaration of Helsinki and were paid for their participation. The 15 hearing subjects were recruited from East China Normal University in China and had no learning experience of sign language or lip reading. The groups were matched for age, gender, handedness, and education.

Suitable deaf participants were selected by means of hearing threshold pretests, conducted within the 2 weeks preceding the fMRI experiment. To facilitate a preliminary screening of the subjects, deaf participants self-reported their level of hearing loss on the basis of their audiologists' diagnoses. Hearing thresholds of all the participants were then measured at the Institute of Speech and Hearing Science, Shanghai. Thresholds were assessed monaurally for both ears, either with or without a hearing aid, at 250, 500, 1000, 2000, 4000, and 8000 Hz, using steps of 5 dB. According to the International Hearing Impairment Classification Standard [40], we divided the 34 deaf participants into two groups in terms of their hearing loss level: profoundly deaf (>90 dB, $n = 19$; in average, the left hearing is 106.8 ± 2.5 dB; the right hearing is 106.7 ± 2.4 dB) and residual hearing (<75 dB, $n = 15$; the left hearing is 73.6 ± 5.5 dB; the right hearing is 76.1 ± 4.4 dB) (Table 1).

2.2. Visual Stimuli. Four different visual materials were presented to participants, a checkerboard pattern to act as a general visual stimulus, and three visual stimuli with language content: words, sign language, and lip-reading (Figure 1, which also see details in Supporting information (available here)). All stimuli were pseudorandomly presented using a block design (Figure 1). Within each block, only one type of stimulus was presented. Each block lasted 20 s and was followed by a 20 s interblock interval. During the 20 s visual presentation, the stimuli were played at a similar rate. During the 20 s interval, a red cross with a black background was presented at the center of the screen and participants were asked to maintain their gaze on the cross. Per subject, twenty blocks in total were included. That is, each type of

Table 1: Demographic data of the participants.

(a) Profoundly deaf

Number	Age (years)	Sex	Cause of deafness	Hearing threshold (dB) Left	Right	Age of SL (years)	Duration of deafness (years)
1	17	M	Hereditary	104	106	N/A	16
2	20	M	Ototoxic drugs	110	110	6	19
3	20	M	Ototoxic drugs	84	79	8	18
4	24	M	Ototoxic drugs	119	118	13	22
5	21	F	Ototoxic drugs	112	108	10	20
6	22	F	Ototoxic drugs	118	120	11	15
7	18	F	Ototoxic drugs	119	120	7	15
8	20	M	Ototoxic drugs	110	93	9	19
9	19	F	Hereditary	109	109	N/A	18
10	20	M	Hereditary	94	93	N/A	20
11	23	F	Meningitis	103	108	6	21
12	22	F	Hereditary	81	95	N/A	22
13	21	F	Unknown	110	109	7	19
14	22	F	Ototoxic drugs	108	117	7	21
15	21	M	Ototoxic drugs	110	110	6	21
16	21	F	Meningitis	104	103	6	20
17	22	M	Ototoxic drugs	105	110	7	20
18	22	M	Ototoxic drugs	>120	109	6	21
19	21	M	Ototoxic drugs	>110	110	13	19

(b) Residual hearing

Number	Age (years)	Sex	Cause of deafness	Hearing threshold (dB) Left (without aid)	Right (without aid)	Duration of deafness (years)	Duration of hearing aid use (years)
1	18	F	Meningitis	60 (105)	55 (101)	18	15
2	19	M	Ototoxic drugs	100	75 (75)	17	14
3	19	F	Ototoxic drugs	48 (73)	35 (70)	19	10
4	20	F	Ototoxic drugs	105	79 (106)	18	10
5	19	M	Meningitis	41 (88)	64 (103)	19	15
6	24	M	Ototoxic drugs	70 (76)	93 (101)	23	11
7	24	F	Head injury	66 (107)	94 (98)	22	22
8	24	F	Ototoxic drugs	47 (68)	65 (93)	23	20
9	21	F	Ototoxic drugs	75 (86)	89	19	14
10	20	M	Ototoxic drugs	69 (99)	75 (103)	18	17
11	21	F	Ototoxic drugs	86 (108)	66 (88)	19	18
12	19	F	Ototoxic drugs	69 (88)	84 (99)	18	15
13	20	F	Ototoxic drugs	96	83 (95)	18	14
14	20	F	Ototoxic drugs	108	84 (110)	18	11
15	23	F	Ototoxic drugs	65 (101)	101	20	19

(c) Hearing participants

Number	Age (years)	Sex
1	19	M
2	23	M
3	19	F

Table 1: Continued.

Number	Age (years)	Sex
4	17	F
5	19	F
6	21	F
7	20	F
8	20	F
9	19	M
10	19	F
11	19	F
12	24	M
13	22	M
14	22	M
15	22	M

The hearing loss of deaf participants was confirmed by testing hearing thresholds with audiometry (see Methods and Materials) in the Institute of Speech and Hearing Science at East China Normal University. The averaged hearing thresholds in decibels of each participant are reported in the table. Profoundly deaf group: $n = 19$, 9 females, mean age = 20.84 ± 1.68 years; residual hearing group: $n = 15$, 11 females, mean age = 20.73 ± 2.05 years. SL: sign language. Note: ototoxic drugs mean the misuse of antibiotics.

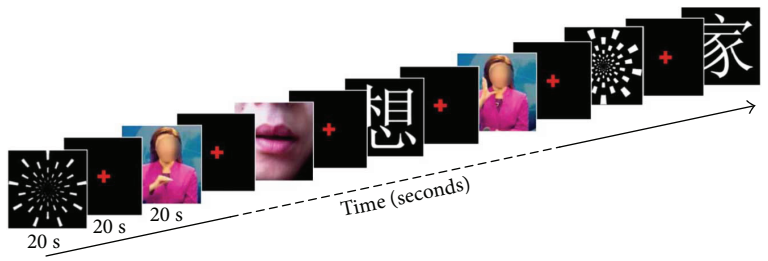

Figure 1: An example session of experimental paradigm. Subjects were presented alternating blocks of four different visual stimuli: checkerboard, words, sign language, and lip-reading. The order of presentation was pseudorandomly assigned. For each subject, there were 20 blocks (four stimuli × five repetitions), with each stimulus presented for 20 s and the black screen sustained for 20 s as an interval. The whole experiment was separated into three sessions for the purpose of avoiding subject fatigue. Throughout a block, subjects were asked to either fixate on a red cross at the center of the screen or concentrate on the visual stimuli. Questions were asked at the end of the experiment to ensure that subjects had paid attention to the visual stimuli (Supporting information).

stimulus was repeated for five times. The blocks were separated into three sessions (6 or 7 blocks per session), with a 5 min intersession interval for rest.

Checkerboard stimuli were presented at 1280×1024 pixels. Each image was presented for 1 s. Word stimuli were composed of 80 Chinese characters (monosyllable) chosen from the List of Frequently Used Characters in Modern Chinese written by the State Language Commission of China. Each character was written in white on a black background and presented as a stimulus for 1 s using a font and size of SimSun 36. For sign language stimuli, five sentences were chosen and expressed by a female presenter moving her hands and arms without facial expression. The video was presented at a resolution of 1024×768 pixels, and each sentence lasting 10 seconds was repeated twice within the same block (20 seconds). The presenter's face in the video was masked to avoid potential interference from the lip-reading. For lip-reading stimuli, consecutive frames of a feminine face pronouncing disyllable Chinese words were presented at a moderate speed. The disyllable words were chosen from the Lexicon of Common Words in Contemporary Chinese by the Commercial Press. Both sign language and lip-reading stimuli were displayed at a rate similar to that used for the word and checkerboard stimuli (~1 Hz). The questionnaire data after scanning showed that all the participants were able to view the stimuli clearly and understand the content of each stimulus (Supporting information).

2.3. Experiment Procedure. The fMRI experiment was approved by the Shanghai Key Laboratory of Magnetic Resonance at East China Normal University. Before scanning, the experimental paradigm and scanning procedures were introduced to the deaf participants through a professional signer. They were asked to stay focused on stimuli and were told that they would be asked questions later after the scan to ensure that attention had been paid to the stimuli. Visual stimuli were displayed on a half-transparent screen hung around 285 cm away from the participant's eyes and displayed via a LCD projector (Epson ELP-7200L, Tokyo, Japan). The participant viewed the screen through a mirror. The

participant's right hand was placed on a button box connected to a computer so that the participant was able to press a button as a sign that he/she wished to withdraw at any stage of the experiment or scan, without having to give a reason.

After scanning, all participants were asked to complete a feedback questionnaire about the content of the experiment and their subjective experiences, to ensure that they were paying attention during the experimental sessions. They were also asked to give ratings on a 3-point scale (3 = all stimuli were very clear, 1 = all stimuli were not clear) to ensure both the clarity of visual stimuli presented and their full engagement in the experiment. Additionally, participants had to describe what they had just seen between trials, the frequency of checkerboard flashing, and the meaning of simple words, sign language, and lip-reading sentences used during the experiment. We did not intend to control the complexity of the language stimuli. The rating scores from stimulus categories did not significantly differ from each other (one-way ANOVA, $p > 0.3$).

2.4. Data Acquisition. The fMRI was performed on a 3-T TimTrio (Siemens, Erlangen, Germany) scanner. During scanning, the participant's head was immobilized using a tight but comfortable foam padding. To avoid nonspecific activation, the participant was asked not to make any sort of response or read aloud during the scan. When presented with visual stimuli, the participant was required to concentrate on the presentation but was not required to perform any mental task or physical operation. Ear defenders were used for all residual and hearing participants throughout the whole procedure. Each participant underwent a T1-weighted structural MR scan (3-D FLASH), with 1 mm-thick slices, a repetition time (TR) of 1900 ms, an echo time (TE) of 3.42 ms, a flip angle of 9°, and a field of view (FOV) of 240×240 mm. FMRI was performed using echo planar imaging (EPI) sequences with the following parameters: 32 axial slices acquired in an interleaved order; TR, 2000 ms; TE, 30 ms; voxel size, $3.75 \times 3.75 \times 3.75$ mm; flip angle, 70°; and FOV, 240×240 mm. A total of 147 sessions (78,400 volumes) were collected from 49 participants.

2.5. Preprocessing. The first two volumes of each run were discarded to allow for T1 equilibration effects. Data were analyzed using SPM8 (Wellcome Trust Centre for Neuroimaging, London, UK) running within Matlab 7.10 (Mathworks Inc., Natick, MA, USA). The image data preprocessing followed standard SPM8 preprocessing procedures and included slice timing correction, realignment for the correction of motion artifacts, coregistration to the participant's structural T1 image, normalization to the Montreal Neurological Institute (MNI) template, and smoothing with a Gaussian kernel of [8 8 8] full width at half maximum. No participants were discarded from the analysis. The head movements were less than 3.75 mm.

2.6. Cross-Modal Activation Analysis. A first-level analysis approach was adopted for the block-design fMRI data using SPM8. In this step, a general linear model encompassing the design and contrasts at the individual subject level was created. The model contained all the information on different conditions, onsets, and durations for all the scans combined across a subject. The twelve predictors included [1–4] the onsets of the four conditions (checkerboard, words, sign language, and lip-reading) in the profoundly deaf group, [5–8] the onsets of the four conditions in the residual deaf group, and [9–12] the onsets of the four conditions in the hearing group. These twelve events were modeled as delta functions convolved with the canonical hemodynamic response function and its temporal and dispersion derivatives. Head motion parameters derived from realignment were also included in the model as covariates of no interest.

The weighted sum of the parameter estimates from the individual analysis was represented as contrast images that were used for the group analysis using a random effect model. The contrast images obtained from the individual analyses represented the normalized condition-related increment of the MR signal of each subject, with the visual stimulus presentations compared with the resting baseline period (stimuli > baseline). The second-level group analysis of the three participant groups (Group: profoundly deaf, residual hearing, and hearing) in the four experimental conditions (Condition: checkerboard, words, sign language, and lip-reading) was performed using SPM. Each contrast image from the relevant condition was firstly submitted to a one-sample *t*-test at the group level for the whole brain to examine the cross-modal activations in the auditory cortex in individual groups. Then, to identify the differences between groups and conditions, a two-way ANOVA with two main factors: Group and Condition, was conducted for the whole brain using a general linear model. To define the regions of interests (ROIs) for following analyses, the peak voxels were selected within the STC (Brodmann areas 41 and 42) in the right hemisphere of the whole-brain map showing a significant main effect of Group (peak at $[66 \quad -27 \quad 13]$) and within language-related brain regions: the left anterior temporal cortex (ATC, peak at $[-57 \quad 7 \quad -9]$) and left inferior frontal gyrus (IFG, peak at $[-47 \quad 22 \quad 13]$) in the map showing the Condition effect. A spherical ROI with a 10 mm radius was then generated and centered on the peak voxel. The mean percent signal change for each participant was extracted from the first-level analysis using the Marsbar software tool (http://marsbar.sourceforge.net).

2.7. Correlation Analysis. In the residual hearing group, most participants communicated by a combination of two or three strategies, which made the analysis of their language learning experience complicated. In the profoundly deaf group, language experience of four participants was not available. Therefore, only 15 profoundly deaf participants were included in the correlation analysis. For the same reason, only the profoundly deaf group was examined to be compared with the hearing group in the functional connectivity analysis and dynamic casual modeling (descripted below). To test the hypothesis that the sign language experience would modulate cross-modal reorganization, we examined the activity in the right superior temporal cortex (STC; using the ROIs defined in the STC showing the Group effect).

Spearman's rank tests for correlations between STC activity and the duration of deafness or between STC activity and the age of learning sign language were performed.

2.8. Functional Connectivity Analysis. A functional connectivity analysis was performed to search for brain areas showing significant differences between the profoundly deaf and hearing groups, with the right STC as a seed region (the same ROI in the above analyses). Functional connectivity analyses were performed using CONN-fMRI Functional Connectivity SPM [41]. EPI images that had been preprocessed as described but had undergone no further statistical analysis were used. Connectivity strength was calculated over the visual presentation period. Before the subject-level analysis, standard preprocessing and depositing procedures using the default settings of the CONN toolbox were performed on the EPI data using the BOLD signal derived from white matter masks and cerebrospinal fluid, as well as motion correction parameters from the realignment stage of the spatial preprocessing as covariates of no interest. The data were further band-pass filtered between 0.008 and 0.09 Hz. For each subject, bivariate regression coefficients were estimated to represent the total linear temporal association between the BOLD signal of the ROIs and the rest of the brain. The subsequent analysis compared correlation strengths by a two-sample t-test (FDR, $p < 0.05$ corrected) on the beta images from the group analysis to examine the differences between the profoundly deaf and the hearing groups at a whole-brain level. To identify the task specificity in each stimulus condition, a further two-sample t-test (FDR, $p < 0.05$ corrected) on the beta images of differences between the groups was performed to examine the differences between the checkerboard condition and the three language conditions.

2.9. Dynamic Causal Modeling. Six different models regarding the language-related visual inputs in deaf participants were compared. These models mainly tested whether STC activations were induced by language stimuli receiving the feedback modulation from IFG and ATC and the feed-forward signal from the primary visual cortex (V1) (see Results). Each model was composed of four regions: IFG, ATC, STC, and V1. The extrinsic input (visual stimulation) always entered the system via the V1. The main differences among the models involved the connections among brain regions: specifically, (1) a model with feedback or feed-forward connections between IFG/ATC and STC, (2) a model with both feed-forward connections between V1 and STC and between V1 and ATC, and (3) a model with only feed-forward connections between V1 and STC or between V1 and ATC. The models were split into two classes of families. The first class tested if models with or without feedback (IFG/ATC to STC) were more likely to explain the data. The family with feedback from IFG/ATC to STC included models [1], [3], and [5], and the family without feedback included models [2], [4], and [6]. The second class tested if models fitted the data which explained the connections between V1 and STC, including V1 to STC (models [1] and [2]), V1 to both STC and ATC (models [3] and [4]), or V1 to only ATC (models [5] and [6]). A group analysis ($p < 0.001$, FDR $p < 0.05$ corrected) of deaf participants (profoundly deaf and residual hearing groups) was conducted to investigate the voxels most significantly activated across all three language-related stimuli in areas of left V1, STC, ATC, and IFG. Specifically, the peak intensities of four regions were identified at V1 $[0 \quad -78 \quad -3]$, STC $[-63 \quad -48 \quad 9]$, ATC $[-57 \quad 7 \quad -9]$, and IFG $[-48 \quad 22 \quad 13]$. The principle eigenvariety (time series) was extracted from the volumes of interest that centered at the coordinates of the nearest voxels within a sphere of 8 mm radius (ROI). Based on the estimated model evidence of each model, using SPM8, random effect Bayesian model selection then calculated the "exceedance probability." When comparing model families, all models within a family were averaged using Bayesian model averaging and the exceedance probabilities were calculated for each model family.

2.10. Representational Similarity Analysis (RSA). The analysis of neural activity within ROIs was conducted with the RSA toolbox (http://www.mrc-cbu.cam.ac.uk/methods-and-resources/toolboxes/) [39]. Both the primary visual area and STC were selected as ROIs defined anatomically by using WFU PickAtlas [42]. We compared the condition-wise patterns amongst fMRI t-maps for the four types of visual stimuli: checkerboard (nonlanguage), words, sign language, and lip-reading (language). Per subject, the representational dissimilarity matrixes (RDMs) comprised correlation distances (1 correlation coefficient) between the images from the blocks for each condition in both the profoundly deaf and the residual hearing group, which yielded a 4×4 matrix. The four conditions were separated into two categories: nonlanguage (checkerboard) and language (words, sign language, and lip-reading). We then compared the correlation coefficient in the three pairs between the nonlanguage and the language conditions (category C-L: checkerboard versus words, checkerboard versus sign language, and checkerboard versus lip-reading) with the three pairs within the language conditions (category L-L: words versus sign language, words versus lip-reading, and sign language versus lip-reading) for each subject. In the individual ROIs, the similarities of the two categories were tested statistically (t-test, $p < 0.05$) in both the profoundly deaf and the residual hearing groups. As there was no plasticity in the auditory cortex with most of visual stimuli in the hearing group, the RSA analysis did not include such group of participants.

3. Results

3.1. Brain Activations in Auditory Areas in Response to Visual Stimuli. We first examined cross-modal activation in the STC of both the deaf and the hearing groups at the group level for each condition (Table 2). We found that the STC was significantly activated by all of the visual stimuli ($p < 0.001$, cluster level $p_{\mathrm{FDR}} < 0.05$ corrected; Figure 2(a)) in the deaf participants. The visual stimuli with language content activated the STC bilaterally, and the checkerboard only induced the STC activation in the right hemisphere (Figure 2(a)). The hearing subjects did not show such cross-modal activity, except for the lip-reading condition. Then, we conducted a

Table 2: Peak activations for BA41 and BA42: profoundly deaf, residual hearing, and hearing groups ($p < 0.001$, uncorrected, minimum cluster size = 10).

Group	Peak coordinates (BA41)			Number of voxels	Peak Z statistic	Peak coordinates (BA42)			Number of voxels	Peak Z statistic
	X	Y	Z			X	Y	Z		
Checkerboard										
Profound	/	/	/	/	/	66	−27	15	19	4.47
Residual	/	/	/	/	/	69	−24	9	30	3.87
Hearing	/	/	/	/	/	/	/	/	/	
Word										
Profound	−48	−33	12	23	4.49	60	−30	15	29	3.78
Residual	/	/	/	/	/	69	−27	9	12	3.64
Hearing	/	/	/	/	/	/	/	/	/	
Sign language										
Profound	54	−24	6	20	4.54	66	−30	12	34	5.54
	/	/	/	/	/	−66	−30	6	11	4.75
Residual	48	−33	9	24	5.07	66	−36	18	31	4.62
	/	/	/	/	/	−63	−30	6	18	4.75
Hearing	/	/	/	/	/	/	/	/	/	
Lip-reading										
Profound	54	−24	6	16	4.72	66	−24	12	39	4.70
	/	/	/	/	/	−66	−30	6	13	3.92
Residual	57	−27	12	18	4.41	63	−24	12	45	5.10
	/	/	/	/	/	−69	−27	6	38	5.36
Hearing	54	−24	6	13	4.44	66	−30	12	33	4.40
	/	/	/	/	/	−69	−27	6	14	4.26

Peak coordinates refer to stereotactic coordinates in MNI (Montreal Neurological Institute) space. BA: Brodmann area.

two-way ANOVA to identify the difference in brain activity between the profoundly deaf, the residual hearing, and the hearing groups and between four visual conditions (Figure 2(b) and Table 3). Results demonstrated that the activations in the right STC had a significant main effect of both Group ($p < 0.001$, $p_{FDR} < 0.05$ corrected, Figure 2(b)) and Condition ($p < 0.001$, $p_{FDR} < 0.05$ corrected, Figure 2(b)). Other brain areas, including the bilateral middle lateral occipital gyrus, bilateral anterior temporal cortex (ATC), and inferior frontal gyrus (IFG), were also activated to the main effect of Condition (Table 3).

We next studied the STC activation in the right hemisphere that was induced by all four visual stimuli (Figures 2(a) and 2(c) and Table 2). For the checkerboard stimulus, we found that the right STC was significantly activated, and the post hoc region of interest (ROI, selected from the map showing the main effect of Group) analysis showed that the cross-modal activation was significantly higher in both the profoundly deaf (t-test, $p < 0.017$) and the residual hearing groups (t-test, $p < 0.002$) than in the hearing group (Figure 2(c), first row). For the visual word stimulus, the activation in the right STC showed significant differences between the profoundly deaf and the hearing groups (t-test, $p < 0.002$) and between the residual- and hearing groups (t-test, $p < 0.001$) (Figure 2(c), second row). For the sign language stimulus, the STC showed enhanced responses in both the profoundly deaf (t-test, $p < 0.003$) and the residual hearing groups (t-test, $p < 0.02$) in comparison with the hearing subjects (Figure 2(c), third row). For the lip-reading stimulus, cross-modal activations were found in the right STC in all subject groups, with no significant differences being found between the profoundly deaf and the hearing groups and between the residual hearing and the hearing groups (t-test, all $p > 0.2$; Figure 2(c), last row).

3.2. Correlations between Developmental Parameters and STC Activations. We then wished to investigate whether activations in auditory regions showed a stronger correlation with the duration of hearing loss or with the age of starting to learn sign language. Most of the residual hearing subjects had a reasonably similar learning duration in reading Chinese words and frequently used multiple language strategies (sign language, speech reading, and spoken language) in their communications. Thus, it is difficult to determine the accurate duration of language learning in the residual hearing group. In the correlation analysis, we only included profoundly deaf subjects and the developmental factors of duration of deafness and the age of learning sign language (Table 1). We first confirmed that the two developmental parameters were not significantly correlated with each other (Spearman's rank, $r = -0.238$, $p > 0.392$).

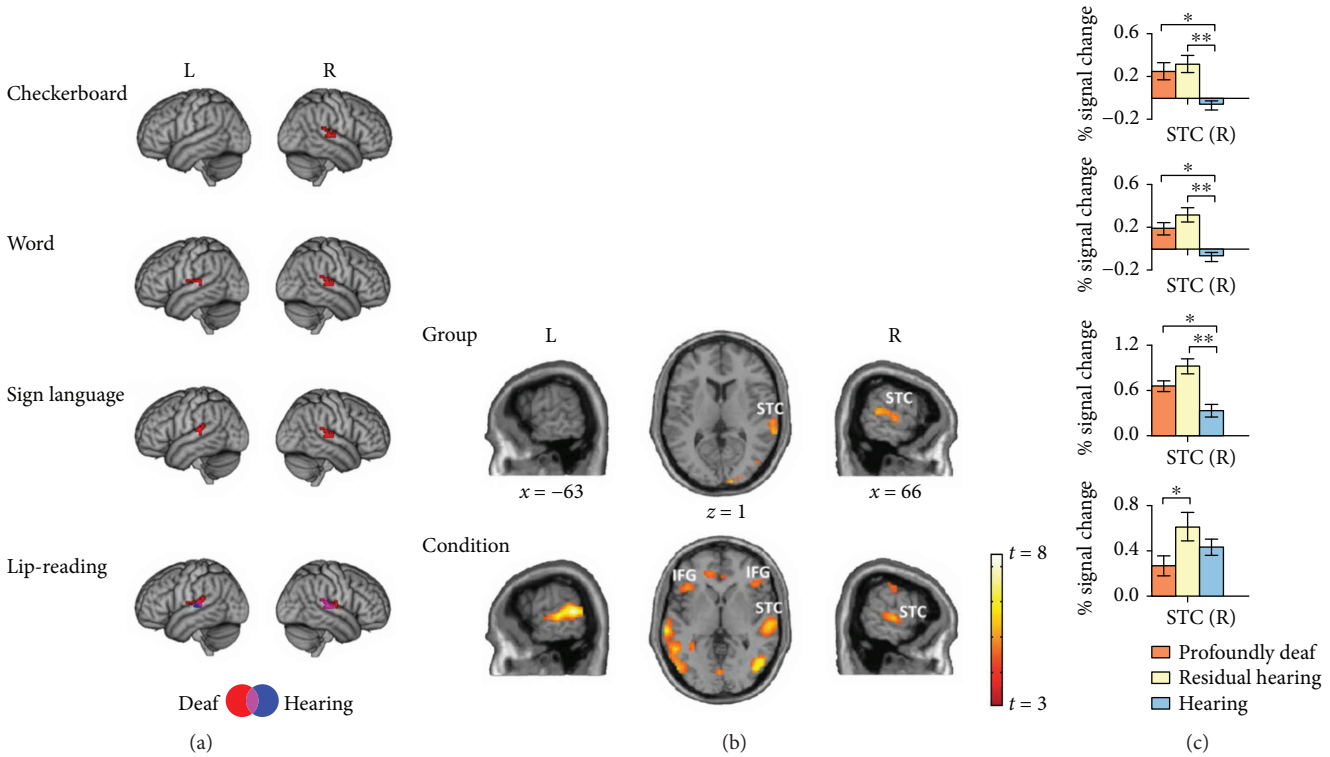

Figure 2: Activations in the superior temporal cortex in response to visual stimuli. (a) Group-level activities for the four visual stimuli are displayed in MNI (Montreal Neurological Institute) standard space. Lateral views of left and right hemispheres showing activity for the checkerboard, word, sign language, and lip-reading stimuli in deaf (red, including both the profoundly deaf and the residual hearing groups, $n = 34$) and hearing (blue, $n = 15$) groups within the brain regions of Brodmann areas (BAs) 41 and 42. The deaf group showed a response to the checkerboard in the right STC region ($p < 0.001$, FDR $p < 0.05$ corrected). Bilateral STC activations were found under the word and sign language conditions in deaf subjects ($p < 0.001$, FDR $p < 0.05$ corrected). Both the deaf and the hearing groups showed bilateral activations for the lip-reading stimuli ($p < 0.001$, FDR $p < 0.05$ corrected). The coordinates and voxel sizes are listed in detail in Table 2. (b) Brain activation to the main effect of Group and Condition are projected on lateral and top views of the brain ($t > 3.0$, $p < 0.001$, FDR $p < 0.05$ corrected). (c) Percent signal change in the regions of interest (10 mm sphere surrounding the peak voxel at $[66 \quad -27 \quad 13]$ in the right STC of the brain map showing the Group effect) of the profoundly deaf (orange, $n = 19$), residual hearing (yellow, $n = 15$), and hearing (blue, $n = 15$) groups. $^{*}p < 0.05$ (Student's t-test), $^{**}p < 0.01$. Error bars indicate 1 standard error. L: left hemisphere; R: right hemisphere; STC: superior temporal cortex; IFG: inferior frontal gyrus.

For profoundly deaf individuals, we found that the right STC activation resulting from the checkerboard was positively correlated with the duration of deafness (Spearman's rank, $r = 0.501$, $p < 0.05$), but not with the age of sign language learning (Spearman's rank, $r = -0.251$, $p > 0.366$; Figure 3(a)). In contrast, the STC activation evoked by sign language stimuli was positively associated with the onset of sign language learning ($r = 0.670$, $p < 0.006$), but not with the duration of deafness ($r = 0.034$, $p > 0.903$; Figure 3(b)). Similar correlations were also found for all the visual stimuli that contained language content. That is, STC activity induced by all of the language stimuli was highly correlated with the onset of sign language learning (Spearman's rank, $r = 0.370$, $p < 0.012$), but not with the duration of deafness (Spearman's rank, $r = -0.04$, $p > 0.792$; Figure 3(c)). Further analyses showed that the activation in the left ATC and left IFG during the presentation of sign language was highly correlated with the onset of sign language learning (ATC: $r = 0.642$, $p < 0.01$; IFG: $r = 0.703$, $p < 0.003$; Figure S1). Interestingly, the activation in the same IFG region under the word condition also demonstrated a significant correlation with the onset of sign language learning (IFG: $r = 0.501$, $p < 0.05$) (Figure S1). However, no areas showing significant correlation with the onset of sign language were found under the checkerboard condition.

3.3. Whole-Brain Functional Connectivity with Cross-Modal Activity in the STC. We next examined the neural sources of cross-modal plasticity in the auditory cortex. We placed a seed region in the reorganized right STC and examined the difference in whole-brain functional connectivity between the profoundly deaf and the hearing subjects ($p < 0.001$, FDR $p < 0.05$ corrected) under the checkerboard condition. We identified significantly greater connection strengths to the STC in the occipital cortex (peak at $[-38 \quad -82 \quad 0]$, t-test, $p < 0.001$) and right thalamus (peak at $[14 \quad -12 \quad 0]$, t-test, $p < 0.01$) of deaf subjects in comparison with hearing subjects (Figure 4(a)).

To explore the difference in functional connectivity between the language stimuli and the checkerboard, we

Table 3: Peak activations for the main effect of Group and Condition (two-way ANOVA, $p < 0.001$, FDR $p < 0.05$ corrected).

Main effect	Brain region	Number of voxels	Peak coordinates			Z score
			X	Y	Z	
Group	Temporal_Superior_Right	151	66	−27	13	4.16
	Occipital_Middle_Left	53	−36	−81	0	4.14
	Occipital_Middle_Right	77	24	−96	3	5.49
	Anglar_Left	34	−54	−60	39	4.02
	Frontal_Middle_Right	21	−33	6	45	4.01
	Precentral_Left	56	−24	−3	36	3.76
	Thalamus_Right	10	24	−27	21	3.92
	Cerebelum_7b_Left	17	−36	−48	−42	3.47
	SupraMarginal_Right	19	42	−39	33	3.35
	Cingulum_Anterior_Right	10	6	42	15	3.17
Condition	Temporal_Superior_Right	426	66	−25	10	6.75
	Temporal_Superior_Left	305	−63	−48	9	7.54
	Frontal_Inferior_Tri_Left	249	−48	22	13	7.58
	Frontal_Inferior_Tri_Right	45	42	30	0	5.85
	Temporal_Middle_Left	234	54	−3	45	6.37
	Temporal_Middle_Right	261	51	−66	3	5.75
	Temporal_Pole_Left	34	−57	7	−9	4.47
	Temporal_Pole_Right	50	57	6	−12	5.19
	Cingulum_Anterior	123	−12	42	0	7.36
	ParaHippocampal_Right	56	30	−36	−9	7.05
	Fusiform_Left	30	−30	−39	−12	6.44
	Frontal_Middle_Right	23	30	24	39	4.12
	Precentral_Left	54	−51	−6	48	5.41
	Precentral_Right	12	54	−3	45	5.19
	Precuneus_Right	49	9	−48	48	6.22
	Lingual_Left	29	0	−78	−3	4.68

Note: peak coordinates refer to stereotactic coordinates in MNI space.

further compared the connectivity contrast (profoundly deaf versus hearing) of each language stimulus with the checkerboard contrast at the whole-brain level ($p < 0.001$, FDR $p < 0.05$ corrected) (Figure 4 and Table 4). For the word stimuli, compared with the checkerboard, we found enhanced connection strengths not only in the left occipital cortex (left hemisphere, peak at $[-42 \quad -58 \quad -14]$, $t = 3.89$) but also in the bilateral ATC (the left hemisphere: peak at $[-40 \quad 2 \quad -14]$, $t = 5.67$; the right hemisphere: peak at $[58 \quad 14 \quad -14]$, $t = 4.97$) and right IFG (peak at $[54 \quad -21 \quad 3]$, $t = 8.73$; Figures 4(b) and 4(e)). The connected area in the left occipital cortex for the word condition was located precisely in the classical visual word form area, which is specific to the processing of visual word information [43–45]. For the sign language stimuli, we identified significantly stronger connections in the bilateral middle temporal areas (the right hemisphere: peak at $[52 \quad -68 \quad 6]$, $t = 6.84$; the left hemisphere: peak at $[44 \quad -70 \quad 8]$, $t = 5.74$), the bilateral FFA (the right hemisphere: peak at $[42 \quad -52 \quad -16]$, $t = 5.70$; the left hemisphere: peak at $[-32 \quad -60 \quad -16]$, $t = 4.20$), right ATC (peak at $[50 \quad 12 \quad -14]$, $t = 5.63$), and bilateral IFG (the right hemisphere: peak at $[54 \quad 21 \quad -6]$, $t = 5.83$; the left hemisphere: peak at $[-48 \quad 21 \quad -10]$, $t = 5.33$; Figures 4(c) and 4(f)). The activated bilateral visual areas were identified to be selective for visual processing of the human body (extrastriate body area, EBA) [46]. For the lip-reading condition, we found significantly greater connection strengths in the bilateral FFA (the right hemisphere: peak at $[38 \quad -58 \quad -12]$, $t = 7.38$; the left hemisphere: peak at $[-26 \quad -56 \quad -10]$, $t = 5.88$, Figure 4(d)), right ATC (peak at $[58 \quad -2 \quad -10]$, $t = 6.13$), and right IFG (peak at $[52 \quad 21 \quad 20]$, $t = 3.80$; Figure 4(g)). The FFA, which is well known as an area involved in the processing of face information [47], was activated in both the sign language and the lip-reading conditions. In short, in comparison with the checkerboard stimulus, the STC activity induced by language stimuli received extra and common connections from the ATC (e.g., the temporal pole) and frontal (e.g., IFG) regions. Additionally, the sensory component was mainly from visual areas (including the VWFA, EBA, and FFA) that seemed highly selective to stimulus features.

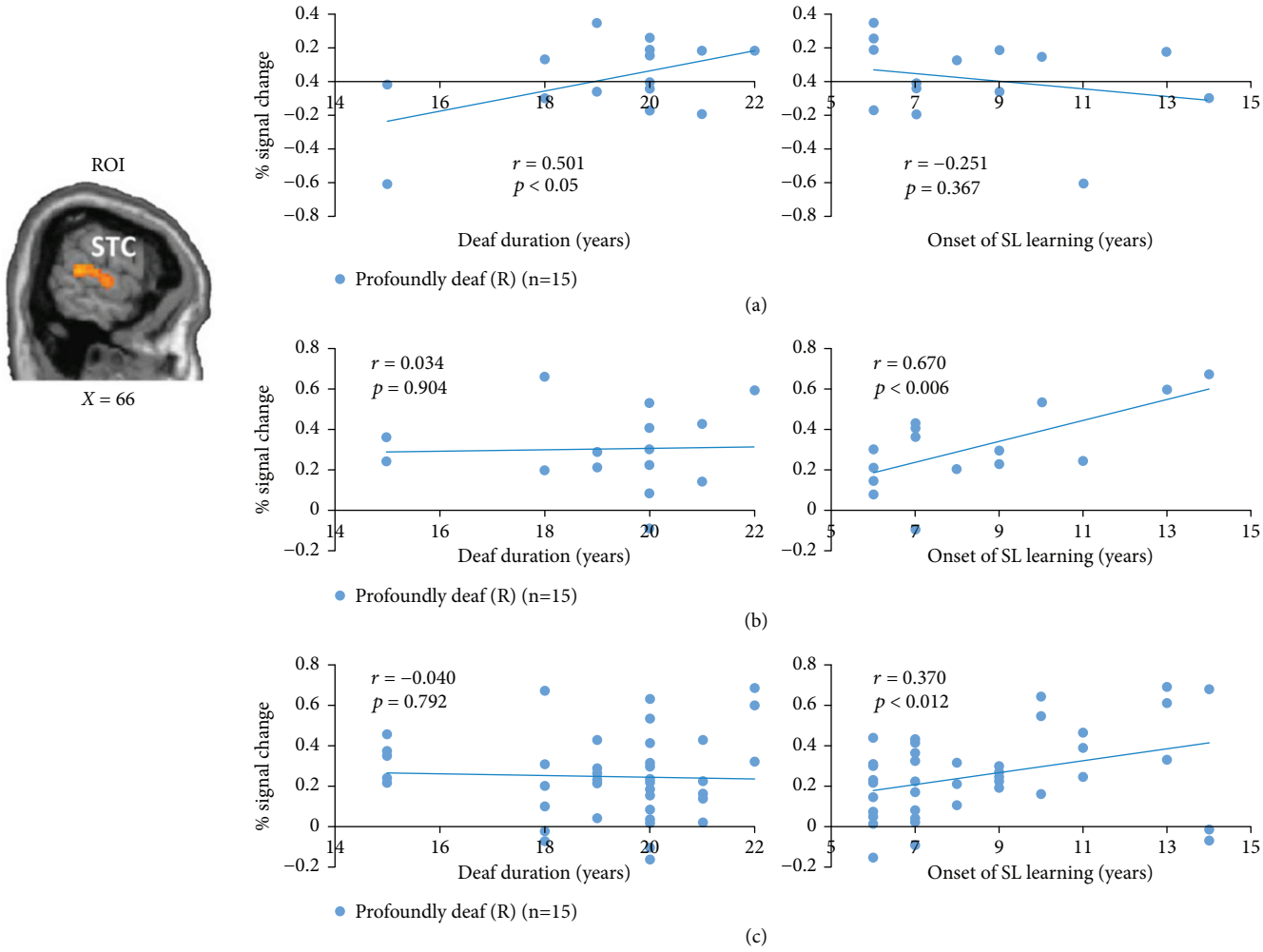

Figure 3: Correlations between superior temporal cortex (STC) activations and duration of deafness and onset of sign language learning in the profoundly deaf group. (a) A sagittal slice depicting the STC region of interest (ROI, selected based on the brain map showing the Group effect, Figure 2(b)) in the right hemisphere. Significant correlations were found in the profoundly deaf group ($n = 15$) between right STC activity for the checkerboard and duration of deafness ($r = 0.501$, $p < 0.05$, Bonferroni corrected), but not between this activation and the onset of sign language learning (the age of starting to learn sign language) ($r = -0.251$, $p = 0.367$). (b) In contrast, significant positive correlation was found between the activation for sign language and the onset of sign language learning ($r = 0.670$, $p < 0.006$, corrected), but not between the activation and hearing loss duration ($r = 0.034$, $p = 0.904$). (c) In the profoundly deaf group ($n = 15$), the STC activity induced by all the visual language stimuli (including words, sign language, and lip-reading) was correlated with the onset of sign language learning ($r = 0.370$, $p < 0.012$, corrected), but not with the duration of deafness ($r = -0.04$, $p = 0.792$).

3.4. Dynamic Causal Modeling. Although we found that the visual cortical areas, ATC, and IFG showed functional connections with STC under the language condition, we still do not know the causal direction between these brain regions. Dynamic causal modeling (DCM) is a generic Bayesian framework for inferring interactions among hidden neural states from measurements of brain activity and has been used in early blind individuals [48, 49]. Thus, we used DCM and Bayesian model selection to explore how language components reach the STC in deaf subjects by comparing six plausible models (Figure 5(a)). Random effects Bayesian model selection showed that cross-modal activity observed in the STC of deaf subjects was best explained by the feedback connection from IFG/ATC (Figure 5(b), left, with feedback; exceedance probability of 0.97) and feed-forward connection from V1 (Figure 5(b) right, V1 to STC; exceedance probability of 0.43; and V1 to STC/ACT; exceedance probability of 0.30) (in model 1, Figure 5(c); exceedance probability of 0.44). The result strongly suggested that the feedback component from language circuit (ATC and IFG) and the feed-forward component from the sensory region were both involved in the induction of cross-modal plasticity in the STC under the language condition.

3.5. Representational Similarity of Cross-Modal Activation in the STC. We finally wanted to explore whether cross-modal activities in the STC shared the same spatial activity pattern when in receipt of distinct contributions from occipital and temporal-frontal areas. We used a multivariate pattern analysis technique known as representational similarity analysis

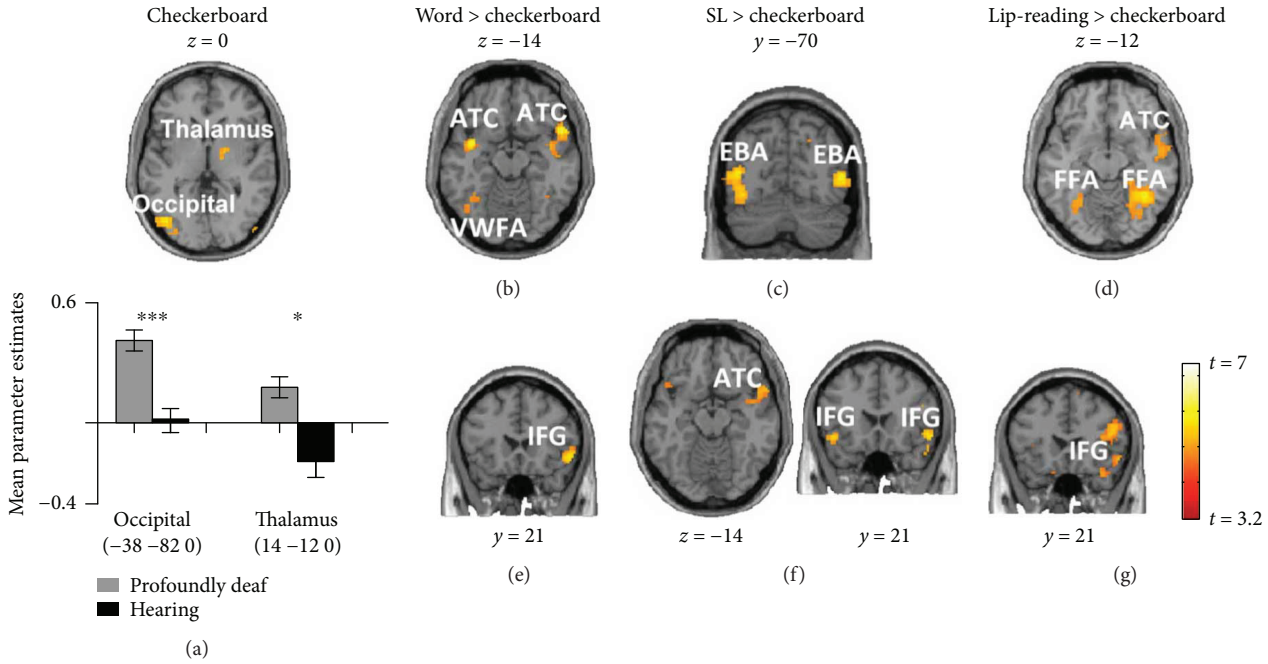

FIGURE 4: Differences in functional connectivity of the superior temporal cortex (STC) between the profoundly deaf and the hearing groups and between the checkerboard and the language conditions. Brain slices depicting the significant differences in functional connectivity between the profoundly deaf and the hearing groups ($p < 0.001$, FDR $p < 0.05$ corrected) with the seed region set in the right STC. For the checkerboard stimulus (a), significantly enhanced functional connectivity between profoundly deaf and hearing subjects was found in the left occipital cortex and right thalamus. In comparison with the checkerboard (whole brain, $p < 0.001$, FDR $p < 0.05$ corrected), for the word condition (b, e), greater connectivity was shown in the visual word form area, bilateral anterior temporal cortex, and right inferior frontal gyrus. For sign language (c, f), the bilateral extrastriate body area, right ATC, the bilateral FFA, and the bilateral IFG were identified as having strong functional connectivity with the right STC. For lip-reading stimuli (d, g), the bilateral FFA, right ATC and right IFG showed higher functional connectivity with the right STC. Asterisks denote a significant difference between the profoundly deaf group and the hearing group. Error bars indicate 1 standard error. $^{***}p < 0.001$ and $^{*}p < 0.05$.

(RSA) [39] to examine how the spatial pattern of BOLD signals over voxels varied in response to different visual stimuli. Per subject, the representational dissimilarity matrixes (RDMs) comprised correlation distances (1 correlation coefficient) between the images from the blocks for each condition in both the profoundly deaf and the residual hearing groups, which yielded a 4×4 matrix. The four conditions were separated into two categories: nonlanguage (checkerboard) and language (words, sign language, and lip-reading). We then compared the correlation coefficient in the three pairs between the nonlanguage and the language conditions (category C-L) with the three pairs within the language conditions (category L-L) for each subject. Results showed that correlation coefficients between the checkerboard and any of the language-related stimuli in the bilateral STC were significantly lower than those between any two language-related stimuli in both the profoundly deaf (Figure 6(a), the left hemisphere, t-test, $p < 0.0001$; the right hemisphere, t-test, $p < 0.005$) and the residual hearing groups (Figure 6(a), the left hemisphere, $p < 0.0001$; the right hemisphere, $p < 0.05$). As a control comparison, no significant differences in RSA were found in the primary visual cortex in either the profoundly deaf (Figure 6(b), the left hemisphere, t-test, $p > 0.65$; the right hemisphere, t-test, $p > 0.81$) or the residual hearing individuals (Figure 6(b), the left hemisphere, t-test, $p > 0.72$; the right hemisphere, t-test, $p > 0.87$).

4. Discussion

Relative to hearing subjects, both profoundly deaf and residual hearing subjects showed enhanced STC responses to checkerboard, word, and sign language stimuli, which confirmed the existence of cross-modal plasticity after auditory deprivation [2, 14, 35, 50, 51]. While Lambertz et al. [51] reported that cortical reorganization of the auditory cortex was only present in profoundly deaf subjects not in subjects with residual hearing ability, our results showed that such plasticity existed in both groups of hearing-impaired subjects. One possible interpretation could be that intensive behavioral and perceptual training caused neuroplasticity in the late-onset sensory deprivation [30]. Despite the fact that there are differences between pre- and postlingually deaf individuals, cross-modal activity is consistently found in postlingually deaf CI patients as well as in mild to moderately hearing impaired individuals [33, 52–54]. Hearing subjects also showed significant STC responses to lip-reading in the present study, which is compatible with previous observations indicating that silent speech reading activates lateral parts of the superior temporal plane in hearing adults [15, 20–23].

Although sensory deprivation triggers cortical reorganization, the origin of anatomical and functional changes observed in the STC of deaf individuals is not only sensory

Table 4: Difference in functional connections with the right STC as a seed region.

Contrast	Brain region	Number of voxels	Peak coordinates			T value
			X	Y	Z	
Checkerboard: profoundly deaf versus hearing group	Occipital_Middle_Left	399	−38	−82	0	5.23
	Occipital_Middle_Left	318	−24	−94	8	5.21
	Cerebellum_Left	40	−32	−60	−48	4.71
	ParaHippocampal_Right	15	30	−16	−28	4.38
	Cingulum_Middle_Right	58	10	26	32	4.15
	Thalamus_Right	35	14	−12	0	3.89
	Supplementary_Motor_Right	11	12	18	60	3.73
	Cerebellum_Left	28	−30	−58	−24	3.71
Word: (word: profoundly deaf versus hearing groups) versus (checkerboard: profoundly deaf versus hearing)	Frontal_Inferior_Orb_Right	74	54	21	3	6.67
	Temporal_Pole_Superior_Right	54	58	14	−16	6.02
	Temporal_Pole_Superior_Left	49	−40	2	−16	4.95
	Visual_word_form_area_Left	47	−42	−58	−14	4.71
	Occipital_Middle_Right	32	42	−74	14	4.06
	Cingulum_Middle_Right	23	6	4	40	3.88
Sign language: (sign language: profoundly deaf versus hearing groups) versus (checkerboard: profoundly deaf versus hearing)	Occipital_Middle_Left	253	−44	−70	8	5.98
	Occipital_Middle_Right	124	52	−68	6	6.84
	Fusiform_Left	67	−32	−60	−16	4.20
	Fusiform_Right	51	42	−52	−16	5.70
	Temporal_Pole_Superior_Right	44	50	12	−14	5.89
	Temporal_Pole_Superior_Left	19	−44	14	−16	4.13
	Frontal_Inferior_Orb_Left	37	54	21	−6	4.31
	Frontal_Inferior_Orb_Right	30	−48	21	−10	5.83
	Supplementary_Motor_Area	39	6	10	64	4.39
	Parietal_Superior_Left	12	−20	−54	50	4.23
Lip-reading: (lip-reading: profoundly deaf versus hearing groups) versus (checkerboard: profoundly deaf versus hearing)	Fusiform_Left	122	−26	−56	−10	5.45
	Fusiform_Right	146	38	−58	−12	7.85
	Temporal_Pole_Superior_Right	97	58	−2	−10	5.77
	Frontal_Inferior_Tri_Right	43	48	22	18	3.79
	Frontal_Inferior_Orb_Right	21	52	21	20	3.53
	Precentral_Left	19	−44	−6	−48	4.25
	Precentral_Right	22	52	4	46	6.87
	Supplementary_Motor_Area	13	−4	6	60	5.13

Note: peak coordinates refer to stereotactic coordinates in MNI space; $p < 0.001$, FDR $p < 0.05$ corrected.

(feed-forward) but also cognitive (feedback), such as in the use of sign language and speech reading [30]. The purely visual stimulus (checkerboard) provoked activations in the right STC, which showed correlations only with the duration of deafness [52], and strong functional connectivity with the visual cortex and thalamus, implying the contribution of sensory components to the plasticity. However, the cognitive stimuli with language content induced activations in both the right and the left STC, which exhibited strong association only with the experience of sign language learning, and enhanced functional connections with not only visual cortical areas but also the ATC and IFG, suggesting a strong potential top-down modulation of plasticity induced by the linguistic components of the cognitive stimuli. The DCM analysis further confirmed the information flow triggered by the visual stimuli with language content, by showing a strong feedback effect from IFG/ATC and a feed-forward effect from V1 to STC.

In deaf humans, it was found that auditory areas preserved the task-specific activation pattern independent of input modality (visual or auditory), suggesting the task-specific reorganization during the cortical plasticity [55]. Cardin et al. [18] showed that auditory deprivation and language experience cause activations of different areas of the auditory cortex when two groups of deaf subjects with different language experience are watching sign language. In the auditory cortical areas of deaf animals, Lomber with his colleagues showed that the neural basis for enhanced visual functions was located to specific auditory cortical subregions. The improved localization of visual stimuli was eliminated by deactivating the posterior auditory cortex, while the enhanced sensitivity to visual motion was blocked

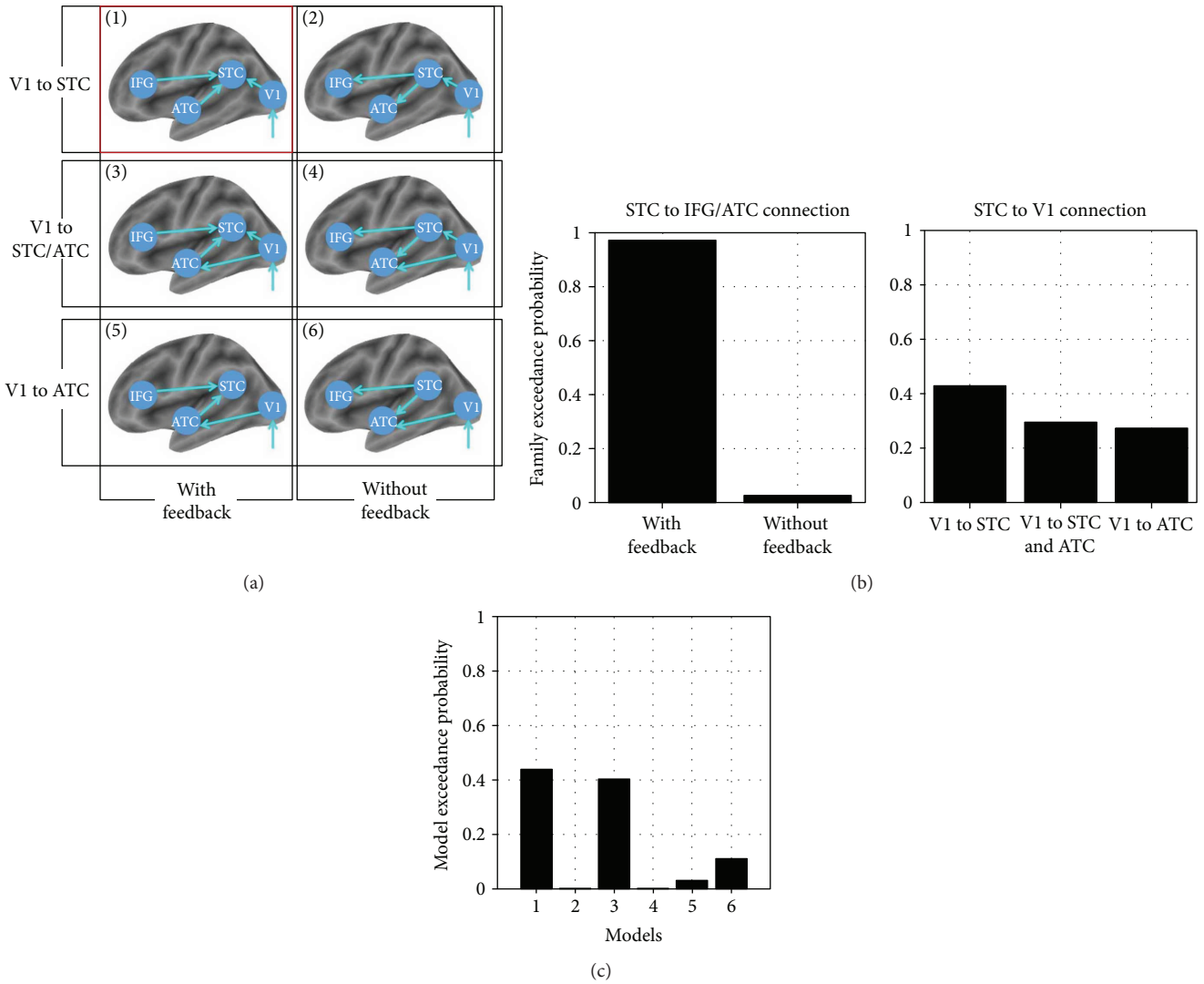

Figure 5: Dynamic causal modeling. (a) The six dynamic causal models used for Bayesian model comparison. Each model receives (parameterized) input at primary visual cortex (V1) source under the language condition in deaf participants. (b) Family-wise Bayesian model selection was used to establish the best neural network architecture for the feedback and feed-forward effect to the STC. Families of models with feedback from IFG/ATC to STC and with feed-forward from V1 to STC/ATC best explained the data. (c) Random effects Bayesian model selection showed model 1 (marked with the red box in (a)) best fits the data for the language condition in deaf individuals.

by disabling the dorsal auditory cortex [25, 56, 57]. Land et al. [58] demonstrated that visually responsive and auditory-responsive neurons in the higher-order auditory cortex of deaf cats form two distinct populations that do not show bimodal interactions. However, we still know little of how other brain regions contribute to the task-specific activations in the auditory cortex. In the present study, although neural reorganization in deaf individuals permits both the sensory and language inputs to reach the STC, the RSA result suggested that the functions of the two components were segregated within the reorganized auditory area, which confirmed the functional segregation hypothesis. Furthermore, our functional connectivity analysis suggested that the stimulus-specific activation in STC was probably developed via different neural pathways. Specifically, the sensory component of stimuli was found to be highly stimulus-specific. During the word presentation, visual areas functionally connected with the STC were located exactly within the visual word form area (only in the left hemisphere, Figure 4(b)) which is a region demonstrated to be involved in the identification of words and letters from lower-level shape images prior to association with phonology or semantics [44, 45, 59]. During the sign language and lip-reading stimuli, the functionally connected visual areas were identified as being in the extrastriate body area and fusiform face area, which is known to be especially involved in facial recognition [47, 60] and human body representation [46]. In contrast, for the language component, the cross-modal plasticity shaped by sign language could also be generalized to the responses to other language stimuli (Figure 3(c) and Figure S1). Additionally, STC activities induced by the word, sign language, and lip-reading stimuli were functionally connected with a similar neural network consisting of the temporal pole areas and inferior frontal regions (part of Broca's

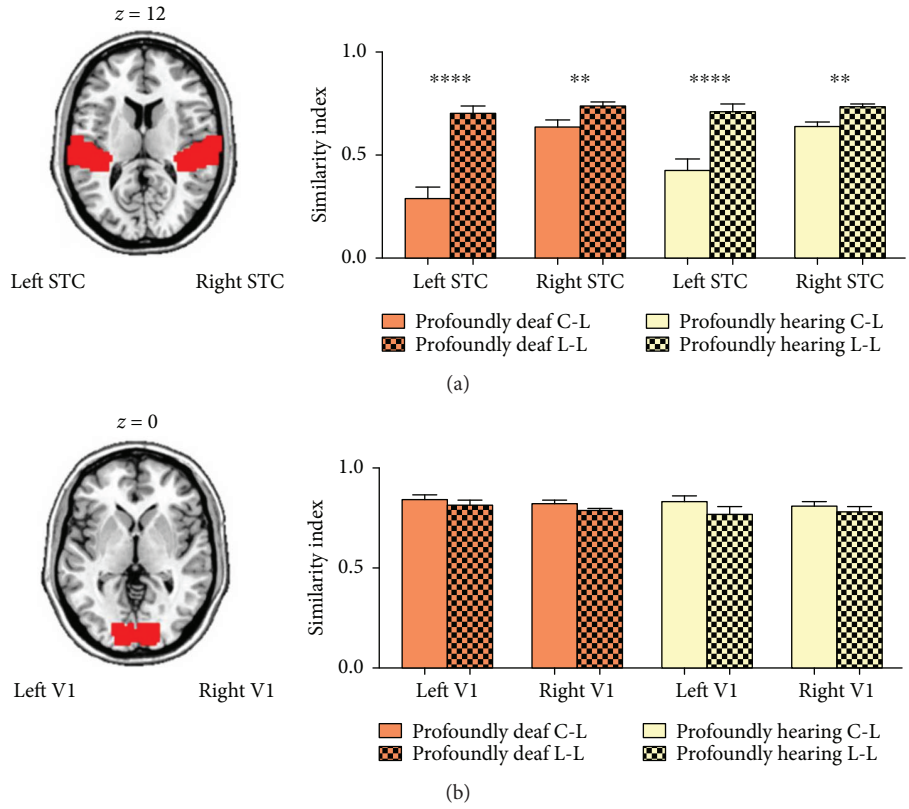

Figure 6: Representational similarities in activation patterns in the superior temporal cortex (STC) and primary visual cortex. (a) Axial slice depicting the auditory region of interest (ROI; Brodmann areas (BAs) 41 and 42) in red. The bars indicate the similarity (correlation coefficient index) of the spatial activation patterns between visual stimuli within the ROI. The solid bars depict the averaged similarities between checkerboard and language-related stimuli (C-L), including sign language, words, and lip-reading, in both the profoundly deaf group (in orange) and the residual hearing group (in yellow). The grid bars depict the average correlation coefficients between language-related stimuli (L-L). The correlation coefficient between language-related stimuli in the bilateral auditory ROIs was significantly higher than that between checkerboard and language-related stimuli in both the profoundly deaf group (left hemisphere: $p < 0.0001$, right hemisphere: $p < 0.001$) and the residual hearing group (left hemisphere: $p < 0.0001$, right hemisphere: $p < 0.0016$). (b) Such differences in representational similarity were not observed in the primary visual cortex (V1; BA17). $^{**}p < 0.01$; $^{****}p < 0.0001$. Error bars represent 1 standard error.

area) (Figure 4), which was shown to be involved in semantic processing in the language system [61]. These results may suggest that the language components from different visual stimuli share a common language circuit for top-down visual-auditory reorganization.

The difference between checkerboard and language-related stimuli (Figure 6(a)) cannot be interpreted by other experimental accounts. For example, one may argue that the language stimuli have a higher visual richness than the purely visual stimuli, which may therefore have induced higher similarity within language stimuli. This seems unlikely, as such a difference in similarity was not shown in the primary visual cortex (Figure 6(b)).

Previous studies on prelingual deaf groups have proposed a link between poor speech outcomes and exposure to a visual language and indicate that the incapacity for processing auditory signals (poorer outcomes of cochlear implant) is due to usurping of the auditory cortex functionality by visual language [31, 32, 62–64]. However, to the contrary, some studies indicate that proficiency with speech reading is linked to better outcomes of cochlear implant [31, 33, 65–68]. Thus, together with other animal studies, our human imaging results on functional segregation suggest that, although exposure to sign language may indeed partially take over the auditory cortex, the auditory regions could still preserve the ability to process auditory signals following cochlear implants, with this being facilitated through the recruitment of new populations of neurons or different spatial activity patterns.

In conclusion, both language and sensory components contribute to the cross-modal plasticity of the STC in deaf people; these are associated with hearing loss duration and language experience, respectively. The feed-forward signal of sensory input is highly stimulus-specific, while the feedback signal from language input is more associated with a common neural network. Finally, even though both pathways activate auditory areas in deaf people, they seem functionally segregated in respect to cross-modal plasticity. In summary, this study provides important and unique evidence for understanding the neural circuits involved in cross-modal plasticity in deaf people and may guide clinicians in consideration of cochlear implants or hearing recovery.

Conflicts of Interest

The authors have no financial conflict of interests.

Authors' Contributions

Mochun Que and Xinjian Jiang contributed equally to this work.

Acknowledgments

The authors are grateful to all participants. They thank the Institute of Speech and Hearing Science, the Shanghai Deaf Youth Technical School, and the Special Education Department of Shanghai Applied Technology Institute. They thank Dr. Yixuan Ku for the initial discussion on this study. They also thank Haidan Lu, Chunyan Lin, Hang Zhao, and Yan Xiu for the recruitment of participants; Di Zhao for the help with data collection; and Dr. Qing Cai, Lei Li, and Shuai Wang for the suggestions on data analysis. The research leading to these results received funding from the National Key Fundamental Research (973) Program of China (Grant 2013CB329501), the National Natural Science Foundation of China (31571084), and Shanghai Pujiang Plan (15PJ1402000) to Liping Wang.

Supplementary Materials

Supplemental information includes one figure, Supplemental visual materials, and Supplemental questionnaire (translated to English) after scanning. *(Supplementary Materials)*

References

[1] T. Kujala, K. Alho, and R. Naatanen, "Cross-modal reorganization of human cortical functions," *Trends in Neurosciences*, vol. 23, no. 3, pp. 115–120, 2000.

[2] E. M. Finney, I. Fine, and K. R. Dobkins, "Visual stimuli activate auditory cortex in the deaf," *Nature Neuroscience*, vol. 4, no. 12, pp. 1171–1173, 2001.

[3] B. A. Armstrong, H. J. Neville, S. A. Hillyard, and T. V. Mitchell, "Auditory deprivation affects processing of motion, but not color," *Cognitive Brain Research*, vol. 14, no. 3, pp. 422–434, 2002.

[4] I. Fine, E. M. Finney, G. M. Boynton, and K. R. Dobkins, "Comparing the effects of auditory deprivation and sign language within the auditory and visual cortex," *Journal of Cognitive Neuroscience*, vol. 17, no. 10, pp. 1621–1637, 2005.

[5] N. Sadato, T. Okada, M. Honda et al., "Cross-modal integration and plastic changes revealed by lip movement, random-dot motion and sign languages in the hearing and deaf," *Cerebral Cortex*, vol. 15, no. 8, pp. 1113–1122, 2005.

[6] P. Vachon, P. Voss, M. Lassonde et al., "Reorganization of the auditory, visual and multimodal areas in early deaf individuals," *Neuroscience*, vol. 245, pp. 50–60, 2013.

[7] D. Bottari, B. Heimler, A. Caclin, A. Dalmolin, M. H. Giard, and F. Pavani, "Visual change detection recruits auditory cortices in early deafness," *NeuroImage*, vol. 94, pp. 172–184, 2014.

[8] M. M. Shiell, F. Champoux, and R. J. Zatorre, "Reorganization of auditory cortex in early-deaf people: functional connectivity and relationship to hearing aid use," *Journal of Cognitive Neuroscience*, vol. 27, no. 1, pp. 150–163, 2015.

[9] T. Allison, A. Puce, and G. McCarthy, "Social perception from visual cues: role of the STS region," *Trends in Cognitive Sciences*, vol. 4, no. 7, pp. 267–278, 2000.

[10] M. MacSweeney, R. Campbell, B. Woll et al., "Dissociating linguistic and nonlinguistic gestural communication in the brain," *NeuroImage*, vol. 22, no. 4, pp. 1605–1618, 2004.

[11] D. Corina, Y. S. Chiu, H. Knapp, R. Greenwald, L. San Jose-Robertson, and A. Braun, "Neural correlates of human action observation in hearing and deaf subjects," *Brain Research*, vol. 1152, pp. 111–129, 2007.

[12] H. J. Neville and D. Bavelier, "Neural organization and plasticity of language," *Current Opinion in Neurobiology*, vol. 8, no. 2, pp. 254–258, 1998.

[13] L. A. Petitto, R. J. Zatorre, K. Gauna, E. J. Nikelski, D. Dostie, and A. C. Evans, "Speech-like cerebral activity in profoundly deaf people processing signed languages: implications for the neural basis of human language," *Proceedings of the National Academy of Sciences of the United States of America*, vol. 97, no. 25, pp. 13961–13966, 2000.

[14] M. MacSweeney, B. Woll, R. Campbell et al., "Neural systems underlying British sign language and audio-visual English processing in native users," *Brain*, vol. 125, no. 7, pp. 1583–1593, 2002.

[15] C. M. Capek, M. MacSweeney, B. Woll et al., "Cortical circuits for silent speechreading in deaf and hearing people," *Neuropsychologia*, vol. 46, no. 5, pp. 1233–1241, 2008.

[16] M. MacSweeney, C. M. Capek, R. Campbell, and B. Woll, "The signing brain: the neurobiology of sign language," *Trends in Cognitive Sciences*, vol. 12, no. 11, pp. 432–440, 2008.

[17] K. Emmorey, J. Xu, and A. Braun, "Neural responses to meaningless pseudosigns: evidence for sign-based phonetic processing in superior temporal cortex," *Brain and Language*, vol. 117, no. 1, pp. 34–38, 2011.

[18] V. Cardin, E. Orfanidou, J. Rönnberg, C. M. Capek, M. Rudner, and B. Woll, "Dissociating cognitive and sensory neural plasticity in human superior temporal cortex," *Nature Communications*, vol. 4, p. 1473, 2013.

[19] A. Moreno, F. Limousin, S. Dehaene, and C. Pallier, "Brain correlates of constituent structure in sign language comprehension," *NeuroImage*, vol. 167, pp. 151–161, 2017.

[20] G. A. Calvert, E. T. Bullmore, M. J. Brammer et al., "Activation of auditory cortex during silent lipreading," *Science*, vol. 276, no. 5312, pp. 593–596, 1997.

[21] G. A. Calvert and R. Campbell, "Reading speech from still and moving faces: the neural substrates of visible speech," *Journal of Cognitive Neuroscience*, vol. 15, no. 1, pp. 57–70, 2003.

[22] M. MacSweeney, G. A. Calvert, R. Campbell et al., "Speechreading circuits in people born deaf," *Neuropsychologia*, vol. 40, no. 7, pp. 801–807, 2002.

[23] R. A. Reale, G. A. Calvert, T. Thesen et al., "Auditory-visual processing represented in the human superior temporal gyrus," *Neuroscience*, vol. 145, no. 1, pp. 162–184, 2007.

[24] A. Kral, R. Hartmann, J. Tillein, S. Heid, and R. Klinke, "Hearing after congenital deafness: central auditory plasticity and sensory deprivation," *Cerebral Cortex*, vol. 12, no. 8, pp. 797–807, 2002.

[25] S. G. Lomber, M. A. Meredith, and A. Kral, "Cross-modal plasticity in specific auditory cortices underlies visual

compensations in the deaf," *Nature Neuroscience*, vol. 13, no. 11, pp. 1421–1427, 2010.

[26] M. A. Meredith, H. R. Clemo, S. B. Corley, N. Chabot, and S. G. Lomber, "Cortical and thalamic connectivity of the auditory anterior ectosylvian cortex of early-deaf cats: implications for neural mechanisms of crossmodal plasticity," *Hearing Research*, vol. 333, pp. 25–36, 2016.

[27] N. Chabot, B. E. Butler, and S. G. Lomber, "Differential modification of cortical and thalamic projections to cat primary auditory cortex following early- and late-onset deafness," *The Journal of Comparative Neurology*, vol. 523, no. 15, pp. 2297–2320, 2015.

[28] B. E. Butler, N. Chabot, and S. G. Lomber, "Quantifying and comparing the pattern of thalamic and cortical projections to the posterior auditory field in hearing and deaf cats," *The Journal of Comparative Neurology*, vol. 524, no. 15, pp. 3042–3063, 2016.

[29] C. R. Lyness, B. Woll, R. Campbell, and V. Cardin, "How does visual language affect crossmodal plasticity and cochlear implant success?," *Neuroscience & Biobehavioral Reviews*, vol. 37, no. 10, pp. 2621–2630, 2013.

[30] L. B. Merabet and A. Pascual-Leone, "Neural reorganization following sensory loss: the opportunity of change," *Nature Reviews Neuroscience*, vol. 11, no. 1, pp. 44–52, 2010.

[31] H. J. Lee, A. L. Giraud, E. Kang et al., "Cortical activity at rest predicts cochlear implantation outcome," *Cerebral Cortex*, vol. 17, no. 4, pp. 909–917, 2007.

[32] A. Sharma, J. Campbell, and G. Cardon, "Developmental and cross-modal plasticity in deafness: evidence from the P1 and N1 event related potentials in cochlear implanted children," *International Journal of Psychophysiology*, vol. 95, no. 2, pp. 135–144, 2015.

[33] M. Stropahl, K. Plotz, R. Schönfeld et al., "Cross-modal reorganization in cochlear implant users: auditory cortex contributes to visual face processing," *NeuroImage*, vol. 121, pp. 159–170, 2015.

[34] J. S. Lee, D. S. Lee, S. H. Oh et al., "PET evidence of neuroplasticity in adult auditory cortex of postlingual deafness," *The Journal of Nuclear Medicine*, vol. 44, no. 9, pp. 1435–1439, 2003.

[35] E. M. Finney, B. A. Clementz, G. Hickok, and K. R. Dobkins, "Visual stimuli activate auditory cortex in deaf subjects: evidence from MEG," *NeuroReport*, vol. 14, no. 11, pp. 1425–1427, 2003.

[36] H. J. Lee, E. Truy, G. Mamou, D. Sappey-Marinier, and A. L. Giraud, "Visual speech circuits in profound acquired deafness: a possible role for latent multimodal connectivity," *Brain*, vol. 130, no. 11, pp. 2929–2941, 2007.

[37] M. K. Leonard, N. Ferjan Ramirez, C. Torres et al., "Signed words in the congenitally deaf evoke typical late lexicosemantic responses with no early visual responses in left superior temporal cortex," *The Journal of Neuroscience*, vol. 32, no. 28, pp. 9700–9705, 2012.

[38] K. J. Friston and R. J. Dolan, "Computational and dynamic models in neuroimaging," *NeuroImage*, vol. 52, no. 3, pp. 752–765, 2010.

[39] N. Kriegeskorte, M. Mur, and P. Bandettini, "Representational similarity analysis - connecting the branches of systems neuroscience," *Frontiers in Systems Neuroscience*, vol. 2, p. 4, 2008.

[40] World Health Organization, *International Classification of Impairments, Disabilities, and Handicaps: A Manual of Classification Relating to the Consequences of Disease; publ. for Trial Purposes in Accordance with Resolution WHA29. 35 for the Twenty-Ninth World Health Assembly, May 1976*, World Health Organization, Geneva, 1980.

[41] S. Whitfield-Gabrieli and A. Nieto-Castanon, "*Conn*: a functional connectivity toolbox for correlated and anticorrelated brain networks," *Brain Connectivity*, vol. 2, no. 3, pp. 125–141, 2012.

[42] J. L. Lancaster, M. G. Woldorff, L. M. Parsons et al., "Automated Talairach atlas labels for functional brain mapping," *Human Brain Mapping*, vol. 10, no. 3, pp. 120–131, 2000.

[43] S. Brem, S. Bach, K. Kucian et al., "Brain sensitivity to print emerges when children learn letter–speech sound correspondences," *Proceedings of the National Academy of Sciences of the United States of America*, vol. 107, no. 17, pp. 7939–7944, 2010.

[44] L. Cohen and S. Dehaene, "Specialization within the ventral stream: the case for the visual word form area," *NeuroImage*, vol. 22, no. 1, pp. 466–476, 2004.

[45] S. Dehaene and L. Cohen, "The unique role of the visual word form area in reading," *Trends in Cognitive Sciences*, vol. 15, no. 6, pp. 254–262, 2011.

[46] P. E. Downing, Y. Jiang, M. Shuman, and N. Kanwisher, "A cortical area selective for visual processing of the human body," *Science*, vol. 293, no. 5539, pp. 2470–2473, 2001.

[47] N. Kanwisher, J. McDermott, and M. M. Chun, "The fusiform face area: a module in human extrastriate cortex specialized for face perception," *The Journal of Neuroscience*, vol. 17, no. 11, pp. 4302–4311, 1997.

[48] O. Collignon, G. Dormal, A. de Heering, F. Lepore, T. L. Lewis, and D. Maurer, "Long-lasting crossmodal cortical reorganization triggered by brief postnatal visual deprivation," *Current Biology*, vol. 25, no. 18, pp. 2379–2383, 2015.

[49] C. Klinge, F. Eippert, B. Roder, and C. Buchel, "Corticocortical connections mediate primary visual cortex responses to auditory stimulation in the blind," *The Journal of Neuroscience*, vol. 30, no. 38, pp. 12798–12805, 2010.

[50] H. Nishimura, K. Hashikawa, K. Doi et al., "Sign language 'heard' in the auditory cortex," *Nature*, vol. 397, no. 6715, p. 116, 1999.

[51] N. Lambertz, E. R. Gizewski, A. de Greiff, and M. Forsting, "Cross-modal plasticity in deaf subjects dependent on the extent of hearing loss," *Cognitive Brain Research*, vol. 25, no. 3, pp. 884–890, 2005.

[52] P. Sandmann, N. Dillier, T. Eichele et al., "Visual activation of auditory cortex reflects maladaptive plasticity in cochlear implant users," *Brain*, vol. 135, no. 2, pp. 555–568, 2012.

[53] M. Stropahl and S. Debener, "Auditory cross-modal reorganization in cochlear implant users indicates audio-visual integration," *NeuroImage: Clinical*, vol. 16, pp. 514–523, 2017.

[54] J. Campbell and A. Sharma, "Cross-modal re-organization in adults with early stage hearing loss," *PLoS One*, vol. 9, no. 2, article e90594, 2014.

[55] Ł. Bola, M. Zimmermann, P. Mostowski et al., "Task-specific reorganization of the auditory cortex in deaf humans," *Proceedings of the National Academy of Sciences of the United States of America*, vol. 114, no. 4, pp. E600–E609, 2017.

[56] S. G. Lomber, "What is the function of auditory cortex when it develops in the absence of acoustic input?," *Cognitive Development*, vol. 42, pp. 49–61, 2017.

[57] M. A. Meredith, H. R. Clemo, and S. G. Lomber, "Is territorial expansion a mechanism for crossmodal plasticity?," *European Journal of Neuroscience*, vol. 45, no. 9, pp. 1165–1176, 2017.

[58] R. Land, P. Baumhoff, J. Tillein, S. G. Lomber, P. Hubka, and A. Kral, "Cross-modal plasticity in higher-order auditory cortex of congenitally deaf cats does not limit auditory responsiveness to cochlear implants," *The Journal of Neuroscience*, vol. 36, no. 23, pp. 6175–6185, 2016.

[59] C. Liu, W. T. Zhang, Y. Y. Tang et al., "The visual word form area: evidence from an fMRI study of implicit processing of Chinese characters," *NeuroImage*, vol. 40, no. 3, pp. 1350–1361, 2008.

[60] N. Kanwisher and G. Yovel, "The fusiform face area: a cortical region specialized for the perception of faces," *Philosophical Transactions of the Royal Society of London Series B: Biological Sciences*, vol. 361, no. 1476, pp. 2109–2128, 2006.

[61] S. Bookheimer, "Functional MRI of language: new approaches to understanding the cortical organization of semantic processing," *Annual Review of Neuroscience*, vol. 25, no. 1, pp. 151–188, 2002.

[62] S. Hirano, Y. Naito, H. Kojima et al., "Functional differentiation of the auditory association area in prelingually deaf subjects," *Auris Nasus Larynx*, vol. 27, no. 4, pp. 303–310, 2000.

[63] D. S. Lee, J. S. Lee, S. H. Oh et al., "Cross-modal plasticity and cochlear implants," *Nature*, vol. 409, no. 6817, pp. 149-150, 2001.

[64] M. E. Doucet, F. Bergeron, M. Lassonde, P. Ferron, and F. Lepore, "Cross-modal reorganization and speech perception in cochlear implant users," *Brain*, vol. 129, no. 12, pp. 3376–3383, 2006.

[65] H. J. Lee, E. Kang, S. H. Oh et al., "Preoperative differences of cerebral metabolism relate to the outcome of cochlear implants in congenitally deaf children," *Hearing Research*, vol. 203, no. 1-2, pp. 2–9, 2005.

[66] T. R. Bergeson, D. B. Pisoni, and R. A. O. Davis, "Development of audiovisual comprehension skills in prelingually deaf children with cochlear implants," *Ear and Hearing*, vol. 26, no. 2, pp. 149–164, 2005.

[67] S. Hassanzadeh, "Outcomes of cochlear implantation in deaf children of deaf parents: comparative study," *The Journal of Laryngology & Otology*, vol. 126, no. 10, pp. 989–994, 2012.

[68] C. A. Anderson, I. M. Wiggins, P. T. Kitterick, and D. E. H. Hartley, "Adaptive benefit of cross-modal plasticity following cochlear implantation in deaf adults," *Proceedings of the National Academy of Sciences of the United States of America*, vol. 114, no. 38, pp. 10256–10261, 2017.

Hindawi
Neural Plasticity
Volume 2018, Article ID 9870985, 11 pages
https://doi.org/10.1155/2018/9870985

Research Article

Region-Dependent Alterations in Cognitive Function and ERK1/2 Signaling in the PFC in Rats after Social Defeat Stress

Qiong Wang,[1,2] Feng Shao,[3] and Weiwen Wang[1,2]

[1]*CAS Key Laboratory of Mental Health, Institute of Psychology, Beijing, China, School of Education, Zhengzhou University, Zhengzhou, China*
[2]*The University of Chinese Academy of Sciences, Beijing, China*
[3]*School of Psychological and Cognitive Sciences, Beijing Key Laboratory of Behavior and Mental Health, Peking University, Beijing, China*

Correspondence should be addressed to Feng Shao; shaof@pku.edu.cn and Weiwen Wang; wangww@psych.ac.cn

Received 13 January 2018; Accepted 26 February 2018; Published 11 April 2018

Academic Editor: Fang Pan

Cognitive dysfunctions are highly comorbid with depression. Impairments of cognitive flexibility, which are modulated by the monoaminergic system of the prefrontal cortex (PFC), are increasingly recognized as an important component of the pathophysiology and treatment of depression. However, the downstream molecular mechanisms remain unclear. Using a classical model of depression, this study investigated the effects of social defeat stress on emotional behaviors, on cognitive flexibility in the attentional set-shifting task (AST), and on the expression of extracellular signal-regulated kinase 1 and 2 (ERK1 and ERK2) and their downstream signaling molecules cAMP-response element binding protein (CREB) and brain-derived neurotrophic factor (BDNF) in two subregions of the PFC, the medial prefrontal cortex (mPFC), and the orbitofrontal cortex (OFC). The results showed that stress induced emotional and cognitive alterations associated with depression, including a decreased sucrose intake ratio and impaired reversal learning and set-shifting performance in the AST. Additionally, rats in the stress group showed a significant decrease only in ERK2 signaling in the mPFC, while more extensive decreases in both ERK1 signaling and ERK2 signaling were observed in the OFC. Along with the decreased ERK signaling, compared to controls, stressed rats showed downregulation of CREB phosphorylation and BDNF expression in both the OFC and the mPFC. Further analysis showed that behavioral changes were differentially correlated with several molecules in subregions of the PFC. These results suggested that social defeat stress was an effective animal model to induce both emotional and cognitive symptoms of depression and that the dysfunction of ERK signaling activities in the PFC might be a potential underlying biological mechanism.

1. Introduction

Depression is the most common serious psychiatric disorder among those with established sets of emotional and cognitive symptoms. Deficits in cognitive flexibility associated with prefrontal lobe dysfunction have been recognized as an important risk factor for the onset of depression [1, 2]. Additionally, antidepressant treatments, which ameliorate emotional symptoms but do not affect cognitive dysfunction, can predict the reoccurrence of depression and of worsened social function and adaptation [3, 4]. Studies across different species (human, primate, and rodent) have demonstrated that prefrontal monoaminergic systems, which are the main targets of antidepressants, are involved in the modulation of cognitive flexibility [5, 6]. For example, monoaminergic neurotransmitters, especially serotonin (5-HT) in the orbitofrontal cortex (OFC) and norepinephrine (NE) in the medial prefrontal cortex (mPFC), regulate reversal learning and set shifting, respectively, two core components of cognitive flexibility [7–10]. In addition, it has been shown that compared with acute antidepressant treatment, chronic antidepressant treatment has better outcomes for the amelioration of cognitive dysfunctions [11] and similar effects on emotional symptoms [12]. These data suggest that there may be a downstream molecular cascade involved in modulating the emotional and cognitive symptoms of depression.

The extracellular signal-regulated kinase (ERK) signaling pathway in neural cells is regarded as the aggregation point for the effects of monoamines in the brain [13]. Previous studies from us and others have shown that ERK signaling is widely involved in the regulation of neuronal plasticity [14], emotion [15], and learning and memory [16, 17]. For example, inhibition of mPFC ERK signaling pathways can induce depressive behaviors such as anhedonia [15] and impair the retention of fear memory [18]. Our previous study also found that acute microinjection of the stress hormone corticotropin-releasing hormone (CRH) into the locus coeruleus exerted an inverse U-shaped dose-response effect on the performance of cognitive flexibility, especially set shifting, and this effect was correlated with the level of ERK phosphorylation in the mPFC [19]. There are two isomers in the ERK family, ERK1 (42 kD) and ERK2 (44 kD). It has been shown that ERK1 and ERK2 have different roles in the regulation of cognitive function. For example, ERK2 mutant mice showed severe cognitive impairment in an associative learning task, and children with decreased ERK2 levels showed impaired cognitive function [20]. In contrast, there is an enhancement of striatum-dependent LTP in ERK1 knock-out mice, and the enhancement of ERK2 in ERK1 knock-out mice was strongly associated with an improvement in learning and memory [21]. However, it remains unclear whether and how ERK1 and 2 modulate different components of cognitive flexibility mediated by different subregions of the PFC.

The present study was designed to examine the effects of chronic stress on depressive-like behaviors and on the ERK1/2 pathways in different areas of the PFC, as well as on the relationships between those subregions. Social defeat stress, a classical animal model of depression [22], was used to induce depressive alterations with emotional and cognitive symptoms. Sucrose preference, a core parameter of depression, and cognitive flexibility were tested. Rodent cognitive flexibility was assessed via the attentional set-shifting task (AST), a task analogue to the Wisconsin card-sorting task, which sensitively reflects cortical function in humans. In addition, the activities of ERK1 and ERK2 signaling and their downstream targets cAMP-response element binding protein (CREB) and brain-derived neurotrophic factor (BDNF) in the mPFC and OFC were examined. These targets were chosen because CREB is one of the most important nuclear transcription factors downstream of ERK signaling [23], and it further regulates the production of BDNF, an activity-dependent molecule that exerts effects on neuronal activity [24]. There is also an activation of the ERK signaling pathway after binding of BDNF and its receptor TrkB. Therefore, the ERK pathway acts as both an upstream and a downstream signaling pathway of BDNF, both of which form a positive feedback loop [25–27].

2. Materials and Methods

2.1. Animals. Adult male Wistar rats (180–220 g) as intruders were obtained from the Lab Animal Center of the China Academy of Military Medical Sciences (Beijing, China). Animals arrived 7 days before the experiment for acclimation (days 1–7). Rats were maintained on a 12 h light/dark cycle (with the light on at 08:00 am) with food and water available ad libitum except for during the saccharine preference test and the restricted diet period in the AST. Body weights were determined once a week across the whole experimental period. As aggressive residents in the social defeat procedure, adult male Long-Evans rats (650–800 g) were obtained from the Lab Animal Center of the Third Military Medical University of the Chinese PLA (Chongqing, China) and singly housed for at least 14 days for a strong territorial effect.

All experimental procedures were performed with the approval of the Institutional Review Board of the Institute of Psychology at the Chinese Academy of Sciences and according to the guidelines of the National Institutes of Health Guide for the Care and Use of Laboratory Animals (NIH Publication number 80-23).

2.2. Social Defeat Stress. Chronic social defeat stress was widely used as an animal model of depression. After 7 days of acclimation, the intruder rats were randomly assigned to either the social defeat stress ($n = 10$) or the control ($n = 6$) groups. Rats in the stress group received 14 d of social defeat (days 8–21), and the controls were free of stress. The social defeat stress in this study was performed using the "resident-intruder" paradigm as described previously [28]. Briefly, each episode of social stress lasted for 45 min; during the first 15 min, a rat was placed into the home cage territory of an unfamiliar Long-Evans resident that was previously screened for high aggression, and the intruder faced different residents every day. A typical agonistic encounter resulted in intruder subordination or defeat, signaled by the intruder assuming a supine position for at least 3 sec. After the defeat, a wire mesh enclosure was placed in the cage to prevent physical contact between the resident and the intruder but allowing visual, auditory, and olfactory contact for the remaining 30 min of the defeat session. Controls were placed into a novel but unoccupied cage for 45 min daily in the same procedure. Rats were returned to their home cages after each session.

2.3. Sucrose Preference Test. Rats were deprived of water and food for 20 h (beginning at 20:00) and then were given a 2 h (16:00–18:00) time window for the sucrose preference test before (day 7) and after (day 21) 2 weeks of social defeat stress. The rats were given two bottles, one containing tap water and the other containing 1% sucrose solution. The amount of each solution consumed was determined by weighing the bottles before and after the test. Total sucrose solution intake and total water intake were recorded. The sucrose preference was assessed by calculating the percentage of sucrose solution intake as total sucrose solution intake/total (sucrose + water) intake. At the end of the preference test, rats were given free access to water and food.

2.4. AST. The procedures for the AST were similar to those described in our previous study [29]. Briefly, rats were restricted to 10–14 g of food per day to maintain 80–85% of their original body weight, with free access to water. Rats were trained to obtain a reward (1/4 of a Honey Nut Cheerio)

by digging in two terracotta pots that were defined by a pair of cues along two stimulus dimensions: the digging medium filling the pots and the odor applied to the inner rim of the pots. The "positive" pot was baited with a reward buried at the bottom of the digging medium. The test contained five successive stages with increasing difficulty: the first stage was simple discrimination (SD), which only presented one relevant stimulus dimension (e.g., the medium). The second stage was compound discrimination (CD) in which the same relevant stimulus dimension as that in the SD stage (medium) was required, and the second dimension (e.g., the odor) was presented as an irrelevant distractor. The third stage was intradimensional shifting (IDS), wherein the medium was still the relevant dimension and the odor was still irrelevant, but new media and new odors were introduced. The fourth stage was reversal learning (REL), in which the same media and odors were used and the medium remained the relevant dimension, but the positive and negative cues from the IDS stage were reversed. The fifth stage was extradimensional shifting (EDS), in which all new media and odors were again introduced, and the relevant dimension was the odor instead of the medium. The test proceeded to the next stage when a rat reached a criterion of six consecutive correct trials. The number of trials to reach the criterion for each stage was recorded.

2.5. Tissue Sampling and Western Blotting Analysis. At 24 h after the end of the behavioral testing, rats were decapitated, and the brains were rapidly removed on ice. Each brain was placed into a freezing microtome (Leica, CM 3050, Germany), according to the atlas of Paxinos and Watson [30]; the mPFC (3.20–2.20 mm from the bregma) and OFC (4.70–3.70 mm from the bregma) were bilaterally punched using a stainless steel cannula with an inner diameter of 0.6 mm at −20°C as described in our previous studies [29, 31]. Then, the tissues were placed into liquid nitrogen for rapid freezing and were stored at −80°C for subsequent processing.

The tissue samples were placed in 50–70 μL of precooled lysate buffer (4°C, pH 7.5, containing 5 μg/mL leupeptin, 5 μg/mL aprotinin, 5 μg/mL pepsin inhibitor, 5 μg/mL trypsin inhibitor, 2 mM EDTA, 2 mM EGTA, 1 mM DTT, and 0.5% NP-40) depending on their volume and were then homogenized using an ultrasonic homogenizer (Sonic Co., Stratford, CT, USA). The protein concentrations in the homogenates were determined by a bicinchoninic acid (BCA) Protein Assay Kit (CW Biotech, Beijing, China). The homogenates were then mixed with 5x sodium dodecyl sulfate (SDS) in proportion to the volume to prepare sample solutions with a certain concentration. The prepared sample solutions were denatured at 95°C for 8 min. Denatured proteins (32 μg) were separated by 12% SDS-PAGE and transferred onto a nitrocellulose (NC) membrane at 230 mA for 1 h. The membrane was blocked with 5% nonfat milk diluted in TBST overnight at 4°C. After being washed in TBST (10 min × 3), the membrane was incubated at RT for 2 h on a shaker with primary antibodies: a rabbit monoclonal ERK1/2 antibody (1 : 1000, Cell Signaling Technology Inc., Beverly, MA, USA) and a rabbit monoclonal pERK1/2 antibody (1 : 2000, Cell Signaling Technology Inc.). After further washing in TBST (10 min × 3), the membrane was incubated at RT for 1 h on a shaker with an HRP-conjugated goat anti-rabbit IgG secondary antibody (1 : 4000, Zhongshan Golden Bridge Biotechnology, Beijing, China) and then washed again. Bands were detected by enhanced chemiluminescence (ECL, Millipore, Bedford, MA, USA) via a FluorChem E System (ProteinSimple, Santa Clara, CA, USA). After exposure, the membranes were stripped and reprobed with a primary mouse monoclonal GAPDH antibody (1 : 1000, Zhongshan Golden Bridge Biotechnology) and secondary HRP-conjugated goat anti-mouse IgG (1 : 4000, Zhongshan Golden Bridge Biotechnology) following the above steps. The pCREB and BDNF levels and the corresponding GAPDH levels were determined in different NC membranes using the same procedures. All bands were quantified using Lab Works TM 4.6 (image acquisition and analysis software). The ratio of the intensity of each target band to that of the GAPDH band was used to analyze differences between the stress and control groups.

2.6. Statistical Analysis. The statistical analysis was performed using "Statistical Package for Social Sciences" software (SPSS, version 11.5). AST data were analyzed by two-way ANOVA (stress × stage) with repeated measures over stages. The body weight and sucrose preference data were analyzed by two-way ANOVA (stress × test day) with repeated measures over tests. The levels of molecular expression in each subregion of the PFC between the stress and control groups were compared using Student's t-test. Pearson's correlation analysis was adopted for correlation analyses of molecular levels and behavioral alterations in the mPFC and OFC, respectively. Differences were considered significant at $p < 0.05$.

3. Results

3.1. Body Weight. As shown in Figure 1, there were significant effects of the test day [$F(2, 13) = 224.3$, $p < 0.001$] and stress condition [$F(1, 14) = 7.5$, $p = 0.016$]. Further analysis showed that there was no difference in body weight between the controls and stressed animals ($t_{15} = -0.713$, $p = 0.488$) before stress exposure (day 7). Animals in the stress group showed a lower body weight compared to that in the controls after 7 days ($t_{15} = -2.760$, $p = 0.015$) and 14 days ($t_{15} = -2.883$, $p = 0.0012$) of stress exposure.

3.2. Sucrose Preference Test. The results indicated the main effects of the test day [$F(1, 12) = 7.279$, $p = 0.019$] and stress [$F(1, 12) = 5.356$, $p = 0.039$]. Further analysis showed that the percentage of sucrose solution intake was not significantly different ($t_{15} = -0.309$, $p = 0.763$) between controls and stressed animals before the stress; however, significant differences were observed after 14 days of stress exposure ($t_{15} = -2.818$, $p = 0.014$) (Figure 2).

3.3. AST. Figure 3 shows significant main effects of stress [$F(1, 14) = 23.35$, $p < 0.001$] and task [$F(4, 56) = 21.517$, $p < 0.001$] and a significant effect of the stress × task interaction [$F(4, 56) = 2.576$, $p = 0.047$]. For the main

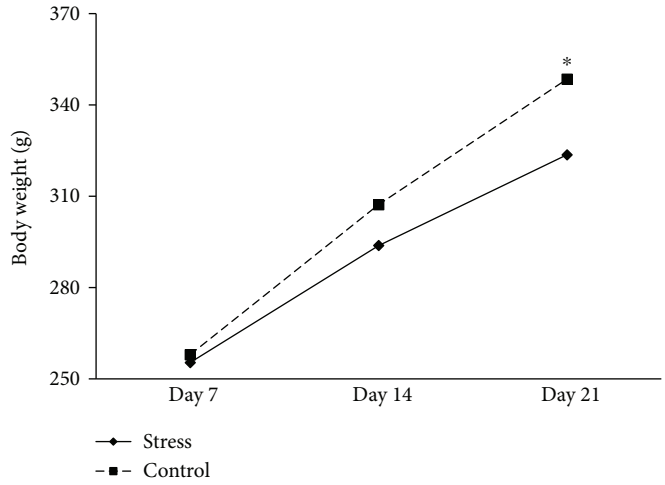

Figure 1: Body weights of controls and stressed rats before the stress (day 7), on the 7th day of stress (day 14), and on the 14th day of stress (day 21). Data are expressed as the mean ± SEM. $^*p < 0.05$ compared to controls.

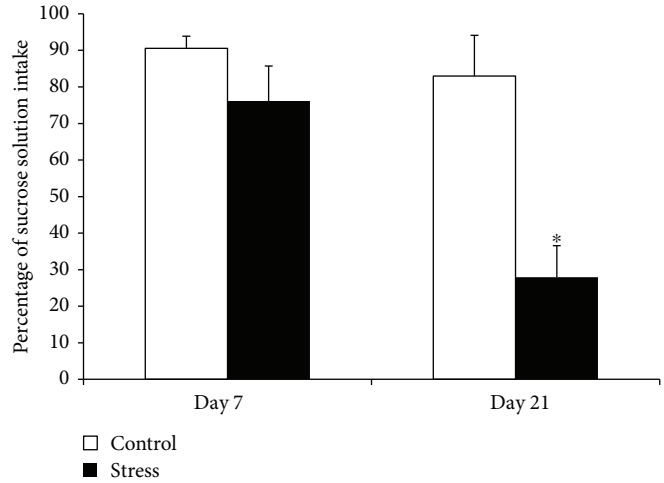

Figure 2: The percentage of sucrose solution intake in the control and stress groups before (day 7) and after stress (day 21). Data are expressed as the mean ± SEM. $^*p < 0.05$ compared to controls.

effect of task, post hoc comparisons showed that significantly more trials were required to reach the criterion during REL and EDS than during the other tasks ($p < 0.001$). Post hoc analysis of the stress effect indicated that stressed rats required significantly more trials to reach the criterion in the REL and EDS stages of the AST than did the controls (REL: $t_{15} = 2.672$, $p = 0.018$; EDS: $t_{15} = 3.41$, $p = 0.005$; Figure 3).

3.4. Protein Expression of ERK1/2, CREB, and BDNF in the mPFC and OFC. The levels of pERK1/2, ERK1/2, pCREB, BDNF, and GAPDH in the OFC and mPFC are shown in Figures 4 and 5, respectively. Stress significantly decreased ERK1, pERK1, pERK2, pCREB, and BDNF levels in the OFC (ERK1: $t_{14} = 3.774$, $p = 0.002$; pERK1: $t_{14} = 4.109$, $p = 0.001$; pERK2: $t_{14} = 3.27$, $p = 0.006$; pCREB: $t_{14} = 2.958$, $p = 0.011$; and BDNF: $t_{14} = 4.765$, $p < 0.001$; Figure 4). There were no changes in ERK2, in the ratio of pERK1 to total ERK1 (pERK1/ERK1), or in the ratio of pERK2 to total ERK2 (pERK2/ERK2) in the OFC. Stress also markedly decreased pERK2, ERK2, pERK2/ERK2, pCREB, and BDNF levels in the mPFC (pERK2: $t_{14} = 3.468$, $p = 0.004$; ERK2: $t_{14} = 2.74$, $p = 0.035$; pERK2/ERK2: $t_{14} = 13.00$, $p < 0.001$; pCREB: $t_{14} = 3.256$, $p = 0.006$; and BDNF: $t_{14} = 5.46$, $p < 0.001$; Figure 5). There were no changes in pERK1, ERK1, or pERK1/ERK1 in the mPFC.

3.5. Correlations between Behavioral and Molecular Alterations in Rats. Results of the correlation analysis are shown in Table 1. In the mPFC, several molecules, including pERK2, ERK2, and BDNF, showed trends of negative association with the number of trials to reach the criterion in the EDS stage of the AST ($r = -0.460$, $p = 0.085$; $r = -0.476$, $p = 0.073$; and $r = -0.485$, $p = 0.067$, resp.), while a marginally or significantly positive correlation was observed between these proteins and sucrose preference ($r = 0.473$,

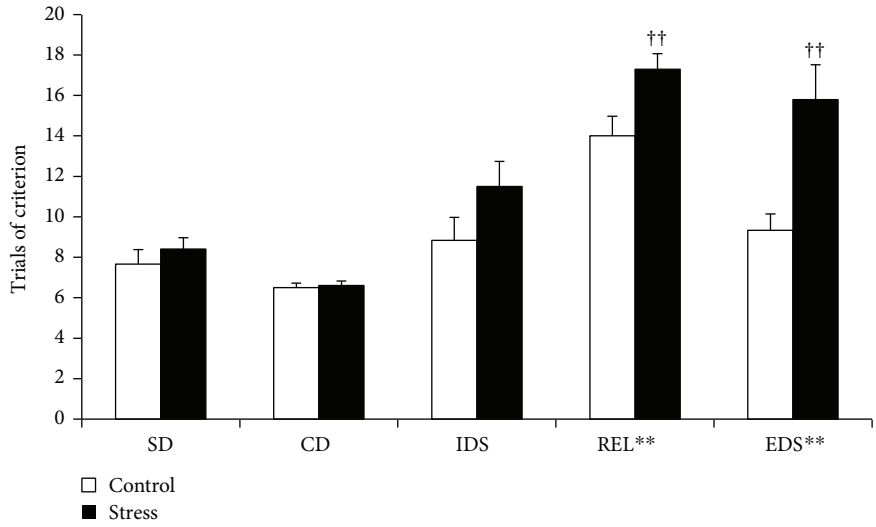

Figure 3: The performance in each stage of the AST in the control and stress groups after social defeat stress. $^{++}p < 0.01$. More trials to reach the criterion were required in the REL and EDS stages compared to those in the SD, CD, and IDS stages. Social defeat induced requirements for significantly higher numbers of trials to reach the criterion in the REL and EDS stages. $^{**}p < 0.01$ compared to controls in the same stage.

$p = 0.075$; $r = 0.482$, $p = 0.069$; and $r = 0.534$, $p = 0.040$, resp.). In the OFC, we observed a significantly negative correlation only between the number of trials to reach the criterion in the REL stage and the BDNF expression level ($r = -0.559$, $p = 0.030$).

4. Discussion

In the present study, chronic social defeat stress induced behavioral and molecular alterations in depression, as manifested by anhedonia and deficits in cognitive flexibility, as well as by inhibited ERK-CREB-BDNF signaling in two subregions of the PFC. Further analysis showed a correlative relationship between behavioral and molecular alterations. These results suggested that the ERK signaling pathway may be a molecular mechanism for emotional and cognitive dysfunction in depression and is a potential target for better pharmaceutical treatment.

Social defeat stress induced a set of behavioral phenotypes of depression, including a decrease in the percentage of sucrose solution intake (reflecting anhedonia, a core symptom of depression) and reduced body weight gain, as well as increased trials to the criterion in the REL and EDS stages of the AST (reflecting deficits in cognitive flexibility in strategy shifting and set shifting, resp.). These results are in accord with those from other studies, in which repeated social defeat resulted in long-lasting loss of body weight [32, 33] and a decreased preference for sweet liquid in rats [34]. Social defeat stress did not significantly reduce sucrose preference of rats until the second week. Some researchers found that the effect of chronic stress on sucrose preference occurred around 10 days after stress [35, 36], while Becker et al. found that social defeat stress significantly decreased the sucrose preference within a short period of time [37]. In addition, other researchers reported that social defeat stress did not significantly change sucrose preference until the third week [38], which may be related to the different experimental paradigm and animal strains used in these studies. In addition, cognitive inflexibility is increasingly recognized as an important risk factor involved in the onset, treatment, and reoccurrence of depression [39]. The deficit profiles of various components of cognitive flexibility induced by chronic stress depend on their consequences on structure and function within the PFC. For example, chronic unpredictable stress and chronic restraint stress induced selective impairment in the EDS with no effect on the REL [11, 40], while chronic intermittent cold stress selectively impaired the REL in the AST but did not affect the EDS [41]. Using the social defeat stress model, this and previous studies by us and Snyder et al. reported impairment in cognitive flexibility in mice and rats [19, 29]. Considering social stress as the main source of life stress, these data suggested that chronic social defeat can be used as a validated social stressor to model both the emotional and cognitive symptoms of depression.

We found that ERK signaling in the PFC was inhibited by social defeat stress. There were significant decreases in the protein levels of ERK and/or phosphorylated ERK (pERK) in different subregions of the PFC, as shown by lower expression levels of ERK1, pERK1, and pERK2 in the OFC and of pERK2, ERK2, and pERK2/ERK2 in the mPFC in stressed rats compared to those in the control rats. Several studies have reported effects of various chronic stressors on ERK signaling in different brain areas. For example, chronic multiple stress impaired spatial cognition in the Morris water maze and significantly reduced the expression of pERK in the hippocampus and PFC of rats [42], while ERK activation caused the upregulation of dendritic spine density in CA1 pyramidal neurons [43–45] and improved spatial learning and memory [25, 46, 47]. It has been shown that social defeat stress can damage the structure and function of the PFC [48], which is involved in a variety of higher brain functions, such as emotion, social behavior, and cognitive function. Considering its important role in neuroplasticity, inhibition of

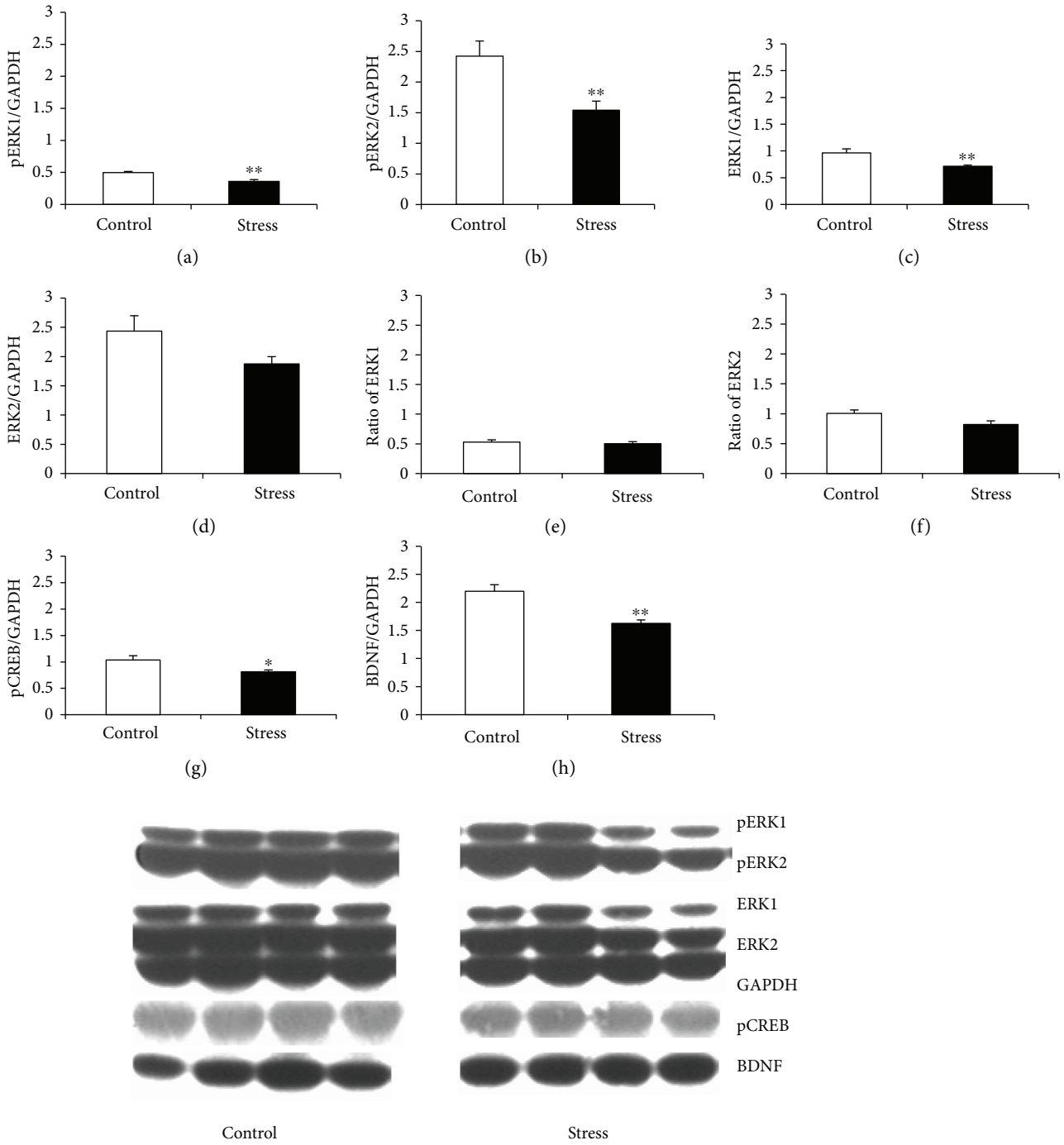

Figure 4: The levels of pERK1 and 2, ERK1 and 2, pCREB, and BDNF and representative blots for each protein from the OFC. (a) pERK1, (b) pERK2, (c) ERK1, (d) ERK2, (e) pERK1/ERK1, (f) pERK2/ERK2, (g) pCREB, and (h) BDNF. Data are expressed as the mean ± SEM. $^{*}p < 0.05$ and $^{**}p < 0.01$ compared to controls.

ERK signaling in the mPFC and OFC in this study suggests that the deficits in cognitive flexibility may be mediated by impairment in corresponding areas.

In addition, this study showed differential alterations in ERK1 and ERK2 signaling in different areas of the PFC after social defeat stress, with a specific decrease in ERK2 signaling in the mPFC and a more extensive reduction in both ERK1 signaling and ERK2 signaling in the OFC. Functional differences in ERK1 and ERK2 signaling in the regulation of brain and behavior have been reported. For example, ERK2 plays a positive role in Ras-dependent cell proliferation, while ERK1 probably affects overall cell signaling output by antagonizing the activation of ERK2 [49]. Consistently, ERK1 knock-out mice exhibited increases in striatum-dependent LTP and ERK2 expression, and those effects were strongly associated [21]. A recent study also showed that

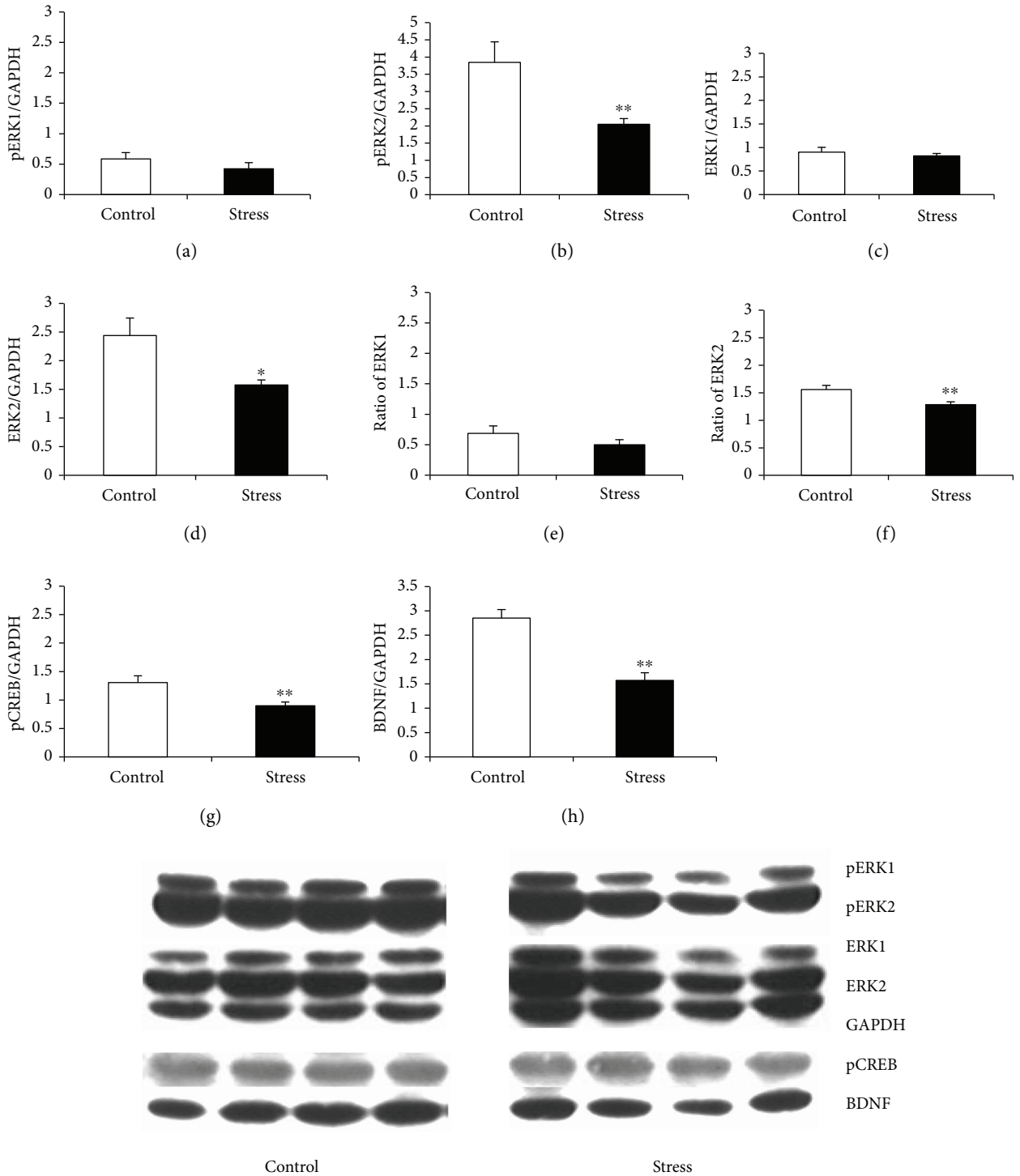

Figure 5: The levels of pERK1 and 2, ERK1 and 2, pCREB, and BDNF and representative blots for each protein from the mPFC. (a) pERK1, (b) pERK2, (c) ERK1, (d) ERK2, (e) pERK1/ERK1, (f) pERK2/ERK2, (g) pCREB, and (h) BDNF. Data are expressed as the mean ± SEM. $^{*}p < 0.05$ and $^{**}p < 0.01$ compared to controls.

ERK1 and ERK2 interacted to balance the process of cytoplasmic-nuclear trafficking [50]. Such differential effects of stress on ERK1 and 2 were also reported by Feng et al., in which depressed animals with early manipulation exhibited differential expression and phosphorylation of ERK1 and ERK2 in the hippocampus and in the frontal cortex [51], suggesting that a balance between ERK1 and 2 may be involved in neural and cognitive responses to stress.

Along with the inhibition of ERK signaling in the mPFC and OFC, expression levels of the downstream targets pCREB and BDNF were also significantly downregulated in this study. Various chronic stressors such as chronic social

Table 1: Correlations between emotional and cognitive alterations.

		Sucrose ratio	EDS
mPFC	pERK2	$r = 0.473$	$r = -0.460$
		$p = 0.075$	$p = 0.085$
	ERK2	$r = 0.482$	$r = -0.476$
		$p = 0.069$	$p = 0.073$
	pERK2/ERK2	$r = 0.373$	$r = -0.380$
		$p = 0.171$	$p = 0.162$
	pCREB	$r = 0.355$	$r = -0.281$
		$p = 0.295$	$p = 0.310$
	BDNF	$r = 0.534^*$	$r = -0.485$
		$\boldsymbol{p = 0.040}$	$p = 0.067$
		Sucrose ratio	REL
OFC	pERK1	$r = 0.362$	$r = -0.308$
		$p = 0.185$	$p = 0.263$
	ERK1	$r = 0.381$	$r = -0.306$
		$p = 0.162$	$p = 0.267$
	pERK2	$r = 0.409$	$r = -0.200$
		$p = 0.130$	$p = 0.476$
	pERK2/ERK2	$r = 0.360$	$r = -0.226$
		$p = 0.188$	$p = 0.419$
	pCREB	$r = 0.380$	$r = -0.127$
		$p = 0.162$	$p = 0.653$
	BDNF	$r = 0.333$	$r = -0.559^*$
		$p = 0.225$	$\boldsymbol{p = 0.030}$

$^*p < 0.05$.

defeat can reduce CREB or pCREB and BDNF expression in the PFC [52–54], though studies do not show uniform results [55, 56] due to differences in experimental conditions, such as stress paradigms, brain areas analyzed, and time of testing. Decreasing or eliminating the expression of CREB or BDNF, due to stress or pharmaceutical or transgenic methods, causes emotional and cognitive impairment, such as in long-term memory consolidation [57] and in spatial cognition in the Morris water maze [33, 58]. In this report, we provide extensive evidence that ERK-CREB-BDNF signaling in the PFC may be involved in the alterations in cognitive flexibility induced by social defeat stress.

The relationship between ERK-CREB-BDNF signaling and the behaviors induced by social defeat were further supported by correlation analysis. First, the sucrose ratios were associated with BDNF levels in the mPFC. Other studies have shown that decreased BDNF expression in the hippocampus and mPFC was associated with chronic stress-induced depressive behaviors, such as anhedonia and despair behavior in the forced swimming test [59]. Snyder et al. found that there was a loss of sucrose preference in hippocampus neurogenesis-deficient mice than intact mice [60]. The present study also found that social defeat stress reduced BDNF expression in the mPFC and OFC, suggesting that the stress-induced reduction of sucrose preference may be related to changes of neurogenesis in the brain. Second, the increased number of trials to reach the criterion in the REL stage was significantly negatively correlated with the BDNF levels in the OFC. Structural and functional impairments in the OFC have been found in depressive patients and animals [61]. Considering that performance in reversal learning and set shifting depends on the normal structure and function of the serotoninergic system in the OFC and of the noradrenergic system in the mPFC, respectively [5, 8–10, 62, 63], these results suggest that different components of cognitive flexibility may be regulated by different ERK signaling pathways downstream of stress-induced changes in monoaminergic signaling, which shows extensive deficiencies in depression.

5. Conclusion

In conclusion, this study confirmed that social defeat stress can be used as a valid model to induce both the emotional and the cognitive domains of depression. Furthermore, we found that social defeat stress inhibited ERK-CREB-BDNF signaling by region-dependent effects on ERK1 and 2 in the PFC, which was correlated with anhedonia and impaired cognitive function. These results suggested that ERK-CREB-BDNF signaling in the PFC could be a common pathway involved in the emotional and cognitive symptoms of depression.

Data Availability

The data used to support the findings of this study are available from the corresponding author upon request.

Conflicts of Interest

The authors declare that they have no conflicts of interest.

Acknowledgments

This work was supported by the National Natural Science Foundation of China (Grant nos. 81471122 and 31470988), the Chinese Academy of Sciences (KJZDEW-L04), and the CAS Key Laboratory of Mental Health, Institute of Psychology, and the Starting Foundation for Youth Teachers from Zhengzhou University (Grant no. 32210394).

References

[1] D. Marazziti, G. Consoli, M. Picchetti, M. Carlini, and L. Faravelli, "Cognitive impairment in major depression," *European Journal of Pharmacology*, vol. 626, no. 1, pp. 83–86, 2010.

[2] P. L. Rock, J. P. Roiser, W. J. Riedel, and A. D. Blackwell, "Cognitive impairment in depression: a systematic review and meta-analysis," *Psychological Medicine*, vol. 44, no. 10, pp. 2029–2040, 2014.

[3] J. Brielmaier, J. M. Senerth, J. L. Silverman et al., "Chronic desipramine treatment rescues depression-related, social and cognitive deficits in *Engrailed-2* knockout mice," *Genes, Brain and Behavior*, vol. 13, no. 3, pp. 286–298, 2014.

[4] R. D. Nebes, B. G. Pollock, P. R. Houck et al., "Persistence of cognitive impairment in geriatric patients following antidepressant treatment: a randomized, double-blind clinical trial with nortriptyline and paroxetine," *Journal of Psychiatric Research*, vol. 37, no. 2, pp. 99–108, 2003.

[5] M. D. S. Lapiz-Bluhm, C. O. Bondi, J. Doyen, G. A. Rodriguez, T. Bédard-Arana, and D. A. Morilak, "Behavioural assays to model cognitive and affective dimensions of depression and anxiety in rats," *Journal of Neuroendocrinology*, vol. 20, no. 10, pp. 1115–1137, 2008.

[6] K. McAlonan and V. J. Brown, "Orbital prefrontal cortex mediates reversal learning and not attentional set shifting in the rat," *Behavioural Brain Research*, vol. 146, no. 1-2, pp. 97–103, 2003.

[7] R. Dias, T. W. Robbins, and A. C. Roberts, "Primate analogue of the Wisconsin card sorting test: effects of excitotoxic lesions of the prefrontal cortex in the marmoset," *Behavioral Neuroscience*, vol. 110, no. 5, pp. 872–886, 1996.

[8] A. A. Kehagia, G. K. Murray, and T. W. Robbins, "Learning and cognitive flexibility: frontostriatal function and monoaminergic modulation," *Current Opinion in Neurobiology*, vol. 20, no. 2, pp. 199–204, 2010.

[9] J. M. Birrell and V. J. Brown, "Medial frontal cortex mediates perceptual attentional set shifting in the rat," *The Journal of Neuroscience*, vol. 20, no. 11, pp. 4320–4324, 2000.

[10] J. Kim and M. Ragozzino, "The involvement of the orbitofrontal cortex in learning under changing task contingencies," *Neurobiology of Learning and Memory*, vol. 83, no. 2, pp. 125–133, 2005.

[11] C. O. Bondi, G. Rodriguez, G. G. Gould, A. Frazer, and D. A. Morilak, "Chronic unpredictable stress induces a cognitive deficit and anxiety-like behavior in rats that is prevented by chronic antidepressant drug treatment," *Neuropsychopharmacology*, vol. 33, no. 2, pp. 320–331, 2008.

[12] S. C. Dulawa, K. A. Holick, B. Gundersen, and R. Hen, "Effects of chronic fluoxetine in animal models of anxiety and depression," *Neuropsychopharmacology*, vol. 29, no. 7, pp. 1321–1330, 2004.

[13] M. Hetman and A. Gozdz, "Role of extracellular signal regulated kinases 1 and 2 in neuronal survival," *European Journal of Biochemistry*, vol. 271, no. 11, pp. 2050–2055, 2004.

[14] X. Zhu, H.-g. Lee, A. K. Raina, G. Perry, and M. A. Smith, "The role of mitogen-activated protein kinase pathways in Alzheimer's disease," *Neurosignals*, vol. 11, no. 5, pp. 270–281, 2002.

[15] X. Qi, W. Lin, J. Li et al., "Fluoxetine increases the activity of the ERK-CREB signal system and alleviates the depressive-like behavior in rats exposed to chronic forced swim stress," *Neurobiology of Disease*, vol. 31, no. 2, pp. 278–285, 2008.

[16] L. M. Igaz, M. Winograd, M. Cammarota et al., "Early activation of extracellular signal-regulated kinase signaling pathway in the hippocampus is required for short-term memory formation of a fear-motivated learning," *Cellular and Molecular Neurobiology*, vol. 26, no. 4–6, pp. 987–1000, 2006.

[17] J. D. Sweatt, "The neuronal MAP kinase cascade: a biochemical signal integration system subserving synaptic plasticity and memory," *Journal of Neurochemistry*, vol. 76, no. 1, pp. 1–10, 2001.

[18] J. D. Runyan and P. K. Dash, "Intra-medial prefrontal administration of SCH-23390 attenuates ERK phosphorylation and long-term memory for trace fear conditioning in rats," *Neurobiology of Learning and Memory*, vol. 82, no. 2, pp. 65–70, 2004.

[19] K. Snyder, W.-W. Wang, R. Han, K. McFadden, and R. J. Valentino, "Corticotropin-releasing factor in the norepinephrine nucleus, locus coeruleus, facilitates behavioral flexibility," *Neuropsychopharmacology*, vol. 37, no. 2, pp. 520–530, 2012.

[20] I. S. Samuels, J. C. Karlo, A. N. Faruzzi et al., "Deletion of ERK2 mitogen-activated protein kinase identifies its key roles in cortical neurogenesis and cognitive function," *The Journal of Neuroscience*, vol. 28, no. 27, pp. 6983–6995, 2008.

[21] C. Mazzucchelli, C. Vantaggiato, A. Ciamei et al., "Knockout of ERK1 MAP kinase enhances synaptic plasticity in the striatum and facilitates striatal-mediated learning and memory," *Neuron*, vol. 34, no. 5, pp. 807–820, 2002.

[22] R. Rygula, N. Abumaria, U. Havemann-Reinecke et al., "Pharmacological validation of a chronic social stress model of depression in rats: effects of reboxetine, haloperidol and diazepam," *Behavioural Pharmacology*, vol. 19, no. 3, pp. 183–196, 2008.

[23] J. Xing, D. D. Ginty, and M. E. Greenberg, "Coupling of the RAS-MAPK pathway to gene activation by RSK2, a growth factor-regulated CREB kinase," *Science*, vol. 273, no. 5277, pp. 959–963, 1996.

[24] X. Tao, S. Finkbeiner, D. B. Arnold, A. J. Shaywitz, and M. E. Greenberg, "Ca^{2+} influx regulates *BDNF* transcription by a CREB family transcription factor-dependent mechanism," *Neuron*, vol. 20, no. 4, pp. 709–726, 1998.

[25] S. W. Ying, M. Futter, K. Rosenblum et al., "Brain-derived Neurotrophic factor induces long-term potentiation in intact adult hippocampus: requirement for ERK activation coupled to CREB and Upregulation of *Arc* synthesis," *The Journal of Neuroscience*, vol. 22, no. 5, pp. 1532–1540, 2002.

[26] T. Pizzorusso, G. M. Ratto, E. Putignano, and L. Maffei, "Brain-derived Neurotrophic factor causes cAMP response element-binding protein phosphorylation in absence of calcium increases in slices and cultured neurons from rat visual cortex," *The Journal of Neuroscience*, vol. 20, no. 8, pp. 2809–2816, 2000.

[27] R. A. Segal, "Selectivity in neurotrophin signaling: theme and variations," *Annual Review of Neuroscience*, vol. 26, no. 1, pp. 299–330, 2003.

[28] S. K. Wood, H. E. Walker, R. J. Valentino, and S. Bhatnagar, "Individual differences in reactivity to social stress predict susceptibility and resilience to a depressive phenotype: role of corticotropin-releasing factor," *Endocrinology*, vol. 151, no. 4, pp. 1795–1805, 2010.

[29] Y. Zhang, F. Shao, Q. Wang, X. Xie, and W. Wang, "Neuroplastic correlates in the mPFC underlying the impairment of stress-coping ability and cognitive flexibility in adult rats exposed to chronic mild stress during adolescence," *Neural Plasticity*, vol. 2017, Article ID 9382797, 10 pages, 2017.

[30] G. Paxinos and C. Watson, *The Rat Brain in Stereotaxic Coordinates-The New Coronal Set*, Academic Press, New York, NY, USA, 2004.

[31] Q. Wang, F. Shao, and W. Wang, "Maternal separation produces alterations of forebrain brain-derived neurotrophic factor expression in differently aged rats," *Frontiers in Molecular Neuroscience*, vol. 8, p. 49, 2015.

[32] P. Meerlo, G. J. F. Overkamp, and J. M. Koolhaas, "Behavioural and physiological consequences of a single social defeat in

Roman high- and low-avoidance rats," *Psychoneuroendocrinology*, vol. 22, no. 3, pp. 155–168, 1997.

[33] J. V. K. Pulliam, A. M. Dawaghreh, E. Alema-Mensah, and P. M. Plotsky, "Social defeat stress produces prolonged alterations in acoustic startle and body weight gain in male Long Evans rats," *Journal of Psychiatric Research*, vol. 44, no. 2, pp. 106–111, 2010.

[34] A. T. Beck, "The evolution of the cognitive model of depression and its neurobiological correlates," *The American Journal of Psychiatry*, vol. 165, no. 8, pp. 969–977, 2008.

[35] R. Rygula, N. Abumaria, G. Flügge, E. Fuchs, E. Rüther, and U. Havemann-Reinecke, "Anhedonia and motivational deficits in rats: impact of chronic social stress," *Behavioural Brain Research*, vol. 162, no. 1, pp. 127–134, 2005.

[36] J. M. Bessa, D. Ferreira, I. Melo et al., "The mood-improving actions of antidepressants do not depend on neurogenesis but are associated with neuronal remodeling," *Molecular Psychiatry*, vol. 14, no. 8, pp. 764–773, 2009.

[37] C. Becker, B. Zeau, C. Rivat, A. Blugeot, M. Hamon, and J.-J. Benoliel, "Repeated social defeat-induced depression-like behavioral and biological alterations in rats: involvement of cholecystokinin," *Molecular Psychiatry*, vol. 13, no. 12, pp. 1079–1092, 2008.

[38] C. M. Deveney and P. J. Deldin, "A preliminary investigation of cognitive flexibility for emotional information in major depressive disorder and non-psychiatric controls," *Emotion*, vol. 6, no. 3, pp. 429–437, 2006.

[39] M. D. S. Lapiz-Bluhm, A. E. Soto-Piña, J. G. Hensler, and D. A. Morilak, "Chronic intermittent cold stress and serotonin depletion induce deficits of reversal learning in an attentional set-shifting test in rats," *Psychopharmacology*, vol. 202, no. 1–3, pp. 329–341, 2009.

[40] C. Liston, M. M. Miller, D. S. Goldwater et al., "Stress-induced alterations in prefrontal cortical dendritic morphology predict selective impairments in perceptual attentional set-shifting," *The Journal of Neuroscience*, vol. 26, no. 30, pp. 7870–7874, 2006.

[41] G. Zheng, W. Luo, Y. Chen, M. Liu, J. Ma, and J. Chen, "Effects of chronic multiple stress on learning and memory and the expression and phosphorylation of cerebral ERK of rats," *Chinese Journal of Applied Physiology*, vol. 27, no. 1, pp. 33–36, 2011.

[42] P. Bekinschtein, M. Cammarota, L. M. Igaz, L. R. M. Bevilaqua, I. Izquierdo, and J. H. Medina, "Persistence of long-term memory storage requires a late protein synthesis- and BDNF-dependent phase in the hippocampus," *Neuron*, vol. 53, no. 2, pp. 261–277, 2007.

[43] M. Alonso, J. H. Medina, and L. Pozzo-Miller, "ERK1/2 activation is necessary for BDNF to increase dendritic spine density in hippocampal CA1 pyramidal neurons," *Learning & Memory*, vol. 11, no. 2, pp. 172–178, 2004.

[44] E. R. Kandel, "The molecular biology of memory storage: a dialogue between genes and synapses," *Science*, vol. 294, no. 5544, pp. 1030–1038, 2001.

[45] M. Mizuno, K. Yamada, N. Maekawa, K. Saito, M. Seishima, and T. Nabeshima, "CREB phosphorylation as a molecular marker of memory processing in the hippocampus for spatial learning," *Behavioural Brain Research*, vol. 133, no. 2, pp. 135–141, 2002.

[46] C. Rendeiro, D. Vauzour, R. J. Kean et al., "Blueberry supplementation induces spatial memory improvements and region-specific regulation of hippocampal BDNF mRNA expression in young rats," *Psychopharmacology*, vol. 223, no. 3, pp. 319–330, 2012.

[47] A. F. T. Arnsten, "Stress signalling pathways that impair prefrontal cortex structure and function," *Nature Reviews Neuroscience*, vol. 10, no. 6, pp. 410–422, 2009.

[48] C. Vantaggiato, I. Formentini, A. Bondanza, C. Bonini, L. Naldini, and R. Brambilla, "ERK1 and ERK2 mitogen-activated protein kinases affect Ras-dependent cell signaling differentially," *Journal of Biology*, vol. 5, no. 5, p. 14, 2006.

[49] M. Marchi, A. D'Antoni, I. Formentini et al., "The N-terminal domain of ERK1 accounts for the functional differences with ERK2," *PLoS One*, vol. 3, no. 12, article e3873, 2008.

[50] P. F. Feng, Z. W. Guan, X. P. Yang, and J. D. Fang, "Impairments of ERK signal transduction in the brain in a rat model of depression induced by neonatal exposure of clomipramine," *Brain Research*, vol. 991, no. 1-2, pp. 195–205, 2003.

[51] R. S. Duman and B. Voleti, "Signaling pathways underlying the pathophysiology and treatment of depression: novel mechanisms for rapid-acting agents," *Trends in Neurosciences*, vol. 35, no. 1, pp. 47–56, 2012.

[52] A. Nair and V. A. Vaidya, "Cyclic AMP response element binding protein and brain-derived neurotrophic factor: molecules that modulate our mood?," *Journal of Biosciences*, vol. 31, no. 3, pp. 423–434, 2006.

[53] H. Xu, Y. Zhang, F. Zhang, S. N. Yuan, F. Shao, and W. Wang, "Effects of duloxetine treatment on cognitive flexibility and BDNF expression in the mPFC of adult male mice exposed to social stress during adolescence," *Frontiers in Molecular Neuroscience*, vol. 9, p. 95, 2016.

[54] S. Fanous, R. P. Hammer Jr., and E. M. Nikulina, "Short- and long-term effects of intermittent social defeat stress on brain-derived neurotrophic factor expression in mesocorticolimbic brain regions," *Neuroscience*, vol. 167, no. 3, pp. 598–607, 2010.

[55] E. M. Nikulina, M. J. Lacagnina, S. Fanous, J. Wang, and R. P. Hammer Jr., "Intermittent social defeat stress enhances mesocorticolimbic ΔFosB/BDNF co-expression and persistently activates corticotegmental neurons: implication for vulnerability to psychostimulants," *Neuroscience*, vol. 212, pp. 38–48, 2012.

[56] B. Bozon, A. Kelly, S. A. Josselyn, A. J. Silva, S. Davis, and S. Laroche, "MAPK, CREB and *zif268* are all required for the consolidation of recognition memory," *Philosophical Transactions of the Royal Society B: Biological Sciences*, vol. 358, no. 1432, pp. 805–814, 2003.

[57] A. Berry, V. Bellisario, S. Capoccia et al., "Social deprivation stress is a triggering factor for the emergence of anxiety- and depression-like behaviours and leads to reduced brain BDNF levels in C57BL/6J mice," *Psychoneuroendocrinology*, vol. 37, no. 6, pp. 762–772, 2012.

[58] X. Xue, S. Shao, W. Wang, and F. Shao, "Maternal separation induces alterations in reversal learning and brain-derived neurotrophic factor expression in adult rats," *Neuropsychobiology*, vol. 68, no. 4, pp. 243–249, 2013.

[59] R. S. Duman and L. M. Monteggia, "A neurotrophic model for stress-related mood disorders," *Biological Psychiatry*, vol. 59, no. 12, pp. 1116–1127, 2006.

[60] J. S. Snyder, A. Soumier, M. Brewer, J. Pickel, and H. A. Cameron, "Adult hippocampal neurogenesis buffers stress

responses and depressive behaviour," *Nature*, vol. 476, no. 7361, pp. 458–461, 2011.

[61] W. C. Drevets, "Orbitofrontal cortex function and structure in depression," *Annals of the New York Academy of Sciences*, vol. 1121, no. 1, pp. 499–527, 2007.

[62] H. F. Clarke, S. C. Walker, J. W. Dalley, T. W. Robbins, and A. C. Roberts, "Cognitive inflexibility after prefrontal serotonin depletion is behaviorally and neurochemically specific," *Cerebral Cortex*, vol. 17, no. 1, pp. 18–27, 2007.

[63] T. W. Robbins and A. F. T. Arnsten, "The neuropsychopharmacology of fronto-executive function: monoaminergic modulation," *Annual Review of Neuroscience*, vol. 32, no. 1, pp. 267–287, 2009.

Hindawi
Neural Plasticity
Volume 2018, Article ID 7051925, 13 pages
https://doi.org/10.1155/2018/7051925

Research Article

Context and Time Matter: Effects of Emotion and Motivation on Episodic Memory Overtime

Qing Sun,[1] Simeng Gu,[2] and Jiongjiong Yang[1]

[1]*School of Psychological and Cognitive Sciences and Beijing Key Laboratory of Behavior and Mental Health, Peking University, Beijing 100080, China*
[2]*Department of Medical Psychology, Jiangsu University Medical School, Zhenjiang 212013, China*

Correspondence should be addressed to Jiongjiong Yang; yangjj@pku.edu.cn

Received 9 December 2017; Accepted 15 January 2018; Published 8 April 2018

Academic Editor: Fang Pan

Previous studies have shown that compared with neutral cues, stimuli with positive and negative/stressful contexts or reward and punishment cues are remembered better. However, it is unclear whether the enhanced effect differs in emotion or motivation dimensions and the passage of time. We addressed these issues by manipulating different contextual cues for neutral words at different time intervals. In experiment 1, subjects were asked to learn words with picture contexts in positive, negative/stressful, and neutral valences and were tested by old/new word recognition and contextual judgment 10 min, 1 day, and 1 week later. In experiment 2, the reward and punishment motivations were manipulated by monetary cues during learning. Word recognition and contextual judgment were assessed 10 min, 1 day, 1 week, and 1 month after the study. Compared with negative and punishment conditions, the words in positive and reward contexts were recognized better at shorter intervals, which was associated with recollection process. In contrast, the words in negative and punishment contexts were recognized better at longer intervals, which was mainly associated with familiarity process. These results clarified how different dimensions of emotional and motivational contexts influence memory at short and long intervals and highlighted the role of contextual features in memory formation and consolidation.

1. Introduction

We encounter enormous information every day, but only a small portion of the information is remembered and remained in the long-term memory. In recent years, studies have suggested that in addition to some salient events (e.g., emotional faces and stressful events), emotional and motivational contexts can also enhance memory for associated neutral events. The negative/stressful and positive stimuli are usually used as emotional contexts [1–4] and monetary reward and punishment/loss as motivational contexts [5, 6]. The electronical shock is used as punishment [7, 8] or negative manipulation [9].

Emotional and motivational contexts influence memory when they are presented in different phases. The contexts can be presented before/with the stimuli (as cues), or after the stimuli, leading to proactive or retroactive memory enhancement. For example, memory for face names was enhanced when happy expressions were presented as cues [10], and memory for neutral pictures was enhanced when negative cues were used in 5 min delay [11]. With regard to motivational contexts, in a study by Adcock et al. [5], participants were presented with pictures that were labeled with high- and low-reward cues. The recognition performance was better in the high- versus low-reward condition 24 h later. The neutral words with shock cues were recognized better than those without shock cues 24 h later [7]. In addition, the enhancement for reward contexts is associated with a high confidence [5] and recollection process [12, 13]. In a study of Gruber et al. [12], subjects learned the object-scene associations in high- or low-reward condition and tested them with object and object-scene associations about 30 min later. Compared with the low-reward condition, the associations that were learned in the high-reward condition were remembered better and relied on the recollection contribution.

One interesting question addressed in this study is whether the memory enhancement by emotional or motivational contexts is time-dependent. As memory is generally forgotten with the passage of time [14], it is unclear whether the enhancements remain for a long time. Previous studies have suggested that emotional and motivational contexts influence both encoding and consolidation stages. Emotional and motivational stimuli could attract more attention during encoding [15–17]. In addition, negative/stressful stimuli are usually highly arousing, which triggers a more efficient consolidation by the interaction of the amygdala and hippocampus system [18]. Motivational stimuli, on the other hand, enhance memory consolidation by the interaction of dopamine and hippocampus system [19]. The studies using the retroactive memory paradigms provided additional evidence for the consolidation mechanisms. For example, Murayama and colleagues showed that monetary reward cues enhanced proactive memory for irrelevant objects, but the effect was observed only after 24 h, not immediately upon testing [20, 21].

Although it is possible that emotional and motivational contexts lead to stable memory enhancement over time, current findings are not clear. Most studies found the enhanced memory for emotional contexts immediately after learning [1–3, 11]. Some studies found the enhanced effect at 24 h but not at short intervals [9, 22]. For the motivational manipulation, some studies found the reward-related memory enhancement for neutral pictures shortly after study (1 min in Shigemune et al.; 30 min in Murty et al.) [8, 23] or 24 h later [5, 7]. But others showed the reward-related enhancement in 3 weeks but not immediately after study [6]. Few studies compared the memory enhancement between different time intervals longer than 1 week [6].

The inconsistent findings may be due to the fact that memory enhancement differs in types of contexts with the passage of time. When memories with different contexts were directly compared, positive contexts enhanced memory more strongly than negative (and neutral) cues for target pictures [2, 3], words [1], and faces [24] at the day of encoding. Other studies using actual shocks during encoding found the enhanced effect at 24 h but not at short intervals [9, 22]. With regard to motivational contexts, a study by Murty et al. [8] compared the effects of monetary reward and mild shock on subsequent recognition of surprise events 30 min after they were learned. The results showed that events with reward motivation resulted in higher memory performance than those with shocks. Note that the memories in positive/reward contexts were enhanced minutes or 1 day after the encoding, which raised the possibility that memory enhancement for the positive and reward contexts occurs earlier, whereas that for the negative contexts occurs later in memory stage. But studies of different emotional and motivational contexts varied in the testing intervals, most only after short delays [8, 23]. We know little about how the memory enhancement changes over time, and it is necessary to include both the time interval and different context as independent factors to address this issue.

If memory enhancement for different contexts differs in time intervals, we would find different contribution of recollection and familiarity processes over time. On the one hand, the memories for positive and reward and the memories for negative and punishment contexts depend on recollection and familiarity differently. For example, the reward-related memory is associated with recollection [6, 12]. The enhanced memory for neutral scenes associated with shock is associated with the familiarity rather than the recollection [9]. On the other hand, previous studies have suggested that memory relying on recollection and familiarity processes differs in forgetting characteristics [25]. As stated in Sadeh et al. [25], memories relying on recollection are forgotten primarily due to decay over time but are relatively resistant to interference from irrelevant information. By contrast, memories relying on familiarity are prone to interference but show less effect of decay. Therefore, when memory enhancement due to different emotional contexts and motivations is associated with recollection and familiarity processes, the forgetting rate would differ over time.

Combining the study for memory with emotional and motivational contexts is important, because both of the contexts are commonly used in memory studies, but it is unclear whether they have similar effects on memory enhancement and whether they rely on similar mechanisms. Some studies showed that both electronical shock and money loss led to similar activation in the striatum [26], and positive emotion evoked value representations in the striatum [27]. In addition, facilitation of memory by punishment motivation may recruit similar neural circuitry as threatening items in the amygdala [7] and medial temporal regions [9]. Clarifying their relationship in behavioral level would provide insights on studies on neural mechanisms.

In sum, the objective of the study was to explore to what extent different emotional and motivational contexts influence memory for neutral targets over time. We addressed these issues by manipulating different contextual cues for neutral words at different time intervals. In experiment 1, pictures with positive, negative/stressful, and neutral valences were used as contexts of words [2, 3, 28]. To dissociate the effects of valence and arousal, the arousal levels of positive and negative/stressful pictures were matched. After subjects learned the associations between words and contexts for 10 min, 1 day, and 1 week, they were tested by old and new word recognition and contextual judgment. We did not include 1-month interval in experiment 1, because that the memory performance was at chance level at 1 month in pilot studies. In experiment 2, the reward and punishment motivation was manipulated by monetary cues during learning and subjects' fees afterward. The motivational levels of punishment and reward were also matched by a separate rating, which was also confirmed by participants' post hoc reports. The word recognition, remember/know judgment, and contextual judgment were performed 10 min, 1 day, 1 week, and 1 month after the study. Based on previous studies, we hypothesized that emotional and motivational contexts enhance memory for subsequent words. In comparisons of different contexts, memory in positive and reward conditions depends on recollection and is higher than that in negative and punishment conditions at shorter intervals, whereas memory enhancement for negative

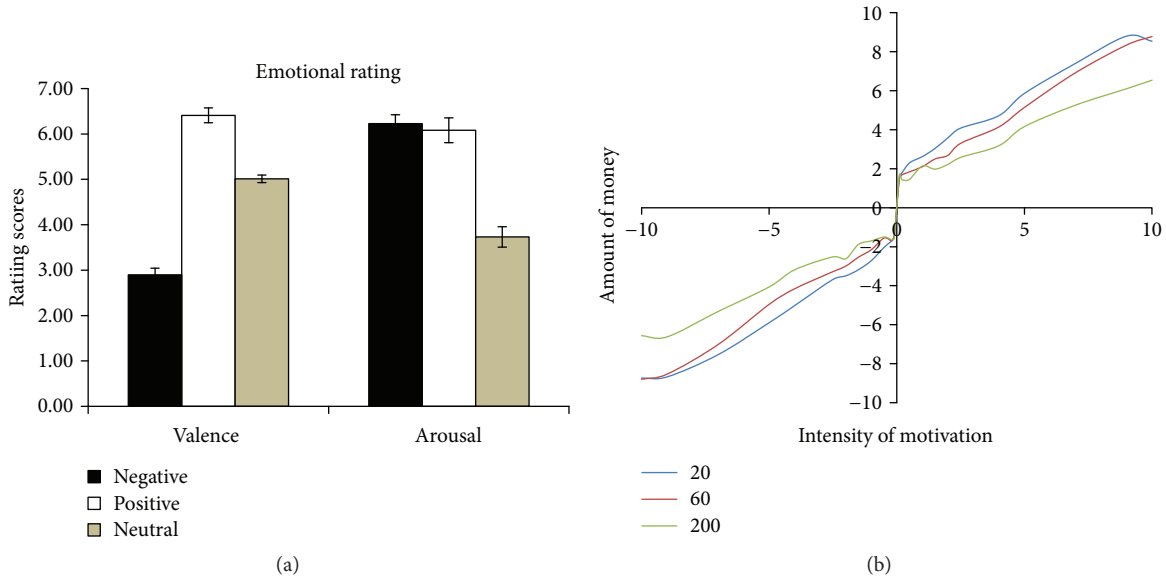

Figure 1: Emotional and motivational rating in experiments 1 and 2.

and punishment pictures may be more familiarity-based and could last for a longer time.

2. Materials and Methods

2.1. Experiment 1. In experiment 1, by using the emotional contextual paradigm, we explored whether negative or positive contexts enhanced memory for neutral words differently over time. The negative and positive pictures were matched in their arousal levels. Participants were first presented with neutral words, followed by pictures of positive, negative, and neutral valences overlaid on the neutral words. They were tested for memories of words and contextual information after 10 min, 1-day, and 1-week intervals.

2.1.1. Participants. Twenty-eight healthy, right-handed participants (10 males) with a mean age of 22.1 ± 2.2 years were recruited in the study. All of the participants were native Chinese speakers, and they all provided written informed consent in accordance with the procedures and protocols approved by the Review Board of School of Psychological and Cognitive Sciences, Peking University.

2.1.2. Material. Two within-subject factors were included in the study: context (positive, negative, and neutral) and time interval (10 min, 1 day, and 1 week). The contexts were 180 pictures, of which negative, neutral, and positive pictures each having 60 pictures. Another 18 participants (11 males, average age 23 ± 1.97 years) rated the pictures in the dimensions of valence and arousal. The three types of contexts differed significantly in valence (2.90 ± 0.61 for negative, 6.41 ± 0.69 for positive, and 5.01 ± 0.36 for neutral, $F(2,34) = 157.90$, $P < 0.001$, $\eta^2 = 0.90$) and arousal (6.23 ± 0.83 for negative, 6.08 ± 1.15 for positive, and 3.73 ± 0.95 for neutral, $F(2,34) = 114.21$, $P < 0.001$, $\eta^2 = 0.87$) ratings (Figure 1(a)). Negative pictures had the lowest valence rating scores (P's < 0.001). More important, the negative and positive pictures were comparable in arousal rating ($P = 0.99$), and both were rated higher in arousal than the neutral pictures (P's < 0.001). Thus, the arousal level was optimally controlled in the experiment.

The neutral words were 360 Chinese nouns, half of which were abstract (e.g., courage) and the other half were concrete (e.g., bedding). They had middle level of word frequency (26.56 ± 92.99) and number of strokes (17.30 ± 4.93). The words were divided into two sets, one set as learning materials and the other as new words during retrieval. Each set was further divided into three subsets. The subsets were matched in frequency and number of strokes (F's < 1). The pictures were divided into four sets. Each set had 20 negative pictures, 20 neutral pictures, and 20 positive pictures. The four sets were used as the contexts for four time intervals. The four sets were matched in their valence and arousal ratings (F's < 1). The 180 pictures and 180 words were formed into 180 pairs that did not have close semantic relationship to each other. The materials were counterbalanced so that each picture-word pair had an equal chance to be the material for each condition.

2.1.3. Procedure. During the study phase (Figure 2(a)), a neutral word was first presented for 2 s for each trial, and the participants were asked to judge whether the word was a concrete noun or an abstract noun. Then the combination of picture and word was presented for 6 s, during which participants were asked to remember the word and its link with the picture to imagine a scene, followed by the task of making a subjective evaluation of the vividness of the imagination they made (1 refers to not vivid at all, and 5 refers to extremely vivid). All stimuli were pseudorandomly presented during the encoding phase so that no more than three stimuli that were tested in the same time interval and with the same valence were presented consecutively.

During the test phase, a word was presented on the screen for 2 s for each trial, and the participants judged whether the word was old or new as accurately and quickly as possible

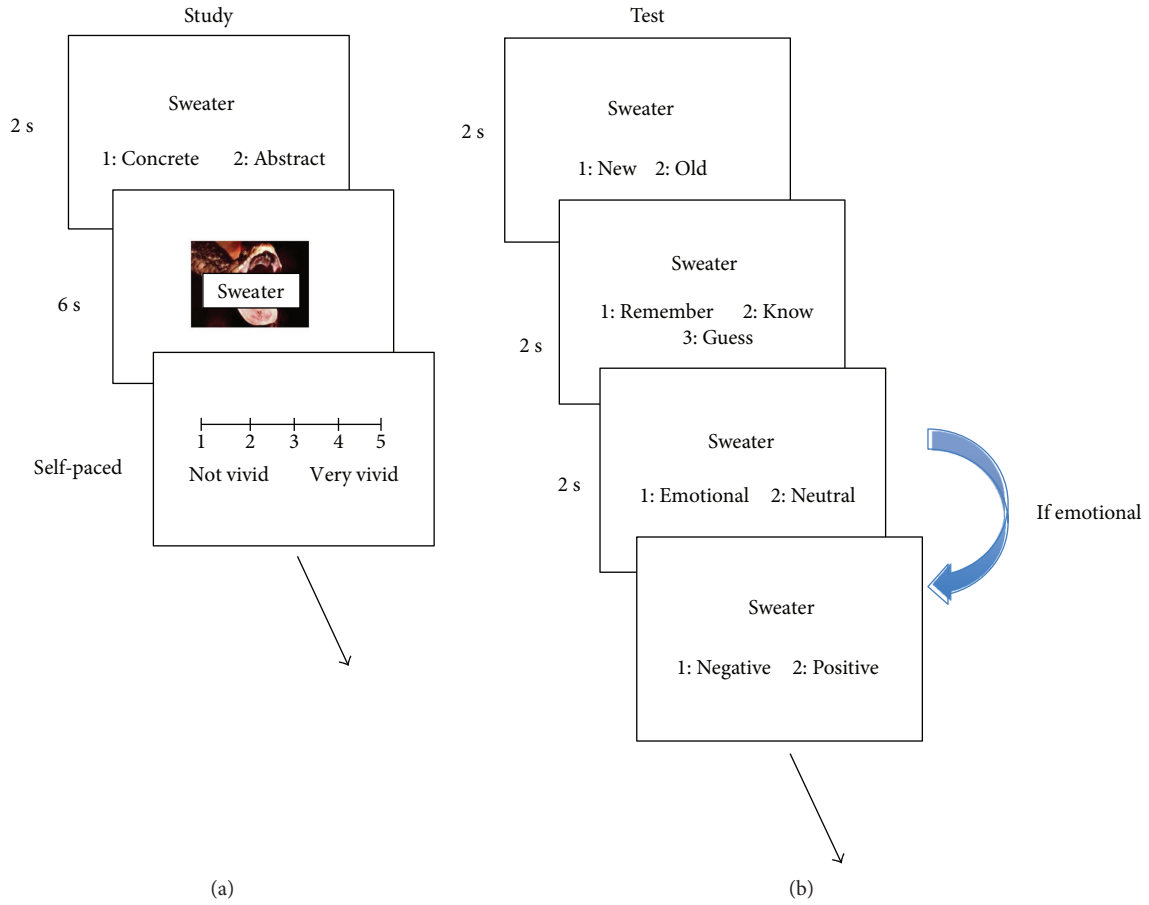

Figure 2: Procedure of the study and test sessions in experiment 1. During encoding, participants first performed a concreteness judgment for each word and then performed an imagination task to combine the picture and the word. During retrieval, the participants made word recognition, R/K/G judgment, and source judgment for each word. Chinese words are replaced by English words for illustration purpose.

(Figure 2(b)). If the word was judged as "old," the word was presented for 1 s again, and the participants were asked to make remember/know/guess judgment. The response with "remember" was made when the participants could retrieve stimulus-related details or contexts; the response with "know" was made when they only felt that the stimulus was familiar without any detailed information. The response of "guess" was made when they retrieved the stimulus by the previously mentioned two processes, they responded with "guess." Finally, the word was presented again, and the participants judged whether the context picture was emotional/neutral or negative/positive. The old and new words were pseudorandomly presented for each time interval, so that no more than three words that were in the same valence were presented consecutively.

The participants learned the 180 words in the same day and then performed the recognition tests at three time intervals (with different words). Before each test phase, a 5 min distraction task was performed to avoid a rehearsal from the study phase (i.e., count backward by 7 continuously from 1000). The participants had separate opportunities to practice the study and test trials before the formal phase.

2.1.4. Data Analysis. The hit rate (Hit), false alarm rate (FA), corrected recognition (Hit-FA), and the mean reaction times (RTs) were calculated and analyzed separately, using a repeated measures ANOVA with the time interval (10 min, 1 day, and 1 week) and the emotional contextual type (positive, negative, and neutral) as within-subject factors. Four subjects' data were excluded due to lower hit rates (>2 SD) at 10 min. The remaining 24 subjects' results were used for data analysis. The d' was also calculated for each subject and averaged according to signal detection theory. Because the results of the d' value and corrected recognition were similar, only the corrected recognition results were reported in detail. The RTs were based on the mean RTs and only correct responses were included in the analysis. The forgetting rate was estimated by the interaction between the retention interval and the memory type [29, 30]. Partial eta squared (η^2) was calculated to estimate the effect size of each analysis. Post hoc pairwise comparisons were Bonferroni-corrected ($P < 0.05$, two-tailed).

Recollection and familiarity processes were estimated using the independent K (IRK) procedure [31, 32], in which R responses were assumed to estimate recollection, whereas familiarity was estimated as the proportion of K responses

divided by the proportion of non-*R* responses. By this, the *R* and *K* responses were not only mutually exclusive but also independently estimated. Then *R* and IRK responses were corrected using the FA: recollection = $p(R, \text{Hit}) - p(R, \text{FA})$; familiarity = $p(K, \text{Hit})/(1 - p(R, \text{Hit})) - p(K, \text{FA})/(1 - p(R, \text{FA}))$ [31–33]. Repeated measures ANOVA with the time interval (10 min, 1 day, and 1 week) and the emotional contextual type (negative, positive, and neutral) as within-subject factors was performed.

2.2. Experiment 2. In experiment 2, we explored whether punishment or reward motivation modulated memory differently over time. Participants learned the same neutral words as those in experiment 1. In one-third of the trials, they were told that if they remembered the word during the test, they would be rewarded afterward. In another third of the trials, if they did not remember the word afterward, they would be punished. In the last third of the trials, if they remembered the words, they were neither rewarded nor punished. The motivational intensity was assessed and matched for reward and punishment conditions to exclude its potential effect on memory performance [34]. Word recognition and source memory were tested after different time intervals.

2.2.1. Participants. Twenty-eight healthy, right-handed participants (12 males) with a mean age of 22.0 ± 2.64 years were recruited in the study. All of the participants were native Chinese speakers, and they all provided written informed consent in accordance with the procedures and protocols approved by the Review Board of School of Psychological and Cognitive Sciences, Peking University.

2.2.2. Materials. Two within-subject factors were included in the study: motivational context (reward, punishment, and control) and retention interval (10 min, 1 day, 1 week, and 1 month). The words were the same as those in experiment 1. The motivation was manipulated with symbols. The symbol "↑ 6 yuan" referred to the reward condition, symbol "↓ 6 yuan" referred to the punishment condition, and "0 yuan" referred to the control condition.

Before the formal experiment, another 10 participants (5 males, 23 ± 1.62 years old) rated the motivational intensity of the punishment and reward conditions. The participants were asked to rate their motivation to remember the word when they would get the reward for remembering or when they would get the punishment for forgetting. We asked the participants to rate their motivational intensity from 1 to 9 (lowest to highest). The amount of money varied from 0.1 yuan to 0.2 yuan, 0.5 yuan, 1 yuan, 5 yuan, and 10 yuan. To control the influence of the total amount of money on the rating, the participants were told that they would pay 20 yuan, 60 yuan, and 200 yuan, respectively, after the test. The results showed that the motivational intensity increased linearly when the reward or punishment levels increased (Figure 1(b)), irrespective of the total test fee. Thus, we chose 6 yuan as the level of punishment and reward in the experiment.

2.2.3. Procedure. During the encoding phase, the participants were told to memorize the words in different motivational conditions. In each trial, participants were first presented a neutral word for 2 s, during which they made a concrete/abstract judgment with the word (Figure 3(a)). Then the word was presented again for 4 s with the motivational cues. Three kinds of symbols represented motivational cues, "0 yuan," "↓ 6 yuan," and "↑ 6 yuan." The "↑ 6 yuan" meant that the participants would get the reward of 6 yuan for each word if the word was correctly recognized in the recognition task; "↓ 6 yuan" meant that the participants would get a deduction of 6 yuan for each word if the word was not correctly recognized in the recognition task; "0 yuan" meant that there was neither reward nor punishment regardless of whether the participants recognized the word in the recognition task. The participants were asked to remember the association of word and the motivational condition. At the end of the learning phase, they were asked to fill in a motivational intensity scale, using numbers 1 to 5 to evaluate the motivational intensity of memorizing words subjectively in different incentive conditions.

During the test phase, in each trial, the participants performed three tasks: an old/new recognition test, a remember/know/guess (R/K/G) judgment, and a motivational condition (reward/control/punishment) judgment (Figure 3(b)). The procedure was the same as experiment 1, except that in the source memory task, the participants were asked to judge the motivational condition the word was associated with. The words were presented in a pseudorandom order, so that no more than three words from the same incentive condition or old/new condition were presented continuously.

To control for the response bias, two steps were further applied. First, before the experiment, the participants were informed that the amount of reward and punishment was independent of the test pay. Second, before the test phase, the participants were told that the judgment of new words would be rewarded and punished. When a new word was judged as new, the participants would be given a 2-yuan reward; when a new word was judged as old, the participants would get a deduction of 2-yuan punishment.

Before the formal test, the participants had an exercise with feedback of their performance, and they saw their own rewards and punishments at the end of the exercise. In the formal test phase, no feedback was provided.

After the study, the participants were asked to fill in the questionnaire about the motivational intensity (range: 1–5): How strong is the motivation to avoid losing money when you see the cue of "↓ 6 yuan"? How strong is the motivation to gain money when you see the cue of "↑ 6 yuan"? How strong is the motivation to gain more money when you see the cue of "0 yuan"?

The participants learned the 240 words in the same day and then performed the recognition tests at four time intervals. The material varied for different time intervals. Before each test phase, to avoid a rehearsal from the study phase, the participants were asked to count backward by 7 continuously from 1000 for 5 minutes. In addition, to prevent the participants from rehearsing the stimuli after the study phase, they were reminded that it was not necessary to retrieve or forget the stimuli intentionally.

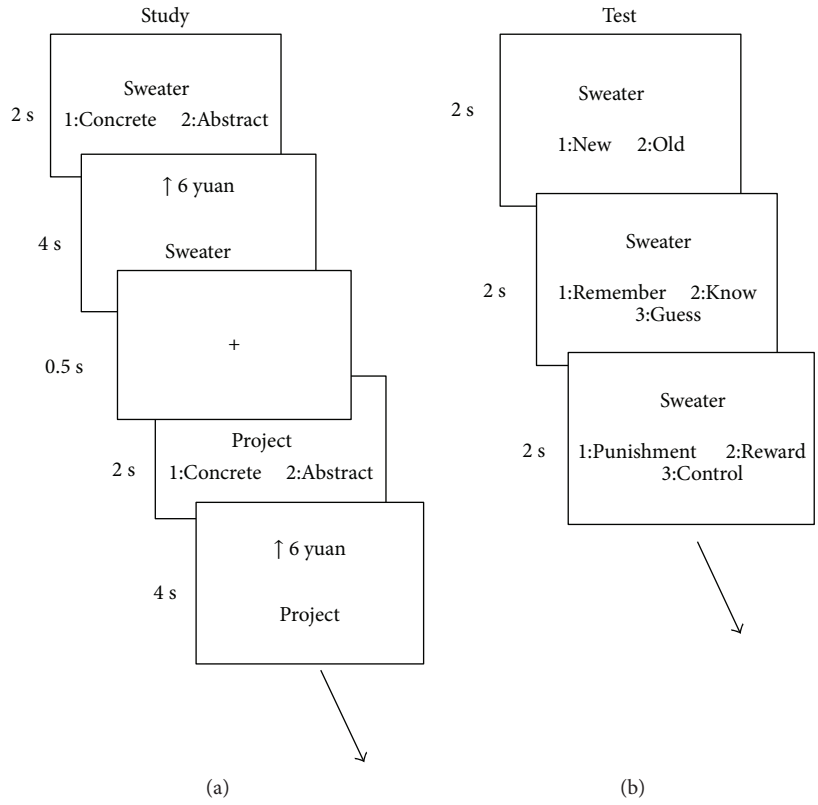

Figure 3: Procedure of the study and test sessions in experiment 2. During encoding, participants first performed a concreteness judgment for each word and then tried to remember the word with different motivational cues. During retrieval, the participants made word recognition, R/K/G judgment, and source judgment for each word. Chinese words are replaced by English words for illustration purpose.

2.2.4. Data Analysis. The analysis was the same as that in experiment 1. The Hit rate, FA rate, corrected recognition (Hit-FA), and mean RTs were calculated and analyzed separately using a repeated measures ANOVA with the time interval (10 min, 1 day, 1 week, and 1 month) and the motivational context (reward, punishment, and control) as within-subject factors. Two subjects' data were excluded due to lower hit rates (>2 SD). The remaining 26 subjects' results were used for data analysis.

3. Results

3.1. Experiment 1. During the encoding task, the participants rated the sentence vividly with an average score of 3.14 ± 0.53. The ANOVA results showed that there was no significant difference in vividness for different contexts (positive: 3.20 ± 0.51; negative: 3.12 ± 0.55; neutral: 3.12 ± 0.58. $P = 0.81$). This ensured that stimuli in each condition were efficiently encoded.

For the corrected recognition, the results showed that memory accuracy decreased over time ($F(2,46) = 130.52$, $P < 0.001$, $\eta^2 = 0.85$) (Figure 4). There was a significant interaction between retention interval and context ($F(4,92) = 5.30$, $P = 0.001$, $\eta^2 = 0.19$). Further analysis showed that there was higher corrected recognition for positive ($P = 0.007$) and negative ($P = 0.003$) conditions than for the neutral condition at 10 min and higher for the positive than for the negative condition at 1 day ($P = 0.05$). There was higher corrected recognition for the negative than for the positive condition ($P = 0.035$) at 1 week (Figure 4(a)). In addition, for memory in negative contexts, recognition performance decreased from 10 min to 1 day ($P < 0.001$) and stayed stable from 1 day to 1 week ($P = 0.149$). For memory in positive and neutral contexts, recognition performance decreased from 10 min to 1 day ($P < 0.001$) and from 1 day to 1 week (P's < 0.005). The corrected recognition in different conditions was significantly higher than expected by chance (0) (P's < 0.05). For the RTs, there was a significant effect for the time interval ($F(2,46) = 5.21$, $P = 0.01$, $\eta^2 = 0.207$) but no significant effect of context or the interaction between context and interval (P's > 0.05).

The Hit rate decreased over time ($F(2,46) = 57.11$, $P < 0.001$, $\eta^2 = 0.713$). The effect of interaction was significant ($F(4, 92) = 4.05$, $P = 0.005$, $\eta^2 = 0.15$). Memories for both negative and positive contexts were higher than those for the neutral context at 10 min interval (P's < 0.01), and the memory for positive and negative contexts did not differ ($P = 0.99$). There were no significant differences among contexts at 1-day and 1-week intervals (P's > 0.10). For the FA rate, there was significant effect of time interval ($F(2,46) = 13.28$, $P < 0.001$, $\eta^2 = 0.37$), increasing from 10 min to 1 day ($P < 0.01$) and from 1 day to 1 week ($P < 0.01$), but the interaction and context effect were not significant (P's > 0.20).

Regarding the contribution of recollection, there was a significant effect of time interval ($F(2, 46) = 40.89$, $P < 0.001$,

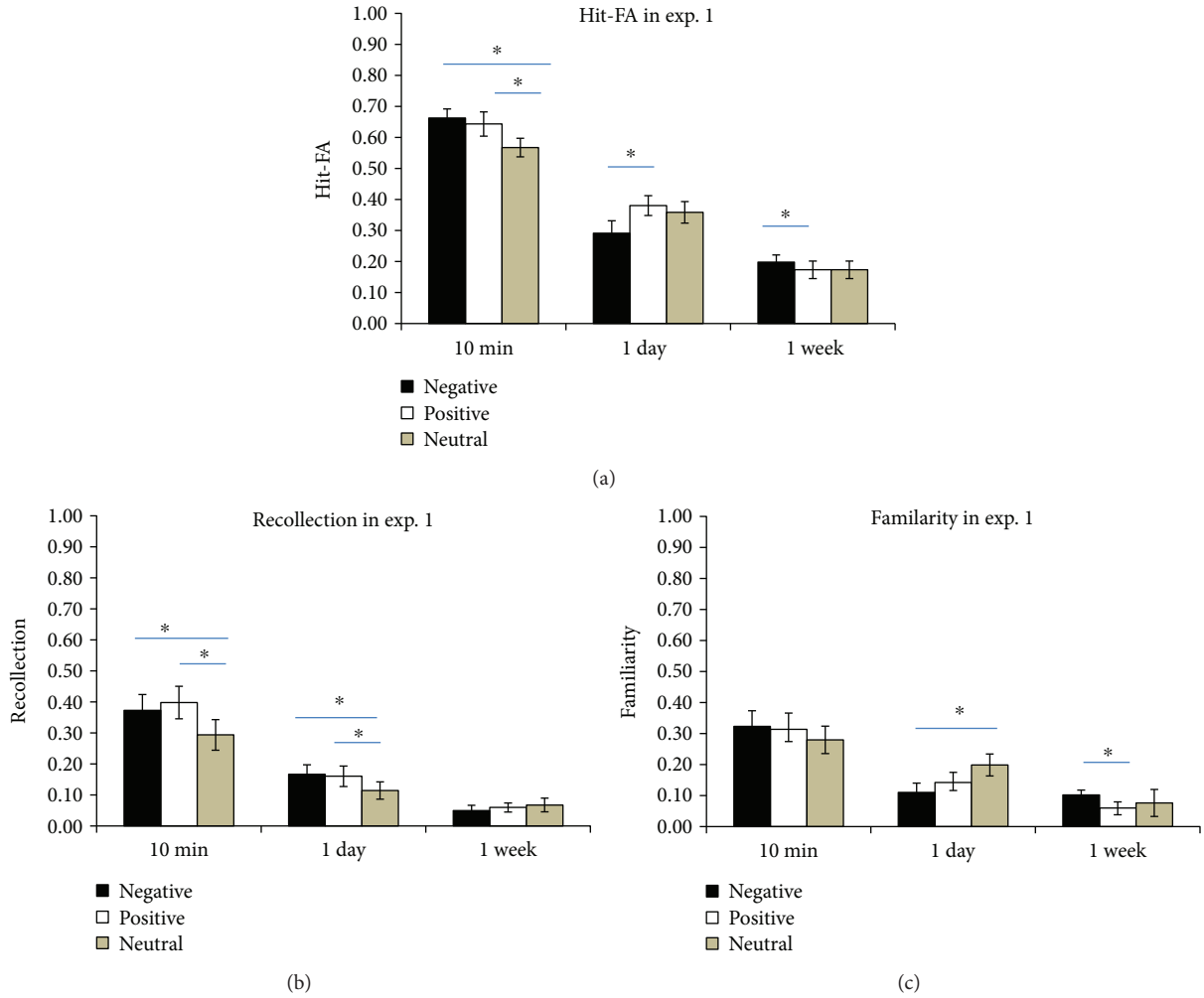

FIGURE 4: Results of experiment 1. Corrected recognition (a). Contribution of recollection (b) and familiarity (c). The error bars represent the standard errors of the means. $*$ represent $P < 0.05$.

$\eta^2 = 0.64$), showing that the recollection estimates decreased over time. The interaction between time interval and context was significant ($F(4, 92) = 3.87$, $P = 0.011$, $\eta^2 = 0.14$). Further analysis showed a higher contribution of recollection for the positive ($P = 0.001$) and the negative ($P = 0.008$) than for the neutral at 10 min. There was a higher contribution of recollection for negative than for neutral at 1 day ($P = 0.022$) (Figure 4(b)). The recollection estimates in different conditions were significantly higher than expected by chance (0) (P's < 0.02).

Regarding the contribution of familiarity, there was a significant effect of time interval ($F(2,46) = 23.58$, $P < 0.001$, $\eta^2 = 0.506$). The interaction between time interval and context was significant ($F(4,92) = 5.506$, $P = 0.002$, $\eta^2 = 0.193$). Further analysis showed that there was a higher contribution of familiarity for the negative than for the positive ($P = 0.019$) at 1 week (Figure 4(c)). In addition, the contribution of familiarity decreased from 10 min to 1 week for the positive condition (P's < 0.01) and decreased from 10 min to 1 day for the negative condition ($P < 0.001$). The familiarity estimates in different conditions were significantly higher than expected by chance (0) (P's < 0.05).

We also included the process (recollection, familiarity) as a factor in the ANOVA analysis. The results showed a significant interaction among process, time, and context ($F(4,84) = 3.51$, $P < 0.01$, $\eta^2 = 0.14$). The effect of process was not significant ($F < 1$). Further analysis showed that there was a higher contribution of familiarity than of recollection for the negative context at 1 week ($P = 0.006$). It suggested that memory performance relies on both recollection and familiarity, and the higher memory for the negative context at 1 week is associated with the familiarity contribution.

Regarding the memory for the emotion/neutral judgment, the results showed that memory accuracy decreased over time ($F(2,46) = 17.60$, $P < 0.001$, $\eta^2 = 0.434$). There was a significant main effect of emotion ($F(1,23) = 11.69$, $P = 0.002$, $\eta^2 = 0.337$), showing a higher accuracy for the neutral than for the emotional ($P = 0.002$). Only the source memory for the neutral contexts was above the chance level. Regarding the memory for the negative/positive judgment, the results showed that memory accuracy decreased over time ($F(2,46) = 3.4$, $P = 0.047$, $\eta^2 = 0.129$). There was no significant main effect of emotion ($F(1,23) = 1.04$, $P = 0.318$,

$\eta^2 = 0.043$), showing no difference of accuracy between negative and positive source memory. The source memory was not above chance level in the negative/positive source judgment. We also calculated the source memory out of the corrected trials, but the result remained the same. It suggested that subjects could not remember the context conditions the words had during encoding.

In sum, the main result of experiment 1 was that there was significant interaction between time and context for corrected recognition. The memory with negative and positive contexts changed over time in different patterns. The positive advantage (versus negative) occurred at the 1-day interval, and negative advantage (versus positive) occurred at the 1-week interval. In addition, the positive advantage at 1 day was driven by both recollection and familiarity processes, whereas the negative advantage at 1 week was driven by the familiarity process. The memory for contextual information was not above chance level; therefore, it was not enhanced.

3.2. Experiment 2. The subjective rating scores after the study showed that the scores of motivation were higher for both reward (4.07 ± 0.71) and punishment (4.24 ± 0.64) conditions than the control (3.07 ± 1.07) condition, $F(2,56) = 21.367$, $P < 0.001$, but there was no significant difference between the reward and the punishment conditions ($P = 0.80$). The post hoc reports ensured that the motivational levels of reward and punishment were matched.

For the corrected recognition, the results showed that memory accuracy decreased over time ($F(3,75) = 196.71$, $P < 0.001$, $\eta^2 = 0.887$) (Figure 5(a)). There was a significant main effect of motivation ($F(2,50) = 4.72$, $P = 0.013$, $\eta^2 = 0.159$), showing that memory for the reward condition was higher than that for the control condition ($P = 0.022$), but the memory for the punishment condition was similar to that of the control condition ($P = 0.53$). There was a significant interaction between time interval and context ($F(6,150) = 4.07$, $P = 0.001$, $\eta^2 = 0.14$). Further analysis showed higher corrected recognition for the reward condition than for the punishment ($P = 0.012$) and control conditions at 10 min (P's < 0.01) and 1 day (P's < 0.05), but there was higher corrected recognition for the punishment than for the reward ($P = 0.007$) and control ($P = 0.026$) at the 1-month interval, with no significant difference between the reward and control condition ($P > 0.05$). It suggested that memory for the punishment condition is forgotten more slowly than the other two conditions. The corrected recognition in different conditions was significantly higher than expected by chance (0) (P's < 0.05). For the RTs, there were no significant effects of time interval, context, or their interaction (P's > 0.05).

Similar to the corrected recognition, the Hit rate decreased over time ($F(3,75) = 70.36$, $P < 0.001$, $\eta^2 = 0.74$). There was a significant main effect of motivational condition ($F(2,50) = 4.85$, $P = 0.013$, $\eta^2 = 0.162$), showing that memory performance for the reward condition was higher than that for the punishment and control conditions (P's < 0.02), but the memory for the punishment and control conditions did not differ ($P = 0.10$). There was no significant interaction between context and time interval ($F(6,150) = 1.56$, $P = 0.18$, $\eta^2 = 0.06$). For the FA rate, there was a significant effect of time interval ($F(3,75) = 56.68$, $P < 0.001$, $\eta^2 = 0.69$), increasing from 10 min to 1 day ($P < 0.001$) and from 1 day to 1 week ($P < 0.001$), and remained stable from 1 week to 1 month ($P > 0.05$). The interaction was significant ($F(6,150) = 2.90$, $P = 0.01$, $\eta^2 = 0.104$). Further analysis showed that the FA rate was higher for the punishment (versus reward) condition at 10 min ($P = 0.06$), but the opposite at the 1-week interval ($P = 0.008$).

Regarding the contribution of recollection, there was a significant effect of time interval ($F(3,75) = 140$, $P < 0.001$, $\eta^2 = 0.848$). The interaction between context and time interval was significant ($F(6,150) = 5$, $P = 0.001$, $\eta^2 = 0.167$). Further analysis showed that there was a higher contribution of recollection for the reward condition than for the punishment and control conditions at 10 min ($P < 0.001$) and 1 day ($P < 0.05$) (Figure 5(b)). The estimates in different conditions were significantly higher than expected by chance (0) (P's < 0.05) except for that in the reward condition at the 1-month interval ($P = 0.17$). It suggested that reward advantage is attributed to the recollection process, but recollection decreased quickly in the reward condition. The contribution of familiarity decreased over time ($F(3,75) = 24.61$, $P < 0.001$, $\eta^2 = 0.50$). The interaction of interval and context was not significant ($F < 1$, $P > 0.60$) (Figure 5(c)). The estimates in different conditions were significantly higher than the expected by chance (0) (P's < 0.05) except for that in the reward condition at the 1-month interval ($P = 0.11$).

We also included the process (recollection, familiarity) as a factor in the ANOVA analysis. The results showed a significant effect of process ($F(1,24) = 14.91$, $P = 0.001$, $\eta^2 = 0.38$). There was a marginally significant interaction among process, time, and context ($F(6,144) = 1.87$, $P = 0.08$, $\eta^2 = 0.07$). Further analysis showed that there was a higher contribution of recollection than familiarity in the positive and neutral contexts at 10 min and 1 day (P's < 0.01) and in the negative context only at 10 min ($P = 0.001$). It suggested that memory performance relies on recollection at shorter intervals, but relies on both processes at longer intervals. The higher memory for the negative context at 1 week might be associated with both recollection and familiarity contributions.

The source memory was not above chance level (0.33) from 1 day to 1 month (P's > 0.05). At the 10 min interval, there was higher accuracy for the reward than for the punishment condition ($P = 0.04$), but both conditions did not significantly differ from the control condition (P's > 0.30). There was no significant effect of interaction ($F(6,150) = 2.05$, $P = 0.081$, $\eta^2 = 0.08$). The result remained the same when corrected values of source memory were used for analysis.

In sum, similar to those in experiment 1, there was significant interaction between time and context for corrected recognition in experiment 2. The memory by reward decreased quickly and depended on the recollection process, whereas the memory by punishment contexts decreased slower after 1 week. The results of experiment 2 suggested that memory by punishment and reward motivation produces different rates of forgetting.

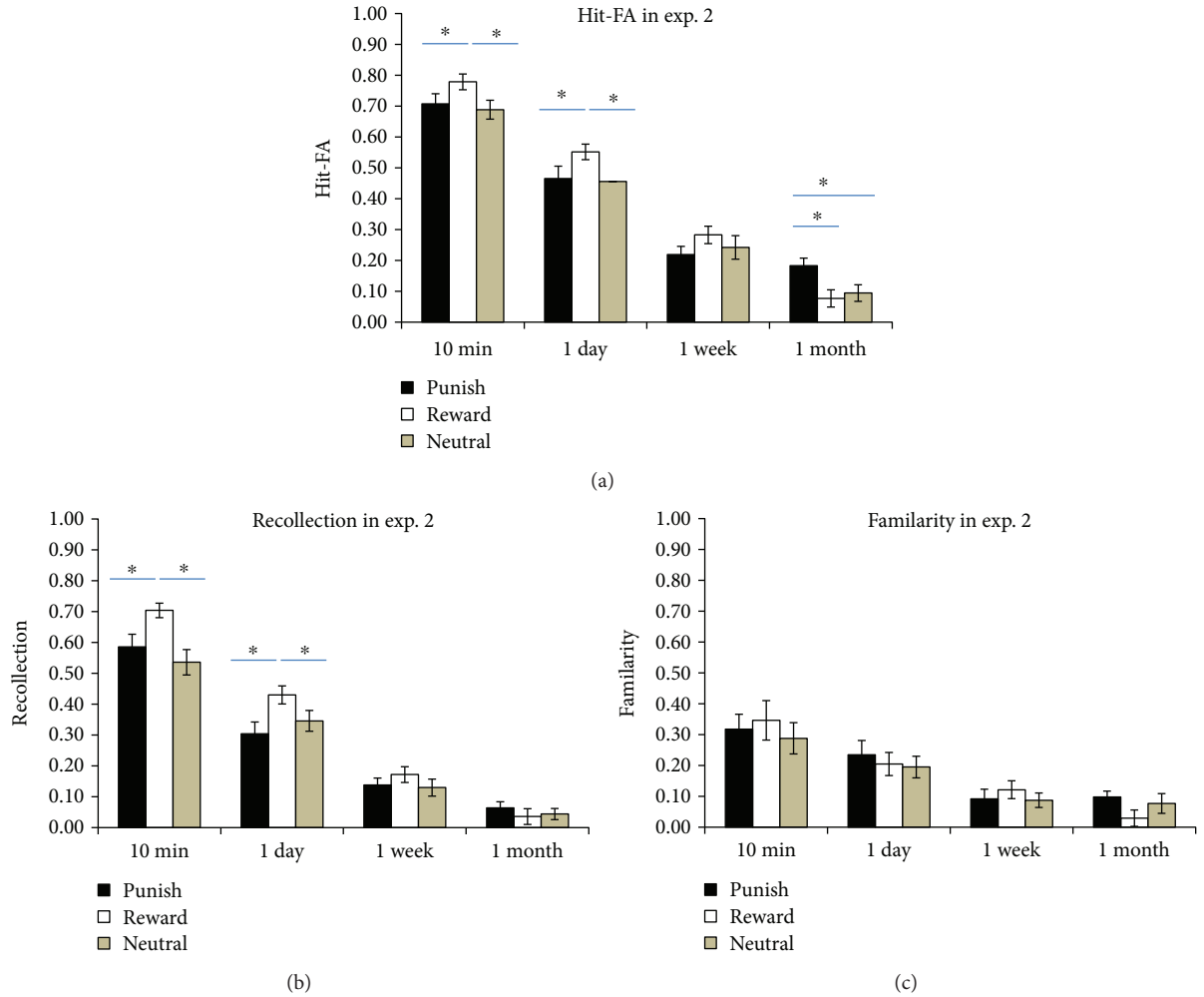

Figure 5: Results of experiment 2. Corrected recognition (a). Contribution of recollection (b) and familiarity (c). The error bars represent the standard errors of the means. ∗ represent $P < 0.05$.

4. Discussion

In this study, the factors of type of context and time interval were manipulated to explore their effects on memory for neutral targets. We asked whether these factors influenced memory after different emotional contexts and motivational conditions over time. By controlling for the arousal level and motivational intensity, the results showed significant interaction between context and time interval in experiments 1 and 2. Compared to negative and punishment conditions, words in positive and reward contexts were recognized better at shorter intervals, which was associated with recollection process. In contrast, the words in negative and punishment contexts were recognized better at longer intervals, which was mainly associated with familiarity process. The results clarified how contextual and motivational cues influence memory at both short and long intervals and highlighted the contextual feature in memory formation and retention.

4.1. Positive versus Negative Contexts from 10 Min to 1 Week. One novelty of the study was that we compared the memory performance in the positive and negative contexts in different time intervals and found that they had different effects on memory of neutral targets over time. Specifically, memory in the positive contexts was forgotten from 10 min to 1 week, whereas memory in the negative contexts was forgotten only from 10 min to 1 day. Thus, the enhanced memory in the positive context was obvious at shorter intervals, which relied on the recollection, whereas the negative (versus positive) enhancement was obvious at longer intervals, which mainly relied on the familiarity process.

The results supported our hypothesis that memory enhancement in the positive and negative contexts is different and time-dependent. The reason for the time-dependent memory enhancement is associated with the underlying processes. First, positive and negative emotions have different characteristics, and memories associated with them rely differentially on recollection and familiarity processes. Compared with negative emotion, positive stimuli broaden the scope of attention [35], which results in increased perceptual processing of task-irrelevant information [15]. The memory for the neutral words may thus have more associated contextual information, leading to increased recollection contribution [36]. In contrast, negative contexts

reduced memory specificity and lead to overgeneralized emotional memory [37]. The enhancement after shock as contexts depended on item familiarity but not recollection [9].

Second, there are different forgetting rates for memories depended on recollection and familiarity [25, 33]. Memory relying on the recollection process is subjected to decay, whereas that relying on familiarity process is more resistant to decay over time [25]. In experiment 1, the interactions between time interval and context were significant for both recollection and familiarity processes. There was higher recollection contribution for the positive and negative contexts than the neutral at 10 min and higher familiarity for the negative than for the positive at 1 week. The contribution of familiarity decreased more slowly for the negative than the positive contexts. This explains why memory in positive contexts was more enhanced at 10 min and 1-day intervals, and memory in negative contexts could remain at 1 week. Cairney et al. also showed that memory of target pictures in negative contexts was less likely to be lost [38]. The results provided evidences that the positive and negative contexts are associated different processes to enhance memory with the passage of time.

4.2. Reward versus Punishment/Stressful Contexts from 10 Min to 1 Month. Previous studies have suggested that the effect of motivational contexts occurs right after the encoding [23], 24 hours later [5], and even three weeks later [6]. The current study clarified the extent the reward and punishment contexts modulated memory at different time intervals. Neutral words in reward contexts were recognized at higher level than those in the punishment and neutral contexts at 10 min and 1 day, and the words in the punishment contexts were recognized better than those in the positive and neutral contexts at 1 month. Thus, words in the stress/punishment context were forgotten more slowly than those presented in the reward contexts.

In this study, we found the reward-related enhancement occurred at both 10 min and 1 day. The memory enhancement was also observed when the test delay was immediately or minutes after encoding [13, 23, 39]. Reward but not punishment context enhanced the memory when the test was performed minutes after encoding [8, 34]. Although Shigemune et al. found comparable enhancement for both reward and punishment contexts immediately after encoding [23], they measured item with source memory correct rather than item memory.

Some studies only found the reward-related enhancement at 24 h but not immediately after study [20, 21]. The results of reward-related enhancement at both 10 min and 1 day in this study are not contradictory to the retroactive enhancement, because we presented the motivational contexts with the neutral words for 4 s, rather than after the neutral words [20, 21]. The mechanisms for proactive or retroactive enhancement are different. When contexts are presented before or right with the stimuli, both encoding and consolidation processes are possible ways to enhance proactive memory [13, 23, 39, 40]. In contrast, the retroactive memory emphasizes that the reward and punishment contexts modulate memory consolidation [20–22]. For example, if neutral objects were paired with shock, the retroactive memory for the objects in the same category was selectively enhanced 6 h and 24 h later [22]. Similar pattern occurred when the category was rewarded [39, 41, 42]. Also note that in Dunsmoor et al. [22], in addition to the retroactive memory enhancement, they found the memory enhancement for the stimuli that were paired with shocks immediately after encoding, 6 h and 24 h later, which was consistent with our findings.

Similar to that for emotional contexts, the reason for the time-dependent memory enhancement for motivational contexts is associated with the underlying processes. The results showed that the enhancement for the reward contexts at short intervals was associated with recollection contribution, and that for the punishment context at longer interval was associated with both recollection and familiarity contribution. It is suggested that under the reward condition, subjects are more likely to remember the details of the neutral stimuli [6]. There was a higher contribution of recollection than familiarity in the positive and neutral contexts at 10 min and 1-day intervals. Previous studies have also shown that reward improved memory by selectively enhancing recollection process rather than familiarity [12, 13, 43]. As the recollection process is subjected to decay over time [25, 33], the memory enhancement for the reward contexts diminished over time. By contrast, punishment motivation facilitates global representation of context [8], so the memory under the punishment is more schematic. At the 1-month interval, the recollection and familiarity estimates were both above chance level for the punishment condition but not for the reward condition. Thus, the different forgetting pattern for the reward and punishment context reflects that the underlying processes support memory representations.

4.3. Memory for Contextual Information. Different from the enhanced memory for the target words, we did not find significant memory enhancement for contextual information. The source memory did not exceed the chance level in most conditions in experiments 1 and 2.

Our results suggested that memory enhancement does not apply to all information related to the targets [11, 13, 44, 45]. The memory of contextual information may be automatic and implicit. Different from remembering the emotional target, the relation between the target and context is sparse. Emotion and motivation selectively affect the recollection of target items rather than the contexts [46, 47] and do not enhance the memory of extrinsic or contextual information [46]. In addition, even participants were more confident that they remembered pictures, the performance was irrespective of actual encoded context [45]. Thus, it is the subjective feeling of the context, not the objective context that determines the memory for contextual information.

On the other hand, even the source memory is implicit, the context could influence the subsequent cognitive processes, such as decision making and valence judgment [37, 48]. These results suggested that emotional and motivational contexts influence memory retrieval in the absence of overt behavioral differences [49]. Participants may reexperience the emotion automatically during retrieval of neutral

targets [49, 50]. Also, note that the source memory may be related to source type. For example, Shigemune et al. tested the position of the word, rather than the contextual condition, and found higher source memory for emotional conditions [23]. Further studies could use implicit memory tasks or other sources to clarify whether the source information is retained.

4.4. Relationships between Emotional and Motivational Contexts. Although emotional pictures and monetary cues were different in various aspects, our results showed that both of them enhanced the memory for the neutral targets. In addition, the memory enhancement in experiments 1 and 2 had similar characteristics. For example, the positive and reward contexts enhanced memory at shorter time intervals, which were driven by the recollection process; whereas, the negative and punishment contexts enhanced memory at longer intervals, which were mainly driven by the familiarity process. In addition, the memory for contextual information was low.

There is a close relationship between emotion and motivation in both behavior and brain activation. For example, in a study by Delgado et al., mild shock and loss of money were used as aversive unconditioned stimuli separately and were paired with one of two conditioned stimuli [26]. The results showed that the striatum was involved in both shock and money conditions. In addition, positive stimuli enhance reward-related memory performance and activation in the midbrain [27, 51]. Arousal level interacted with the motivational condition to influence subsequent memory performance [34]. These results suggested that positive and reward and negative and punishment may interact and share similar brain mechanisms, including the midbrain reward system and the amygdala. The results in our study provided behavioral evidences that the positive and reward and negative and punishment context had similar mechanisms in enhancing memory of the neutral targets. Both types of the contexts could modulate the medial temporal memory system, making the behavioral consequences similar.

On the other hand, the effects of the two types of contexts differed in several aspects. In this study, although we are unable to compare the two types of contexts directly due to various experimental manipulations, some differences may be inferred from our results. First, memory performance in the motivational contexts was higher than that in the emotional contexts, especially at shorter intervals. The memory enhancement for the motivational contexts depended more on recollection, because the results showed higher recollection estimates than familiarity in experiment 2, but the two processes were comparable in experiment 1. Second, the memory in the emotional contexts seemed to be forgotten more quickly than that in the motivational contexts. Particularly, memory enhancement for the negative contexts occurred at 1 week, whereas that for the punishment contexts at 1 month. We call for caution in interpreting this result and advise further studies to clarify whether the memory in the motivational contexts lasts longer than that in the emotional contexts. The difference in memory performance may be a possible source of divergent results. Third, the memory for motivational contexts was above chance level at the 10 min interval, but the memory for emotional contexts was not above chance level from 10 min to 1 week. These results suggested that reward and punishment contexts might facilitate memory details of both target item and source information at shorter intervals. How these differences happen at the level of neural activation needs future investigations.

4.5. Conclusions. In summary, the results of this study clarified the cognitive mechanisms of how contextual and motivational cues influence memory formation and consolidation. The positive and reward contexts enhanced memory by recollection process and lasted for a shorter time. The negative and punishment contexts enhanced memory mainly be familiarity process and lasted at longer intervals. The results provided evidence that emotional and motivational cues influence memory processes in different dimensions and highlight that different processes mediate memory enhancement in different contexts.

The current findings have significant implications for practice. It is clear that different contexts had impacts on recent and remote memories that were associated with these contexts. On the one hand, we are exposed to a large amount of information, and most of it is devoid of emotional and motivational values. To enhance memory, one possible way is to combine emotional or motivational contexts with the information. Moreover, because these contexts differ in their effects on retention time and detail or gist part of memory, different contexts could be chosen to enhance memory. On the other hand, it sheds light on how stress induces long-term consequences in memory and many mental disorders [52, 53]. For example, acute stress could be induced by negative events, so the results are similar to those in negative and punishment contexts [4]. But as stress level differs in its intensity and duration, the effects of stress on memory are complicated and need careful manipulation and interpretations.

Disclosure

The funder had no role in study design, data collection and analysis, decision to publish, or preparation of the manuscript.

Conflicts of Interest

The authors declare that they have no conflicts of interest.

Acknowledgments

This research was supported by the grant from the National Science Foundation of China (31571114, Jiongjiong Yang).

References

[1] S. Erk, M. Kiefer, J. Grothe, A. P. Wunderlich, M. Spitzer, and H. Walter, "Emotional context modulates subsequent memory effect," *NeuroImage*, vol. 18, no. 2, pp. 439–447, 2003.

[2] S. APR, H. RNA, R. J. Dolan, and M. D. Rugg, "fMRI correlates of the episodic retrieval of emotional contexts," *NeuroImage*, vol. 22, no. 2, pp. 868–878, 2004.

[3] A. P. R. Smith, R. N. A. Henson, M. D. Rugg, and R. J. Dolan, "Modulation of retrieval processing reflects accuracy of emotional source memory," *Learning & Memory*, vol. 12, no. 5, pp. 472–479, 2005.

[4] M. J. A. G. Henckens, E. J. Hermans, Z. Pu, M. Joels, and G. N. Fernandez, "Stressed memories: how acute stress affects memory formation in humans," *Journal of Neuroscience*, vol. 29, no. 32, pp. 10111–10119, 2009.

[5] R. A. Adcock, A. Thangavel, S. Whitfield-Gabrieli, B. Knutson, and G. JDE, "Reward-motivated learning: mesolimbic activation precedes memory formation," *Neuron*, vol. 50, no. 3, pp. 507–517, 2006.

[6] B. C. Wittmann, B. H. Schott, S. Guderian, J. U. Frey, H. J. Heinze, and E. Duzel, "Reward-related fMRI activation of dopaminergic midbrain is associated with enhanced hippocampus-dependent long-term memory formation," *Neuron*, vol. 45, no. 3, pp. 459–467, 2005.

[7] V. P. Murty, K. S. LaBar, and R. A. Adcock, "Threat of punishment motivates memory encoding via amygdala, not midbrain, interactions with the medial temporal lobe," *Journal of Neuroscience*, vol. 32, no. 26, pp. 8969–8976, 2012.

[8] V. P. Murty, K. S. LaBar, and R. A. Adcock, "Distinct medial temporal networks encode surprise during motivation by reward versus punishment," *Neurobiology of Learning and Memory*, vol. 134, Part A, pp. 55–64, 2016.

[9] U. Schwarze, U. Bingel, and T. Sommer, "Event-related nociceptive arousal enhances memory consolidation for neutral scenes," *Journal of Neuroscience*, vol. 32, no. 4, pp. 1481–1487, 2012.

[10] T. Tsukiura and R. Cabeza, "Orbitofrontal and hippocampal contributions to memory for face–name associations: the rewarding power of a smile," *Neuropsychologia*, vol. 46, no. 9, pp. 2310–2319, 2008.

[11] V. Sterpenich, A. D'Argembeau, M. Desseilles et al., "The locus ceruleus is involved in the successful retrieval of emotional memories in humans," *Journal of Neuroscience*, vol. 26, no. 28, pp. 7416–7423, 2006.

[12] M. J. Gruber, M. Ritchey, S.-F. Wang, M. K. Doss, and C. Ranganath, "Post-learning hippocampal dynamics promote preferential retention of rewarding events," *Neuron*, vol. 89, no. 5, pp. 1110–1120, 2016.

[13] J. P. Hennessee, A. D. Castel, and B. J. Knowlton, "Recognizing what matters: value improves recognition by selectively enhancing recollection," *Journal of Memory and Language*, vol. 94, pp. 195–205, 2017.

[14] E. E. Ebbinghaus, *Memory*T, editors. New York: Original work published; 1964..

[15] G. Rowe, J. B. Hirsh, and A. K. Anderson, "Positive affect increases the breadth of attentional selection," *Proceedings of the National Academy of Sciences of the United States of America*, vol. 104, no. 1, pp. 383–388, 2007.

[16] D. Talmi, A. K. Anderson, L. Riggs, J. B. Caplan, and M. Moscovitch, "Immediate memory consequences of the effect of emotion on attention to pictures," *Learning & Memory*, vol. 15, no. 3, pp. 172–182, 2008.

[17] E. A. Kensinger and S. Corkin, "Two routes to emotional memory: distinct neural processes for valence and arousal," *Proceedings of the National Academy of Sciences of the United States of America*, vol. 101, no. 9, pp. 3310–3315, 2004.

[18] J. L. McGaugh, "The amygdala modulates the consolidation of memories of emotionally arousing experiences," *Annual Review of Neuroscience*, vol. 27, no. 1, pp. 1–28, 2004.

[19] D. Shohamy and R. A. Adcock, "Dopamine and adaptive memory," *Trends in Cognitive Sciences*, vol. 14, no. 10, pp. 464–472, 2010.

[20] K. Murayama and C. Kuhbandner, "Money enhances memory consolidation – but only for boring material," *Cognition*, vol. 119, no. 1, pp. 120–124, 2011.

[21] K. Murayama and S. Kitagami, "Consolidation power of extrinsic rewards: reward cues enhance long-term memory for irrelevant past events," *Journal of Experimental Psychology: General*, vol. 143, no. 1, pp. 15–20, 2014.

[22] J. E. Dunsmoor, V. P. Murty, L. Davachi, and E. A. Phelps, "Emotional learning selectively and retroactively strengthens memories for related events," *Nature*, vol. 520, no. 7547, pp. 345–348, 2015.

[23] Y. Shigemune, T. Tsukiura, T. Kambara, and R. Kawashima, "Remembering with gains and losses: effects of monetary reward and punishment on successful encoding activation of source memories," *Cerebral Cortex*, vol. 24, no. 5, pp. 1319–1331, 2014.

[24] J. Graciela Martinez-Galindo and S. Cansino, "Positive and negative emotional contexts unevenly predict episodic memory," *Behavioural Brain Research*, vol. 291, pp. 89–102, 2015.

[25] T. Sadeh, J. D. Ozubko, G. Winocur, and M. Moscovitch, "How we forget may depend on how we remember," *Trends in Cognitive Sciences*, vol. 18, no. 1, pp. 26–36, 2014.

[26] M. R. Delgado, R. L. Jou, and E. A. Phelps, "Neural systems underlying aversive conditioning in humans with primary and secondary reinforcers," *Frontiers in Neuroscience*, vol. 5, p. 71, 2011.

[27] M. E. Speer, J. P. Bhanji, and M. R. Delgado, "Savoring the past: positive memories evoke value representations in the striatum," *Neuron*, vol. 84, no. 4, pp. 847–856, 2014.

[28] S. Erk, S. Martin, and H. Walter, "Emotional context during encoding of neutral items modulates brain activation not only during encoding but also during recognition," *NeuroImage*, vol. 26, no. 3, pp. 829–838, 2005.

[29] J. M. Gardiner and R. I. Java, "Forgetting in recognition memory with and without recollective experience," *Memory & Cognition*, vol. 19, no. 6, pp. 617–623, 1991.

[30] N. J. Slamecka, "On comparing rates of forgetting – comment on loftus," *Journal of Experimental Psychology: Learning, Memory, and Cognition*, vol. 11, no. 4, pp. 812–816, 1985.

[31] A. P. Yonelinas, "The nature of recollection and familiarity: a review of 30 years of research," *Journal of Memory and Language*, vol. 46, no. 3, pp. 441–517, 2002.

[32] A. P. Yonelinas and B. J. Levy, "Dissociating familiarity from recollection in human recognition memory: different rates of forgetting over short retention intervals," *Psychonomic Bulletin & Review*, vol. 9, no. 3, pp. 575–582, 2002.

[33] J. J. Yang, L. X. Zhan, Y. Y. Wang et al., "Effects of learning experience on forgetting rates of item and associative memories," *Learning & Memory*, vol. 23, no. 7, pp. 365–378, 2016.

[34] V. P. Murty, K. S. LaBar, D. A. Hamilton, and R. A. Adcock, "Is all motivation good for learning? Dissociable influences of approach and avoidance motivation in declarative memory," *Learning & Memory*, vol. 18, no. 11, pp. 712–717, 2011.

[35] B. L. Fredrickson and C. Branigan, "Positive emotions broaden the scope of attention and thought-action repertoires," *Cognition & Emotion*, vol. 19, no. 3, pp. 313–332, 2005.

[36] A. K. Anderson, P. E. Wais, and G. JDE, "Emotion enhances remembrance of neutral events past," *Proceedings of the National Academy of Sciences of the United States of America*, vol. 103, no. 5, pp. 1599–1604, 2006.

[37] B. RMWJ, F. Klumpers, and G. Fernandez, "Medial prefrontal–hippocampal connectivity during emotional memory encoding predicts individual differences in the loss of associative memory specificity," *Neurobiology of Learning and Memory*, vol. 134, Part A, pp. 44–54, 2016.

[38] S. A. Cairney, S. J. Durrant, R. Jackson, and P. A. Lewis, "Sleep spindles provide indirect support to the consolidation of emotional encoding contexts," *Neuropsychologia*, vol. 63, pp. 285–292, 2014.

[39] P. Ripolles, J. Marco-Pallares, H. Alicart, C. Tempelmann, A. Rodriguez-Fornells, and T. Noesselt, "Intrinsic monitoring of learning success facilitates memory encoding via the activation of the SN/VTA-hippocampal loop," *eLife*, vol. 5, article e17441, 2016.

[40] K. D. Duncan and D. Shohamy, "Memory states influence value-based decisions," *Journal of Experimental Psychology: General*, vol. 145, no. 11, pp. 1420–1426, 2016.

[41] A. Patil, V. P. Murty, J. E. Dunsmoor, E. A. Phelps, and L. Davachi, "Reward retroactively enhances memory consolidation for related items," *Learning & Memory*, vol. 24, no. 1, pp. 65–69, 2016.

[42] J. P. Oyarzun, P. A. Packard, R. De Diego-Balaguer, and L. Fuentemilla, "Motivated encoding selectively promotes memory for future inconsequential semantically-related events," *Neurobiology of Learning and Memory*, vol. 133, pp. 1–6, 2016.

[43] B. C. Wittmann, R. J. Dolan, and E. Duezel, "Behavioral specifications of reward-associated long-term memory enhancement in humans," *Learning & Memory*, vol. 18, no. 5, pp. 296–300, 2011.

[44] P. A. Lewis, S. Cairney, L. Manning, and H. D. Critchley, "The impact of overnight consolidation upon memory for emotional and neutral encoding contexts," *Neuropsychologia*, vol. 49, no. 9, pp. 2619–2629, 2011.

[45] A. Takashima, F. van der Ven, K. MCW, and G. Fernandez, "Retrieved emotional context influences hippocampal involvement during recognition of neutral memories," *NeuroImage*, vol. 143, pp. 280–292, 2016.

[46] A. P. Yonelinas and M. Ritchey, "The slow forgetting of emotional episodic memories: an emotional binding account," *Trends in Cognitive Sciences*, vol. 19, no. 5, pp. 259–267, 2015.

[47] M. Mather, "Emotional arousal and memory binding: an object-based framework," *Perspectives on Psychological Science*, vol. 2, no. 1, pp. 33–52, 2007.

[48] G. E. Wimmer and C. Buechel, "Reactivation of reward-related patterns from single past episodes supports memory-based decision making," *Journal of Neuroscience*, vol. 36, no. 10, pp. 2868–2880, 2016.

[49] T. W. Buchanan, "Retrieval of emotional memories," *Psychological Bulletin*, vol. 133, no. 5, pp. 761–779, 2007.

[50] J. S. Feinstein, M. C. Duff, and D. Tranel, "Sustained experience of emotion after loss of memory in patients with amnesia," *Proceedings of the National Academy of Sciences of the United States of America*, vol. 107, no. 17, pp. 7674–7679, 2010.

[51] B. C. Wittmann, K. Schiltz, C. N. Boehler, and E. Duezel, "Mesolimbic interaction of emotional valence and reward improves memory formation," *Neuropsychologia*, vol. 46, no. 4, pp. 1000–1008, 2008.

[52] B. Roozendaal, B. S. McEwen, and S. Chattarji, "Stress, memory and the amygdala," *Nature Reviews Neuroscience*, vol. 10, no. 6, pp. 423–433, 2009.

[53] D. De Quervain, L. Schwabe, and B. Roozendaal, "Stress, glucocorticoids and memory: implications for treating fear-related disorders," *Nature Reviews Neuroscience*, vol. 18, no. 1, pp. 7–19, 2017.

Hindawi
Neural Plasticity
Volume 2018, Article ID 6473728, 12 pages
https://doi.org/10.1155/2018/6473728

Research Article

Metabolic Changes Associated with a Rat Model of Diabetic Depression Detected by Ex Vivo ^{1}H Nuclear Magnetic Resonance Spectroscopy in the Prefrontal Cortex, Hippocampus, and Hypothalamus

Kun Liu,[1,2] Liangcai Zhao,[2] Wen Xu,[1] Qiuting Lin,[2] Yongjin Zhou,[1] Xiaoyan Huang,[1] Xinjian Ye,[1] Jiawei He,[1] Guanghui Bai,[1] Zhihan Yan,[1] and Hongchang Gao[2]

[1]*Radiology Department of the Second Affiliated Hospital and Yuying Children's Hospital, Wenzhou Medical University, Wenzhou 325035, China*
[2]*School of Pharmaceutical Sciences, Wenzhou Medical University, Wenzhou 325035, China*

Correspondence should be addressed to Zhihan Yan; zhihanyan@hotmail.com and Hongchang Gao; gaohc27@wmu.edu.cn

Received 9 December 2017; Revised 12 February 2018; Accepted 11 March 2018; Published 8 April 2018

Academic Editor: Fang Pan

Diabetic patients often present with comorbid depression. However, the pathogenetic mechanisms underlying diabetic depression (DD) remain unclear. To explore the mechanisms underpinning the pathogenesis of the disease, we used ex vivo ^{1}H nuclear magnetic resonance spectroscopy and immunohistochemistry to investigate the main metabolic and pathological changes in various rat brain areas in an animal model of DD. Compared with the control group, rats in the DD group showed significant decreases in neurotransmitter concentrations of glutamate (Glu) and glutamine (Gln) in the prefrontal cortex (PFC), hippocampus, and hypothalamus and aspartate and glycine in the PFC and hypothalamus. Gamma-aminobutyric acid (GABA) was decreased only in the hypothalamus. Levels of the energy product, lactate, were higher in the PFC, hippocampus, and hypothalamus of rats with DD than those in control rats, while creatine was lower in the PFC and hippocampus, and alanine was lower in the hypothalamus. The levels of other brain metabolites were altered, including N-acetyl aspartate, taurine, and choline. Immunohistochemistry analysis revealed that expressions of both glutamine synthetase and glutaminase were decreased in the PFC, hippocampus, and hypothalamus of rats with DD. The metabolic changes in levels of Glu, Gln, and GABA indicate an imbalance of the Glu-Gln metabolic cycle between astrocytes and neurons. Our results suggest that the development of DD in rats may be linked to brain metabolic changes, including inhibition of the Glu-Gln cycle, increases in anaerobic glycolysis, and disturbances in the lactate-alanine shuttle, and associated with dysfunction of neurons and astrocytes.

1. Introduction

As a chronic and progressive disease, diabetes is commonly associated with several neuropsychiatric comorbidities, such as depression, dementia, schizophrenia, and bipolar disorder [1]. The incidence of depression is two to three times higher in patients with diabetes than in healthy persons [2, 3]. Depression is also one of the most neglected symptoms in patients with diabetes and is directly linked with reduced quality of life, lower medical adherence, poor nutrition, lower physical and mental wellbeing, and even higher mortality [4–6]. Studies examining the pathogenesis of diabetic depression (DD) may contribute to developing novel interventions or therapeutic targets.

The mechanisms unpinning DD remain unclear. However, oxidative stress has been suggested as an important underlying mechanism on the basis of results from pathophysiology studies [7–9]. Oxidative stress causes significant changes in the function of several macromolecules (proteins, lipids, and DNA), and the persistent effects of these changes are related to the etiology of diabetes and depression. Hypothalamic-pituitary-adrenal axis dysregulation also plays

crucial roles in the pathogenesis of DD [8]. In addition, DD may be attributed to impaired neurogenesis and brain-derived neurotrophic factor synthesis [8]. Despite these findings, more questions than answers regarding the mechanisms underpinning DD remain.

Studies have shown that depression may be induced by unbalanced glutamatergic and GABAergic neurotransmitter metabolism. An in vivo magnetic resonance spectroscopy (MRS) study has reported that, compared with those in healthy participants, the glutamate (Glu) and the glutamate and glutamine (Glx) levels were significantly lower in the anterior cingulate in patients with major depression [10]. Gamma-aminobutyric acid (GABA) and Glx levels were also decreased in the prefrontal regions of patients with depression, and Glu and glutamine (Gln) levels were decreased in the subcortical area in type 2 diabetic patients with major depression [11, 12]. These suggest a possible role of decreased glutamatergic and GABAergic neurotransmission within these brain regions in the pathogenesis of depression. However, studies have also shown that increased glutamatergic and GABAergic neurotransmission may be involved in depression. Xu et al. found that the Glx/creatine value was significantly increased in the thalamus in patients with bipolar depression compared with that in healthy controls [13]. Glodzik-Sobanska et al. revealed an elevation of GABA levels in the frontal lobes of poststroke patients with depression [14]. These inconsistencies in the changes of glutamatergic and GABAergic neurotransmission may stem from several factors, including the poor sensitivity of in vivo MRS, other pathophysiological conditions of the patients, and differences in the brain regions investigated.

Usually, ex vivo ^{1}H nuclear magnetic resonance (NMR) spectroscopy is conducted at higher field strength than in vivo ^{1}H NMR spectroscopy. Hence, the detection sensitivity, regional specificity, and dispersion of metabolite peaks are remarkably improved in ex vivo ^{1}H NMR spectroscopy [15]. One of our previous studies done by this approach found that hyperbilirubinemia can result in region-specific perturbation of metabolic pathways including neurotransmitter transition and energy metabolism in the brain [15]. These results have contributed to the understanding of the pathogenesis of bilirubin encephalopathy. Thus, we used this same approach in the present study along with pathological analyses of key proteins to investigate the features of metabolism in samples of the prefrontal cortex (PFC), hippocampus, and hypothalamus obtained from rats modeling DD. The purpose of the present study was to explore metabolic variations in these brain regions, which may provide important clues for understanding the mechanisms of DD or for identifying novel interventions.

2. Materials and Methods

2.1. Animals. Male Wistar rats (about 6 weeks of age, weighing 163.4 ± 3.9 g) were purchased from the SLAC Laboratory Animal Co. Ltd. (Shanghai, China). The animals were allowed to adapt to the laboratory environment for 1 week before the experiments. During the whole experimental process, rats were kept in a temperature- and humidity-controlled environment on a 12 h light/dark cycle. Food and water were available ad libitum. All animals were treated in strict accordance with the National Institutes of Health's *Guide for the Care and Use of Laboratory Animals*.

2.2. Rat Model of DD. The induction of DD was conducted according to a previously described procedure [16, 17]. The animals were randomly allocated to the control group ($n = 8$) or the DD group ($n = 18$). After a 12 h fast, rats in the DD group were injected intraperitoneally with streptozotocin (Sigma, St. Louis, MO, USA) dissolved in 0.01 mol/L citric acid solution (pH = 4.5) at a single dose of 64 mg/kg. Control rats received injections of citrate buffer alone. Seventy-two hours after streptozotocin administration, blood glucose was measured after obtaining blood through tail nicking with a Glucotrend monitor (Roche Diagnostics, Switzerland). The rats with increased blood glucose level (≥16.70 mmol/L) were subjected to the chronic unpredictable mild stress (CUMS) procedure. The stress procedure consisted of a range of stressors, including crowding (10 rats cohabiting in one cage for 24 h), cage tilt (40° for 24 h), white noise (80 ± 2 db for 6 h), wet bedding (24 h), cold swim (4°C for 5 min), stroboscopic illumination (300 flashes/min for 6 h), and tail pinch (for 1 min). Over a period of 28 days, one of these stimuli was randomly chosen and used to the rats in case the rats were capable of anticipating the stimulus. For each rat, every stimulus was applied four times within 28 days. Control animals were housed in a separate room and had no contact with the stressed group. Body weight was measured on days 0, 14 (2 weeks), and 28 (4 weeks) after the CUMS procedure.

2.3. Open-Field Test. The open-field test is an evaluation of spontaneous and exploratory activities as well as of anxiety-like behavior in a novel environment in rodents [16, 18]. The rats in the DD group were subjected to this test after the 4-week CUMS procedure. The open-field apparatus was made of opaque materials. Its bottom was 90 × 90 cm square and divided into 25 equilateral squares. The height of the wall surrounding the bottom was 40 cm. Being placed in the central square, the rat was permitted to explore freely for 5 min. A video-tracking system was used to record the distances traveled and the time spent in the central and peripheral areas. After each rat finished the test, the apparatus was cleaned with 100% alcohol and dried so that the next rat would not be influenced by the smell of the preceding rat. A behavioral analysis system was used to analyze the acquired video-tracking data.

2.4. Morris Water Maze Test. Spatial learning and memory were tested using the Morris water maze [19]. The Morris water maze apparatus was a water tank (110 cm in diameter, 30 cm high) with a platform (7 cm in diameter) inside the tank (raised 19 cm from the tank bottom) that was not visible to the rats. The tank was filled with 20 cm height of water maintained at a temperature of 24–26°C. The rats were trained for 4 consecutive days, and on each training day, the rats swam four 60 s trials (initial placement rotated for each trial) or until they reached to the hidden platform. On the fifth day, the platform was removed for a 60 s trial and

the swim path as well as the time spent swimming were recorded by a video-tracking computer system.

2.5. Sample Collection. After the behavioral tests were completed, 14 rats in the DD group and 6 control rats were decapitated and the brain was rapidly removed. The bilateral PFC, hippocampus, and hypothalamus were quickly dissected, frozen in liquid nitrogen, and stored at −80°C until they were treated for use in ^{1}H NMR studies. The remaining rats were anesthetized with 4% chloral hydrate and perfused intracardially with phosphate-buffered saline (PBS) followed by 4% paraformaldehyde in PBS. Then, brain tissues were collected, fixed in 10% formalin for 24 h, imbedded in paraffin, and stored at 4°C until used for immunohistochemical studies.

2.6. Brain Metabolite Extraction and Acquisition of ^{1}H NMR Spectra. Our previously reported method was used to prepare brain tissue extracts and acquire ^{1}H-NMR spectra [15, 20]. Briefly, the tissue was weighed into a centrifuge tube. Then, ice-cold methanol (4 mL/g) and distilled water (0.85 mL/g) were added into the tube, homogenized by vortex at 4°C. Subsequently, chloroform (2 mL/g) and distilled water (2 mL/g) were added to the tube and mixed by vortex. After being kept on ice for 15 min, the final mixture was centrifuged at 1000 ×g for 15 min at 4°C. The supernatant was extracted and lyophilized for approximately 24 h. The dried metabolite mixture was weighted and then dissolved in 0.6 mL of 99.5% D_2O for NMR analyses.

A Bruker Avance III 600 MHz NMR spectrometer was used to conduct all ^{1}H NMR experiments. The crucial parameters were set as follows: spectral width, 12,000 Hz; acquisition time, 2.65 s per scan; relaxation delay, 10 s; and number of scans, 256. By using the TopSpin software (v2.1 pl4, Bruker BioSpin, Germany), all spectra were preprocessed with a reference of the lactate peak (CH_3, 1.33 ppm) and manual correction of the phase and baseline.

2.7. Data Processing of NMR Spectra and Multivariate Pattern Recognition. For exploiting whole metabolic information in the spectra, AMIX software package was used to divide all NMR spectra into integral regions, which had an equal width of 0.01 and 0.0015 ppm. Due to the residual peak from the suppressed water resonance, the integral of the NMR region (δ 5.85–4.60) was set to zero. Other integral regions were normalized to the total sum of the spectral intensity. Then, the normalized integral values were entered into SIMCA-P+ 12.0 software (Umetrics, Umeå, Sweden) as variables and were mean-centered for multivariate data analysis. The projection to latent structures-discriminant analysis (PLS-DA) was used to discriminate the class and identify the biomarkers [21]. In order to acquire the most efficient 2-D representation of the information, the principal component (PC) score plot of the first two principal components (PC1 and PC2) was applied to visualize the data. Each point on the PC score plot represented an individual spectrum of the sample [15]. The position of each point along a given axis in the score plot was influenced by variables in the same axis in the loading plot [22]. PLS-DA revealed differences in the composition of different groups, which were necessary to eliminate outliers and enhance the quality of the PCA model. Differences in the metabolites between groups were shown as coefficient of variation plots, which facilitate interpretation because the loadings resemble NMR spectra. The scores and loading plots complemented each other. The loading plot—wherein differential peaks of metabolites are shown as positive and negative signals suggest the relative metabolite changes—was applied to determine which spectral variables were the main contributors to the discrimination of the samples on the score plot [15, 20, 23].

2.8. Immunohistochemistry. For immunohistochemical staining, tissue sections were cut to a thickness of 3 μm, deparaffinized with xylene, and rehydrated in a graded series of ethanol. Immunohistochemistry was performed according to procedures described in previous studies [24, 25]. Briefly, fixed brains were incubated with glutamine synthetase (GS) (1 : 200, Santa Cruz Biotechnology, CA) and glutaminase (GLS) (1 : 200, Abcam, ab156876) antibodies overnight at 4°C. The sections were washed in PBS 3 times, then incubated with horseradish peroxidase-conjugated secondary antibodies at 37°C for 1 h, and finally terminated by 3,3′-diaminobenzidine. The images were photographed with a Nikon Eclipse 80i (Nikon, Japan). For each immunohistochemical stain, the signal densities were analyzed using three selected sections from the PFC, hippocampus, and hypothalamus with Image-Pro Plus software (version 6.0, Rockville, MD, USA).

2.9. Target Metabolic Changes in Tissues and Statistical Analysis. By reference to internal trimethylsilyl-propionic-2,2,3,3-d4 acid, the concentrations of metabolites were determined from the spectra and expressed as mmol/kg wet tissue weight. Significant statistical difference between the rats modeling DD and the control rats for the identified metabolites, body weight, and behavioral data was determined using Student's *t*-test with SPSS software (version 13.0, SPSS Inc., USA). The level of statistical significance was set at $p < 0.05$.

3. Results

3.1. Body Weights and Behavioral Analyses. Compared with the control group, rats in the DD group showed a significant decrease in body weight on days 0, 14, and 28 after the CUMS procedure (Figure 1(a)).

In the open-field test, the total distance traveled by rats in the DD group was significantly lower than that traveled by rats in the control group. A reduction in activity time and time spent in locomotion indicated less spontaneous activity in these rats (Figures 1(b)–1(d)). These data suggested that rats treated with streptozotocin and CUMS had less interest than control rats in exploring a new environment.

In the Morris water maze test, the number of times the rats crossed the location where the platform had been hidden and the amount of time spent in the platform quadrant were significantly different between the two groups (Figures 1(e) and 1(f)). Compared with rats in the control group, rats in

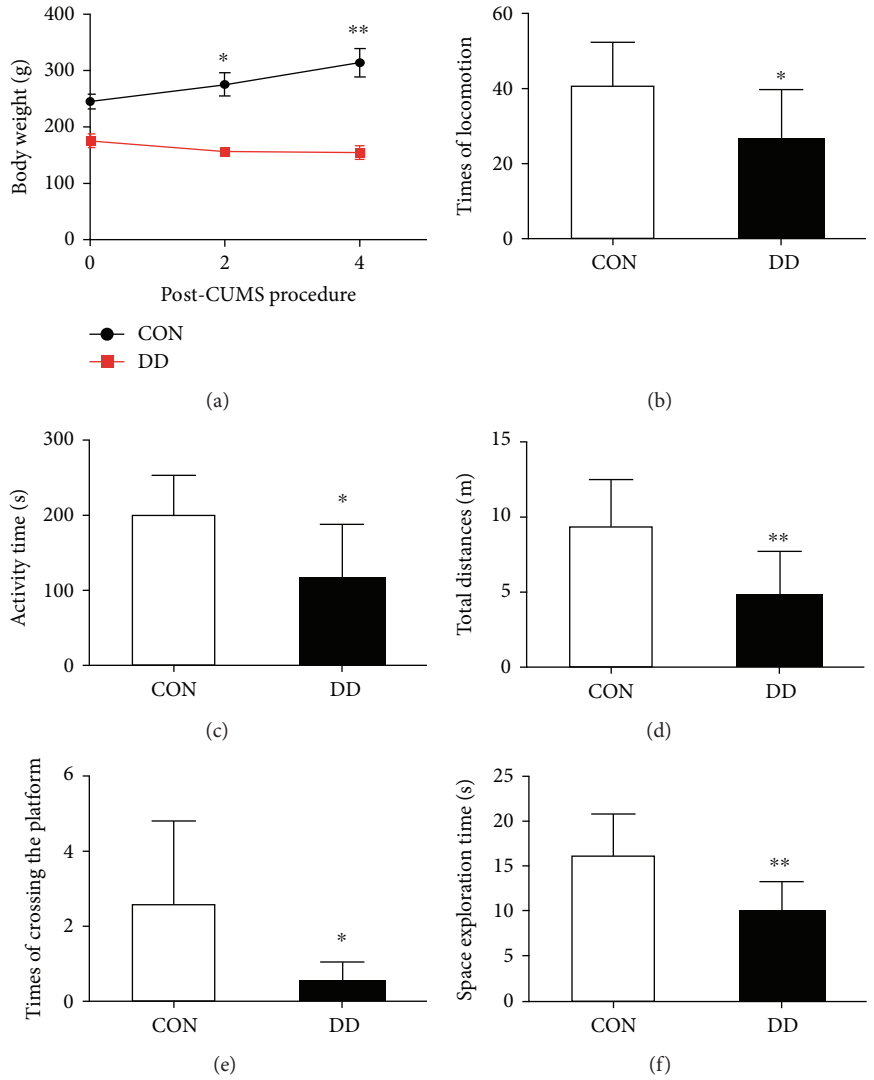

Figure 1: Changes in body weight, performance on the open-field test and Morris water maze test for rats in the control (CON) and DD groups. (a) body weight, (b) times of locomotion, (c) activity time, (d) total time, (e) times of crossing the platform, (f) space exploration time. Significant level: $^{*}p < 0.05$, $^{**}p < 0.01$.

the DD group traveled irregularly during the 1 min probe test, with significantly fewer crossings of the area where the platform had been located and less time spent in the platform quadrant. This suggested that after 4 days of training, rats in the DD group appeared to perform worse in learning and consolidating the platform location, which can be interpreted as an expression of memory impairment in these rats.

3.2. ^{1}H NMR Spectra and PLS-DA Analysis. Figure 2 shows representative ^{1}H NMR spectra of the PFC extracts obtained from rats in the DD and control groups. Assignments presented in Figure 2 are based on our previous publication and were verified by 2D ^{1}H-^{1}H COSY and TOCSY spectra (data not shown) [20]. Many endogenous metabolites can be measured from the ^{1}H NMR spectra, including lactate (Lac), Glu, Gln, GABA, aspartate (Asp), succinate (Suc), creatine (Cre), alanine (Ala), N-acetyl aspartate (NAA), taurine (Tau), myo-inositol (m-Ins), glycine (Gly), and choline (Cho).

After the segmentation of the NMR spectra of PFC extracts, a multivariate data analysis was used to determine metabolic profile changes in rats in the DD group. Marked separation was found between the DD and control groups in the $t(1)$ direction on PLS-DA score plots (Figure 3), which indicates a different spectral feature of the two groups in the PFC. The corresponding coefficient-coded loading plot (Figure 3) showed that Glu, Lac, NAA, and Cre contribute to the separation. Similar patterns of metabolism were found in the score plots and loading plots of the spectra from the hippocampal and hypothalamic extracts (Figure 3).

3.3. Quantitative Analysis of Metabolic Alterations. The changes in the metabolites of the PFC, hippocampus, and hypothalamus obtained from rats in the DD group are shown in Figures 4 and 5. DD induced a significant increase in Lac but no apparent change in Suc in the PFC, hippocampus, and hypothalamus. Cre was decreased in the PFC and

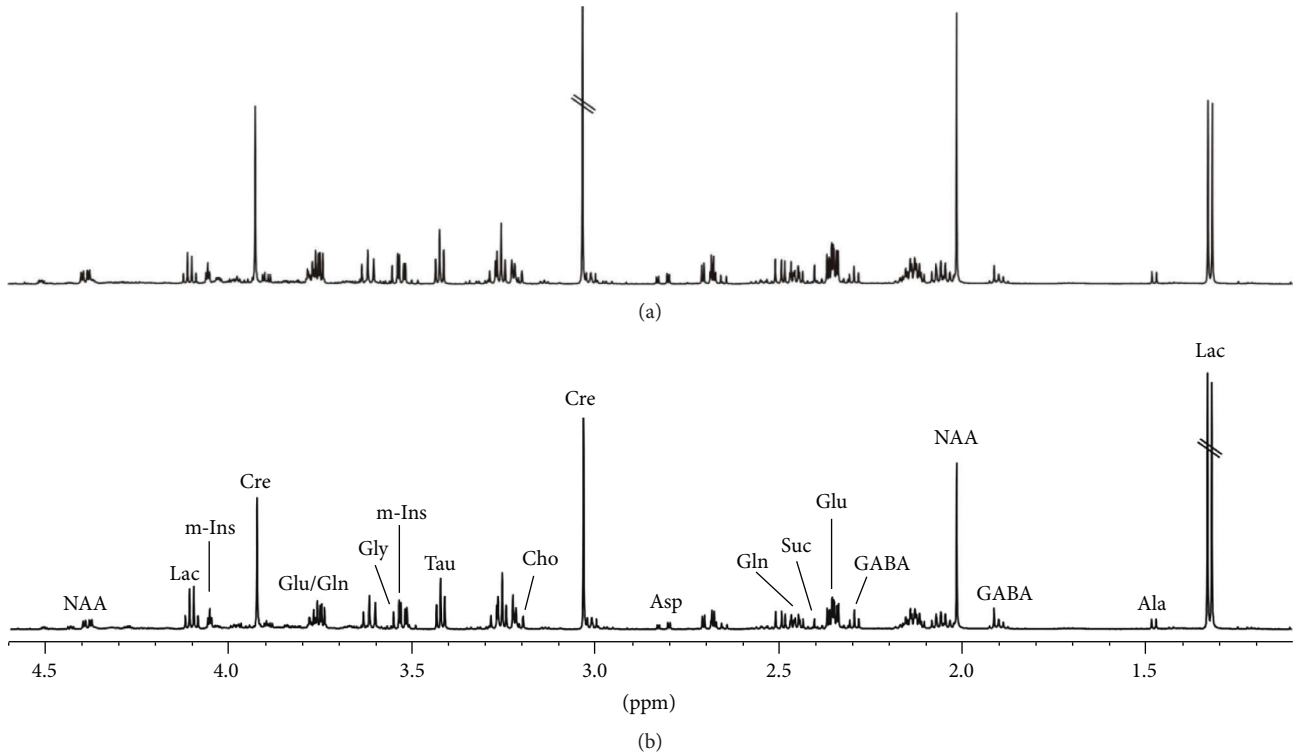

Figure 2: Representative ^{1}H NMR spectra of the PFC extracts obtained from rats in the control (a) and DD (b) groups.

hippocampus of these rats. NAA was significantly decreased in the PFC, hippocampus, and hypothalamus, and Cho was decreased in the latter two brain areas, while Tau was increased in the former two regions. Ala was decreased only in the hypothalamus, and m-Ins was increased only in the hippocampus. Marked decreases in Glu and Gln neurotransmitter concentrations were found in the hippocampus of rats in the DD group. Similar decreases in these neurotransmitters along with Asp and Gly were found in the PFC and hypothalamus. GABA was decreased only in the hypothalamus.

3.4. Key Enzymes in the Glu-Gln Cycle. As a crucial enzyme in the cytoplasm of astrocyte, GS results in the formation of Gln from Glu [24]. GLS is an important enzyme in neuronal axons and generates Glu from Gln. Immunohistochemical staining showed that GS was decreased in the PFC, hippocampus, and hypothalamus of rats in the DD group, indicating inhibition of the pathway from Glu to Gln (Figure 6). Decreased labeling of GLS neurons was found in these brain areas (Figure 7), which was in accordance with the reduction of Gln to Glu.

4. Discussion

In this study, we successfully established a rat model of DD and comprehensively reported metabolic alterations in the PFC, hippocampus, and hypothalamus in these rats as determined by ex vivo ^{1}H NMR spectroscopy. We found marked metabolic changes of neurochemicals containing some crucial neurotransmitters and energy products, as well as disruption in the markers of neuronal and astrocytic activity in these brain areas in rats modeling DD.

4.1. Establishment of the Rat Model of DD. Streptozotocin is frequently used to induce diabetes in rats [26]. After an adequate dose of streptozotocin is injected, rats generally maintain a high level of blood glucose and fail to gain body weight. Near the end of the present study, rats in the DD group exhibited approximately half the body weight of control rats. The CUMS procedure is thought to simulate unpredictable, stressful daily life events [27]. It has a significant impact on anxiety and metabolism and results in anhedonia, which is a major symptom of human depression. The CUMS procedure is commonly used to develop depression in rats. In our study, rats in the DD group subjected to the CUMS procedure exhibited significant decreases in locomotion and in exploratory activity in the open-field test, representing both a loss of interest in new stimulating situations and a deficit in motivation. In the Morris water maze test, rats in the DD group spent less time in the target quadrant and had fewer crossings over the hidden platform, indicating impaired memory function and spatial learning deficits after the CUMS treatment. Taking together, the body weight change and the results of the behavioral tests indicated the successful establishment of a rat model of DD.

4.2. Changes in Neurotransmitter Metabolism. As an important metabolic cycle between astrocytes and neurons, the Glu-Gln cycle regulates homeostasis of neurotransmitters such as Glu, Gln, and GABA in the brain. Glu is the main excitatory neurotransmitter, and GABA is the main

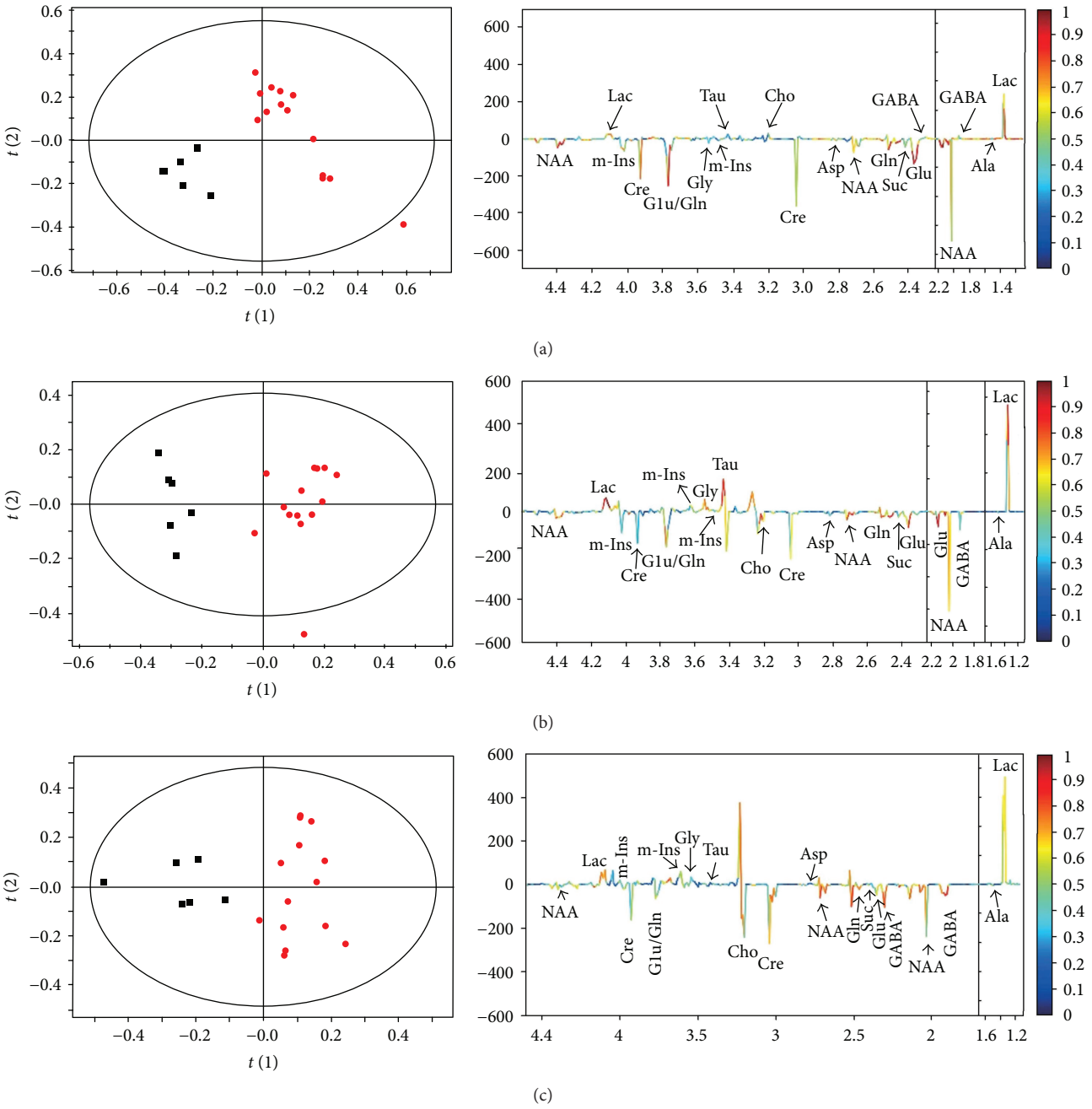

Figure 3: PLS-DA scores (left) and coefficient-coded loading plots (right) for the models discriminating the rats in the DD group (red dots) from control rats (blank squares) for data obtained in PFC (a), hippocampus (b), and hypothalamus (c) samples.

inhibitory neurotransmitter. In this study, both Glu and Gln levels were significantly decreased in the PFC, hippocampus, and hypothalamus of rats modeling DD, which is consistent with previous studies showing a significant reduction of Glu and Gln levels in the subcortical region of the brain in patients with type 2 diabetes and major depression [12]. Glu and Gln were significantly increased in the frontal region of diabetic patients [28], but were significantly decreased in the PFC and hippocampus of depressed rats [29]. We speculated that the changes of Glu and Gln in our study is likely due to the effect of depression. Compared with that in controls, GABA was significantly decreased only in the hypothalamus of the rats modeling DD. This is similar to the previous observation that major depression is associated with reduced GABA levels in the dorsomedial/dorsal anterolateral PFC of the brain [11]. Decreased GABA was also observed in the hippocampus of diabetic rats [30]. Both depression and diabetes result in the decreased GABA in human and rat brain. Thus, it cannot be concluded whether the observed change of GABA in our study is rather due to diabetes or depression. Since the metabolic pathways

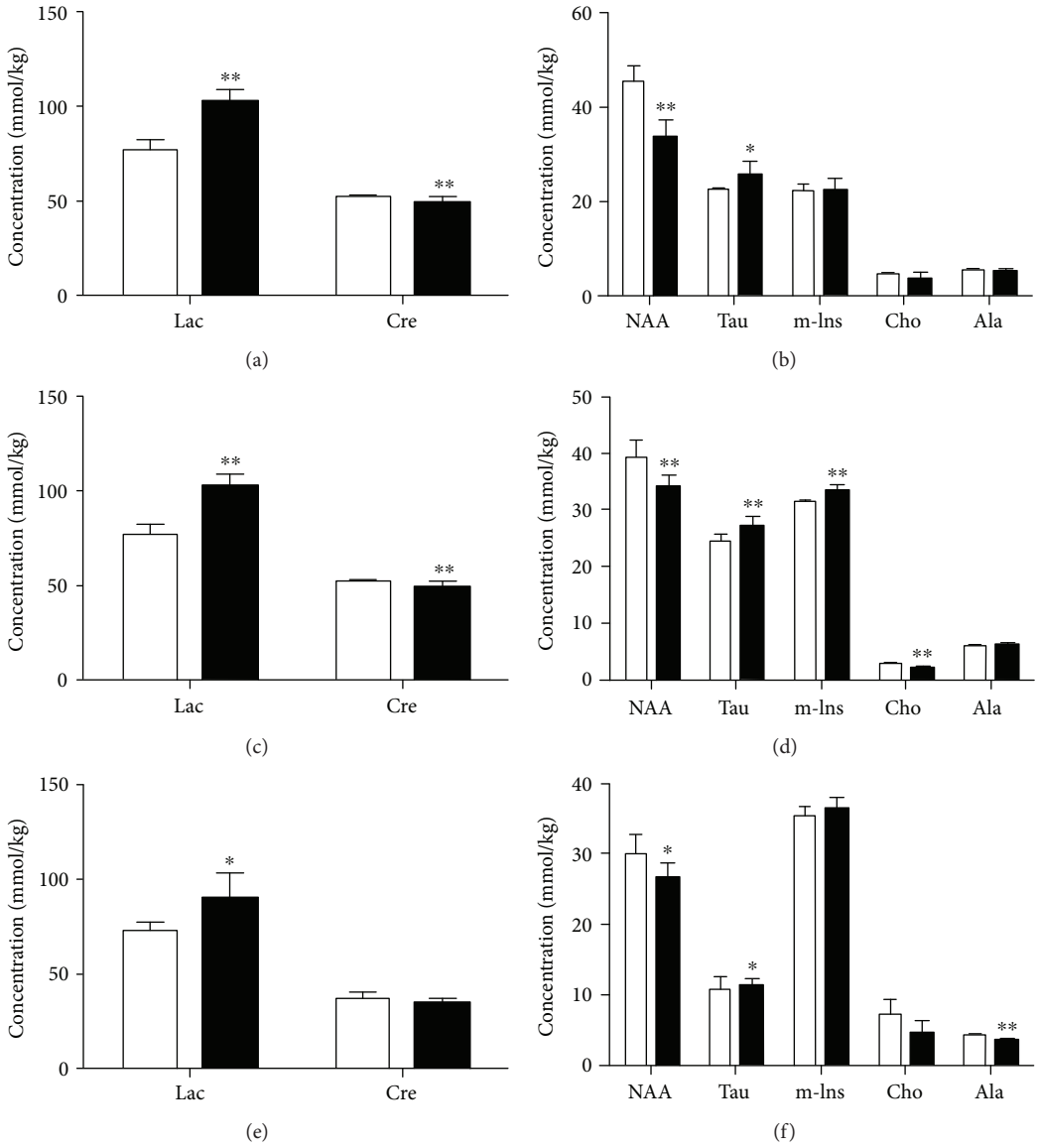

Figure 4: Changes in concentrations of energy and other brain metabolites in the PFC (a, b), hippocampus (c, d), and hypothalamus (e, f) in the control (white bars) and DD (black bars) groups. Significant level: $^{*}p < 0.05$, $^{**}p < 0.01$.

which regulate the producing and the cycling of Glu, Gln, and GABA are closely coupled, alterations in these neurotransmitters reflect change of the balance of the Glu-Gln shuttling between astrocytes and neurons in the PFC, hippocampus, and hypothalamus of rats modeling DD. This perhaps resulted from decreased Glu synthesis in neurons via GS and/or reduced Glu uptake by astrocytes, where Glu is transformed into Gln by GLS. Interestingly, our immunohistochemical staining showed that both GS and GLS were attenuated in the PFC, hippocampus, and hypothalamus of rats in the DD group. The decreases in Glu and Gln were in agreement with the alterations of these key proteins in the Glu-Gln cycle.

The reduced levels of Glu and Gln also suggested reduced precursor pools, which may have been caused by diabetes-induced impairment of glucose metabolism and depression-induced dysfunction of astrocyte. Studies have revealed that changed astrocyte metabolism is necessary for maintaining cerebral Glu and GABA levels in diabetic rats and impaired astrocyte function is responsible for the reduction of Glu and Gln concentrations in depressed patients [31, 32].

Depression may be ascribed to a change in the function of glutamatergic and GABAergic neurons. Glu and GABA play crucial roles in the regulation of emotion and stress [33]. Glu is released from the presynaptic cell and acts on postsynaptic receptors, such as N-methyl-D-aspartate (NMDA) receptors [34]. GABA acts at inhibitory synapses in the brain by binding to specific transmembrane receptors, including $GABA_A$ and $GABA_B$ receptors [35, 36]. It has been demonstrated that the expression levels of NMDA and GABA receptors are changed in synaptic densities in the brains of diabetic rats

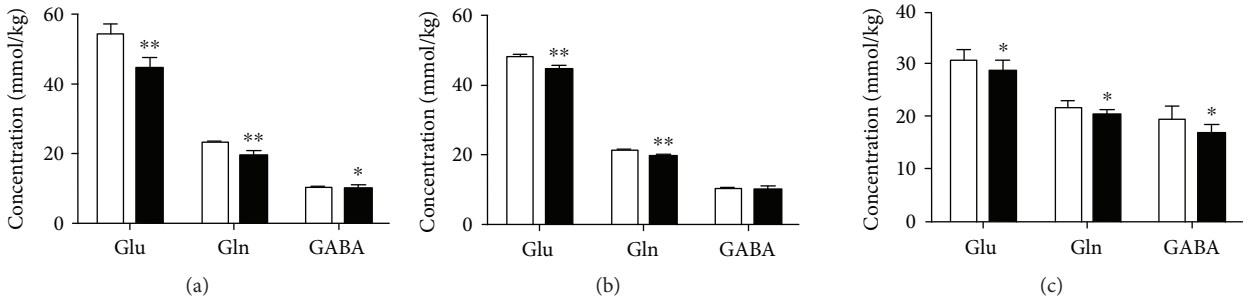

Figure 5: Changes in concentrations of glutamate (Glu), glutamine (Gln), and GABA in the PFC (a), hippocampus (b), and hypothalamus (c) in the control (white bars) and DD (black bars) groups. Significant level: $^{*}p < 0.05$, $^{**}p < 0.01$.

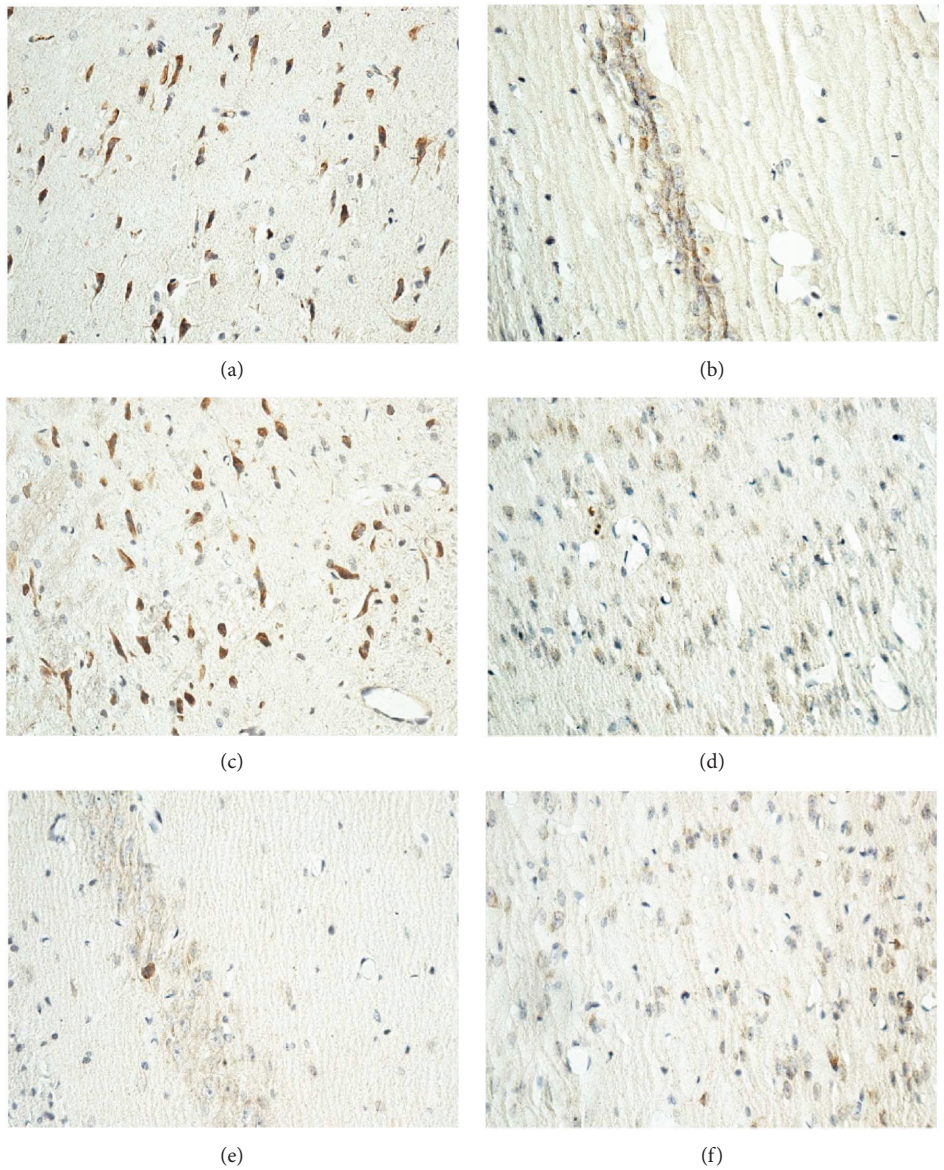

Figure 6: Immunohistochemistry of glutamine synthetase (GS) in the PFC, hippocampus, and hypothalamus of rats in the control (a, b, c) and DD (d, e, f) groups.

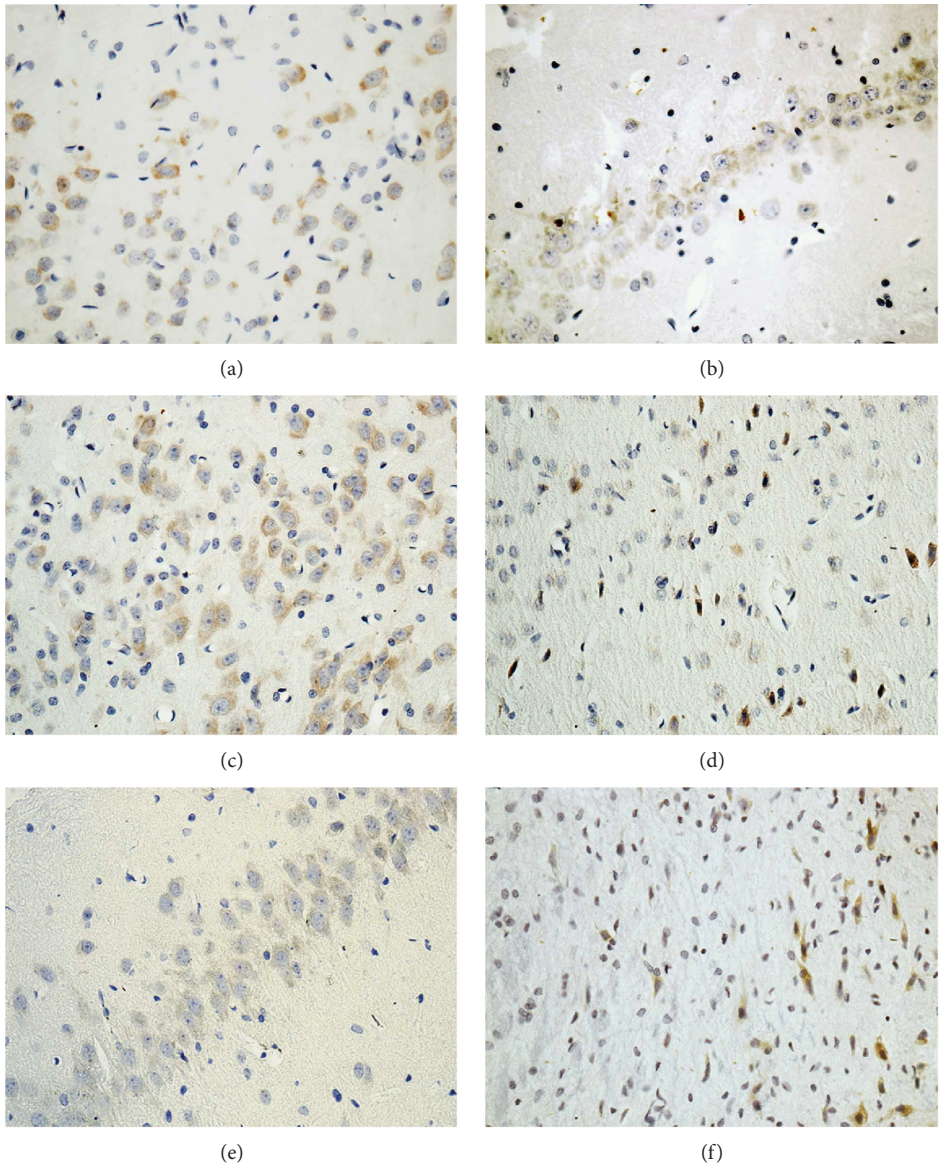

Figure 7: Immunohistochemistry of glutaminase (GLS) in the PFC, hippocampus, and hypothalamus of rats in the control (a, b, c) and DD (d, e, f) groups.

[37, 38]. However, the relationship between DD and the changes in Glu and GABA levels as well as NMDA and GABA receptor activity remains ambiguous and needs further study.

4.3. Changes in Energy Metabolism. Brain energy supply relies almost entirely on glucose oxidative metabolism in the mitochondria. When brain energy requirements exceed the oxidative metabolism rate, the anaerobic glycolysis pathway will be enhanced and the production of Lac will be markedly increased. Lac will then be used as the energy substrate to maintain normal cerebral energy homeostasis and metabolism [39]. In this study, the increased Lac level may indicate that anaerobic glycolysis was increased and the mitochondrial function was impaired in the PFC, hippocampus, and hypothalamus of rats modeling DD. Similarly, an increased Lac level is associated with diabetes in humans [23]. Thus, the change of Lac in our study is likely due to the effect of diabetes. Besides, the lactate-alanine shuttle is responsible for nitrogen exchange in the brain of mammals. Compared with control rats, Lac was increased and Ala was decreased in the present study, suggesting a disorder in the lactate-alanine shuttle of the hypothalamus in the DD group. Cre also takes part in the regulation of cellular energy metabolism and is utilized as an energy reservoir in cells with a high energy demand [40]. Compared with that in control rats, Cre was significantly decreased in the PFC and hippocampus but not in the hypothalamus of rats in the DD group. However, Cre was significantly increased in the ventral lateral prefrontal region of bipolar depressed patients [41] and also in the hippocampus of diabetic rats [42]. This suggested that the observed reduction of Cre in our study only occurs when

diabetes and depression appear together and may be the result of a combined effect of diabetes and depression. In addition, the change of Cre could be considered as one of the specific changes in DD. The changes in Cre also reflect abnormal energy metabolism in the PFC and hippocampus of rats in the DD group.

4.4. Changes in Other Metabolites. NAA is regarded as a surrogate marker of the status of the neuronal function. Sharp decreases in the levels of NAA were found in the PFC, hippocampus, and hypothalamus of rats in the DD group. Similarly, a significant reduction in NAA has been reported in patients with depression [43] and also in patients with diabetes [28, 44]. Thus, it cannot be concluded whether the reduction of NAA in our study is due to diabetes or depression. Our results indicated that neuronal dysfunction occurred in rats of the DD group.

As markers of astrocytic activity, Tau, m-Ins, and Cho have crucial functions in regulating the intracellular osmolarity in astrocytes [45, 46]. Disturbances in their levels have been interpreted as a compensatory response to an increase in intracellular osmolarity in glial cells [47]. In our study, brain region-specific changes of these metabolites were observed in rats in the DD group. For example, Tau was increased in the PFC and hippocampus and m-Ins was increased in the hippocampus, while Cho was decreased in the hippocampus and hypothalamus. Both depression and diabetes result in the increased Cho in human brain [41, 48]. Hence, the decreased Cho in our study only occurs when diabetes and depression appear together and may be the result of a combined effect of diabetes and depression. In addition, the decreased Cho may be one of the specific changes in DD. Both depression and diabetes cause the increased Tau in rat hippocampus [29, 49], while depression causes the decreased Tau in rat PFC [50]. Thus, it cannot be concluded whether the observed change of Tau in our study is due to diabetes or depression. The level of m-Ins in the hippocampus was found increased in the animal model of diabetes [23, 49], but decreased in the animal model of depression [29], suggesting that diabetes plays a dominant role in the change of m-Ins in this study. The changes of Tau, m-Ins, and Cho are likely mechanisms compensating for changed astrocytic osmolarity in the PFC, hippocampus, and hypothalamus.

5. Conclusion

The current study was designed to detect changes of numerous metabolites in the rat brain to explore the mechanisms underpinning DD. Changes in the metabolism of the neurotransmitters Glu, Gln, GABA, Asp, and Gly and the energy products Lac and Cre as well as other metabolites in the PFC, hippocampus, and hypothalamus were observed. Our results suggested that DD may be associated with metabolic changes, such as inhibition of the Glu-Gln cycle, increase in anaerobic glycolysis, and disruption of the lactate-alanine shuttle, as well as with the dysfunction of neurons and astrocytes. Our results will advance the understanding of the underlying mechanisms of DD.

Conflicts of Interest

The authors declare that they have no competing interests regarding the publication of this paper.

Authors' Contributions

Kun Liu, Liangcai Zhao, and Wen Xu contributed equally to this work.

Acknowledgments

This work was supported by the grants from National Natural Science Foundation of China (nos. 81400863, 21575105 and 31601083), Zhejiang Provincial Natural Science Foundation (nos. LY18H070003 and LY17H160049), and Department of Health of Zhejiang Province (nos. 2018KY522, 2014KYA141, and 2014KYA145).

References

[1] F. Rotella and E. Mannucci, "Depression as a risk factor for diabetes: a meta-analysis of longitudinal studies," *The Journal of Clinical Psychiatry*, vol. 74, no. 1, pp. 31–37, 2013.

[2] T. Roy and C. E. Lloyd, "Epidemiology of depression and diabetes: a systematic review," *Journal of Affective Disorders*, vol. 142, pp. S8–21, 2012.

[3] K. Semenkovich, M. E. Brown, D. M. Svrakic, and P. J. Lustman, "Depression in type 2 diabetes mellitus: prevalence, impact, and treatment," *Drugs*, vol. 75, no. 6, pp. 577–587, 2015.

[4] R. D. Goldney, P. J. Phillips, L. J. Fisher, and D. H. Wilson, "Diabetes, depression, and quality of life: a population study," *Diabetes Care*, vol. 27, no. 5, pp. 1066–1070, 2004.

[5] W. J. Katon, C. Rutter, G. Simon et al., "The association of comorbid depression with mortality in patients with type 2 diabetes," *Diabetes Care*, vol. 28, no. 11, pp. 2668–2672, 2005.

[6] S. Moussavi, S. Chatterji, E. Verdes, A. Tandon, V. Patel, and B. Ustun, "Depression, chronic diseases, and decrements in health: results from the World Health Surveys," *Lancet*, vol. 370, no. 9590, pp. 851–858, 2007.

[7] C. A. Wayhs, C. P. Mescka, C. S. Vanzin et al., "Brain effect of insulin and clonazepam in diabetic rats under depressive-like behavior," *Metabolic Brain Disease*, vol. 28, no. 4, pp. 563–570, 2013.

[8] J. M. Zanoveli, H. de Morais, I. C. da Silva Dias, A. K. Schreiber, C. P. de Souza, and J. M. da Cunha, "Depression associated with diabetes: from pathophysiology to treatment," *Current Diabetes Reviews*, vol. 12, no. 3, pp. 165–178, 2016.

[9] H. de Morais, C. P. de Souza, L. M. da Silva et al., "Increased oxidative stress in prefrontal cortex and hippocampus is related to depressive-like behavior in streptozotocin-diabetic rats," *Behavioural Brain Research*, vol. 258, pp. 52–64, 2014.

[10] D. P. Auer, B. Putz, E. Kraft, B. Lipinski, J. Schill, and F. Holsboer, "Reduced glutamate in the anterior cingulate cortex in depression: an in vivo proton magnetic resonance spectroscopy study," *Biological Psychiatry*, vol. 47, no. 4, pp. 305–313, 2000.

[11] G. Hasler, J. W. van der Veen, T. Tumonis, N. Meyers, J. Shen, and W. C. Drevets, "Reduced prefrontal glutamate/glutamine and γ-aminobutyric acid levels in major depression

determined using proton magnetic resonance spectroscopy," *Archives of General Psychiatry*, vol. 64, no. 2, pp. 193–200, 2007.

[12] O. Ajilore, E. Haroon, S. Kumaran et al., "Measurement of brain metabolites in patients with type 2 diabetes and major depression using proton magnetic resonance spectroscopy," *Neuropsychopharmacology*, vol. 32, no. 6, pp. 1224–1231, 2007.

[13] J. Xu, U. Dydak, J. Harezlak et al., "Neurochemical abnormalities in unmedicated bipolar depression and mania: a 2D ^{1}H MRS investigation," *Psychiatry Research*, vol. 213, no. 3, pp. 235–241, 2013.

[14] L. Glodzik-Sobanska, A. Slowik, P. McHugh et al., "Single voxel proton magnetic resonance spectroscopy in post-stroke depression," *Psychiatry Research*, vol. 148, no. 2-3, pp. 111–120, 2006.

[15] W. Hu, X. Cheng, X. Ye et al., "Ex vivo ^{1}H nuclear magnetic resonance spectroscopy reveals systematic alterations in cerebral metabolites as the key pathogenetic mechanism of bilirubin encephalopathy," *Molecular Brain*, vol. 7, no. 1, p. 87, 2014.

[16] Y. H. Wang, L. T. Yin, H. Yang, X. L. Li, and K. G. Wu, "Hypoglycemic and anti-depressant effects of Zuogui Jiangtang Jieyu formulation in a model of unpredictable chronic mild stress in rats with diabetes mellitus," *Experimental and Therapeutic Medicine*, vol. 8, no. 1, pp. 281–285, 2014.

[17] P. Willner, "Validity, reliability and utility of the chronic mild stress model of depression: a 10-year review and evaluation," *Psychopharmacology*, vol. 134, no. 4, pp. 319–329, 1997.

[18] M. Zhou, M. Wang, X. Wang et al., "Abnormal expression of microRNAs induced by chronic unpredictable mild stress in rat hippocampal tissues," *Molecular Neurobiology*, vol. 55, no. 2, pp. 917–935, 2018.

[19] R. Morris, "Developments of a water-maze procedure for studying spatial learning in the rat," *Journal of Neuroscience Methods*, vol. 11, no. 1, pp. 47–60, 1984.

[20] K. Liu, X. J. Ye, W. Y. Hu et al., "Neurochemical changes in the rat occipital cortex and hippocampus after repetitive and profound hypoglycemia during the neonatal period: an ex vivo ^{1}H magnetic resonance spectroscopy study," *Molecular Neurobiology*, vol. 48, no. 3, pp. 729–736, 2013.

[21] M. Coen, E. M. Lenz, J. K. Nicholson, I. D. Wilson, F. Pognan, and J. C. Lindon, "An integrated metabonomic investigation of acetaminophen toxicity in the mouse using NMR spectroscopy," *Chemical Research in Toxicology*, vol. 16, no. 3, pp. 295–303, 2003.

[22] J. A. Westerhuis, E. J. J. van Velzen, H. C. Hoefsloot, and A. K. Smilde, "Multivariate paired data analysis: multilevel PLSDA versus OPLSDA," *Metabolomics*, vol. 6, no. 1, pp. 119–128, 2010.

[23] Y. Zheng, Y. Yang, B. Dong et al., "Metabonomic profiles delineate potential role of glutamate-glutamine cycle in *db*/*db* mice with diabetes-associated cognitive decline," *Molecular Brain*, vol. 9, no. 1, p. 40, 2016.

[24] L. Hertz, R. Dringen, A. Schousboe, and S. R. Robinson, "Astrocytes: glutamate producers for neurons," *Journal of Neuroscience Research*, vol. 57, no. 4, pp. 417–428, 1999.

[25] C. Zhao and S. C. Gammie, "Glutamate, GABA, and glutamine are synchronously upregulated in the mouse lateral septum during the postpartum period," *Brain Research*, vol. 1591, pp. 53–62, 2014.

[26] S. N. Goyal, N. M. Reddy, K. R. Patil et al., "Challenges and issues with streptozotocin-induced diabetes - a clinically relevant animal model to understand the diabetes pathogenesis and evaluate therapeutics," *Chemico-Biological Interactions*, vol. 244, pp. 49–63, 2016.

[27] G. Biala, K. Pekala, A. Boguszewska-Czubara, A. Michalak, M. Kruk-Slomka, and B. Budzynska, "Behavioral and biochemical interaction between nicotine and chronic unpredictable mild stress in mice," *Molecular Neurobiology*, vol. 54, no. 2, pp. 904–921, 2017.

[28] S. Sinha, M. Ekka, U. Sharma, P. Raghunandan, R. M. Pandey, and N. R. Jagannathan, "Assessment of changes in brain metabolites in Indian patients with type-2 diabetes mellitus using proton magnetic resonance spectroscopy," *BMC Research Notes*, vol. 7, no. 1, p. 41, 2014.

[29] B. S. Hemanth Kumar, S. K. Mishra, P. Rana, S. Singh, and S. Khushu, "Neurodegenerative evidences during early onset of depression in CMS rats as detected by proton magnetic resonance spectroscopy at 7 T," *Behavioural Brain Research*, vol. 232, no. 1, pp. 53–59, 2012.

[30] H. Zheng, Y. Zheng, D. Wang et al., "Analysis of neuron-astrocyte metabolic cooperation in the brain of *db*/*db* mice with cognitive decline using ^{13}C NMR spectroscopy," *Journal of Cerebral Blood Flow & Metabolism*, vol. 37, no. 1, pp. 332–343, 2016.

[31] M. A. Garcia-Espinosa, M. L. Garcia-Martin, and S. Cerdan, "Role of glial metabolism in diabetic encephalopathy as detected by high resolution ^{13}C NMR," *NMR in Biomedicine*, vol. 16, no. 6-7, pp. 440–449, 2003.

[32] G. Sanacora, D. L. Rothman, G. Mason, and J. H. Krystal, "Clinical studies implementing glutamate neurotransmission in mood disorders," *Annals of the New York Academy of Sciences*, vol. 1003, no. 1, pp. 292–308, 2003.

[33] A. D. Stan, C. V. Schirda, M. A. Bertocci et al., "Glutamate and GABA contributions to medial prefrontal cortical activity to emotion: implications for mood disorders," *Psychiatry Research*, vol. 223, no. 3, pp. 253–260, 2014.

[34] W. Krzyzanowska, B. Pomierny, M. Filip, and J. Pera, "Glutamate transporters in brain ischemia: to modulate or not?," *Acta Pharmacologica Sinica*, vol. 35, no. 4, pp. 444–462, 2014.

[35] F. C. Roth and A. Draguhn, "GABA metabolism and transport: effects on synaptic efficacy," *Neural Plasticity*, vol. 2012, Article ID 805830, 12 pages, 2012.

[36] C. Wu and D. Sun, "GABA receptors in brain development, function, and injury," *Metabolic Brain Disease*, vol. 30, no. 2, pp. 367–379, 2015.

[37] S. Antony, T. P. Kumar, K. P. Kuruvilla, N. George, and C. S. Paulose, "Decreased GABA receptor binding in the cerebral cortex of insulin induced hypoglycemic and streptozotocin induced diabetic rats," *Neurochemical Research*, vol. 35, no. 10, pp. 1516–1521, 2010.

[38] F. Gardoni, A. Kamal, C. Bellone et al., "Effects of streptozotocin-diabetes on the hippocampal NMDA receptor complex in rats," *Journal of Neurochemistry*, vol. 80, no. 3, pp. 438–447, 2002.

[39] C. P. Chih and E. L. Roberts Jr., "Energy substrates for neurons during neural activity: a critical review of the astrocyte-neuron lactate shuttle hypothesis," *Journal of Cerebral Blood Flow & Metabolism*, vol. 23, no. 11, pp. 1263–1281, 2003.

[40] A. Sartorius, P. Lugenbiel, M. M. Mahlstedt, G. Ende, P. Schloss, and B. Vollmayr, "Proton magnetic resonance

spectroscopic creatine correlates with creatine transporter protein density in rat brain," *Journal of Neuroscience Methods*, vol. 172, no. 2, pp. 215–219, 2008.

[41] N. C. Patel, K. M. Cecil, S. M. Strakowski, C. M. Adler, and M. P. DelBello, "Neurochemical alterations in adolescent bipolar depression: a proton magnetic resonance spectroscopy pilot study of the prefrontal cortex," *Journal of Child and Adolescent Psychopharmacology*, vol. 18, no. 6, pp. 623–627, 2008.

[42] M. van der Graaf, S. W. Janssen, J. J. van Asten et al., "Metabolic profile of the hippocampus of Zucker diabetic fatty rats assessed by *in vivo* ^{1}H magnetic resonance spectroscopy," *NMR in Biomedicine*, vol. 17, no. 6, pp. 405–410, 2004.

[43] N. Mao, J. Fang, H. Xie et al., "Correlation between neurochemical metabolism and memory function in adolescent patients with depression: a multi-voxel ^{1}H magnetic resonance spectroscopy study," *Psychiatry and Clinical Neurosciences*, vol. 70, no. 4, pp. 167–174, 2016.

[44] S. Mangia, A. F. Kumar, A. A. Moheet et al., "Neurochemical profile of patients with type 1 diabetes measured by ^{1}H-MRS at 4 T," *Journal of Cerebral Blood Flow & Metabolism*, vol. 33, no. 5, pp. 754–759, 2013.

[45] N. Fayed, J. Garcia-Campayo, R. Magallon et al., "Localized ^{1}H-NMR spectroscopy in patients with fibromyalgia: a controlled study of changes in cerebral glutamate/glutamine, inositol, choline, and N-acetylaspartate," *Arthritis Research & Therapy*, vol. 12, no. 4, p. R134, 2010.

[46] X. Zhang, H. Liu, J. Wu, X. Zhang, M. Liu, and Y. Wang, "Metabonomic alterations in hippocampus, temporal and prefrontal cortex with age in rats," *Neurochemistry International*, vol. 54, no. 8, pp. 481–487, 2009.

[47] J. Cordoba, F. Sanpedro, J. Alonso, and A. Rovira, "^{1}H magnetic resonance in the study of hepatic encephalopathy in humans," *Metabolic Brain Disease*, vol. 17, no. 4, pp. 415–429, 2002.

[48] S. Makimattila, K. Malmberg-Ceder, A. M. Hakkinen et al., "Brain metabolic alterations in patients with type 1 diabetes-hyperglycemia-induced injury," *Journal of Cerebral Blood flow and Metabolism*, vol. 24, no. 12, pp. 1393–1399, 2004.

[49] H. Zhang, M. Huang, L. Gao, and H. Lei, "Region-specific cerebral metabolic alterations in streptozotocin-induced type 1 diabetic rats: an in vivo proton magnetic resonance spectroscopy study," *Journal of Cerebral Blood Flow and Metabolism*, vol. 35, no. 11, pp. 1738–1745, 2015.

[50] C. X. Li, Y. Wang, H. Gao et al., "Cerebral metabolic changes in a depression-like rat model of chronic forced swimming studied by ex vivo high resolution ^{1}H magnetic resonance spectroscopy," *Neurochemical Research*, vol. 33, no. 11, pp. 2342–2349, 2008.

Hindawi
Neural Plasticity
Volume 2018, Article ID 7254016, 12 pages
https://doi.org/10.1155/2018/7254016

Research Article

TLR4-NF-κB Signal Involved in Depressive-Like Behaviors and Cytokine Expression of Frontal Cortex and Hippocampus in Stressed C57BL/6 and ob/ob Mice

Yihe Wang,[1] **Jingjing Xu**,[2] **Yuan Liu**,[2] **Ziyang Li**,[3] **and Xiaohong Li**[4]

[1]*School of Medicine, Shandong University, Jinan, Shandong 250012, China*
[2]*Department of Medical Psychology, School of Basic Medical Sciences, Shandong University, Jinan, Shandong 250012, China*
[3]*Department of Psychology, Jiangsu University Medical Center, Zhenjiang, Jiangsu 212013, China*
[4]*Department of Neurology, Jinan Central Hospital Affiliated to Shandong University, Jinan, Shandong 250013, China*

Correspondence should be addressed to Xiaohong Li; xiaohong-li@sdu.edu.cn

Received 14 December 2017; Accepted 11 February 2018; Published 22 March 2018

Academic Editor: Fushun Wang

Studies found that elevated levels of cytokines such as interleukin- (IL-) 1β, IL-6, and tumor necrosis factor-α (TNF-α) are closely associated with the pathogenesis of depression. Obesity providing a low-grade inflammation state was proposed to be implicated in susceptibility to depression in obesity. However, the alterations of cytokines and the TLR4-NF-κB signal in the brain of normal-weight and obese mice under stress have not been fully elucidated. This study used chronic unpredictable mild stress (CUMS) to induce a depressive-like behavior in an animal model and examine depressive-like behaviors, memory changes, and serum corticosterone levels, as well as the expressions of cytokines and NF-κB in the frontal cortex and hippocampus. We aimed to observe the role of neuroinflammation in susceptibility to depression in obesity under CUMS. In addition, we investigated the protective effect of inhibiting the TLR4-NF-κB signal. Our results demonstrated that CUMS induced depressive-like behavior and spatial memory damage, higher level of serum corticosterone, and overexpression of cytokines and NF-κB in the frontal cortex and hippocampus in both C57BL/6 and ob/ob mice. ob/ob mice displayed serious behavioral disorder and higher levels of IL-1β, IL-6, TNF-α, and NF-κB. Our results concluded that a hyperactive TLR4-NF-κB signal and higher level of cytokines are involved in susceptibility to depression in stressed obese mice.

1. Introduction

An increasing amount of literatures have reported that neuroinflammation is linked with etiology of depression [1–3]. Immune activation and elevated levels of cytokines in the brain are closely associated with severity of depression [4–6]. Further, some cytokines such as interleukin- (IL-) 1β, IL-6, and tumor necrosis factor-α (TNF-α) were believed to be contributors of the onset and progression of depression [7–9] because these cytokines affected the neuron function and neuroactive molecule production which were associated with depression [10–12]. Meanwhile, some anti-inflammation medications could relieve symptoms of depression by reducing the overexpression of cytokines [7, 13–15].

Recently, a great body of researches has demonstrated that depression and obesity are coexisting [16–18]. The high-fat diet combined with chronic unpredictable mild stress (CUMS) could induce a serious depressive-like behavior in rats [19]. Neuroinflammation was the link of the pathophysiology of obesity comorbidity with depression as obesity provided a low-grade inflammation state [17, 18, 20]. Specially, increased damage-associated molecular pattern (DAMP), an active element of the TLR4/NF-κB signal, has been found in stress reaction which was regarded as the major reason of depression [16]. Higher levels of IL-1β, IL-6, and TNF-α in the brain were believed to induce depression due to DAMPs under stress [21]. Our previous studies revealed that both long-term mild stress and lipopolysaccharide (LPS) induced depressive-like behaviors

as well as IL-1β, IL-6, and TNF-α expression in the frontal cortex and hippocampus [7, 22]. These results supported the conclusion that the activation of TLR4-NF-κB is involved in the pathogenesis of both depression and obesity. However, the role of the TLR/NF-κB signal in susceptibility to depression of stressed obesity remains unclear.

TLR4 belongs to the TLR family, which is composed of evolutionarily conserved microbe-specific structural motifs and the endogenous molecule recognition transmembrane TLR4 expressed in various sentinel cells of the central nervous system and formed the first line of defense in the brain [23, 24]. The sustained expression of TLR4 induced neuroinflammation which constitutes the reason of psychiatric disorders [21]. LPS induced both depressive-like behavior and cytokine expression in the hippocampus of mice, and mice lacking caspase-1 resisted LPS-induced depressive-like behavior [22]. The above studies suggested that activated TLR4 might play a crucial role in the pathophysiology of depression. NF-κB is a transcription factor which induces a certain cytokine expression and regulates the inflammatory cascade [25, 26]. More importantly, studies have clearly shown that NF-κB increased IL-1β and TNF-α expression in the hippocampus and frontal cortex during stress [7] and regulated neurogenesis in the hippocampus which were closely related with depression [27, 28].

In the study, CUMS was used to establish an animal model for depression, which replicates the specific neuroendocrinological and cytokine expression abnormalities of depression patients [29]. In addition, ob/ob mice with higher levels of blood lipid and C57BL/6 mice were used in order to distinguish the differences in behavioral alteration and cytokine expression between normal-weight and obese mice. Given that a higher level of blood lipid is one of the DAMPs that could initiate TLR4 and inhibition of the TLR4-NF-κB signaling pathway, which might be a potential strategy in depression treatment, the aim of the study was to compare the depressive-like behaviors and the levels of cytokines (IL-1β, IL-6, and TNF-α) and NF-κB in the brain between C57BL/6 mice and ob/ob mice after CUMS and whether the TLR4 antagonist Tak242 could reverse the depressive-like behaviors and overexpressions of cytokines and NF-κB in stressed mice.

2. Materials and Methods

2.1. Animals. Thirty male C57BL/6 mice, seven to eight weeks old, weighing 18–22 grams and thirty male ob/ob mice, seven to eight weeks old, weighing 40–45 grams obtained from Vital River Laboratory Animal Technology Co., Ltd. (Beijing, China), were housed (5 per cage) and maintained under a 12 hr light-dark cycle, at 20–24°C with free access to food and water. The weights of mice were recorded at baseline and every week during the CUMS procedure and on the day after behavioral tests. The order of behavioral tests was sucrose preference test, open-field test, and Morris water maze test. All procedures used in this study were reviewed and approved by the Ethics Committee of School of Medicine, Shandong University, which complies with the National Institutes of Health's *Guide for the Care and Use of Laboratory Animals* (NIH publication no. 85-23, revised 1985).

2.2. Experimental Groups and Drug Administration. After 7 days of adaptation, C57BL/6 mice and ob/ob mice were randomly divided into 6 groups (10 mice per group): C57BL/6 control group (Ctrc57), C57BL/6 CUMS group (CUMSc57), C57BL/6 CUMS + Tak242 (Takc57), ob/ob control group (Ctrob), ob/ob CUMS group (CUMSob), and ob/ob CUMS + Tak242 group (Takob). Two CUMS groups received CUMS procedure, and two Tak242 groups received both CUMS procedure and a daily intraperitoneal injection of TLR4 antagonist Tak242 (3 mg/kg, freshly suspended in 80% polyethylene glycol 400) at 30 min prior to stress exposure [30]. The control and CUMS groups were given 80% polyethylene glycol 400 (vehicle) to balance the systematic error.

2.3. Chronic Unpredictable Mild Stress. Mice in the CUMS and CUMS + Tak242 groups were repeatedly exposed to a series of chronic unpredictable mild stressors that included the following: 8 hours of food deprivation, 8 hours of water deprivation, 45° lean cage, white noise (1500 Hz, 92 PB, 1 h), day and night confusion, foot shock for 15 min (50 mV, 10 s duration, average 1 shock/min), and horizontal oscillation for 20 min. Each stressor was applied per day, and the entire stress procedure lasted for 3 weeks, with stressors applied in a completely random order, inducing a depressive state [31].

2.4. Behavior Tests

2.4.1. Sucrose Preference Test. A decreased sucrose preference is considered to be homologous to anhedonia, the inability to experience pleasure, which simulates the defining symptom of major depression [32, 33]. Mice were individually housed during the sucrose preference test. Prior to the test, there was a 48-hour adaptation period for mice to habituate to sucrose solution or water. After that, a 23-hour period of water and food deprivation was carried out. Then, each mouse was given free access to two bottles for 1 hour, one with 200 ml 1% (w/v) sucrose solution and the other with 200 ml water. The drinking bottles were weighed to calculate the consumption of fluids 1 hour later. The sucrose preference percentage was evaluated by the amount of sucrose solution consumed during consumption of all fluids, the decrease of which indicated the depression symptom.

2.4.2. Open-Field Test. An open-field test was used to test the exploration motivation of mice [34, 35]. The open-field apparatus is made of black acrylic (90 cm diameter and 45 cm wall height). Mice were placed individually at the center of the apparatus and left free to explore the arena for 5 min. The following indices were recorded: number of grid crossings (horizontal movement), defined as crossing into the nearby grids with more than three paws or half of the body; number of rears (vertical movement), defined as both forelimbs raised at least 1 cm above the ground; frequency of grooming behaviors; and time in centre squares, defined as the time spent in the central nine grids before stepping into the outer grids of the apparatus. The box was thoroughly

cleaned between tests. The time in centre squares, horizontal and vertical movements, and number of grooming were recorded by a camera linked with a computer which fitted with a SMART video tracking system in the study (SMART v3.0, Panlab, Spain).

2.4.3. Morris Water Maze. A version of the conventional Morris water maze test was performed to evaluate spatial reference learning and memory [36]. The maze was a blue pool (0.8 m in diameter) filled with water (0.3 m deep, $25 \pm 1^{\circ}$C). Geometric pictures pasted on the surrounding walls were used by the mice for space orientation. Four equal quadrants were divided according to four directions: I, II, III, and IV. Movement tracks of the mice were captured by a CCD camera connected with a computer. All mice were allowed to swim for 60 s freely within 24 hours before the formal training. During the following 4 consecutive days, mice were trained to find a platform (12 cm diameter) hidden under the water surface in quadrant IV 4 times per day. If a mouse failed to find the platform within 60 s, it was manually guided to the platform and allowed to remain there for 10 s. The escape latency was scored as 60 s for these mice. On the fifth day, all mice were released into the maze without the hidden platform from an identical point of quadrant I and allowed to swim freely for 60 seconds. The percentage of time spent in quadrant IV of mice on the fifth day was analyzed.

2.5. Serum Corticosterone Measurement. At the end of the experiment, the animals (six per group) were sacrificed under deep anesthesia; all blood samples were obtained and centrifuged for 10 min at 3000 rpm. Serum corticosterone (CORT) was measured using a commercially available radioimmunoassay (RIA) kit (Nanjing Jiancheng Bioengineering Institute, China). RIA was performed according to the manufacturer's instruction.

2.6. Enzyme-Linked Immunosorbent Assay. Animals (six per group) were sacrificed under deep anesthesia, and both sides of the frontal and parietal bones were pulled off to collect the whole brain from the cranial cavity. After that, the frontal cortex and hippocampus were collected and immersed immediately in liquid nitrogen and stored at −80°C for further protein isolation. The tissue was dissociated using an ultrasonic cell disruptor and lysed in cold lysis buffer containing 10 mM Tris-HCl, pH 8.0, 240 mM NaCl, 5 mM EDTA, 1 mM dithiothreitol, 0.1 mM phenylmethanesulfonyl fluoride, 1% Triton X-100, 1 mM sodium vanadate, and 1 g/ml of leupeptin, pepstatin, and aprotinin. Tissue lysates were incubated at 4°C for 20 min. The sample was centrifuged at 12,000 rpm for 10 min at 4°C, then the supernatant was collected and protein content was determined by BCA protein assay reagents (Pierce, Rockford, IL). The levels of IL-1β, IL-6, and TNF-α were measured using commercially available enzyme-linked immunosorbent assay (ELISA) kits according to the manufacturer's instructions (Beijing Ke Ying Mei Technology Co., Ltd, China). Briefly, serial dilutions of protein standards and samples were added to 96-well ELISA plates, followed by biotinylated antibodies of IL-1β, IL-6, and TNF-α. After rinsing with wash buffer, a prepared solution of the avidin-horseradish peroxidase conjugated complex was added followed by addition of substrate solution. The reaction was stopped by the stopping solution. The optical density was detected at 450 nm using the iMark Microplate Absorbance Reader (Bio-Rad Labs, Hercules, CA, USA). The concentration of each sample was calculated from the linear equation derived from the standard curve of known concentrations of the cytokines.

2.7. Western Blotting

2.7.1. Protein Isolation. Brain tissue was homogenized in a lysis buffer supplemented with 1% protease inhibitor phenylmethanesulfonyl fluoride (PMSF) in a ratio of 1 : 5 (1 g tissue/5 ml reagent). The lysed tissue sample was centrifuged at 14000g at 4°C for 30 min, and then the protein-containing supernatant obtained was either immediately used or stored at −80°C. The protein concentration was detected with a BCA Protein Assay Kit (Beyotime Institute of Biotechnology) using the iMark Microplate Absorbance Reader (Bio-Rad, CA, USA).

2.7.2. NF-κB Western Blotting. Brain protein samples containing the same amount of total protein were mixed with a 5x Laemmli loading buffer (protein volume : loading buffer = 4 : 1). The mixed protein sample was heated at 99°C for 5 min to cause protein denaturation, and then 20 μg of protein sample was separated on 12% sodium dodecyl sulfate-polyacrylamide (SDS-PAGE) gel and electrotransferred to polyvinylidene difluoride (PVDF) membranes (Bio-Rad, CA, USA). The membrane was blocked with 5% skim milk in TBS containing 0.1% Tween-20 (TBST) for 1 h and incubated with primary antibodies against NF-κB p65 protein (anti-rabbit, 1 : 2500, Abcam, USA) or GAPDH (anti-rabbit, 1 : 5000, Biogot Technology Co., Ltd) at 4°C overnight in a refrigerator. The following day, after washing with TBST three times for 5 min, the PVDF membrane was incubated for 1 h at room temperature with the secondary antibody (anti-rabbit, 1 : 10000, ZSGB-BIO, China). Then, the PVDF membrane was washed again with TBST three times for 15 min; the Western blots were visualized after being incubated with ECL solution (Millipore Corp., Billerica, Massachusetts, USA) for 1 min and exposed onto photographic films (Eastman Kodak Company, Rochester, New York, USA) for 10–90 sec. Signal intensities were quantified using the ImageJ 14.0 software, and the density value of the objective protein band was normalized according to that of the GAPDH band of the same sample.

2.8. Immunohistochemistry. The animals (four per group) were anesthetized with pentobarbital and perfused with 50 ml of 0.1 M PBS, followed by 100 ml ice-cold 4% paraformaldehyde (PFA). Paraffin-embedded frontal cortex and hippocampus tissues were cut to a thickness of the 5 μm section on a microtome. After rehydration, the sections were incubated with fresh 3% H_2O_2 for 10 min under room temperature, washed with distilled water, and heated at 95–98°C in 0.01 M citrate buffer (pH 6.0) for 15 min, then cooled at room temperature for 30 min and washed with PBS. Then the sections were blocked with normal goat

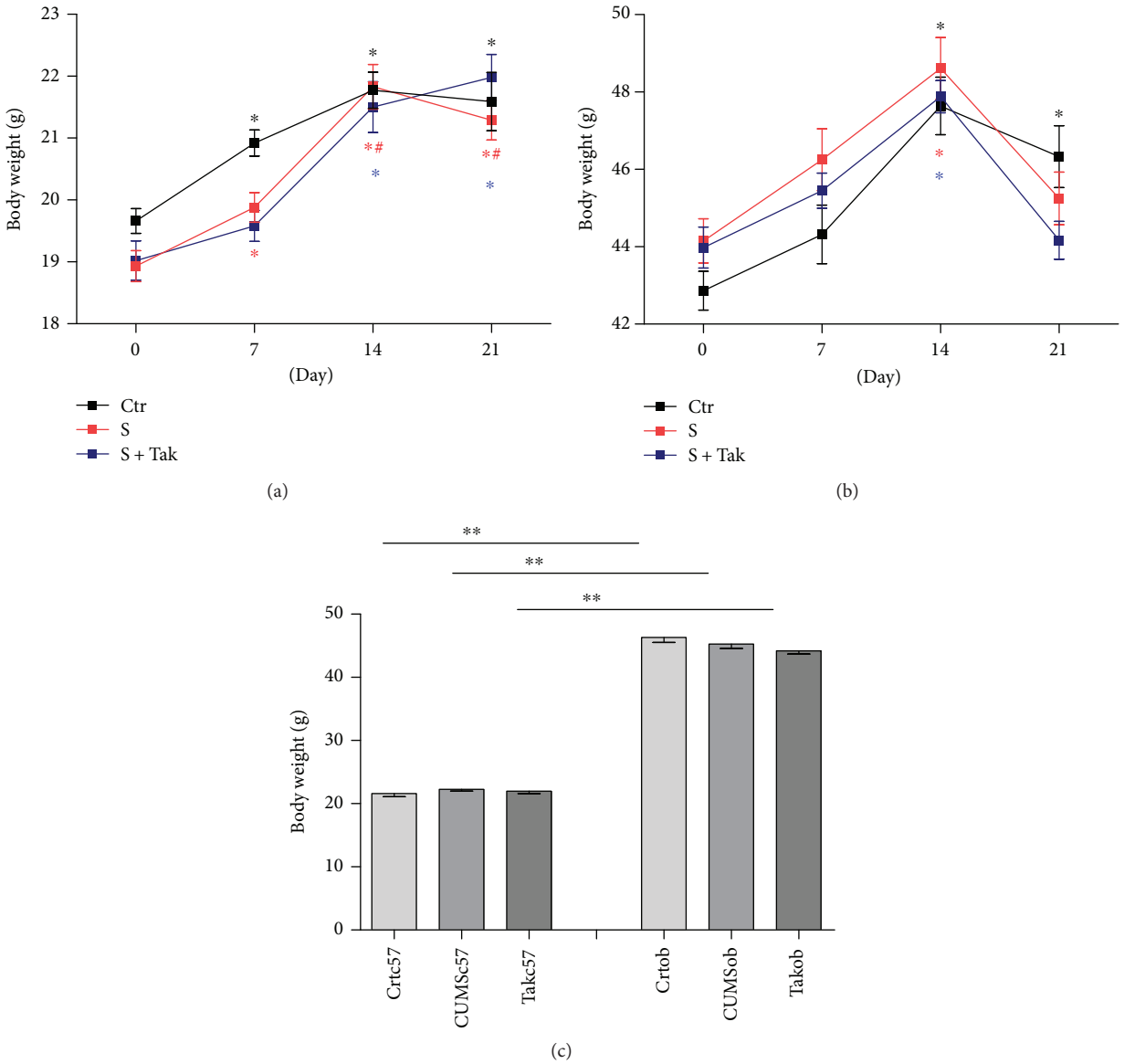

Figure 1: The comparison of body weight in different groups. (a) Body weight changes during CUMS of C57BL/6 mice; $^{*}p < 0.05$ compared with 0 day and $^{\#}p < 0.05$ compared with 7 days. (b) Body weight changes during CUMS of ob/ob mice; $^{*}p < 0.05$ compared with 14 days. (c) The body weight on the day after behavioral tests. Results are expressed as mean ± SEM ($n = 10$ in each group); $^{**}p < 0.01$.

serum for 20 min, incubated with rabbit anti-NF-κB p65 antibody (1 : 250, GeneTex, USA) at 4°C overnight, and washed with PBS. After that, the sections were incubated with biotinylated goat anti-rabbit IgG antibodies at 37°C for 15 min, rewashed with PBS, incubated with the streptavidin-biotin complex (SABC) at 37°C for 15 min, and then stained with diaminobenzidine under a microscope. At the end, the sections were dehydrated, cleared, and mounted. After all the staining was finished, each section was viewed under 400x magnification, and NF-κB p65 expression was observed.

2.9. Statistics. Data were presented as the mean ± SEM. Statistical analysis of data was carried out by one-way analysis of variance (ANOVA) with S-N-K post hoc test and independent samples t-test. Further, two-way ANOVA was used to analyze the change in bodyweight during the CUMS procedure. Differences were considered statistically significant if the p value was less than 0.05.

3. Results

3.1. Body Weight. The results showed that the main effect of group on body weight was not significant ($F = 2.093$, $p = 0.128$; $F = 1.764$, $p = 0.177$), but the time effect on body weight was significant in C57BL/6 groups ($F = 42.227$, $p < 0.001$) and ob/ob groups ($F = 24.327$, $p < 0.001$) during the period of CUMS (Figures 1(a) and 1(b)). The body weight of both C57BL/6 and ob/ob mice increased during 14 days of the CUMS procedure. Briefly, the body weights of the C57BL/6 control group and CUMS group significantly increased at 7 days of the CUMS procedure compared with

those at baseline ($F = 9.157$, $p < 0.001$) ($p < 0.05$, resp.), and the body weight of the C57BL/6 Tak242 group significantly increased at 14 days of the CUMS procedure compared with that at baseline ($p < 0.05$, resp.). The body weights of all ob/ob groups significantly increased at 14 days of CUMS procedure compared with those at baseline ($p < 0.05$, resp.). There were significant differences in body weight between C57BL/6 mice and ob/ob mice in control groups ($t = 27.731$, $p < 0.001$), CUMS groups ($t = 32.160$, $p < 0.001$), and Tak242 groups ($t = 36.014$, $p < 0.001$) after behavioral tests (Figure 1(c)). The results indicated that there was no effect of the CUMS regimen on body weight of both C57BL/6 mice and ob/ob mice, but ob/ob mice had greater body weight than C57BL/6 mice had on the day after behavioral tests due to the animal strains.

3.2. Behavioral Tests

3.2.1. Sucrose Preference Test. As shown in Figure 2(a), CUMS exposure significantly reduced the percentage of sucrose consumption in both stressed C57BL/6 mice and ob/ob mice in comparison with the control animals [$F = 76.236$, $p < 0.001$; $F = 22.252$, $p < 0.001$], while treatment with Tak242 significantly prevented the decrease in sucrose consumption, as compared to the CUMS-exposed mice ($p < 0.01$; $p < 0.01$). In addition, the Ctrob and CUMSob groups had lower percentage of sucrose consumption than the Ctrc57 and CUMSc57 groups had ($t = 6.827$, $p < 0.001$; $t = 20.646$, $p < 0.001$). The results indicated that stress decreased sucrose preference in C57BL/6 mice and ob/ob mice, while the antagonist reversed the alteration. Both unstressed and stressed ob/ob mice had lower sucrose consumption than C57BL/6 mice had.

3.2.2. Open-Field Test. As shown in Figure 2(b), CUMS increased the time in centre squares in C57BL/6 mice [$F = 16.483$, $p < 0.001$] ($p < 0.01$), but Tak242 could not relieve the alteration ($p < 0.01$). There was a significant difference in the time in centre squares among ob/ob mice [$F = 4.334$, $p = 0.025$], unstressed and stressed mice had a longer time in centre squares compared with the antagonist group ($p < 0.05$; $p < 0.01$). Moreover, all ob/ob groups had a longer time in centre squares than their C57BL/6 counterparts had ($t = 3.378$, $p = 0.004$; $t = 6.531$, $p < 0.001$; and $t = 2.706$, $p = 0.015$). As shown in Figure 2(c), the C57BL/6 mice in the CUMS group showed decreased horizontal and vertical movements [$F = 3.496$, $p = 0.045$] in comparison to the control group ($p < 0.05$). Treatment with Tak242 significantly reversed the behavioral alteration as compared to the CUMS groups ($p < 0.05$). In ob/ob mice, unstressed and stressed mice had lower horizontal and vertical movements compared with the antagonist group [$F = 6.463$, $p = 0.006$], Tak242 prevented the lower exploratory behaviors ($p < 0.01$). In addition, all ob/ob groups had decreased horizontal and vertical movements compared with the C57BL/6 group ($t = 8.860$, $p < 0.001$; $t = 5.268$, $p < 0.001$; and $t = 3.860$, $p = 0.001$). As shown in Figure 2(d), CUMS increased the number of grooming in ob/ob mice [$F = 8.915$, $p = 0.001$] ($p < 0.01$) while Tak242 relieved the change ($p < 0.05$). The control ob/ob group and CUMS ob/ob group displayed a much higher number of grooming than did C57BL/6 groups ($t = 3.344$, $p = 0.004$, and $t = 3.291$, $p = 0.004$, resp.).

The results indicated that stress induced lower interest in a new environment. Behavior suppression of both C57BL/6 mice and ob/ob mice was explored; ob/ob mice had obvious behavioral disorders in the OFT compared with C57BL/6 mice, and the antagonist improved most of the abnormal behaviors in both mice and ob/ob mice.

3.2.3. Morris Maze Test. As shown in Figure 2(e), CUMS mice showed less target quadrant time in the Morris maze test [$F = 22.123$, $p = 0.001$, and $F = 4.283$, $p = 0.026$] in comparison to the control mice (C57BL/6 mice: $p < 0.01$; ob/ob mice: $p < 0.05$). Treatment with Tak242 significantly reversed the behavioral alteration as compared to the CUMS C57BL/6 mice ($p < 0.01$), while Tak242 treatment did not improve the behavioral change in the Tak242 ob group ($p > 0.05$). Moreover, the CUMSc57 group had less target quadrant time compared with the CUMSob group ($t = 2.889$, $p = 0.010$), while Tak242 c57 had a longer target quadrant time compared with the Takob group in the Morris maze test ($t = 3.451$, $p = 0.003$). The results indicated that CUMS induced less target quadrant time in both C57BL/6 mice and ob/ob mice in the Morris maze test, and the antagonist relived the alteration in C57BL/6 mice.

3.3. The Level of Serum Corticosterone. As shown in Figure 3, CUMS induced a higher level of serum corticosterone in stressed ob/ob mice [14.070, $p < 0.001$] compared with unstressed mice ($p < 0.01$). Tak242 could reverse the increased level of corticosterone in ob/ob mice ($p < 0.01$).

3.4. The Levels of Cytokines in the Frontal Cortex and Hippocampus. Cytokine expression in the frontal cortex is shown in Figures 4(a)–4(c). As shown in Figure 4(a), the level of IL-1β increased in both stressed C57BL/6 mice [$F = 244.847$, $p < 0.001$] ($p < 0.01$) and ob/ob mice as compared to controls [$F = 251.203$, $p < 0.001$] ($p = 0.01$), while Tak242 could reverse the alteration in C57BL/6 mice and ob/ob mice ($p < 0.01$; $p < 0.01$). ob/ob mice in the control group, CUMS group, and Tak242 group had higher levels of IL-1β than C57BL/6 mice had ($t = 39.963$, $p < 0.001$; $t = 298.468$, $p < 0.001$; and $t = 27.188$, $p < 0.001$). As shown in Figure 4(b), CUMS significantly increased the levels of IL-6 in C57BL/6 mice [$F = 32.093$, $p = 0.001$] ($p < 0.01$) and ob/ob mice [$F = 67.729$, $p < 0.001$] ($p < 0.01$) as compared to controls, while Tak242 decreased the levels of IL-6 in C57BL/6 mice ($p < 0.01$) and ob/ob mice ($p < 0.01$). Further, ob/ob mice in the control group, CUMS group, and Tak242 group had higher levels of IL-6 than C57BL/6 mice had ($t = 11.741$, $p < 0.001$; $t = 13.777$, $p < 0.001$; and $t = 82.866$, $p < 0.001$). As shown in Figure 4(c), stress significantly increased TNF-α in C57BL/6 mice [$F = 215.849$, $p < 0.001$] ($p < 0.01$) and ob/ob mice [$F = 54.251$, $p < 0.001$] ($p < 0.01$), while Tak242 could reverse the change in TNF-α level ($p < 0.01$; $p < 0.01$). The Ctrob, CUMSob, and Tak242 ob groups had higher levels of TNF-α than

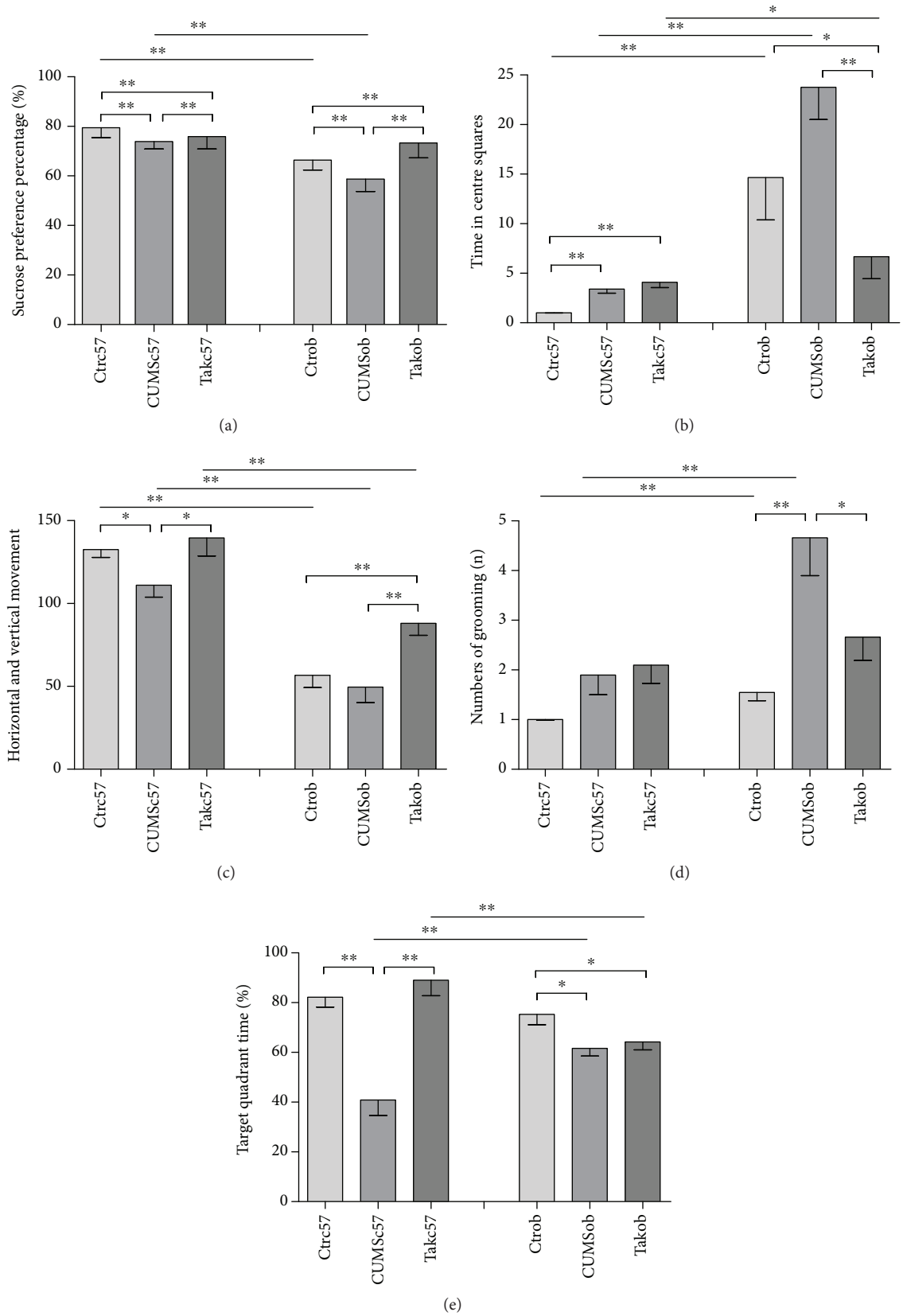

Figure 2: The comparison of behavior changes in different groups: (a) sucrose preference percentage in the SPT; (b) time in centre squares in the OFT; (c) number of horizontal and vertical movements in the OFT; (d) number of grooming in the OFT; (e) percentage of time spent in the target quadrant in the MWM test. Results are shown as mean ± SEM ($n = 10$ in each group). $^{*}p < 0.05$ and $^{**}p < 0.01$.

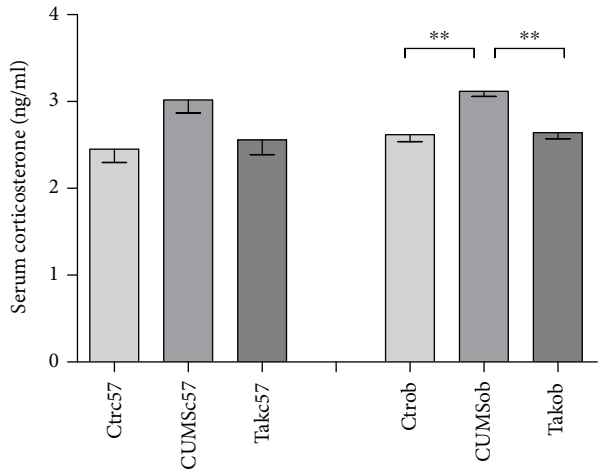

FIGURE 3: The comparison of serum corticosterone levels in different groups. Data are expressed as means ± SEM ($n = 6$ in each group). $^{**}p < 0.01$.

C57BL/6 groups had, respectively ($t = 20.156$, $p < 0.001$; $t = 353.631$, $p < 0.001$; and $t = 11.044$, $p < 0.001$).

The results indicated that CUMS induced increased IL-1β, IL-6, and TNF-α levels in the frontal cortex in both C57BL/6 and ob/ob mice, while the antagonist reversed the alteration; ob/ob mice had higher levels of cytokines in the frontal cortex than C57BL/6 mice had.

Cytokine expression in the hippocampus is shown in Figures 4(d)–4(f). The change tendency was similar to the frontal cortex. Figure 4(d) shows that the levels of IL-1β increased in both CUMS C57BL/6 group [$F = 167.546$, $p < 0.001$] ($p < 0.01$) and CUMS ob/ob group compared to the control group [$F = 24.858$, $p = 0.001$] ($p < 0.01$); however, Tak242 reversed the alteration in C57BL/6 mice and ob/ob mice ($p < 0.01$; $p < 0.01$). Unstressed, stressed, and Tak242 ob/ob mice had higher levels of IL-1β than C57BL/6 mice had ($t = 10.107$, $p = 0.001$; $t = 12.004$, $p < 0.001$; and $t = 13.796$, $p < 0.001$). Figure 4(e) shows that CUMS significantly increased the levels of IL-6 in C57BL/6 [$F = 41.508$, $p < 0.001$] ($p < 0.01$) and ob/ob mice [$F = 13.651$, $p = 0.006$] ($p < 0.01$) compared to the control, while Tak242 decreased the levels of IL-6 in C57BL/6 mice ($p < 0.01$) and ob/ob mice ($p < 0.01$). Meanwhile, unstressed, stressed, and Tak242 ob/ob mice had higher levels of IL-6 than C57BL/6 mice had ($t = 7.676$, $p = 0.002$; $t = 5.443$, $p = 0.006$; and $t = 15.702$, $p < 0.001$). Figure 4(f) shows that stress increased TNF-α in C57BL/6 [$F = 94.544$, $p < 0.001$] ($p < 0.05$) and ob/ob mice [$F = 47.300$, $p < 0.001$] ($p < 0.01$), while Tak242 could reverse the change in TNF-α level ($p < 0.01$; $p < 0.01$). ob/ob mice in the control, CUMS, and antagonist groups had higher levels of TNF-α than C57BL/6 groups had ($t = 4.381$, $p = 0.012$; $t = 21.203$, $p < 0.001$; and $t = 37.023$, $p < 0.001$).

The results suggested that CUMS induced increased IL-1β, IL-6, and TNF-α levels in the hippocampus in C57BL/6 mice and ob/ob mice, while the antagonist reversed the alteration; ob/ob mice in unstressed, stressed, and antagonist groups had higher levels of cytokines in the hippocampus than C57BL/6 mice had.

3.5. NF-κB p65 Expression in the Frontal Cortex and Hippocampus

3.5.1. NF-κB p65 Expression in the Frontal Cortex and Hippocampus in Western Blot. Figure 5(a) shows the NF-κB p65 expression in the frontal cortex in Western blot. The CUMS procedure induced a marked increase in NF-κB p65 level in C57BL/6 mice compared to control animals [$F = 4.043$, $p = 0.035$] ($p < 0.05$), and Tak242 could relieve the alteration ($p > 0.05$ control group versus Tak242 group). CUMS did not induce a significant increase in NF-κB p65 level in ob/ob mice [$F = 2.359$, $p = 0.123$]. Moreover, the NF-κB p65 level of ob/ob mice in the control group was higher than that of the C57BL/6 mice in the control group ($t = 4.669$, $p = 0.001$). The results suggested that both unstressed and stressed ob/ob mice had higher levels of NF-κB p65 than C57BL/6 mice in the frontal cortex, but the antagonist could not reverse the alteration of the NF-κB p65 level in ob/ob mice.

Figure 5(b) shows the NF-κB p65 expression in the hippocampus in Western blot. CUMS induced a higher level of NF-κB p65 expression in C57BL/6 mice compared to control animals [$F = 4.177$, $p = 0.032$] ($p < 0.05$), while Tak242 relieved the alteration ($p > 0.05$, control group versus Tak242 group). CUMS induced an increase in NF-κB p65 expression in ob/ob mice compared to control mice [$F = 5.641$, $p = 0.015$] ($p < 0.01$), while Tak242 could reverse the alteration ($p < 0.05$). Further, there were significant differences in NF-κB p65 expression in the hippocampus between control groups ($t = 5.548$, $p < 0.001$), CUMS groups ($t = 8.350$, $p < 0.001$), and Tak242 groups ($t = 4.592$, $p = 0.001$) of C57BL/6 mice and ob/ob mice. The results indicated that ob/ob mice had a higher level of NF-κB p65 in the hippocampus than C57BL/6 mice had; stress worsened the situation, while the antagonist normalized it.

3.5.2. NF-κB p65 Expression in the Frontal Cortex and Hippocampus in IHC. Figure 5(c) shows the NF-κB p65 expression in the frontal cortex (above) and hippocampus (below) in immunohistochemistry (IHC). Figures 5(b) and 5(c) show the cell counting of NF-κB p65 expression in the frontal cortex and hippocampus. The NF-κB expression in IHC confirmed the change tendency of NF-κB p65 expression in the frontal cortex and hippocampus in Western blot.

In Figure 5(d), CUMS induced significant NF-κB p65 expression in the frontal cortex of C57BL/6 mice [$F = 50.864$, $p < 0.001$] ($p < 0.01$), while Tak242 reversed the change in mice of the Takc57 group ($p < 0.01$). CUMS induced an obvious NF-κB p65 expression in the frontal cortex of ob/ob mice, but the differences in the number of NF-κB p65-positive expression cells among the three groups did not reach significance [$F = 2.275$, $p = 0.159$]. There were no significant differences in the number of positive expression cells in the frontal cortex between C57BL/6 mice and ob/ob mice in control groups ($t = 0.333$, $p = 0.750$),

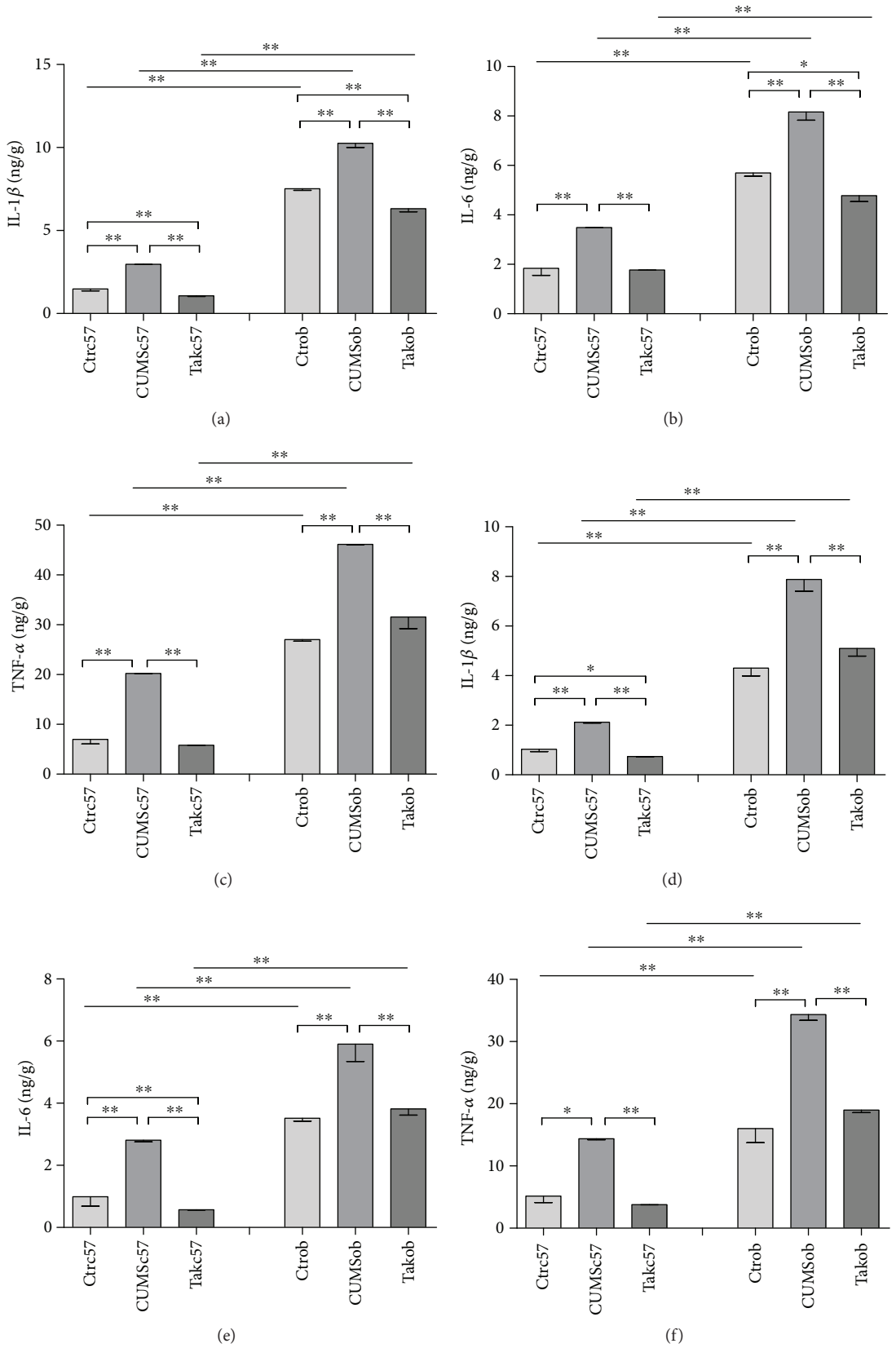

Figure 4: Cytokine expression in the frontal cortex and hippocampus measured in different groups: (a) IL-1β expression in the frontal cortex; (b) IL-6 expression in the frontal cortex; (c) TNF-α expression in the frontal cortex; (d) IL-1β expression in the hippocampus; (e) IL-6 expression in the hippocampus; (f) TNF-α expression in the hippocampus. Data are expressed as means ± SEM ($n = 6$ in each group). $^{*}p < 0.05$ and $^{**}p < 0.01$.

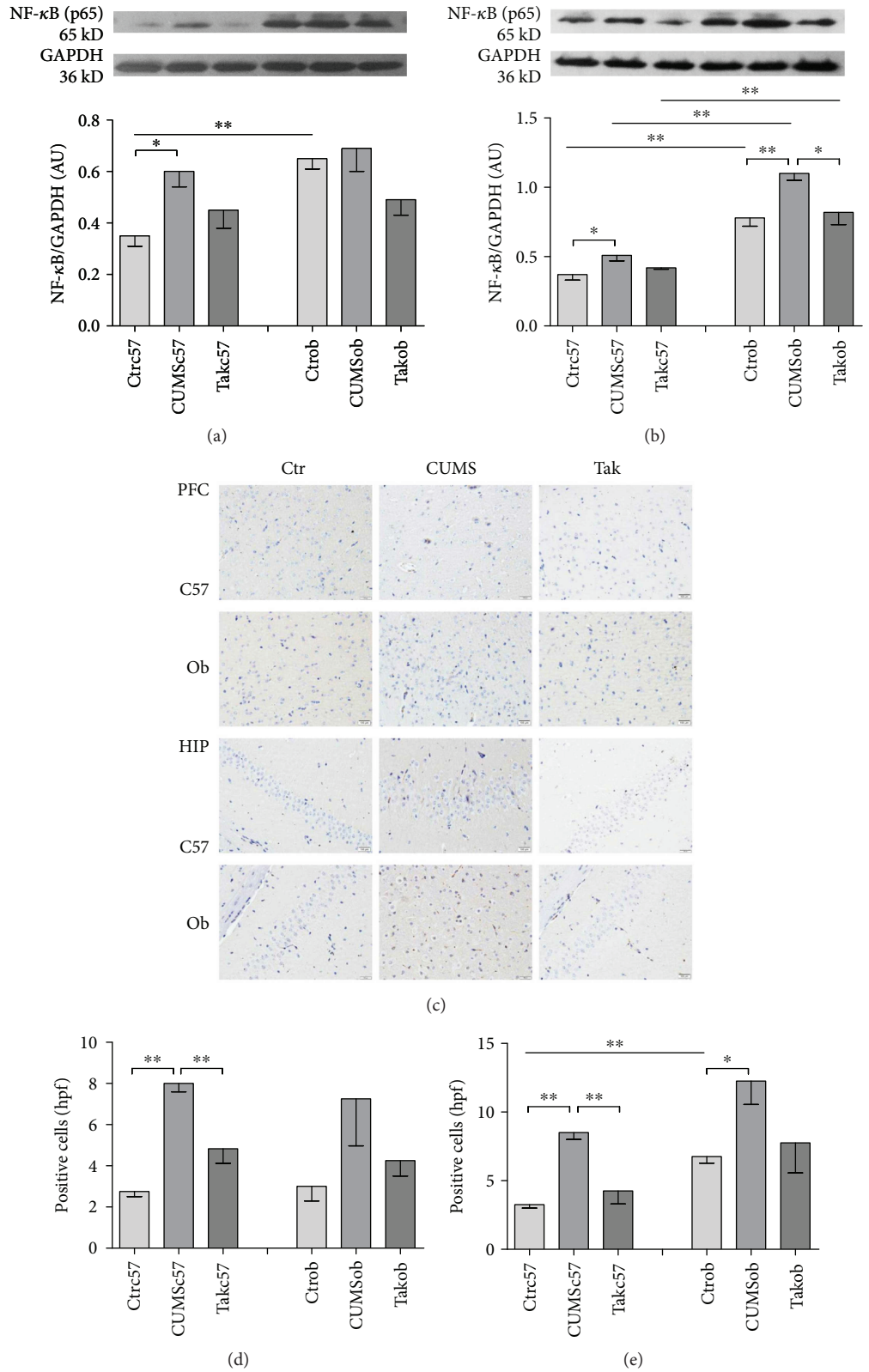

Figure 5: NF-κB p65 expression in the frontal cortex and hippocampus. (a) NF-κB p65 expression in the frontal cortex measured in Western blot. (b) NF-κB p65 expression in the hippocampus measured in Western blot. (c) NF-κB p65 expression in the frontal cortex and hippocampus in immunohistochemistry (×400). Above: frontal cortex; below: hippocampus. (d) Positive expression neuron counting in the frontal cortex in a high-power field (hpf). (e) Positive expression neuron counting in the hippocampus in a high-power field (hpf). Data are expressed as means ± SEM ($n = 6$ in each group and $n = 4$ in each group). $^{*}p < 0.05$ and $^{**}p < 0.01$.

CUMS groups ($t = 0.323$, $p = 0.758$), and Tak242 groups ($t = 0.562$, $p = 0.595$).

In Figure 5(e), CUMS induced a significant NF-κB p65 expression in the hippocampus in the CUMSc57 group compared with the control group [$F = 19.293$, $p < 0.001$] ($p < 0.01$). Tak242 changed the alteration of NF-κB p65-positive expression in the hippocampus in the Takc57 group ($p < 0.01$). CUMS induced a much more NF-κB p65-positive expression in the hippocampus in the CUMSob group [$F = 4.162$, $p = 0.053$] ($p < 0.05$), while Tak242 relieved the increased NF-κB p65 expression of the hippocampus in the Tak242 ob group ($p > 0.05$). ob/ob mice in the control group had significantly more positive expression cells than C57BL/6 mice had in the control group ($t = 6.481$, $p = 0.001$); no significant differences in the number of positive expression cells were found between C57BL/6 mice and ob/ob mice in the CUMS group ($t = 2.114$, $p = 0.079$) and Tak242 group ($t = 1.759$, $p = 0.129$).

4. Discussion

Studies have confirmed that stress was associated with elevated inflammation and depression, and increased cytokines in the brain played a crucial role in the etiology of depression [1]. Meanwhile, a low-grade inflammation state might constitute vulnerability to depression in an obese population [16] because the higher levels of certain cytokines in the prefrontal cortex and hippocampus were regarded as contributors of emotional disorder and memory damage [7]. The present study probed the depressive-like behaviors induced by CUMS between normal-body weight mice and ob/ob mice [37, 38] and the protective effects of the TLR4 antagonist on behavioral changes [22, 27, 28]. The results demonstrated that CUMS induced lower sucrose consumption, more time spent in the central squares, low number of movements in OFT, and less target quadrant time in MWM in both C57BL/6 mice and ob/ob mice. The results all suggested that the stressed animals displayed anhedonia and disinterest in a new environment and were in a state of low excitement and memory impairment [21, 22]. Inconsistent with the hypotheses, TLR4 antagonist Tak242 displayed different effects on preventing the behavioral disorders by showing that Tak242 remarkably reversed lower sucrose consumption and induced behavioral disorders in OFT and memory impairment except anhedonia in C57BL/6 mice and memory impairment in ob/ob mice. The findings implicated that overexpression of cytokines in the frontal cortex and hippocampus could not interpret all depressive symptoms; dysfunction of the hypothalamic-pituitary-adrenal axis (HPA) and the neurotransmitter system played important roles in the pathogenesis of depression [39, 40]. However, it was noticed that ob/ob mice in both control group and CUMS group displayed serious anhedonia and autonomic activity suppression than did C57BL/6 mice which suggested that obese animals might be more vulnerable to depression than normal weight animals under stress [41, 42].

Studies showed that certain cytokines such as IL-1β were involved in the pathogeneses of depression [2, 3]. TNF-α was closely related with locomotor activity suppression, anhedonia, and fatigue, as well as alterations in cognition, and might cause depressive symptoms through the HPA axis [40]. Our previous study also confirmed that the reduction level of IL-1β, IL-6, and TNF-α in the hippocampus could relieve depressive-like behaviors [5, 17]. In the study, CUMS increased the IL-1β and IL-6 expression in both C57BL/6 and ob/ob mice, while Tak242 prevented the alterations. The results supported the conclusion that stress elevated the inflammation condition and induced depression. Moreover, the present study showed that ob/ob mice in unstressed, stressed, and antagonist groups had higher levels of IL-1β, IL-6, and TNF-α in both frontal cortex and hippocampus than C57BL/6 mice which indicated that ob/ob mice had higher baseline of cytokines in certain brain areas; stress worsened the situation, while the TLR4 antagonist could not completely reverse the increased cytokines in ob/ob mice. Combined with the results that both unstressed and stressed ob/ob mice had serious depressive-like behaviors than C57BL/6 mice had, the study reached the conclusion that higher levels of cytokines of the frontal cortex and hippocampus might be the reason for the susceptibility to depression in obese mice [20].

TLR4-mediating innate immune response was associated with neuroinflammation [23, 24]. NF-κB was a cardinal transcriptional regulator of inflammation and apoptosis of neurons [1, 10]. DAMPs activated the TLR4-NF-κB pathway and induced elevated levels of IL-1β, IL-6, and TNF-α [16]. In order to clarify the role of TLR4-NF-κB signaling in the regulation of inflammatory responses during CUMS, we examined the NF-κB expression in the frontal cortex and hippocampus which are closely related with cognition and emotion using Western blot and immunohistochemistry. In the results of Western blot, CUMS induced a significant increase in NF-κB expression in the frontal cortex and the TLR4 antagonist reversed the overexpression of NF-κB in C57BL/6 mice. However, both CUMS and antagonist did not change the NF-κB expression in the frontal cortex in ob/ob mice. This explains that ob/ob mice in the control group had high NF-κB expression at baseline than C57BL/6 mice had, and CUMS failed to increase the level of NF-κB in the frontal cortex. In addition, the present study shows that CUMS induced a significant increase in NF-κB expression in the hippocampus while the TLR4 antagonist could reverse the overexpression of NF-κB in both C57BL/6 mice and ob/ob mice, but all ob/ob mice displayed higher NF-κB levels in the hippocampus than C57BL/6 mice did. The results suggested that the high NF-κB expression at baseline was the crucial reason for the overexpression of cytokines in the hippocampus; CUMS stimulated higher levels of NF-κB, but the antagonist could normalize in ob/ob mice. In the IHC result, CUMS induced NF-κB overexpression in the frontal cortex and hippocampus in both C57BL/6 and ob/ob mice, and ob/ob mice in the control group had more obvious NF-κB expression in the hippocampus than C57BL/6 mice had, which was consistent with the results in Western blot. Based on the findings, the study concluded that ob/ob mice had a hyperactive TLR4-NF-κB signal and higher level of cytokines under CUMS [1, 21]. Our study may provide novel insights into

the development of new therapeutic approaches for obesity comorbidity depression [39, 43].

5. Conclusions

Our results demonstrated that CUMS induced a depressive-like behavior, spatial memory damage, higher level of serum corticosterone, and overexpression of cytokines and NF-κB in the frontal cortex and hippocampus. Obese mice displayed serious depressive-like behaviors and an upregulated TLR4-NF-κB signal. The implications for understanding the pathoetiology of vulnerability to depression of obesity and the development of new treatments are also considered.

Abbreviations

IL: Interleukin
TNF-α: Tumor necrosis factor-α
TLR4: Toll-like receptor 4
NF-κB: Nuclear factor kappa B
CUMS: Chronic unpredictable mild stress
HPA: Hypothalamic-pituitary-adrenal
PFC: Prefrontal cortex
HIP: Hippocampus
ANOVA: Analysis of variance
SEM: Standard error of the mean.

Conflicts of Interest

The authors have no conflict of interests to declare.

Authors' Contributions

Xiaohong Li was involved in the study design and data interpretation; Yihe Wang and Ziyang Li contributed to the analysis of data and writing of the manuscript; and Yihe Wang, Yuan Liu, and Jingjing Xu performed the majority of the laboratory work and were responsible for the animal model.

Acknowledgments

This work was supported by funding from the National Natural Science Foundation of China (no. 81373635) and the Jinan Municipal Science and Technology Development Program (no. 201212012).

References

[1] G. M. Slavich and M. R. Irwin, "From stress to inflammation and major depressive disorder: a social signal transduction theory of depression," *Psychological Bulletin*, vol. 140, no. 3, pp. 774–815, 2014.

[2] F. Lamers, Y. Milaneschi, P. de Jonge, E. J. Giltay, and B. W. J. H. Penninx, "Metabolic and inflammatory markers: associations with individual depressive symptoms," *Psychological Medicine*, pp. 1–11, 2017.

[3] Y. Lu, C. S. Ho, X. Liu et al., "Chronic administration of fluoxetine and pro-inflammatory cytokine change in a rat model of depression," *PLoS One*, vol. 12, no. 10, article e0186700, 2017.

[4] A. J. Dunn, A. H. Swiergiel, and R. de Beaurepaire, "Cytokines as mediators of depression: what can we learn from animal studies?," *Neuroscience and Biobehavioral Reviews*, vol. 29, no. 4-5, pp. 891–909, 2005.

[5] R. Dantzer, J. C. O'Connor, G. G. Freund, R. W. Johnson, and K. W. Kelley, "From inflammation to sickness and depression: when the immune system subjugates the brain," *Nature Reviews Neuroscience*, vol. 9, no. 1, pp. 46–56, 2008.

[6] J. Levine, Y. Barak, K. N. R. Chengappa, A. Rapoport, M. Rebey, and V. Barak, "Cerebrospinal cytokine levels in patients with acute depression," *Neuropsychobiology*, vol. 40, no. 4, pp. 171–176, 1999.

[7] H. Jiang, Z. Wang, Y. Wang et al., "Antidepressant-like effects of curcumin in chronic mild stress of rats: involvement of its anti-inflammatory action," *Progress in Neuro-Psychopharmacology & Biological Psychiatry*, vol. 47, pp. 33–39, 2013.

[8] C. L. Raison, L. Capuron, and A. H. Miller, "Cytokines sing the blues: inflammation and the pathogenesis of depression," *Trends in Immunology*, vol. 27, no. 1, pp. 24–31, 2006.

[9] D. G. A. Janssen, R. N. Caniato, J. C. Verster, and B. T. Baune, "A psychoneuroimmunological review on cytokines involved in antidepressant treatment response," *Human Psychopharmacology*, vol. 25, no. 3, pp. 201–215, 2010.

[10] A. H. Miller, "Norman Cousins Lecture. Mechanisms of cytokine-induced behavioral changes: psychoneuroimmunology at the translational interface," *Brain, Behavior, and Immunity*, vol. 23, no. 2, pp. 149–158, 2009.

[11] R. Sapolsky, C. Rivier, G. Yamamoto, P. Plotsky, and W. Vale, "Interleukin-1 stimulates the secretion of hypothalamic corticotropin-releasing factor," *Science*, vol. 238, no. 4826, pp. 522–524, 1987.

[12] C. E. Wright, P. C. Strike, L. Brydon, and A. Steptoe, "Acute inflammation and negative mood: mediation by cytokine activation," *Brain, Behavior, and Immunity*, vol. 19, no. 4, pp. 345–350, 2005.

[13] O. Köhler, M. E. Benros, M. Nordentoft et al., "Effect of anti-inflammatory treatment on depression, depressive symptoms, and adverse effects: a systematic review and meta-analysis of randomized clinical trials," *JAMA Psychiatry*, vol. 71, no. 12, pp. 1381–1391, 2014.

[14] X. H. Yang, S. Q. Song, and Y. Xu, "Resveratrol ameliorates chronic unpredictable mild stress-induced depression-like behavior: involvement of the HPA axis, inflammatory markers, BDNF, and Wnt/β-catenin pathway in rats," *Neuropsychiatric Disease and Treatment*, vol. 13, pp. 2727–2736, 2017.

[15] M. Jia, C. Li, Y. Zheng et al., "Leonurine exerts antidepressant-like effects in the chronic mild stress-induced depression model in mice by inhibiting neuroinflammation," *The International Journal of Neuropsychopharmacology*, vol. 20, no. 11, pp. 886–895, 2017.

[16] C. D. Rethorst, I. Bernstein, and M. H. Trivedi, "Inflammation, obesity, and metabolic syndrome in depression: analysis of the 2009-2010 National Health and Nutrition Examination Survey (NHANES)," *The Journal of Clinical Psychiatry*, vol. 75, no. 12, pp. e1428–e1432, 2014.

[17] Y. Milaneschi, E. M. Simonsick, N. Vogelzangs et al., "Leptin, abdominal obesity, and onset of depression in older men and women," *The Journal of Clinical Psychiatry*, vol. 73, no. 9, pp. 1205–1211, 2012.

[18] A. M. Lasserre, J. Glaus, C. L. Vandeleur et al., "Depression with atypical features and increase in obesity, body mass index, waist circumference, and fat mass: a prospective, population-based study," *JAMA Psychiatry*, vol. 71, no. 8, pp. 880–888, 2014.

[19] J. L. Yang, X. Liu, H. Jiang, F. Pan, C. S. Ho, and R. C. Ho, "The effects of high-fat-diet combined with chronic unpredictable mild stress on depression-like behavior and leptin/LepRb in male rats," *Scientific Reports*, vol. 6, no. 1, article 35239, 2016.

[20] J. Schachter, J. Martel, C. S. Lin et al., "Effects of obesity on depression: a role for inflammation and the gut microbiota," *Brain, Behavior, and Immunity*, 2017.

[21] G. Singhal, E. J. Jaehne, F. Corrigan, C. Toben, and B. T. Baune, "Inflammasomes in neuroinflammation and changes in brain function: a focused review," *Frontiers in Neuroscience*, vol. 8, no. 315, 2014.

[22] Y. Zhao, Y. Zhang, and F. Pan, "The effects of EGb761 on lipopolysaccharide-induced depressive-like behaviour in C57BL/6J mice," *Central European Journal of Immunology*, vol. 40, no. 1, pp. 11–17, 2015.

[23] B. B. Mishra, U. M. Gundra, and J. M. Teale, "Toll-like receptors in CNS parasitic infections," *Current Topics in Microbiology and Immunology*, vol. 336, pp. 83–104, 2009.

[24] H. Kumar, T. Kawai, and S. Akira, "Toll-like receptors and innate immunity," *Biochemical and Biophysical Research Communications*, vol. 388, no. 4, pp. 621–625, 2009.

[25] W. Teng, L. Wang, W. Xue, and C. Guan, "Activation of TLR4-mediated NFκB signaling in hemorrhagic brain in rats," *Mediators of Inflammation*, vol. 2009, Article ID 473276, 6 pages, 2009.

[26] D. Li, N. Zhang, Y. Cao et al., "Emodin ameliorates lipopolysaccharide-induced mastitis in mice by inhibiting activation of NF-κB and MAPKs signal pathways," *European Journal of Pharmacology*, vol. 705, no. 1–3, pp. 79–85, 2013.

[27] A. Lanzillotta, V. Porrini, A. Bellucci, M. Benarese, C. Branca, E. Parrella et al., "NF-κB in innate neuroprotection and age-related neurodegenerative diseases," *Frontiers in Neurology*, vol. 6, p. 98, 2015.

[28] V. Bortolotto, B. Cuccurazzu, P. L. Canonico, and M. Grilli, "NF-κB mediated regulation of adult hippocampal neurogenesis: relevance to mood disorders and antidepressant activity," *BioMed Research International*, vol. 2014, Article ID 612798, 11 pages, 2014.

[29] T. Cheng, S. Dimitrov, C. Pruitt, and S. Hong, "Glucocorticoid mediated regulation of inflammation in human monocytes is associated with depressive mood and obesity," *Psychoneuroendocrinology*, vol. 66, pp. 195–204, 2016.

[30] H. Fang, P. F. Wang, Y. Zhou, Y. C. Wang, and Q. W. Yang, "Toll-like receptor 4 signaling in intracerebral hemorrhage-induced inflammation and injury," *Journal of Neuroinflammation*, vol. 10, no. 1, article 794, 2013.

[31] P. Willner, M. Wilkes, and A. Orwin, "Attributional style and perceived stress in endogenous and reactive depression," *Journal of Affective Disorders*, vol. 18, no. 4, pp. 281–287, 1990.

[32] P. Willner, A. Towell, D. Sampson, S. Sophokleous, and R. Muscat, "Reduction of sucrose preference by chronic unpredictable mild stress, and its restoration by a tricyclic antidepressant," *Psychopharmacology*, vol. 93, no. 3, pp. 358–364, 1987.

[33] A. J. Grippo, J. A. Moffitt, and A. K. Johnson, "Cardiovascular alterations and autonomic imbalance in an experimental model of depression," *American Journal of Physiology-Regulatory, Integrative and Comparative Physiology*, vol. 282, no. 5, pp. R1333–R1341, 2002.

[34] K. Y. Sarkisova and M. A. Kulikov, "Prophylactic actions of the antioxidant agent AEKOL on behavioral (psychoemotional) disturbances induced by chronic stress in rats," *Neuroscience and Behavioral Physiology*, vol. 31, no. 5, pp. 503–508, 2001.

[35] R. Adamec, M. Hebert, J. Blundell, and R. F. Mervis, "Dendritic morphology of amygdala and hippocampal neurons in more and less predator stress responsive rats and more and less spontaneously anxious handled controls," *Behavioural Brain Research*, vol. 226, no. 1, pp. 133–146, 2012.

[36] F. Dellu, W. Mayo, J. Cherkaoui, M. Le Moal, and H. Simon, "A two-trial memory task with automated recording: study in young and aged rats," *Brain Research*, vol. 588, no. 1, pp. 132–139, 1992.

[37] S. J. Fan, H. Jiang, L. J. Yang, X. Liu, J. Song, and F. Pan, "Effects of adrenergic agents on stress-induced brain microstructural and immunochemical changes in adult male Wistar rats," *Annals of Anatomy*, vol. 193, no. 5, pp. 418–424, 2011.

[38] L. J. Yang, X. Liu, D. X. Liu et al., "Effects of different adrenergic blockades on the stress resistance of Wistar rats," *Neuroscience Letters*, vol. 511, no. 2, pp. 95–100, 2012.

[39] M. Martinac, D. Babić, M. Bevanda et al., "Activity of the hypothalamic-pituitary-adrenal axis and inflammatory mediators in major depressive disorder with or without metabolic syndrome," *Psychiatria Danubina*, vol. 29, no. 1, pp. 39–50, 2017.

[40] K. Ma, H. Zhang, and Z. Baloch, "Pathogenetic and therapeutic applications of tumor necrosis factor-α (TNF-α) in major depressive disorder: a systematic review," *International Journal of Molecular Sciences*, vol. 17, no. 12, 2016.

[41] Y. Zhang, L. Liu, Y. L. Peng et al., "Involvement of inflammasome activation in lipopolysaccharide-induced mice depressive-like behaviors," *CNS Neuroscience & Therapeutics*, vol. 20, no. 2, pp. 119–124, 2014.

[42] M. C. Morris and U. Rao, "Cortisol response to psychosocial stress during a depressive episode and remission," *Stress*, vol. 17, no. 1, pp. 51–58, 2014.

[43] O. Guillemot-Legris and G. G. Muccioli, "Obesity-induced neuroinflammation: beyond the hypothalamus," *Trends in Neurosciences*, vol. 40, no. 4, pp. 237–253, 2017.

Hindawi
Neural Plasticity
Volume 2018, Article ID 3281040, 7 pages
https://doi.org/10.1155/2018/3281040

Research Article

Examination Stress Results in Attentional Bias and Altered Neural Reactivity in Test-Anxious Individuals

Xiaocong Zhang[1,2] **Yunying Dong**[3] **and Renlai Zhou**[1,4,5]

[1]*Research Center for Learning Science, Southeast University, Nanjing 210096, China*
[2]*School of Psychology, Nanjing University of Chinese Medicine, Nanjing 210023, China*
[3]*School of Education, Jiangsu University of Technology, Changzhou 213001, China*
[4]*Department of Psychology, School of Social and Behavioral Sciences, Nanjing University, Nanjing 210023, China*
[5]*National Key Laboratory of Cognitive Neuroscience and Learning, Beijing Normal University, Beijing 100875, China*

Correspondence should be addressed to Renlai Zhou; rlzhou@nju.edu.cn

Received 6 December 2017; Accepted 28 January 2018; Published 20 March 2018

Academic Editor: Jason H. Huang

Examination stress occurs so frequently in the lives of students. The neural mechanisms of attentional bias induced by examination stress in test-anxious individuals remain unclear. Accordingly, we investigated the attentional bias toward test-related threatening words in selected high and low test-anxious participants under the stress of final examinations by using an event-related potential (ERP) technique. A classic dot-probe paradigm was adopted with a test-related/test-unrelated threatening word and a neutral word pair as cues. Results showed attention bias and enhanced N200 amplitude toward test-related threat in high test-anxious individuals, whereas avoidance of test-related threat and decreased N200 amplitude were shown in low test-anxious individuals. Additionally, ERP data revealed the relatively enhanced LPP amplitude in low test-anxious participants compared with that in high test-anxious participants. No attentional bias toward test-unrelated threat was found. In conclusion, examination stress resulted in attentional bias and functional perturbations of a brain circuitry that reacted rapidly to test-related threat in high test-anxious individuals.

1. Introduction

Examinations occur so frequently and assume so much importance in the lives of students. College students report that examinations are the main sources of considerable stress [1]. Routine experiences of examination stress can lead to adverse psychological and physiological health [2, 3]. It has been estimated that about 15% to 20% of college students suffer from test anxiety [4]. Test anxiety is characterized by feelings of tension, worrisome thoughts, and the activation of the autonomic nervous system when an individual faces evaluative achievement-demanding situations [5]. Test anxiety can magnify stressful experiences about an examination situation. High test-anxious (HTA) individuals produce significantly higher physiological responses during examination settings than low test-anxious (LTA) individuals, and larger increases in physiological arousal are often associated with poorer exam or task performance [6].

The issue of how test-anxious individuals process threat (especially test-related threat) under examination stress is of particular interest because of the important implications of developing coping strategies and effective treatments for students [7, 8]. Previous studies showed that the attention system of anxious individuals might be abnormally sensitive to threat-related stimuli in the environment [9]. This attention pattern has been implicated in the etiology and maintenance of anxiety disorders [10]. As far as we know, only a few studies have investigated the attentional bias of test-anxious individuals. The existing studies suggested that test-anxious individuals show attentional bias toward test-related threatening information under examination stress [11–13]. However, these studies have not examined test-anxious individuals' attentional bias toward test-unrelated threatening stimuli. This issue has critical implications for providing the impetus for interventions through attentional bias modification

training. Recently, researchers have tried to use computerized attention-training tasks to modify attentional bias patterns of test-anxious participants and revealed significant reduction in anxiety vulnerability [7]. The attentional bias pattern needs to be systematically investigated before more effective interventions are carried out. If test-anxious individuals also show attentional bias toward test-unrelated threat, attention training should be carried out to help them modify the attentional bias pattern.

Furthermore, no research has investigated the neural mechanisms of attentional bias induced by examination stress in test-anxious subjects. The existing studies relying on reaction times (RTs) and attentional bias scores (ABS) are insufficient to identify the underlying neural correlates of attentional processing and their timing. In contrast to RTs and ABS, which reflect the combined effects of a sequence of many distinct neural processes, the ERP technique can obtain an online measure of attentional processing and show how the allocation of attention unfolds over the course of a trial [14]. The present research investigated neural mechanisms of attentional bias in test-anxious subjects, by using the ERP technique in conjunction with the traditional RT measure. ERP studies have revealed an initial shift of attention toward threat in trait-anxious individuals, as measured with the larger amplitudes for the P1 [15, 16] and/or N200 component [17], and sustained engagement with threat over time, as measured with the late positive potential (LPP) [18, 19]. Augmentation of the P1 component was found among high trait-anxious individuals, which was attributed to greater attention allocation to the threatening relative to neutral stimuli [15]. The N200 component has been well validated and was used to examine the allocation of attention to emotional stimuli [17, 20]. LPP was also used to investigate whether a threatening stimulus elicits sustained engagement. If attention was initially shifted to threatening stimuli (reflected by P1 or N200) but not maintained on them, threat-related modulation of the LPP would likely not to be observed.

The present study employed the classic dot-probe task to investigate the attentional bias of test-anxious individuals. Attentional bias was inferred from different RTs toward probes that replaced threatening stimuli (i.e., test-related and test-unrelated words) compared to probes that replaced neutral stimuli [21]. If a test-anxious individual's attention was abnormally sensitive to a threatening stimulus, RTs would be shorter for probes that replaced threatening stimuli compared to RTs for probes that replaced neutral stimuli. The research question is as follows: Do HTA individuals undergoing examination stress, compared with LTA individuals, show attentional bias and altered neural reactivity toward test-related threat rather than test-unrelated threat (test-unrelated threatening words)? Test-anxious individuals were sensitive to environmental stimuli that are relevant to their specific anxiety-related schemas [5]. That is, HTA participants' attention should be oriented toward the location and direction of test-related threats in examination settings [12]. Therefore, we expected to see stronger evidence of attentional bias toward test-related threat rather than toward test-unrelated threat in the HTA group. More specifically, this pattern of results would be typified in both behavioral and electrophysiological data. In the behavioral data, this prediction would be achieved if test-anxious individuals show faster RTs or positive attention bias scores for test-related threat. In the ERP data, this prediction would be supported by the finding of a larger amplitude for the P1 and/or N200 components in HTA relative to LTA individuals in response to cued test-related threatening words. In a word, we expected to further illuminate the association between examination stress, attentional bias, and brain activation by using the classic dot-probe task.

2. Materials and Methods

2.1. Participants. Forty-five volunteers were selected from a larger pool of undergraduate students who had completed the short form of the Test Anxiety Inventory [22] in Chinese (short form of the TAI-C) [23]. HTA participants ($N = 22$; mean age, 19.86 ± 1.28 years; 11 females) were defined as those scoring more than 13 ($M = 16.09$, SD = 1.87); LTA participants ($N = 23$; mean age, 19.67 ± 1.27 years; 9 females) were those scoring less than 8 ($M = 6.04$, SD = .88) in our study. These cut-off points represented approximately the upper and lower 16% of preliminary norms of the short form of the TAI-C (one standard deviation above and below the mean) [20]. The groups differed in TAI-C, $t(43) = 22.85$, $p < .001$. All participants signed the written informed consent and had self-reported normal or corrected-to-normal eyesight.

2.2. Stimuli and Task. Stimuli consisted of 72 test-related threatening words (TR) and 72 test-unrelated threatening words (TU), individually matched with 144 neutral words (*N*). Word pairs were presented one above the other in Song font size 21 and were 3 cm apart. Whether a threatening or neutral word was presented at the top was randomly chosen.

The words were drawn from the Test Anxiety Word System [24], which provides a standardized set of emotional stimuli with normative ratings of threat dimension, test-related dimension, and familiar dimension. In the threat dimension, the TR set and the TU set did not significantly differ between each other, but both differed from the *N* set significantly (TR = $5.13 \pm .37$, TU = $5.18 \pm .31$, $N = 2.65 \pm .16$; $F_{(2,285)} = 3290.07$, $p < .001$, $\eta^2_p = .96$). In the test-related dimension, the TU set and the *N* set did not significantly differ between each other, but both differed from the TR set significantly (TR = $5.54 \pm .34$, TU = $2.66 \pm .24$, $N = 2.64 \pm .15$; $F_{(2,285)} = 4160.76$, $p < .001$, $\eta^2_p = .97$). In the familiar dimension, the three sets did not significantly differ between each other (TR = $5.51 \pm .60$, TU = $5.55 \pm .57$, $N = 5.40 \pm .48$; $F_{(2,285)} = 2.19$, $p = .11$, $\eta^2_p = .02$).

In the dot-probe task (see Figure 1), each trial began with a central fixation cross, presented for 500/520/540/560 ms, followed by a word pair (i.e., cue) displayed for 200 ms. Immediately (300 ms) following the word pair, the probe stimulus (either left or right arrows) was randomly presented with equal regularity in the location of the centre of one of the words for 200 ms. Then, a blank screen was presented until a response was made or until 2000 ms had elapsed. Participants

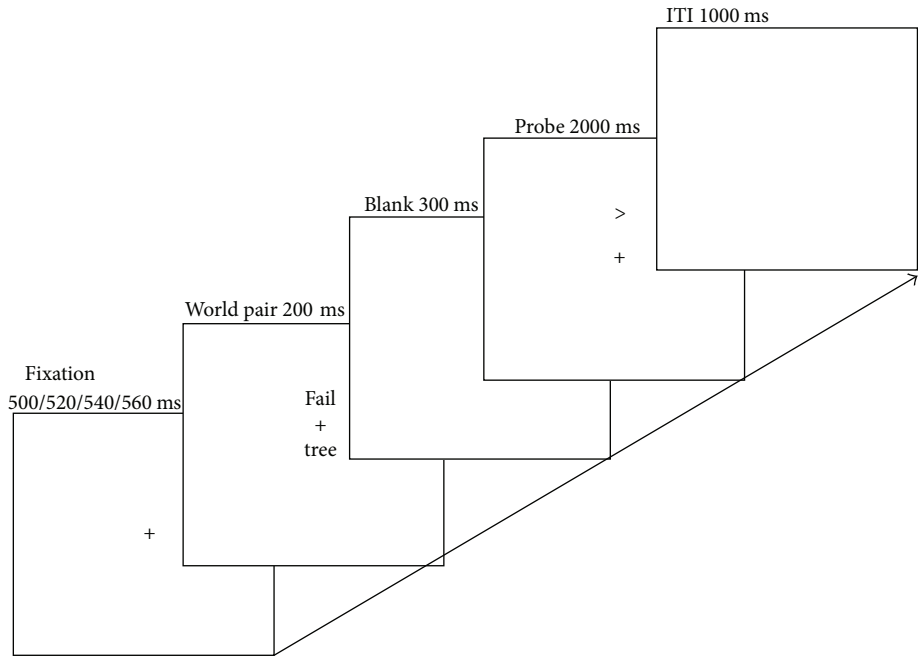

Figure 1: Example trial sequence in the dot-probe task.

had to determine the orientation of the probes by pressing one of two prespecified buttons. Participants were instructed to respond as quickly and accurately as possible. The intertrial interval was 1000 ms. The task was split into four experimental blocks; each of the blocks contained 72 trials. The practice block including 12 trials was shown prior to the experimental blocks. The trials were presented in a new random order for each participant.

2.3. EEG Recording and Artifact Scoring. Electroencephalograms were recorded using a 256-channel system (Electrical Geodesics (EGI), USA). All electrode impedances were kept below 40 kΩ. All channels were referenced to the Cz channel, and data were collected using a 0.1–100 Hz bandpass filter. Signals were collected at 500 samples per second and digitized with a 16-bit A/D converter.

Trials with incorrect responses were eliminated from analysis, as well as trials containing eye blinks or artifacts exceeding ±70 μV. Prior to data analyses, all ERP waveforms were low-pass filtered at 30 Hz, using a zero-phase shift digital filter [15]. Mean cue-evoked ERP amplitudes were epoched from −200 ms to 800 ms after the word pair onset, and probe-evoked ERP amplitudes were epoched from −200 ms to 500 ms after the probe onset [18].

2.4. Procedure. To investigate the neural reactivity induced by examination stress, participants carried out the procedures 1 week before their final examination. All participants were seated in a comfortable chair 80 cm from the computer screen in a sound-attenuated room. Instructions for the task were presented. Participants completed the practice block and the dot-probe task. Between blocks, several minutes of rest were taken appropriately. The EEG was recorded throughout the experiment. Finally, participants were thanked, paid, and debriefed after participation.

2.5. Data Analyses

2.5.1. Behavioral Reaction Times. Erroneous responses were excluded from statistical analyses. RTs shorter than 200 ms or longer than 1500 ms were removed. Furthermore, RTs deviating more than 3 SDs from the individual mean RTs were excluded. Statistical analyses were run on 98% of the data. RTs were subjected to a 2 (groups: HTA and LTA) × 2 (word types: TR and TU) × 2 (congruency: congruent and incongruent) mixed-design ANOVA. Congruent corresponds to the probes replacing threatening words, while incongruent corresponds to the probes replacing neutral words. All variables were within subjects except for group. If the higher-order interactions including congruency were significant, an attentional bias index would be calculated (see below).

For each of the types of threatening words (TR and TU), the bias score was calculated following MacLeod et al. [25]. Bias score $= 0.5 \times (\mathrm{RT}_{\mathrm{incongruent}} - \mathrm{RT}_{\mathrm{congruent}})$, where incongruent corresponds to the probes replacing neutral words and congruent corresponds to the probes replacing threat words. Positive values reflect attention toward the threatening words, and negative values reflect attention away from the threatening words. A value of zero implies no attentional bias. Bias scores were analyzed using a 2 (groups: HTA and LTA) × 2 (word types: TR and TU) mixed-design ANOVA with the between-subjects factor group and the within-subjects factor word type.

2.5.2. ERP Analysis. Based on previous reports in the literature [14, 15, 18, 26] and inspection of the grand mean ERPs,

Table 1: Mean reaction times (in ms) in the dot-probe task for HTA and LTA participants (standard deviations in parentheses).

	Test-related threatening word		Test-unrelated threatening word	
	Incongruent	Congruent	Incongruent	Congruent
HTA group ($n = 22$)	621.13 (231.43)	595.16 (208.05)	602.03 (214.92)	599.59 (215.09)
LTA group ($n = 23$)	488.77 (150.79)	509.32 (155.56)	500.59 (153.32)	500.96 (157.67)

Table 2: Bias scores in the dot-probe task for HTA and LTA participants.

	Test-related threatening word		Test-unrelated threatening word	
	Mean (SD)	t-test[a]	Mean (SD)	t-test[a]
HTA group ($n = 22$)	12.98 (19.02)	3.20*	1.22 (16.83)	.34
LTA group ($n = 23$)	−10.27 (12.70)	−3.88*	−.18 (13.59)	−.07

[a]Results from a one-sample t-test between bias scores and zero (*$p < .05$).

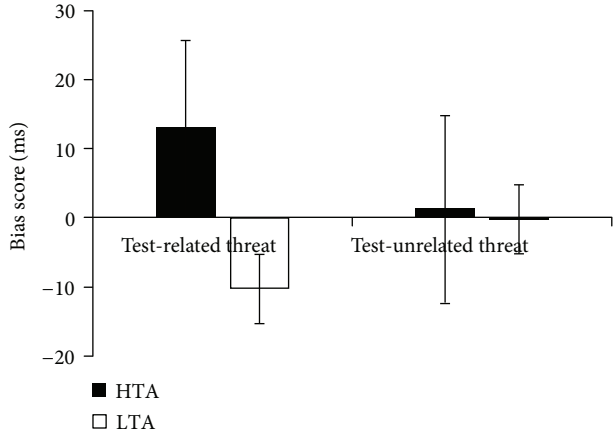

Figure 2: Bias scores to test-related (TR) and test-unrelated (TU) threat for HTA and LTA participants.

ERP analyses focused on the mean amplitudes of the P1 elicited by the word pairs (i.e., the cue) and the N200 and LPP evoked by the probe. Attention allocation was known to modulate P1 over occipital electrode sites. Thus, P1 was analyzed over occipital electrodes (O1 and O2) [15]. The N200 was analyzed at posterior electrode sites (P7 and P8), where N200 was typically maximal [14]. The LPP was analyzed at POz as it was typically maximal at posterior and parietal sites [18].

The P1 mean amplitude was computed between 120 and 140 ms after the presentation of word pairs and analyzed by repeated-measures analysis of variance (ANOVA), with group (HTA and LTA) as between-subjects factor and word type (TR and TU) and electrodes (O1 and O2) as within-subjects factors. The N200 peak amplitude was measured within the latency window of 180–200 ms and analyzed by repeated-measures analysis of variance (ANOVA), with group (HTA and LTA) as between-subjects factor and word type (TR and TU), congruency (congruent and incongruent), and electrodes (P7 and P8) as within-subjects factors. Finally, the LPP was scored as the mean activity between 300 and 500 ms at the electrode site POz and analyzed by repeated-measures analysis of variance (ANOVA), with group (HTA and LTA) as between-subjects factor and word type (TR and TU) and congruency (congruent and incongruent) as within-subjects factors. Planned comparisons were run to compare effects within the HTA and LTA groups. The Greenhouse-Geisser correction was used.

3. Results

3.1. Reaction Time Data. The $2 \times 2 \times 2$ ANOVA on RTs revealed a significant interaction of group × word type × congruency, $F_{(1,43)} = 8.656$, $p = .005$, $\eta^2_p = .168$. Table 1 shows the RTs for the three-way interaction effect.

The 2×2 ANOVA on bias scores revealed a significant main effect of group, $F_{(1,43)} = 18.799$, $p < .001$, $\eta^2_p = .304$ and a significant group × word type interaction, $F_{(1,43)} = 8.656$, $p = .005$, $\eta^2_p = .168$ (see Table 2). Follow-up tests revealed that HTA individuals had a larger bias score for TR words compared with the LTA individuals, $F_{(1,43)} = 23.469$, $p < .001$, $\eta^2_p = .353$. There was no significant difference between HTA and LTA individuals for the bias scores on TU words, $F_{(1,43)} = .095$, $p = .760$, $\eta^2_p = .002$. As predicted, a comparison against zero revealed that HTA individuals had a positive bias score, $t(21) = 3.20$, $p = .004$, and LTA individuals had a negative bias score, $t(22) = -3.88$, $p = .001$, both for TR words (see Figure 2).

3.2. Analyses of Cue-Evoked ERPs. No significant effects were found for the P1 component time-locked to cue onset.

3.3. Analyses of Probe-Evoked ERPs. For the peak amplitude of the N200 component, the interaction of group × word type × congruency × electrodes was significant, $F_{(1,43)} = 10.16$, $p = .003$, $\eta^2_p = .19$. Planned comparisons conducted on each group showed that for the HTA group, the amplitudes at the electrode site P7 in the incongruent TR-N condition ($M = -6.96$, SE = .72) are marginally more negative than those in the incongruent TU-N condition ($M = -6.19$, SE = .71), $p = .051$, while for the LTA group, the amplitudes at the electrode site P7 in the incongruent TR-N condition ($M = -6.63$, SE = .70) are significantly less negative than those in the incongruent TU-N condition ($M = -7.40$, SE = .69),

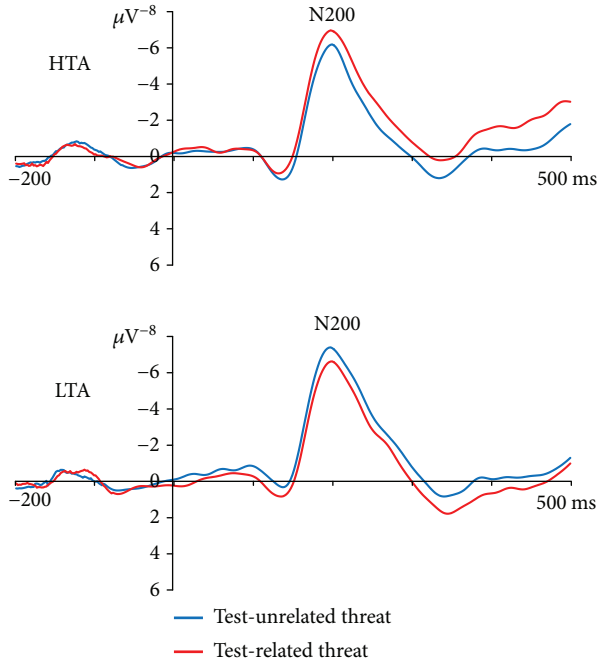

Figure 3: Grand-averaged ERPs evoked by probes in the incongruent test-unrelated (TU) condition and test-related (TR) condition at the P7 electrode site for HTA and LTA participants.

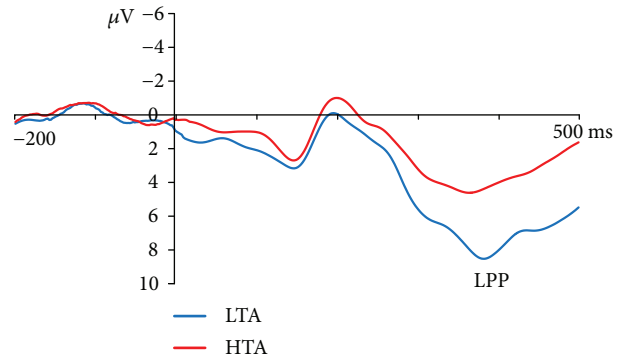

Figure 4: Grand-averaged late positive potential (LPP) evoked by probes at the POz electrode site for HTA (red) and LTA (blue) participants.

$p = .047$ (see Figure 3). None of the other comparisons resulted in significant differences in N200 amplitude between the word pairs' conditions.

Grand-averaged ERP waveforms time-locked to the onset of the probe at the electrode site POz are presented in Figure 4. There was a significant main effect of group on the LPP such that the LTA group ($M = 6.98$, SE = 1.10) elicited a larger LPP compared with the HTA group ($M = 3.57$, SE = 1.12), $F_{(1,43)} = 4.72$, $p = .04$, $\eta^2_p = .10$, and a significant word type × congruency interaction, $F_{(1,43)} = 4.15$, $p = .048$, $\eta^2_p = .09$. Follow-up analyses revealed that for the congruent condition, a significantly higher LPP amplitude was elicited by the TU-N word pairs ($M = 5.86$, SE = .82) relative to the TR-N word pairs ($M = 4.84$, SE = .80), $F_{(1,43)} = 5.51$, $p = .02$, $\eta^2_p = .11$. For incongruent condition, the LPP amplitude elicited by the TU-N word pairs ($M = 5.29$, SE = .86) did not, however, differ from that elicited by the TR-N word pairs ($M = 5.10$, SE = .85), $F_{(1,43)} = .18$, $p = .67$, $\eta^2_p = .004$. No other main or interaction effects emerged from this analysis, Fs < 2.29, ps > .08, η^2_ps < .06.

4. Discussion

The present study found that HTA participants undergoing the stress of academic examinations showed attentional bias toward TR with enhanced N200 amplitude, while LTA participants showed avoidance of them with decreased N200 amplitude. In addition, the electrophysiological data revealed no threat-related modulation of the LPP but relatively enhanced LPP amplitude in low test-anxious participants compared with that in high test-anxious participants.

The behavioral results of this study confirmed our predictions. In accord with the extant literature on attentional bias in test-anxious subjects [12, 13], this study provided evidence that test anxiety was characterized by an attentional bias toward test-related threatening stimuli under examination stress. Test anxiety predisposes HTA individuals to be susceptible to distraction and interference of test-related threat [5]. HTA individuals tend to consume a disproportionate amount of cognitive resources to scan the test environment for possible signs of test-related threat. This can help explain why HTA individuals are often associated with poorer exam or task performance under examination stress [27]. This study further clarified that test-anxious individuals did not show attentional bias toward test-unrelated threat. It confirmed the notion that test anxiety was a situation-specific form of trait anxiety and was characterized by intrusive anxiety-related behaviors and cognitions elicited by testing stimuli in academic or evaluative settings [5]. More effective interventions for test anxiety (e.g., attentional bias modification training [7]) should be carried out to help HTA individuals modify attentional bias patterns toward test-related threat.

In the present study, ERP results revealed that HTA individuals showed attentional bias toward TR with enhanced N200 amplitude and LTA individuals showed avoidance toward TR with decreased N200 amplitude. In previous studies of anxiety, N200 was used to examine the allocation of attention to emotional stimuli [14]. A larger N200 amplitude was associated with processing emotional than neutral stimuli in dot-probe task [17, 18]. The ERP results directly indicated that HTA individuals can quickly detect the threatening stimulus within about 200 ms after the emergence. We believed that N200 was likely to be consistent with the behavioral results, reflecting a significant initial shift of attention to test-related threat.

However, the electrophysiological data revealed no threat-related modulation of the LPP, which indicated that after initially shifting to threatening stimuli, HTA individuals did not show sustained attention to them [28]. This result was consistent with previous eye-tracking research which

suggested that HTA individuals were characterized by initially attending to test-related threat but avoiding such stimuli later on [13]. Some ERP researches also found no evidence of sustained engagement with the threat-related stimuli in high trait-anxious participants [14, 18]. It meant that in order to reduce increased internal distress, highly anxious subjects may try to counterbalance their initial attention to threat by quickly disengaging attention away from the threat [29].

The present study also found that compared with LTA individuals, HTA individuals elicited decreased LPP amplitude. LPP is susceptible to top-down processing influences, and its magnitude can be modulated by psychological resources [30]. This result indicated that HTA individuals may have less cognitive resources to complete the dot-probe task. The attentional control theory proposes that anxiety affects the efficiency of the inhibition function, which can prevent attention being directed to task-irrelevant stimuli (e.g., test-related threat) [31]. As a consequence, HTA individuals may consume too much cognitive resources for task-irrelevant stimuli.

The present study failed to find threat-related ERP differences in the P1 component locked to the cue-processing phase of the dot-probe task. Previous studies were inconsistent in their findings on such modulation. Augmentation of the P1 component was found among anxious individuals [15], while a reduction in this component was also shown in anxious individuals [26]. Hence, although the behavioral results in the present study indicated that HTA individuals were selectively biased toward test-related threat, this was not mirrored by selective modulation of the P1 component to the cue display. This null result might be due to no difference in the threat level between test-related and test-unrelated threatening words in the classic dot-probe used here. The current study did not provide a definitive answer regarding threat- and anxiety-related modulations in the P1 component, leaving this issue open for future researches.

A noteworthy limitation of the present study is that although a facilitated response to probes that appear at the location of a test-related threat is interpreted as vigilance for threat, results can also be interpreted as a difficulty to disengage from the threat [32]. These data suggest that it is time to modify the dot-probe task (e.g., adding N-N trials) and to index the components of attentional bias toward test-related threat.

5. Conclusion

In summary, the present study demonstrated that examination stress resulted in attentional bias and functional perturbations of a brain circuitry that reacted rapidly to test-related threat in high test-anxious individuals.

Abbreviations

ABS: Attentional bias scores
HTA: High test-anxious
LTA: Low test-anxious
LPP: Late positive potential
RTs: Reaction times
TR: Test-related threatening words
TU: Test-unrelated threatening words.

Ethical Approval

This study was approved by the ethics committee of Southeast University in agreement with the Declaration of Helsinki.

Conflicts of Interest

The authors declare that there is no conflict of interest regarding the publication of this article.

Acknowledgments

This study was funded by the Project of Philosophy and Social Science in Colleges and Universities in Jiangsu (2017SJB0306), the Key Project of Philosophy and Social Science Research in Colleges and Universities in Jiangsu (2015JDXM001), and the Jiangsu University of Technology Social Science Fund (KYY16519).

References

[1] K. M. Conley and B. J. Lehman, "Test anxiety and cardiovascular responses to daily academic stressors," *Stress and Health*, vol. 28, no. 1, pp. 41–50, 2012.

[2] L. B. Clutter, W. T. Potter, A. Alarbi, and J. F. Caruso, "Test anxiety and salivary cortisol levels in nursing students," *Nurse Educator*, vol. 42, no. 1, pp. 28–32, 2017.

[3] P. Loft, M. G. Thomas, K. J. Petrie, R. J. Booth, J. Miles, and K. Vedhara, "Examination stress results in altered cardiovascular responses to acute challenge and lower cortisol," *Psychoneuroendocrinology*, vol. 32, no. 4, pp. 367–375, 2007.

[4] T. Ergene, "Effective interventions on test anxiety reduction," *School Psychology International*, vol. 24, no. 3, pp. 313–328, 2003.

[5] C. D. Spielberger and P. R. Vagg, "Test anxiety: a transactional process model," in *Test Anxiety: Theory, Assessment and Treatment*, C. D. Speilberger and P. R. Vagg, Eds., pp. 3–14, Taylor & Frances, Bristol, UK, 1995.

[6] Q. Jiang, Y. Zhao, Q. Hou, H. Sui, H. Lv, and Z. Liu, "Test anxiety correlates with 24-hour ambulatory blood pressure and angiotensin II in high school students," *Journal of Hypertension*, vol. 35, no. 9, pp. 1908–1913, 2016.

[7] W. P. Cai, Y. Pan, H. Chai et al., "Attentional bias modification in reducing test anxiety vulnerability: a randomized controlled trial," *BMC Psychiatry*, vol. 18, no. 1, pp. 1–9, 2018.

[8] E. de Hullu, B. E. Sportel, M. H. Nauta, and P. J. de Jong, "Cognitive bias modification and CBT as early interventions for adolescent social and test anxiety: two-year follow-up of a randomized controlled trial," *Journal of Behavior Therapy and Experimental Psychiatry*, vol. 55, pp. 81–89, 2017.

[9] T. J. Barry, B. Vervliet, and D. Hermans, "An integrative review of attention biases and their contribution to treatment for anxiety disorders," *Frontiers in Psychology*, vol. 6, p. 968, 2015.

[10] J. M. Kuckertz and N. Amir, "Attention bias modification for anxiety and phobias: current status and future directions," *Current Psychiatry Reports*, vol. 17, no. 2, pp. 1–8, 2015.

[11] E. Keogh and C. C. French, "Test anxiety, evaluative stress, and susceptibility to distraction from threat," *European Journal of Personality*, vol. 15, no. 2, pp. 123–141, 2001.

[12] D. W. Putwain, H. C. Langdale, K. A. Woods, and L. J. Nicholson, "Developing and piloting a dot-probe measure of attentional bias for test anxiety," *Learning and Individual Differences*, vol. 21, no. 4, pp. 478–482, 2011.

[13] Y. Y. Dong, A. D. Beuckelaer, L. Yu, and R. L. Zhou, "Eye-movement evidence of the time-course of attentional bias for threatening pictures in test-anxious students," *Cognition and Emotion*, vol. 31, no. 4, pp. 781–790, 2016.

[14] E. S. Kappenman, J. L. Farrens, S. J. Luck, and G. H. Proudfit, "Behavioral and ERP measures of attentional bias to threat in the dot-probe task: poor reliability and lack of correlation with anxiety," *Frontiers in Psychology*, vol. 5, no. 1368, pp. 1–9, 2014.

[15] S. Eldar, R. Yankelevitch, D. Lamy, and Y. Bar-Haim, "Enhanced neural reactivity and selective attention to threat in anxiety," *Biological Psychology*, vol. 85, no. 2, pp. 252–257, 2010.

[16] M. Rossignol, S. Campanella, C. Bissot, and P. Philippot, "Fear of negative evaluation and attentional bias for facial expressions: an event-related study," *Brain and Cognition*, vol. 82, no. 3, pp. 344–352, 2013.

[17] S. M. Sass, W. Heller, J. E. Fisher et al., "Electrophysiological evidence of the time course of attentional bias in non-patients reporting symptoms of depression with and without co-occurring anxiety," *Frontiers in Psychology*, vol. 5, no. 7, p. 301, 2014.

[18] E. S. Kappenman, A. MacNamara, and G. H. Proudfit, "Electrocortical evidence for rapid allocation of attention to threat in the dot-probe task," *Scan*, vol. 10, no. 4, pp. 577–583, 2015.

[19] H. T. Schupp, A. Ohman, M. Junghofer, A. I. Weike, J. Stockburger, and A. O. Hamm, "The facilitated processing of threatening faces: an ERP analysis," *Emotion*, vol. 4, no. 2, pp. 189–200, 2004.

[20] A. Holmes, K. Mogg, J. Fockert, M. Nielsen, and B. Bradley, "Electrophysiological evidence for greater attention to threat when cognitive control resources are depleted," *Cognitive, Affective and Behavioral Neuroscience*, vol. 14, no. 2, pp. 827–835, 2014.

[21] R.v. Rooijen, A. Ploeger, and M. Kret, "The dot-probe task to measure emotional attention: a suitable measure in comparative studies?," *Psychonomic Bulletin & Review*, vol. 24, no. 6, pp. 1686–1717, 2017.

[22] J. Taylor and F. P. Deane, "Development of a short form of the Test Anxiety Inventory (TAI)," *The Journal of General Psychology*, vol. 129, no. 2, pp. 127–136, 2002.

[23] Y. Y. Dong, R. L. Zhou, X. Gao, F. Jiao, and W. Guo, "Reliability and validity of the Chinese version of Test Anxiety Inventory (TAI) Short Form in college students," *Chinese Mental Health Journal*, vol. 25, no. 11, pp. 872–876, 2011.

[24] X. Gao and R. L. Zhou, "On the inhibition of selective attention by people with test anxiety," *Chinese Journal of Special Education*, vol. 20, no. 151, pp. 85–91, 2013.

[25] C. MacLeod, A. Mathews, and P. Tata, "Attentional bias in emotional disorders," *Journal of Abnormal Psychology*, vol. 95, no. 1, pp. 15–20, 1986.

[26] E. M. Mueller, S. G. Hofmann, D. L. Santesso, A. E. Meuret, S. Bitran, and D. A. Pizzagalli, "Electrophysiological evidence of attentional biases in social anxiety disorder," *Psychological Medicine*, vol. 39, no. 07, pp. 1141–1152, 2009.

[27] Z. Shi, X. Gao, and R. L. Zhou, "Emotional working memory capacity in test anxiety," *Learning and Individual Differences*, vol. 32, no. 3, pp. 178–183, 2014.

[28] J. K. Olofsson, S. Nordin, H. Sequeira, and J. Polich, "Affective picture processing: an integrative review of ERP findings," *Biological Psychology*, vol. 77, no. 3, pp. 247–265, 2008.

[29] M. G. Calvo and P. Avero, "Time course of attentional bias to emotional scenes in anxiety: gaze direction and duration," *Cognition and Emotion*, vol. 19, no. 3, pp. 433–451, 2005.

[30] M. I. Núñez-Peña and M. Suárez-Pellicion, "Processing of multi-digit additions in high math-anxious individuals: psychophysiological evidence," *Frontiers in Psychology*, vol. 6, no. 1268, pp. 1–11, 2015.

[31] M. W. Eysenck and N. Derakshan, "New perspectives in attentional control theory," *Personality and Individual Differences*, vol. 50, no. 7, pp. 955–960, 2011.

[32] E. H. W. Koster, G. Crombez, B. Verschuere, and J. De Houwer, "Selective attention to threat in the dot probe paradigm: differentiating vigilance and difficulty to disengage," *Behaviour Research and Therapy*, vol. 42, no. 10, pp. 1183–1192, 2004.

Hindawi
Neural Plasticity
Volume 2018, Article ID 9360203, 11 pages
https://doi.org/10.1155/2018/9360203

Research Article

Recovery of Chronic Stress-Triggered Changes of Hippocampal Glutamatergic Transmission

Min Lin,[1] Gonglin Hou,[1] Ying Zhao,[1] and Ti-Fei Yuan[2,3]

[1]*Department of Psychology, Zhejiang Sci-Tech University, Hangzhou, Zhejiang, China*
[2]*Shanghai Key Laboratory of Psychotic Disorders, Shanghai Mental Health Center, Shanghai Jiao Tong University School of Medicine, Shanghai, China*
[3]*Co-innovation Center of Neuroregeneration, Nantong University, Nantong, Jiangsu, China*

Correspondence should be addressed to Gonglin Hou; 13505818948@163.com and Ti-Fei Yuan; ytf0707@126.com

Received 3 August 2017; Revised 6 November 2017; Accepted 28 November 2017; Published 30 January 2018

Academic Editor: Fang Pan

Chronic stress results in neurochemical, physiological, immune, molecular, cellular, and structural changes in the brain and often dampens the cognition. The hippocampus has been one major focus in studying the stress responsivity and neural mechanisms underlying depression. Both acute and chronic stress stimuli lead to dynamic changes in excitatory transmission in the hippocampus. The present study examined the potential effects of spontaneous recovery after chronic stress on spatial memory function and glutamatergic transmission in the hippocampus. The results showed that chronic unpredicted mild stress transiently increased AMPA receptor GluA2/3 subunit expression, together with elevated PICK-1 protein expression. Spontaneous recovery restored the behavioral deficits in Barnes maze test, as well as the glutamate receptor expression changes. In conclusion, spontaneous recovery acts as an important mechanism in system homeostasis.

1. Introduction

Chronic stress results in neurochemical, physiological, immune, molecular, cellular, and structural changes in the brain and often dampens the cognition [1–4]. The hippocampus is believed to be responsible for the decreased learning and memory abilities following chronic stress. It has been found that chronic stress decreases adult hippocampal neurogenesis, blocks LTP induction, downregulates expression of neurotrophic factors, and exacerbates neuronal apoptosis in the hippocampus [5–7]. In addition, chronic stress alters glia homeostasis [8–10], such as triggering microglial cell proliferation and activation, suppresses astrocyte proliferation, and decreases the expression of GFAP protein and excitatory amino acid transporters (EAATs) in astrocytes, which might contribute to the altered excitatory transmission (e.g., glutamatergic) of hippocampal neurons following chronic stress. Limited evidences revealed that suppressed hippocampal neurogenesis is recovered following removal of stress [11].

The hippocampus has been one major focus in studying the stress responsivity and neural mechanisms underlying depression. The excitatory transmission in the hippocampus is mainly mediated by glutamatergic synapses, with two types of inotropic glutamate receptors: AMPA receptor and NMDA receptor, respectively. AMPA receptors are composed of GluA1–4 subunits, which bind to scaffolding proteins postsynaptically to be functional on the membrane. PICK-1 and PSD-95 interact with the glutamatergic receptors, regulating their membrane distribution and functions [12–14].

Acute stress potentiates the AMPA receptor transmission in the hippocampus, inducing insertion of GluA2-lacking AMPA receptors in the CA1 region (reflected by increased AMPA/NMDA ratio and lack of change in NMDA-mEPSCs) [15, 16], while chronic stress might impair or have no effect on AMPA transmission in the hippocampus [17, 18]. In the present study, we examined the potential effects of spontaneous recovery after chronic stress on spatial memory function and glutamatergic transmission in the hippocampus. The

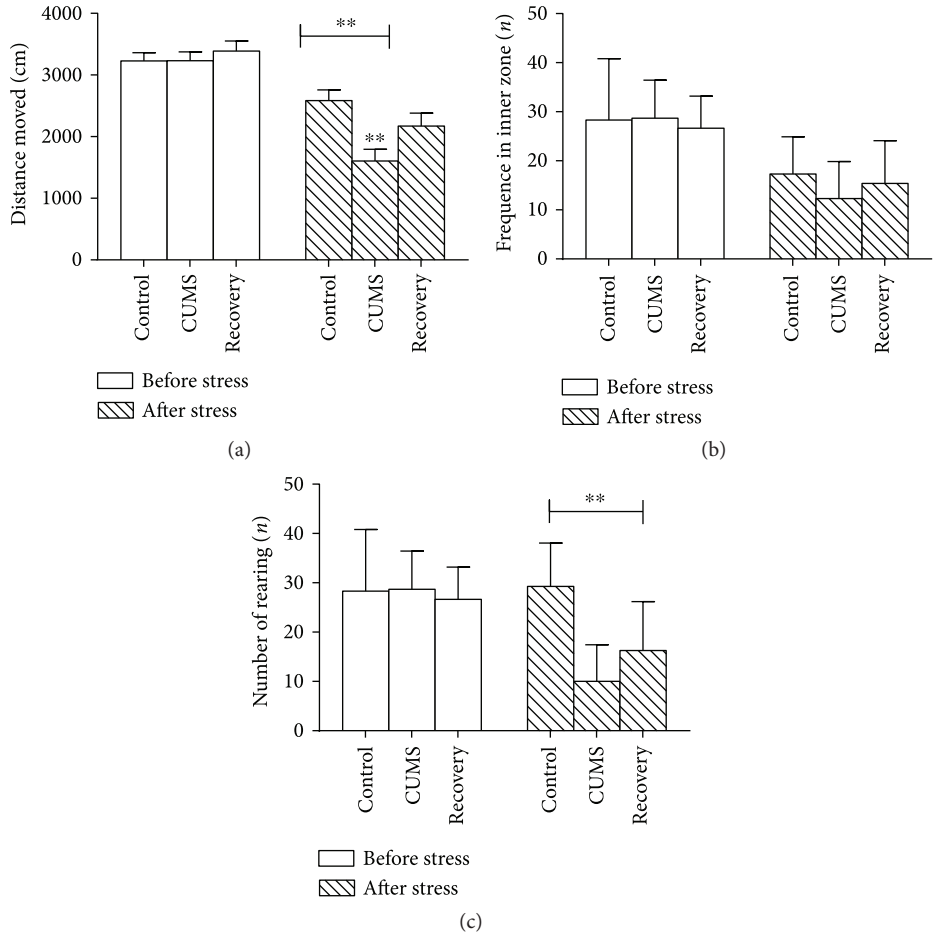

Figure 1: Open field test results. (a) The animals in the CUMS group exhibited decreased movement after stress, which was restored in the recovery group. (b) There was no significant difference among the three groups in frequencies crossing the inner zone. (c) The animals in the CUMS group exhibited decreased vertical rearing exploration after stress, which was restored in the recovery group. $^{**}P < 0.01$.

results suggested that spontaneous recovery might act as an important endogenous mechanism in self-repair.

2. Materials and Methods

2.1. Ethics. The study has been approved by Ethics Committee of Animal Experiments in Zhejiang Sci-Tech University, and all procedures followed the guidelines to animal experiments in Zhejiang Sci-Tech University.

2.2. Animals. 36 male Sprague-Dawley rats were purchased from Animal Experiment Center, Chinese academy of Sciences, and raised under temperature $22 \pm 2^{\circ}$C, humidity 50–60%, 12/12 hours L/D cycle, and free access to food/water. All animals were subjected for a 10-day adaptation period before being randomly assigned into control group, model (chronic stress) group, or recovery (recovery from chronic stress) group (12 in each group). The control group animals were housed as 3 rats per cage, while the CUMS rats were housed alone and subjected to chronic unpredictable mild stress (CUMS) of 35 days. For the recovery group, the animals received CUMS and then left for recovery of another 35 days.

Table 1: The results of open field test (M ± SD).

	Locomotion (cm)	Central cross times	Rearing times
Control ($n = 12$)	2585.1 ± 173.0	17 ± 8	29.3 ± 8.8
CUMS ($n = 10$)	1605.5 ± 189.5**	12 ± 8	10.0 ± 7.4**
Recovery ($n = 8$)	2171.2 ± 211.8	15 ± 9	16.3 ± 9.9
F	7.297	1.115	14.065
P value	0.003	0.343	0.000

$^{**}P < 0.01$.

2.3. Procedures for CUMS. CUMS procedures included as follows: food deprivation (24 hours), water deprivation (24 hours), tail pinch (1 minute), food shock (1.0 mA for 10 seconds, 30 times with interval of 1 minute), ice water swimming (4°C, 5 minutes), wet bedding (24 hours), and reversed light/dark cycle. The seven types of stress were randomly presented to animals with each per day [6].

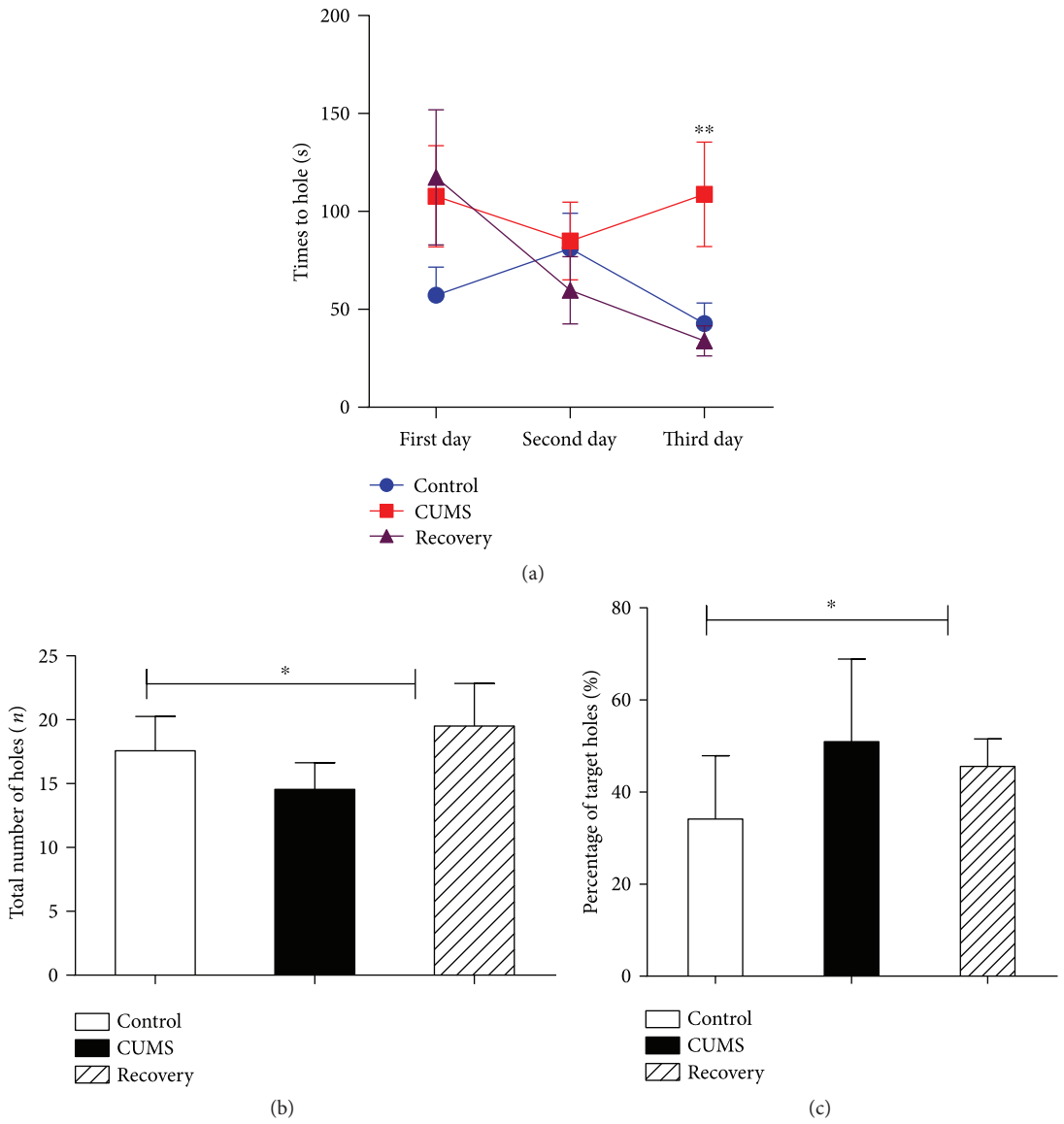

Figure 2: Barnes maze test results. (a) The animals in the CUMS group exhibited decreased learning ability in Barnes maze test, which was restored in the recovery group. (b) In the test phase, the animals in the CUMS group exhibited decreased exploration ability (reflected by total number of holes explored). (c) In the test phase, the CUMS group animals exhibited deficits in short-term working memory (reflected by repeated exploration of the target hole). $*$ suggests for $P < 0.05$ and $**$ for $P < 0.01$.

2.4. Open Field Test. Open filed is 80 cm × 80 cm × 40 cm (length, width, and height), and the central field was set as 40 cm × 40 cm in Noldus software (Noldus Co., Netherlands). The animal was let freely in the open field for 5 minutes.

2.5. Barnes Maze Test. Barnes maze was built as previously described [19]. The maze is composed of a 122 cm diameter plate with 18 holes (diameter 10 cm) under bright light. One dark box was under the plate, and the animal can hide into the box through one of the hole on the plate. For each test, the plate was turned while the dark box was in fixed position. The animal was trained once per day for three continuous days. In the test phase, the animal was placed in the central of the plate with random head direction and the behavior trace was recorded.

2.6. Corticosterone Measurement. 1 ml cardiac blood was sampled in the morning and centrifuged at 3000 r/min under 4 degrees Celsius for serum isolation. The supernatant was kept at −80 degrees before measuring with Corticosterone ELISA kit (Abcam). The procedure was performed following the kit brochure, and the corticosterone concentration was calculated from the standard curve.

2.7. Western Blot. The acutely dissociated hippocampus tissue was weighted and homogenized for protein extraction. The primary antibody was mice-anti-Rat GluA1/2/3/PICK-1/PSD-95 (Millipore, 1 : 100). The blot was finally revealed with ECL system and imaged in Tanon-2500 system.

2.8. Immunohistochemistry. The animals were sacrificed, and brains were harvested for paraffin embedding, sectioning,

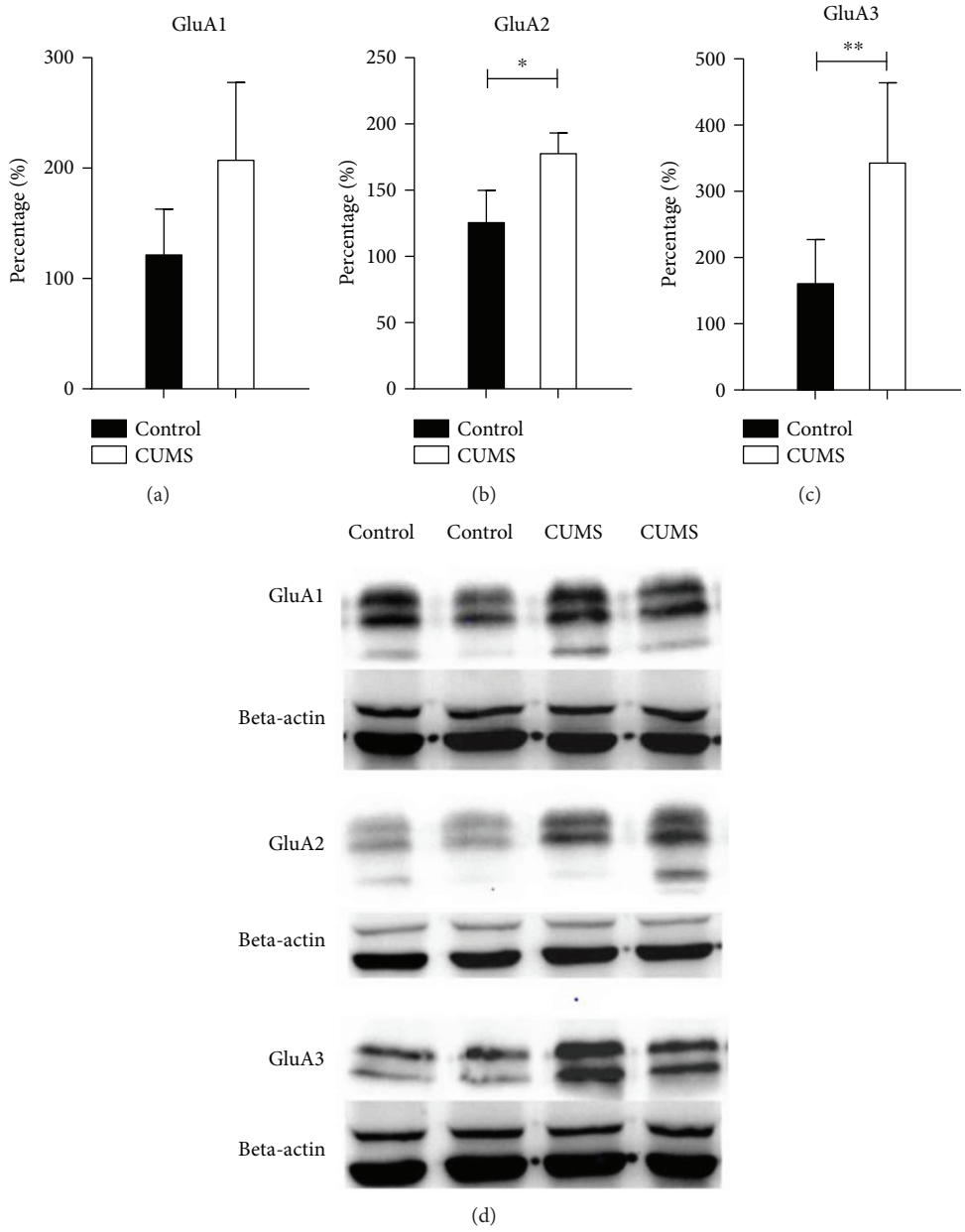

Figure 3: Western blot results of GluA1–3 subunit expression in the whole hippocampus. There was no clear increase of GluA1 subunit, while the expression levels of GluA2/3 subunits were significantly upregulated. $*$ suggests for $P < 0.05$ and $**$ for $P < 0.01$.

and immunostaining (or HE staining). Briefly, the sections were firstly incubated with primary antibody mice-anti-Rat GluA1/2/3/PICK-1/PSD-95 (Millipore, 1 : 400) overnight at 4 degrees, then secondary antibody goat-anti-mice IgG conjugated for Envision kit (1 : 400, Boshide, Wuhan, China). The images were taken under a Zeiss fluorescence microscope and analyzed by Image-Pro plus software (Media Cybernetics, USA). For stereological analyses, six sections of the hippocampus were chosen from each side (Bregma −3.3, −3.6, −3.9, −4.2, −4.5, and −4.8 mm). The boundary of the hippocampus was defined as previously described [20].

2.9. Statistics. The data were presented as mean ± SD and analyzed with SPSS 13.0 software (Chicago, USA). The differences between two groups were compared by independent sample t-test and ANOVA for the three groups. $P < 0.05$ was considered as statistically significant.

3. Results

3.1. Serum Corticosterone Response and Behavior Changes. Chronic stress induced significant elevation in serum corticosterone concentration of the CUMS group (101.4 ± 20.3 ng/ml), compared to the control group (67.7 ± 15.4 ng/ml) ($F_{(2,19)} = 12.233$, $P < 0.01$). In the recovery group, the corticosterone concentration (59.6 ± 11.2 ng/ml) went back to control level.

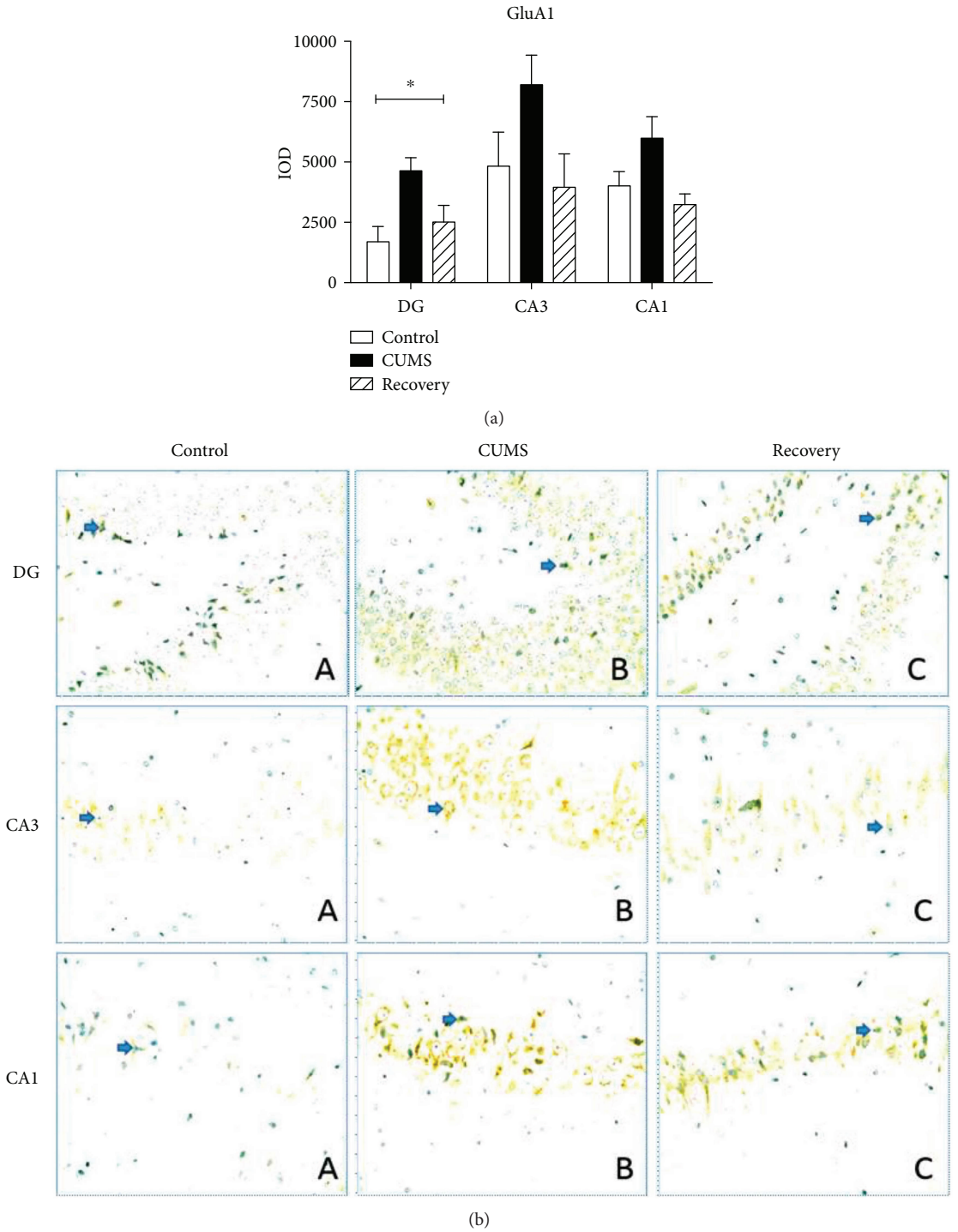

Figure 4: Immunohistochemistry results showing the expression of GluA1 in the subregion of the hippocampus. $^{*}P < 0.05$.

In the open field test, the CUMS group animals exhibited decreased locomotion in the maze, as well as decreased vertical rearing (Figures 1(a) and 1(c)), but not the frequencies of central crosses (Figure 1(b)). In addition, the recovery group animals rehabilitated and demonstrated restored behavior responses (Table 1).

In the Barnes maze test, the CUMS group showed decreased ability of learning in the first 3 days (Figure 2(a)): one-way ANOVA revealed significant effect ($F_{(2,27)} = 7.277$, $P < 0.01$). In the test phase, the CUMS group explored fewer holes than the control group and spent more time in the target hole area (Figure 2(b), one-way ANOVA ($F_{(2,27)} = 8.125$, $P < 0.01$); Figure 2(c), one-way ANOVA ($F_{(2,27)} = 3.490$, $P < 0.05$)), suggesting for impaired short-term memory and spatial learning ability. On the other hand, the recovery group exhibited control level performance in the test.

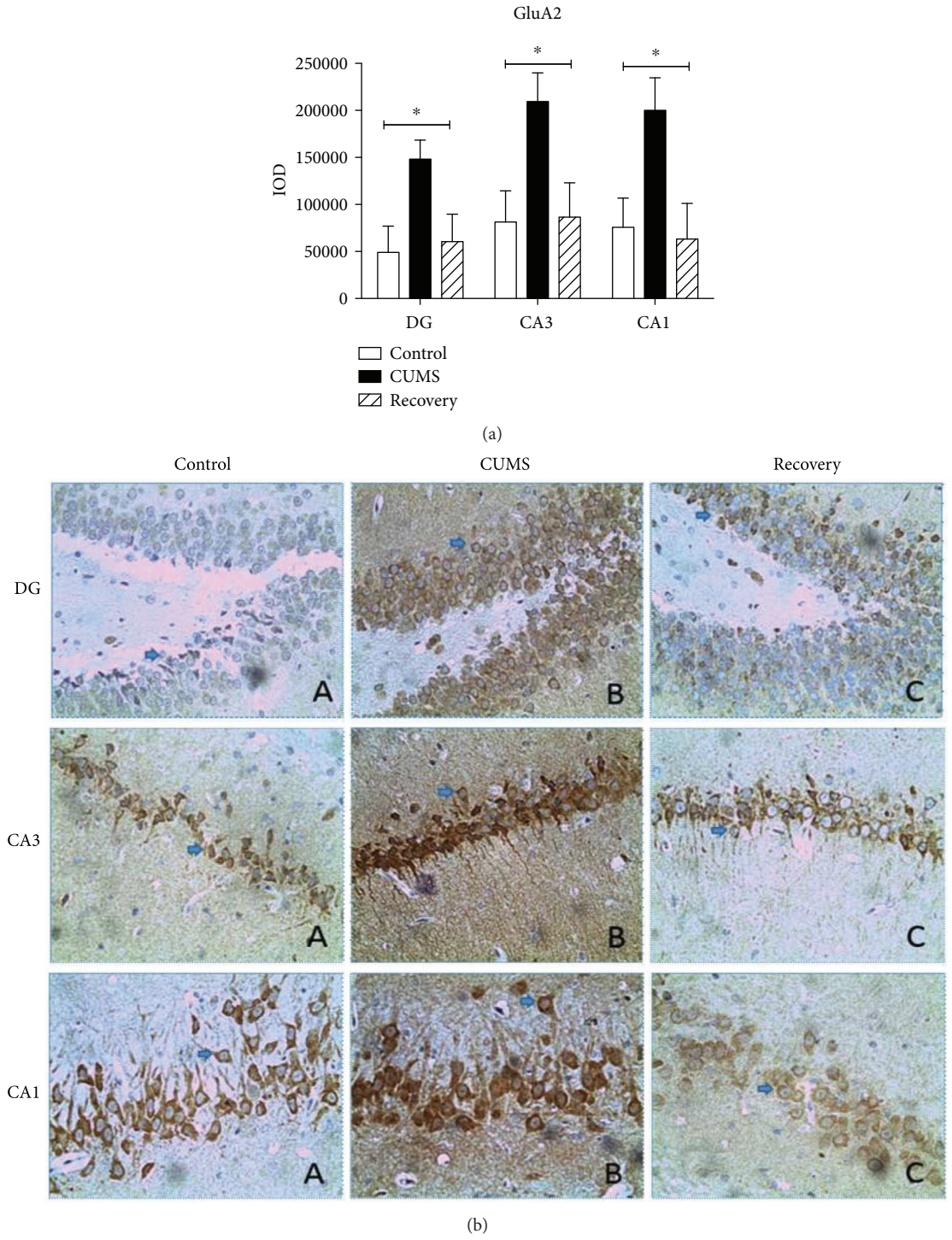

Figure 5: Immunohistochemistry results showing the expression of GluA2 in the subregion of the hippocampus. $^{*}P < 0.05$.

3.2. Expression Changes of AMPA Receptor Subunits. AMPA receptors are important components in excitatory transmission. We therefore examined the changes of AMPA receptors subunits GluA1–3 in the hippocampus following chronic stress. With Western blot of full hippocampus tissue, we found that in the CUMS group, the expression levels of GluA2 (independent sample t-test, $t = 6.893$, $P < 0.05$, $n = 8$) and GluA3 (independent sample t-test, $t = 12.966$, $P < 0.01$, $n = 8$) subunits were significantly elevated, but not the GluA1 subunit (independent sample t-test, $t = 4.381$, $P = 0.08$, $n = 8$) (Figure 3).

We further compared the expression changes of GluA1–3 subunits in the subregion of the hippocampus (DG, CA3, and CA1) with immunohistochemistry and semiquantitative

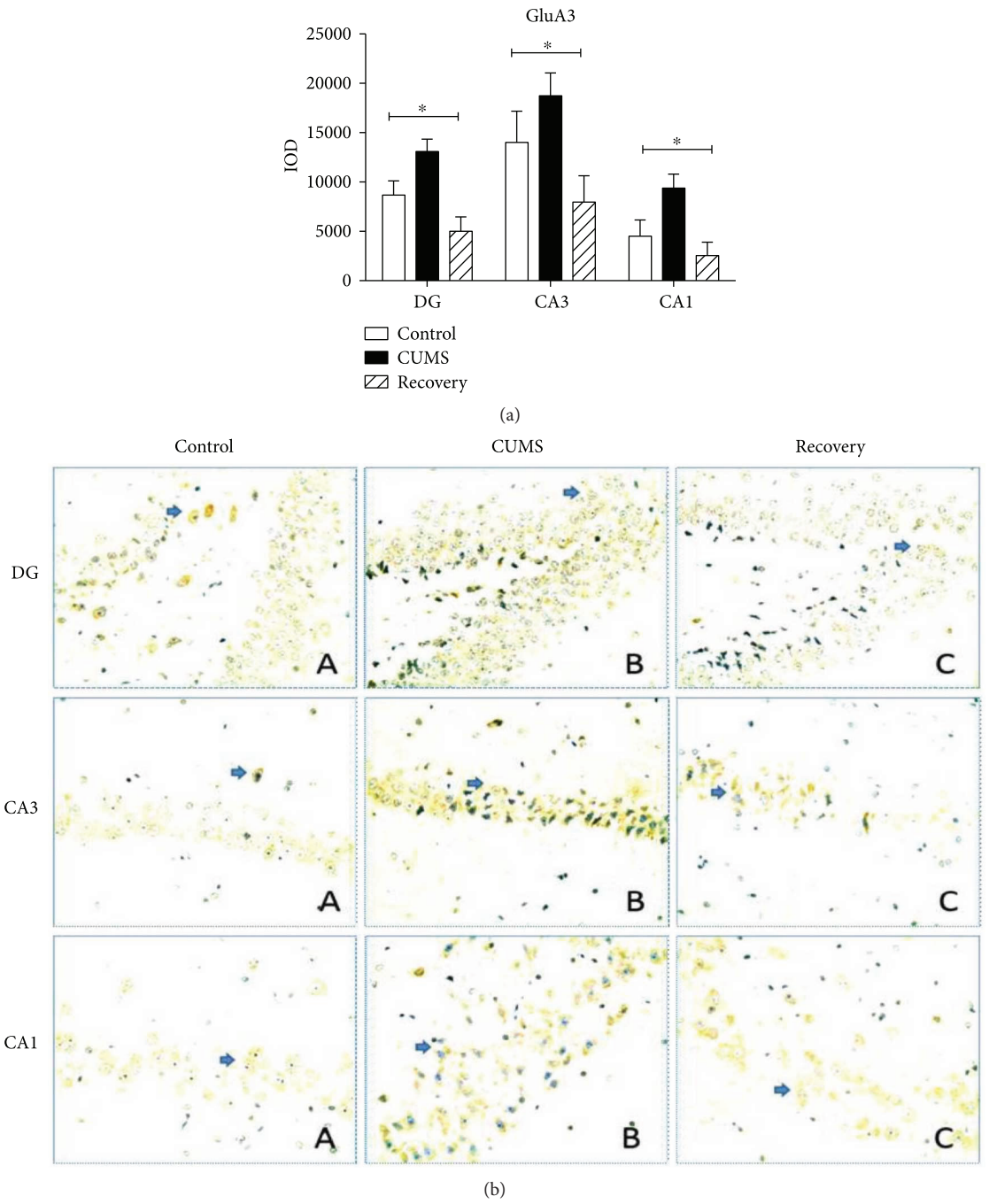

Figure 6: Immunohistochemistry results showing the expression of GluA3 in the subregion of the hippocampus. $^{*}P < 0.05$.

measurement by optic density. For GluA1 subunit, we found that the expression in the DG region is upregulated in the CUMS group when compared to the control (one-way ANOVA, $F_{(2,25)} = 3.491$, post hoc test, $P < 0.05$), but not in the CA3 ($F_{(2,25)} = 2.991$, $P = 0.063$) and CA1 regions ($F_{(2,25)} = 1.861$, $P = 0.17$). In addition, the recovery group showed restored level of GluA1 expression (Figure 4).

For GluA2 subunits, in the DG, CA3, and CA1 regions, we all found the upregulated expression in the CUMS group, compared to the control group (post hoc test, $P < 0.05$) and the recovery group (post hoc test, $P < 0.05$) (Figure 5). Compared by one-way ANOVA, CUMS increased GluA2 expression in DG ($F_{(2,31)} = 3.729$, $P < 0.05$), CA3 ($F_{(2,31)} = 4.658$, $P < 0.05$), and CA1 ($F_{(2,31)} = 4.406$, $P < 0.05$). Meanwhile for GluA3 subunits, compared to the control group, one-way ANOVA reveals a significant effect of CUMS in the DG/CA1 regions (in the DG region, $F_{(2,23)} = 9.102$, $P < 0.01$, post hoc test, $P < 0.01$; in the CA1 region, $F_{(2,23)} = 5.364$, $P < 0.01$, post hoc test, $P < 0.01$) and in the CA3 region ($F_{(2,23)} = 4.629$, $P < 0.05$, post hoc

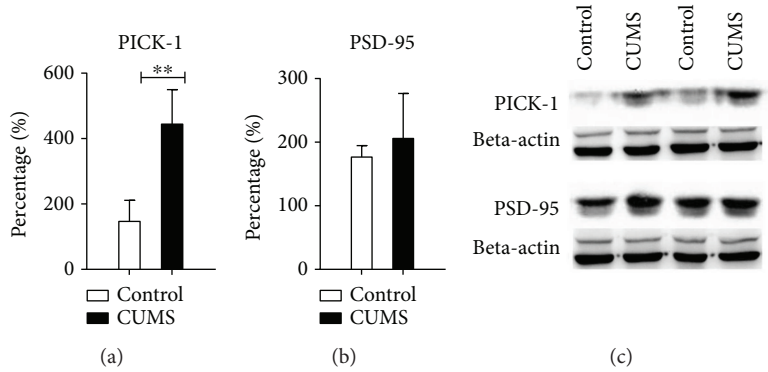

Figure 7: Western blot results of PICK-1 and PSD-95 expression in the whole hippocampus. There was no clear change for PSD-95 expression, while the expression level of PICK-1 was significantly upregulated. $^{**}P < 0.01$.

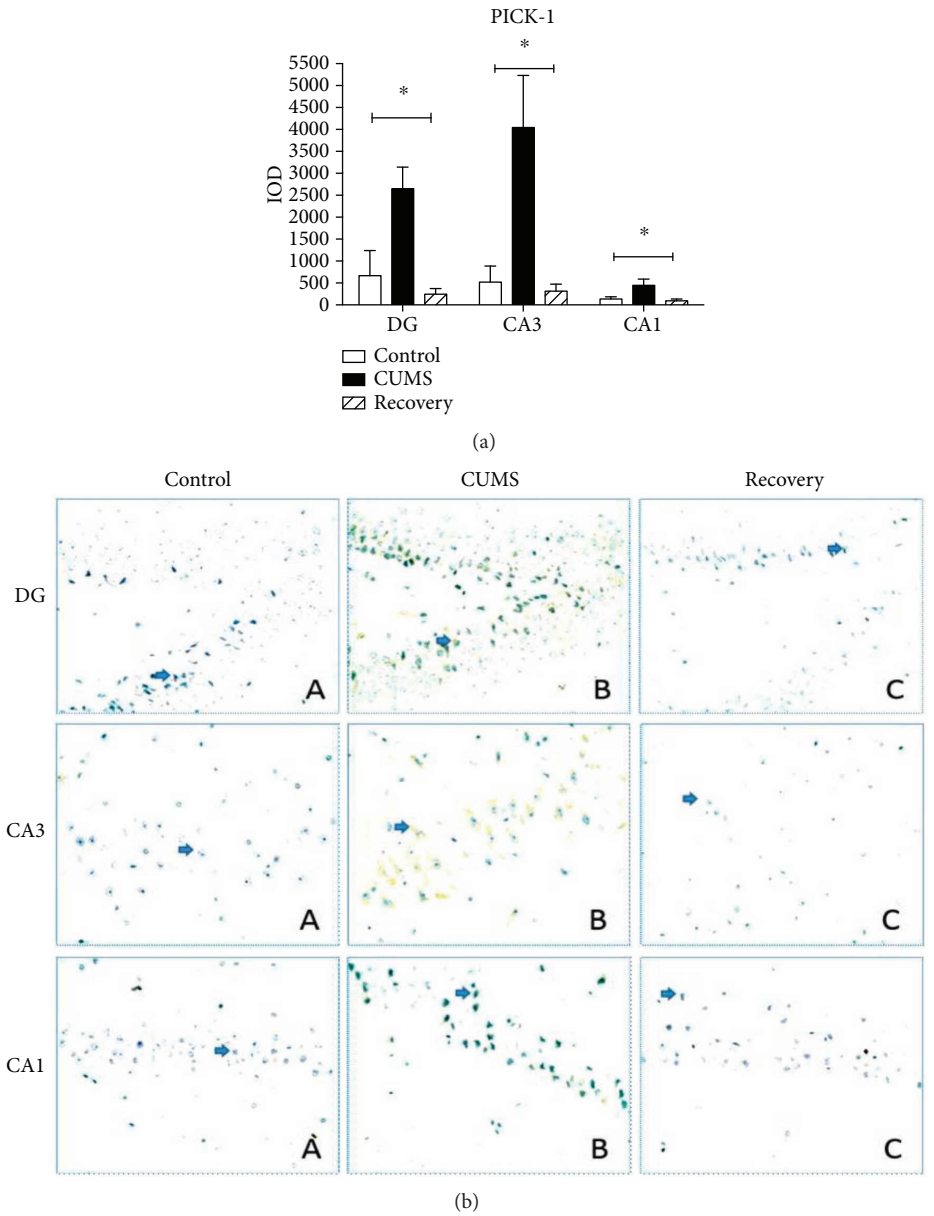

Figure 8: Immunohistochemistry results showing the expression of PICK-1 in the subregion of the hippocampus. $^{*}P < 0.05$.

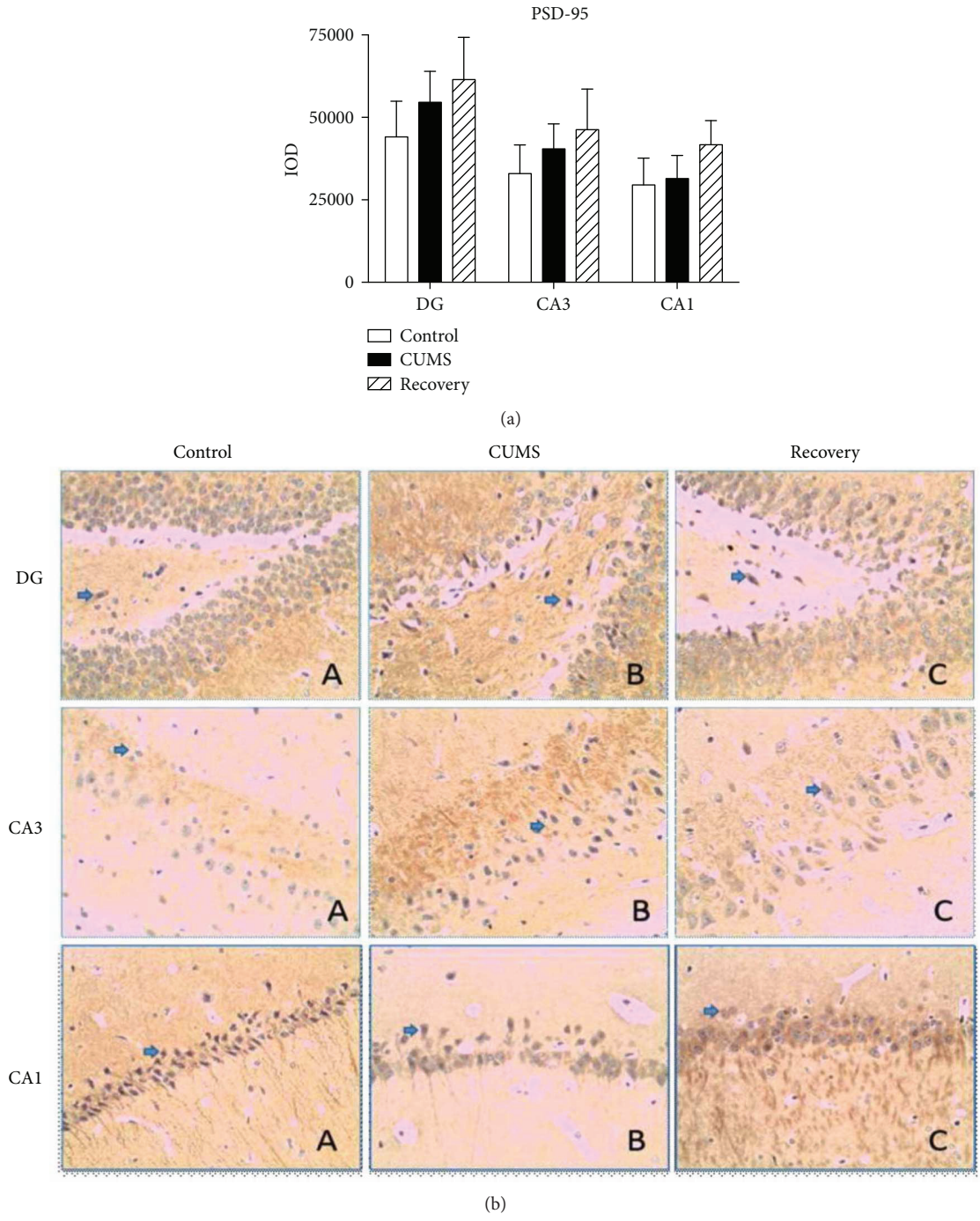

Figure 9: Immunohistochemistry results showing the expression of PSD-95 in the subregion of the hippocampus.

test, $P < 0.05$). In addition, compared with the CUMS group, the recovery group exhibited restored level of GluA3 expression in the DG and CA1 regions (post hoc test, $P < 0.01$) (Figure 6).

3.3. Expression Changes of AMPA Receptor-Associated Proteins. In order to explore the potential molecular mechanism underlying AMPA receptor subunit changes, we then examined the postsynaptic scaffolding proteins that bind to AMPA receptor, such as PICK-1 and PSD-95. With Western blot of full hippocampus tissue, we found that in the CUMS group, the expression level of PICK-1 (independent sample t-test, $t = 23.260$, $P < 0.01$, $n = 8$) protein was significantly elevated compared to the control group, but not the PSD-95 protein (independent sample t-test, $P = 0.34$) (Figure 7).

We further compared the expression changes of PICK-1 and PSD-95 in the subregion of the hippocampus (DG, CA3, and CA1) with immunohistochemistry and semiquantitative measurement by optic density. For PICK-1, one-way ANOVA analysis in the DG and CA1, respectively, yielded

$F_{(2,37)} = 6.013$ ($P < 0.01$) and $F_{(2,37)} = 17.219$ ($P < 0.01$), while in the CA3 region, it yielded $F_{(2,37)} = 4.805$ ($P < 0.05$) all exhibiting a significant different expression among the three groups. There was an upregulated expression of PICK-1 in the CUMS group compared to the control group (post hoc test, in DG/CA3, $P < 0.05$, and in CA1, $P < 0.01$) and the recovery group (post hoc test, in the DG/CA1, $P < 0.01$, and in CA3, $P < 0.05$) (Figure 8). On the other hand, in line with the Western blot result, there was no significant change of PSD-95 expression across all groups (Figure 9).

4. Discussion

Disrupted glutamatergic transmission is reported in both animal models of depression and postmortem brain from depression patients [21]. We here showed that, together with the restored brain function after a recovery period after chronic stress, the glutamatergic transmission is also recovered. The hippocampus has been one major focus in studying the stress responsivity and neural mechanisms underlying depression. Acute stress potentiates the AMPA receptor transmission in the hippocampus, inducing insertion of GluA2-lacking AMPA receptors in the CA1 region (reflected by increased AMPA/NMDA ratio and lack of change in NMDA-mEPSCs) [15, 16], while chronic stress might impair or have no effect on AMPA transmission in the hippocampus [17, 18, 22]. In present study, we reported that the expression of AMPAR subunits were increased following chronic stress, which decreased to baseline following a period of recovery, in line with the behavioral restoration.

In our results, we detected significant elevation of GluA2/3 expression in the hippocampus, but not GluA1. This suggested for insertion or synthesis of GluA2-containing AMPA receptors, which might act in replacement of GluA2-lacking AMPA receptors that are recruited in acute stress phases. However, one limitation of the study is that we did not discriminate synaptic and somatic AMPA receptors and if these receptors are involved in synaptic transmission. It should also be noted that the receptor changes could be pathway-specific in CA1 [17], which requires electrophysiological investigations (such as measuring the synaptic strength in projection-specific manner) in the future.

PICK-1 is important in AMPA receptor trafficking during long-term synaptic plasticity [12, 13]. In fact, PICK-1 interacts with GluA2 subunit directly and is involved in the incorporation of GluA2-containing AMPA receptors as the replacement of GluA2-lacking AMPA receptors [23]. The expression level of PICK-1 was tightly linked to the expression of GluA2 subunit [24], as well as the strength of AMPA receptor transmission [14]. The present study reported the elevation of PICK-1 protein in the CUMS group, which is consistent with the previous data on AMPA receptor subunits. In addition, the results indicate that the upregulated AMPA receptors are functional, since they interact with PICK-1 at postsynaptic site. On the other hand, we did not detect clear changes in PSD-95 proteins. It is possible that they are in much higher quantity compared to AMPA receptor, and therefore the AMPA receptor trafficking did not affect their expression significantly.

In conclusion, recovery of chronic stress is able to restore the glutamatergic transmission in the hippocampus, as well as the impaired cognitive behaviors. In the future study, it is yet to confirm investigate the functional aspects of AMPA receptor expression changes, such as with electrophysiological approaches.

Conflicts of Interest

The authors declare no conflicts of financial interest.

Authors' Contributions

Min Lin, Gonglin Hou, and Ti-Fei Yuan designed the study. Min Lin and Ying Zhao performed the study and analyzed the data. All authors wrote the paper together and approved the final version of the manuscript.

Acknowledgments

This work was supported by Science Philosophy Betterment Society (Registered British Virgin Islands). Ti-Fei Yuan received supports from the National Natural Science Foundation of China (31771215, 81501164, and 81611130224) and Young Elite Scientists Sponsorship Program by CAST (YESS).

References

[1] C. D. Conrad, "A critical review of chronic stress effects on spatial learning and memory," *Progress in Neuro-Psychopharmacology and Biological Psychiatry*, vol. 34, no. 5, pp. 742–755, 2010.

[2] G. Hou, W. Xiong, M. Wang, X. Chen, and T. F. Yuan, "Chronic stress influences sexual motivation and causes damage to testicular cells in male rats," *The Journal of Sexual Medicine*, vol. 11, no. 3, pp. 653–663, 2014.

[3] R. Tian, G. Hou, L. Song, J. Zhang, and T. F. Yuan, "Chronic grouped social restriction triggers long-lasting immune system adaptations," *Oncotarget*, vol. 8, no. 20, pp. 33652–33657, 2017.

[4] E. S. Wohleb, T. Franklin, M. Iwata, and R. S. Duman, "Integrating neuroimmune systems in the neurobiology of depression," *Nature Reviews Neuroscience*, vol. 17, no. 8, pp. 497–511, 2016.

[5] R. S. Duman and G. K. Aghajanian, "Synaptic dysfunction in depression: potential therapeutic targets," *Science*, vol. 338, no. 6103, pp. 68–72, 2012.

[6] G. Hou, Y. Zhao, X. Yang, and T. F. Yuan, "Autophagy does not lead to the asymmetrical hippocampal injury in chronic stress," *Physiology & Behavior*, vol. 144, pp. 1–6, 2015.

[7] P. J. Lucassen, V. M. Heine, M. B. Muller et al., "Stress, depression and hippocampal apoptosis," *CNS & Neurological Disorders Drug Targets*, vol. 5, no. 5, pp. 531–546, 2006.

[8] C. Nasca, B. Bigio, D. Zelli et al., "Role of the astroglial glutamate exchanger xCT in ventral hippocampus in resilience to stress," *Neuron*, vol. 96, pp. 402–413.e5, 2017.

[9] M. A. Woodbury-Farina, "The importance of glia in dealing with stress," *The Psychiatric Clinics of North America*, vol. 37, no. 4, pp. 679–705, 2014.

[10] T. F. Yuan, G. Hou, Y. Zhao, and O. Arias-Carrion, "Commentary: the effects of psychological stress on microglial cells in the brain," *CNS & Neurological Disorders Drug Targets*, vol. 14, no. 3, pp. 304–308, 2015.

[11] V. M. Heine, J. Zareno, S. Maslam, M. Joels, and P. J. Lucassen, "Chronic stress in the adult dentate gyrus reduces cell proliferation near the vasculature and VEGF and Flk-1 protein expression," *The European Journal of Neuroscience*, vol. 21, no. 5, pp. 1304–1314, 2005.

[12] J. G. Hanley, "Molecular mechanisms for regulation of AMPAR trafficking by PICK1," *Biochemical Society Transactions*, vol. 34, no. 5, pp. 931–935, 2006.

[13] W. Lu and E. B. Ziff, "PICK1 interacts with ABP/GRIP to regulate AMPA receptor trafficking," *Neuron*, vol. 47, no. 3, pp. 407–421, 2005.

[14] A. Terashima, L. Cotton, K. K. Dev et al., "Regulation of synaptic strength and AMPA receptor subunit composition by PICK1," *The Journal of Neuroscience*, vol. 24, no. 23, pp. 5381–5390, 2004.

[15] H. Karst and M. Joels, "Corticosterone slowly enhances miniature excitatory postsynaptic current amplitude in mice CA1 hippocampal cells," *Journal of Neurophysiology*, vol. 94, no. 5, pp. 3479–3486, 2005.

[16] E. Y. Yuen, W. Liu, I. N. Karatsoreos et al., "Mechanisms for acute stress-induced enhancement of glutamatergic transmission and working memory," *Molecular Psychiatry*, vol. 16, no. 2, pp. 156–170, 2011.

[17] A. J. Kallarackal, M. D. Kvarta, E. Cammarata et al., "Chronic stress induces a selective decrease in AMPA receptor-mediated synaptic excitation at hippocampal temporoammonic-CA1 synapses," *The Journal of Neuroscience*, vol. 33, no. 40, pp. 15669–15674, 2013.

[18] H. Karst and M. Joels, "Effect of chronic stress on synaptic currents in rat hippocampal dentate gyrus neurons," *Journal of Neurophysiology*, vol. 89, no. 1, pp. 625–633, 2003.

[19] C. A. Barnes, "Memory deficits associated with senescence: a neurophysiological and behavioral study in the rat," *Journal of Comparative and Physiological Psychology*, vol. 93, no. 1, pp. 74–104, 1979.

[20] L. J. Kjonigsen, T. B. Leergaard, M. P. Witter, and J. G. Bjaalie, "Digital atlas of anatomical subdivisions and boundaries of the rat hippocampal region," *Frontiers in Neuroinformatics*, vol. 5, p. 2, 2011.

[21] T. F. Yuan and G. Hou, "The effects of stress on glutamatergic transmission in the brain," *Molecular Neurobiology*, vol. 51, no. 3, pp. 1139–1143, 2015.

[22] T. F. Yuan, A. Li, X. Sun et al., "Transgenerational inheritance of paternal neurobehavioral phenotypes: stress, addiction, ageing and metabolism," *Molecular Neurobiology*, vol. 53, no. 9, pp. 6367–6376, 2016.

[23] N. Jaafari, J. M. Henley, and J. G. Hanley, "PICK1 mediates transient synaptic expression of GluA2-lacking AMPA receptors during glycine-induced AMPA receptor trafficking," *The Journal of Neuroscience*, vol. 32, no. 34, pp. 11618–11630, 2012.

[24] D. F. Yu, P. F. Wu, H. Fu et al., "Aging-related alterations in the expression and distribution of GluR2 and PICK1 in the rat hippocampus," *Neuroscience Letters*, vol. 497, no. 1, pp. 42–45, 2011.

Hindawi
Neural Plasticity
Volume 2017, Article ID 1230713, 18 pages
https://doi.org/10.1155/2017/1230713

Review Article

Relationship between Insulin Levels and Nonpsychotic Dementia: A Systematic Review and Meta-Analysis

Qiu-xia Pan, Xiao-juan Li, Yue-yun Liu, Fang-fang Wang, Ya-jing Hou, Qing-lai Bian, Wen-qi Qiu, Zhi-yi Yan, You-ming Jiang, and Jia-xu Chen

School of Basic Medical Science, Beijing University of Chinese Medicine, No. 11 North Third Ring Road, Chaoyang, Beijing 100029, China

Correspondence should be addressed to Jia-xu Chen; chenjiaxu@hotmail.com

Received 20 August 2017; Accepted 16 October 2017; Published 27 December 2017

Academic Editor: Fushun Wang

Objectives. To explore the relationship between insulin levels and nonpsychotic dementia. *Methods*. Six electronic databases (PubMed, Cochrane, SCI, CNKI, VIP, and Wanfang) were searched from January 1, 2007, to March 1, 2017. Experimental or observational studies that enrolled people with nonpsychotic dementia or abnormal insulin levels in which insulin levels or MMSE scores (events in nonpsychotic dementia) were the outcome measures. Random-effects models were chosen for this meta-analysis. Sample size, mean, s.d., and events were primarily used to generate effect sizes (with the PRIMA registration number CRD42017069860). *Results*. 50 articles met the final inclusion criteria. Insulin levels in cerebrospinal fluid were lower (Hedges' $g = 1.196$, 95% CI = 0.238 to 2.514, and $P = 0.014$), while the levels in peripheral blood were higher in nonpsychotic dementia patients (Hedges' $g = 0.853$ and 95% CI = 0.579 to 1.127), and MMSE scores were significantly lower in the high insulin group than in the healthy control group (Hedges' $g = 0.334$, 95% CI = 0.249 to 0.419, and $P = 0.000$). *Conclusions*. Our comprehensive results indicate that blood insulin levels may increase in patients with nonpsychotic dementia.

1. Introduction

Dementia is a general term for a decline in mental ability severe enough to interfere with daily life, and it is a common clinical syndrome that is not only a leading cause of death globally but also a burden on families and society. There is no one test to determine if someone has dementia. Doctors diagnose Alzheimer's and other types of dementia based on a careful medical history, a physical examination, laboratory tests, and the characteristic changes in thinking, day-to-day function, and behavior associated with each type. At present, all of the Mini-Mental State Examination (MMSE), Hasegawa's dementia scale, clinical dementia rating, cognitive abilities screening instrument, Alzheimer's disease assessment scale-cognitive section, activity of living, Functional Activities Questionnaire, and clock-drawing test can be used in the diagnosis of dementia, among which, the MMSE is widely used.

As it is harder to determine the exact type of dementia because the symptoms and brain changes of different dementias can overlap, and in some cases, a doctor may diagnose "dementia" and not specify a type. In these cases, we divided the dementia into two aspects (psychotic dementia and nonpsychotic dementia) according to the day-to-day functions, behaviors, and medical history of the patients. Psychotic dementia is caused by mental illness, which means that dementia is caused by depression, schizophrenia, and other mental disorders, while nonpsychotic dementia excludes the dementia caused by mental illness (psychotic dementia) [1], for example, Alzheimer's disease (AD), vascular dementia (VD), and brain lesions. In addition, mild cognitive impairment (MCI) is a "clinical" diagnosis representing a doctor's best professional judgment about the reason for a person's symptoms. MCI causes a slight but noticeable and measurable decline in cognitive abilities, including memory and thinking skills. A person with MCI is at an increased risk

of developing Alzheimer's or another dementia. Medical history, assessment of independent function and daily activities, input from a family member or trusted friend, assessment of mental status, in-office neurological examination, evaluation of mood, and laboratory tests were the primary diagnostic route.

Many risk factors are associated with nonpsychotic dementia. These include older age, gender (i.e., female), a low educational level, a low socioeconomic level, certain physical diseases, and a family genetic history. Recently, abnormal insulin levels were shown to be an important factor that influences the occurrence of nonpsychotic dementia. Umegaki et al. [2] performed a prospective study in which cognitive function scores were assessed at baseline and after 3 years in the same patient group. The results suggested that higher insulin and glycol-hemoglobin levels were associated with diabetes-related cognitive dysfunction.

Insulin is an active substance with a variety of biological functions that affect growth and apoptosis in neurons by participating in blood glucose metabolism [3–8]. The discovery of insulin in the brain suggested that insulin not only participates in metabolism and growth but is also involved in higher cognitive functions, such as learning and memory [3–5]. Insulin has been shown to increase the expression of amyloid precursor protein (APP), beta-amyloid 42 (Aβ42), and hyperphosphorylated tau in the hippocampus and frontal cortex in rats [6, 9]. Thus, there may be mechanistic and sequential associations among insulin, impaired cognitive function, and structural AD-like changes.

In humans, aging is associated with decreased metabolic turnover, decreased glucose utilization, and decreased insulin levels because of effects on the regulation of the insulin signaling pathway. Some authors have argued that abnormal insulin metabolism is caused by aging and does not share a causal relationship with nonpsychotic dementia. For example, Burns et al. [8] assessed the relationship between insulin resistance and conditions including cognitive decline and brain atrophy for two years in patients with early AD and nondemented controls. The authors found that insulin was differentially associated with cognitive decline and atrophy in AD and elderly patients. Furthermore, higher levels of peripheral insulin may exert AD-specific benefits, and insulin signaling may be affected by AD-associated systemic physiological changes. Finally, Dorrance et al. [10] supported the notion that insulin resistance exerts positive effects on cerebral vasculature dementia.

Furthermore, exogenous insulin interventions or treatments have been shown to alleviate nonpsychotic dementia symptoms in patients with insulin resistance and improve their Mini-Mental State Examination (MMSE) scores [11, 12]. However, other studies have demonstrated that insulin levels are negatively correlated with nonpsychotic dementia [13]. In addition, some studies have found no relationship between the occurrence of nonpsychotic dementia and insulin levels when patients were compared with healthy control subjects (HCs) [14, 15]. Therefore, both negative and positive correlations have been observed, resulting in controversy regarding whether high insulin levels or low insulin levels cause nonpsychotic dementia. Thus, a meta-analysis of this subject is warranted.

The present meta-analysis was aimed at determining whether nonpsychotic dementia is associated with altered levels of insulin in the blood or cerebrospinal fluid (CSF). We used meta-analytical techniques because they allow data from individual studies to be quantitatively combined to improve the strength of preclinical and clinical evidence.

2. Materials and Methods

The meta-analyses performed in this study adhered to the guidelines recommended by the Preferred Reporting Items for Systematic Reviews and Meta-Analysis (PRISMA) statement [16] and are registered with the international prospective register of systematic reviews (PROSPERO). Its PRISMA registration number is CRD42017069860.

2.1. Literature Search. Two investigators (Qiu-xia Pan and Xiao-juan Li) independently performed a systematic review of English language publications using the PubMed, SCI, and Cochrane Library databases and Chinese language publications using the CNKI, VIP, and Wanfang databases.

The following search terms were used in the database search: (Dementia or Alzheimer's disease/AD or Mild cognitive impairment/MCI) and (Insulin or insulin signaling pathway). The search was performed to obtain articles published from January 1, 2007, to March 1, 2017. The initial search generated 1287 records, including 474 English and 813 Chinese records. After we screened the titles and abstracts, 263 appropriate articles, including 120 English and 143 Chinese papers, that were related to the present subject were selected for full-text scrutiny. Original studies that reported data on peripheral blood and CSF insulin concentrations in at least two groups of subjects (i.e., dementia or AD and MCI) were included.

2.2. Quality Assessment. Studies were appraised for methodological quality using the Newcastle-Ottawa Scale (NOS). The NOS defines the study quality of observational studies (i.e., case-control studies and cross-sectional studies) using an 8-item scale (scored 0–9 points). Two investigators (Qiu-xia Pan and Xiao-juan Li) independently assessed the quality of each paper, and any disagreements were resolved by consensus in a group meeting.

2.3. Study Selection. After further evaluating the 135 originally selected articles, 50 high-quality (i.e., had 5–9 points on the NOS, Table 1) [17] articles describing observational studies were included in this study. The remaining 85 articles were excluded for the following reasons: there were no necessary data on insulin concentrations [13, 18–27]; related genes and insulin signaling pathway proteins were the main study outcomes [28–36]; there was no clear description or record of a cognitive function evaluation [37–42]; the design of the experiments was unreasonable for the purpose of this study [43–52]; the experimental methods were incomplete [53–60]; the papers did not provide completely related data [61–66]; data from only one group were reported [2, 67–74]; the papers reported data from the same cohort of

Table 1: Quality assessment of the included studies according to the Newcastle-Ottawa Scale (NOS)*.

Study names	S1	S2	S3	S4	C1a	C1b	E1a	E1b	E2	E3	Total points
Si-ling Liu, 2011	1	1	1	1	0	1	1	0	0	0	6
Qin-yun Li, 2015	1	1	1	1	0	1	1	0	1	0	7
Zong-yuan Wang, 2008	1	1	1	1	0	1	1	0	1	0	7
Abimbola A. Akintola, 2015	0	1	1	0	0	1	1	0	1	0	5
Angela J. Hanson, 2016	1	1	0	0	1	0	1	0	1	0	5
J.K. Morris, 2016	1	1	0	0	0	1	1	0	1	0	5
G. Stennis Watson, 2009	1	1	1	1	0	1	1	0	1	0	7
Robert Krikorian, 2012	1	1	0	0	0	1	1	0	1	0	5
E. Rönnemaa, B. Zethelius, and J. Sundelöf, 2009	1	1	0	1	1	0	0	1	1	0	6
Galit Weinstein, 2015	0	1	1	1	0	1	1	0	1	0	6
Jeffrey M. Burns, 2012	0	1	1	1	0	1	1	0	1	0	6
Auriel A. Willette, 2015	0	1	1	1	0	1	1	0	1	0	6
Amber S. Watts, 2013	1	1	1	1	1	1	1	0	1	1	9
Josh D. Woolley, 2014	1	1	0	0	1	0	1	0	1	1	6
Xiao-hong Sun, 2010	1	1	0	1	1	0	1	0	1	0	6
Lu Zhang, 2011	1	1	0	1	1	0	1	0	1	0	6
Wei-gang Liu, 2009	1	1	0	0	1	0	1	0	1	0	5
Gui-qing Chen, 2015	1	1	0	1	1	0	1	0	1	1	7
Zhi-juan Wang, 2014a	1	1	0	1	1	0	1	0	1	0	6
Jun-shi Zhang, 2016	1	0	0	1	1	1	1	0	1	1	7
Jin-geng Li, 2013	1	1	0	1	1	1	1	0	1	1	8
Zhi-dong Yang, 2007	1	0	1	1	0	1	1	0	1	0	6
Hong-mei Yue, 2014	1	1	0	1	1	1	1	0	1	0	7
Liang-mi Li, 2015	1	1	1	1	1	1	1	0	1	0	8
Qing-chun Xia, 2015	1	1	0	1	1	1	1	1	1	0	8
Ran Song, 2015	1	1	0	1	1	1	1	0	1	1	8
Yu-mei Yang, 2009	1	0	0	1	1	1	1	0	1	0	6
Xiao-lan Liu, 2008	1	1	0	1	1	1	1	0	1	1	8
Rong-wei Zhang, 2008	1	1	0	0	1	0	1	0	1	0	5
Bin-bin Zang, 2011	1	1	0	1	1	1	1	0	1	0	7
Zhi-juan Wang, 2014b	1	1	1	1	1	0	1	0	1	0	7
Hong-shan Pan, 2016	1	1	0	1	1	0	1	0	1	0	6
Nan Mu, 2010	1	1	1	1	1	0	1	0	1	0	7
Yan-Wu, 2008	1	1	0	1	1	0	1	0	1	0	6
Hong-li Li, 2013	1	1	0	1	1	0	1	0	1	0	6
Jill K. Morris, 2014	1	0	0	0	1	1	1	0	1	1	6
Wen-qing Xia, 2016	1	1	1	1	1	0	1	0	1	0	7
Chin-Chou Huang, 2014	1	1	1	1	0	1	1	0	1	0	7
Rosebud O. Roberts, 2014	1	1	1	0	0	1	1	0	1	0	6
Mkaya Mwamburi, 2016*	1	1	0	1	0	0	1	1	1	0	6
Heather Kenna, 2013	1	1	1	1	1	0	1	0	1	0	7
Yen-Chun Fan, 2017	1	1	1	1	0	1	1	0	1	0	7
Laura D. Baker, 2011	0	1	1	1	0	1	1	0	1	0	6
M.S. Beeri, 2008	0	1	1	1	0	1	1	0	1	0	6
Hannah Bruehl, 2009	1	1	1	1	1	1	1	1	1	0	9
Xiao-bing Zhou, 2012	0	1	0	1	1	0	1	0	1	0	5
Qiong-yu Zhang, 2012	1	1	0	0	1	1	1	0	1	0	6

Table 1: Continued.

Study names	S1	S2	S3	S4	C1a	C1b	E1a	E1b	E2	E3	Total points
Xiao-hong, Zhao, 2009	1	1	0	1	1	1	1	0	1	0	7
Jun-yi Wu, 2013	1	1	0	1	1	1	1	0	1	0	7
Sheng Huang, 2015	1	1	0	1	1	1	1	0	1	0	7

Note. S1: eligibility criteria; S2: representativeness of the cases; S3: community controls; S4: the controls had no history of disease (endpoint); C1a: important factor basis between two groups; C1b: study controls for additional factor basis between two groups; E1a: secure record of exposure; E1b: structured interview where blind to case about the exposure; E2: same method of ascertainment for cases and controls; E3: nonresponse rate. *Cross-sectional study.

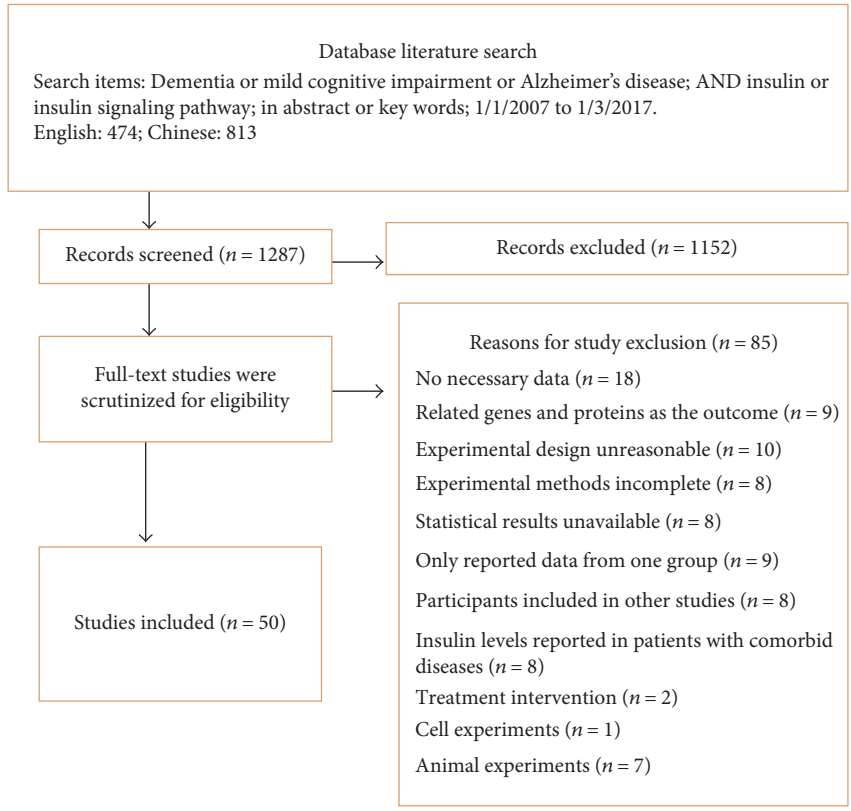

Figure 1: Preferred Reporting Items for Systematic Reviews and Meta-Analysis flowchart of the literature search.

patients who were used in another study [75–81]; insulin levels were reported in patients with comorbid diseases (in addition to diabetes, metabolic syndrome and related diseases can also lead to nonpsychotic dementia [82–89]), such as cognitive dysfunction caused by depression or anxiety [85]; serum insulin was measured before and after insulin treatment or other treatments that could influence insulin metabolism in patients with nonpsychotic dementia; only changes in the MMSE scores before and after the treatment were analyzed, while differences between the observation group and the control group were not analyzed [11, 12]; and the studies involved cell experiments [90] or animal experiments [6, 91–96] (for the flowchart, see Figure 1).

2.4. Data Extraction. Data regarding sample size, mean, standard deviation (s.d.), events, and *P* values were extracted as the primary outcomes. Two investigators (Qiu-xia Pan and Xiao-juan Li) independently extracted the data, and the results were verified by another team member (Zhi-yi Yan). Any inconsistencies were resolved by consensus. Tables 2 and 3 summarized the included studies and present the demographic and clinical characteristics of the included patients.

2.5. Statistical Analysis. Comprehensive Meta-Analysis Version 2 software (Biostat, Englewood, NJ, USA) was used for all statistical analyses. The sample size, mean, s.d., and events were primarily used to generate effect sizes (ESs) (the sample size and *P* value were used in some studies in which the mean, s.d., and events were not available). The ESs were calculated as the standardized mean difference in insulin levels or MMSE scores between groups and converted to Hedges' *g*, which provides an unbiased ES that is adjusted for the sample size. In pooled ESs, 95% confidence intervals (95% CIs) were used to assess significant differences. Random-effects models were chosen for this meta-analysis because we hypothesized that within-study and

Table 2: Baseline subject characteristics (nonpsychotic dementia and HCs).

Names (IN) mmol/l	Age		Edu	Sex		Number		Nonpsychotic dementia		HC		Sample	State	Drug	P value
	Ex	HC		Men	Women	Ex	HC	Mean	s.d.	Mean	s.d.				
Si-ling Liu, 2011 AD	72	72	11.2	34	19	23	30	—	—	—	—	Serum	Fast	—	$P < 0.05$ H
Qin-yun Li, 2015 AD	77	75	10.1	126	120	126	120	11.78	6.6	6.28	3.36	Serum	Fast	No	$P = 0.04$ H
Zong-yuan Wang, 2008 a AD L	70	72	—	—	—	14	12	5.7	6.9	4.5	3.5	Plasma	Fast	No	$P < 0.05$ H
Zong-yuan Wang, 2008 b AD (MH)	70	72	—	—	—	9	12	10.3	9.8	4.5	3.5	Plasma	Fast	No	$P < 0.05$ H
Zong-yuan Wang, 2008 c AD L	70	72	—	—	—	14	12	3.4	0.3	3.3	0.4	CSF	Fast	No	$P > 0.05$
Zong-yuan Wang, 2008 d AD (MH)	70	72	—	—	—	9	12	2.4	0.2	3.3	0.4	CSF	Fast	No	$P < 0.05$ L
Abimbola A. Akintola, 2015 multi	66	66	—	62	70	75	57	—	—	—	—	Plasma	Fast	No	$P = 0.07$
Angela J. Hanson, 2016 AD	68	72	—	163	156	199	120	15.6	—	11.7	—	Plasma	Fast	—	$P = 0.0005$ H
J.K. Morris, 2016 AD L	71	72	17	22	29	14	37	8.73	7.8	4.19	3.8	Plasma	Fast	Yes	$P = 0.023$ H
G. Stennis Watson, 2009 AD	76	74	15	13	22	16	19	8.2	4.3	8.9	4.8	Plasma	Fast	No	$P > 0.05$
Robert Krikorian, 2012 MCI	71	68	15	—	—	11	12	14.4	6	16.9	6	—	Fast	No	$P = 0.40$
E. Rönnemaa, B. Zethelius, and J. Sundelöf, 2009 multi	71	71	—	—	—	257	868	—	1.0	—	0.96	Plasma	Fast	Yes	$P = 0.04$ H
Galit Weinstein, 2015 multi	47	47	—	2156	1782	215	3723	—	—	—	—	—	Fast	Yes	$P = 0.036$ H
Jeffrey M. Burns, 2012 AD	75	73	16	59	50	48	61	8.4	5.4	7.2	4.6	Serum	Fast	—	$P = 0.19$
Auriel A. Willette, 2015 a MCI	76	76	15	95	185	194	26	2.78	3.08	2.98	3.10	Plasma	Fast	—	$P = 0.589$
Auriel A. Willette, 2015 AD b	76	76	15	95	185	60	26	2.41	1.46	2.98	3.10	Plasma	Fast	—	$P = 0.589$
Amber S. Watts, 2013 AD	75	74	—	61	87	75	73	—	—	—	—	Serum	Fast	—	$P = 0.001^*$
Josh D. Woolley, 2014 a AD	59	57	15	16	19	17	18	—	—	—	—	Serum	-3 min	—	$P < 0.01$ H
Josh D. Woolley, 2014 b (bvFTD)	59	57	15	18	19	19	18	—	—	—	—	Serum	−30 min	—	$P < 0.05$ H
Xiao-hong Sun, 2010 AD	—	—	—	32	58	45	44	12.36	8.627	6.541	9.120	Serum	Fast	—	$P < 0.05$ H
Lu Zhang, 2011 a AD L	72	72	—	59	44	41	35	1.07	0.21	1.51	0.27	CSF	—	—	$P < 0.05$ L
Lu Zhang, 2011 b AD MH	72	72	—	59	44	27	35	0.68	0.11	1.51	0.27	CSF	—	—	$P < 0.01$ L
Wei-gang Liu, 2009 a AD L	71	71	—	66	59	31	70	7.9	2.0	6.8	2.5	—	Fast	—	$P < 0.01$ H
Wei-gang Liu, 2009 b AD MH	71	71	—	66	59	24	70	8.0	2.4	6.8	2.5	—	Fast	—	$P < 0.01$ H
Wei-gang Liu, 2009 c AD L	71	71	—	45	38	27	35	0.27	0.08	0.29	0.10	CSF	—	—	$P > 0.05$
Wei-gang Liu, 2009 d AD MH	71	71	—	45	38	21	35	0.22	0.12	0.29	0.10	CSF	—	—	$P < 0.05$ L
Gui-qing Chen, 2015 AD	78	78	7	94	81	95	80	9.758	7.42	6.384	5.89	Serum	Fast	—	$P = 0.023$ H
Zhi-juan Wang, 2014 a AD	67	67	—	28	22	30	20	7.94	6.81	9.25	5.51	Serum	Fast	—	$P > 0.05$
Zhi-juan Wang, 2014 b VD	67	67	—	29	23	30	20	7.89	6.55	9.25	5.51	Serum	Fast	—	$P > 0.05$
Jun-shi Zhang, 2016 AD	76	76	—	47	39	43	43	11.79	6.62	6.25	3.34	Serum	Fast	—	$P < 0.05$ H
Jin-geng Li, 2013 a AD L	73	73	7	39	46	18	30	10.667	10.51	6.793	14.75	—	Fast	—	$P < 0.01$ H
Jin-geng Li, 2013 b AD M	73	73	7	39	46	20	30	9.203	5.36	6.793	14.75	—	Fast	—	$P < 0.01$ H

Table 2: Continued.

Names (IN) mmol/l	Age		Edu	Sex		Number		Nonpsychotic dementia		HC		Sample	State	Drug	P value
	Ex	HC		Men	Women	Ex	HC	Mean	s.d.	Mean	s.d.				
Jin-geng Li, 2013 c AD H	73	73	7	39	46	17	30	9.324	7.48	6.793	14.75	—	Fast	—	$P < 0.01$ H
Jin-geng Li, 2013 d AD (total)	73	73	7	39	46	55	30	9.718	10.31	6.793	14.75	—	Fast	—	$P < 0.01$ H
Zhi-dong Yang, 2007a AD L	—	—	—	36	43	21	31	16.1	3.7	11.6	4.3	Plasma	Fast	—	$P < 0.05$ H
Zhi-dong Yang, 2007 b AD MH	—	—	—	36	43	27	31	22.1	5.2	11.6	4.3	Plasma	Fast	—	$P < 0.05$ H
Zhi-dong Yang, 2007 c AD L	—	—	—	36	43	21	31	0.98	0.33	1.12	0.31	CSF	Fast	—	$P > 0.05$
Zhi-dong Yang, 2007 d AD MH	—	—	—	36	43	27	31	0.63	0.17	1.12	0.31	CSF	Fast	—	$P < 0.05$ L
Hong-mei Yue, 2014 a MCI	72	72	10	—	—	116	76	19.90	1.62	11.15	1.60	Serum	Fast	—	$P < 0.05$ H
Hong-mei Yue, 2014 b AD L	72	72	10	—	—	81	76	17.90	5.6	11.15	1.6	Serum	Fast	—	$P < 0.05$ H
Hong-mei Yue, 2014 c AD M	72	72	10	—	—	72	76	27.08	1.6	11.15	1.6	Serum	Fast	—	$P < 0.05$ H
Hong-mei Yue, 2014 d AD H	72	72	10	—	—	34	76	34.10	1.61	11.15	1.6	Serum	Fast	—	$P < 0.05$ H
Liang-mi Li, 2015 a AD	73	73	—	117	103	80	70	7.94	0.83	8.23	1.04	Serum	Fast	—	$P > 0.05$
Liang-mi Li, 2015 b VD	73	73	—	117	103	70	70	7.89	0.89	8.23	1.04	Serum	Fast	—	$P > 0.05$
Qing-chun Xia, 2015 a AD L	70	70	—	27	63	34	30	30.29	20.00	20.15	20.50	Plasma	Fast	No	$P < 0.05$ H
Qing-chun Xia, 2015 b AD MH	70	70	—	27	63	26	30	40.29	21.10	20.15	20.50	Plasma	Fast	No	$P < 0.05$ H
Ran Song, 2015 VD	65	65	—	53	32	39	46	8.88	0.31	4.97	2.01	Serum	Fast	Yes	$P < 0.001$ H
Yu-mei Yang, 2009 MCI	63	63	—	81	114	51	144	10.50	—	8.10	—	—	Fast	—	$P = 0.001$ H
Xiao-lan Liu, 2008 VD	74	74	—	88	32	40	40	10.01	—	8.7	—	—	Fast	No	$P > 0.05$
Rong-wei Zhang, 2008 a MVCI	73	73	—	56	38	37	34	13.5	1.4	10.40	1.2	Serum	Fast	—	$P < 0.05$
Rong-wei Zhang, 2008 b VD	73	73	—	56	38	23	34	15.4	2.0	10.40	1.2	Serum	Fast	—	$P < 0.05$ H
Bin-bin Zang, 2011 multi	76	76	—	33	27	30	30	6.42	0.58	5.53	1.03	Serum	Fast	—	$P < 0.05$ H
Zhi-juan Wang, 2014 c AD	74	74	—	69	35	68	36	7.82	6.46	8.37	5.31	Serum	Fast	—	$P > 0.05$
Hong-shan Pan, 2016 AD	69	69	—	50	40	45	45	7.7	4.5	9.4	4.9	—	Fast	No	$P > 0.05$
Nan Mu 2010, a AD L	81	81	—	—	—	13	32	25.38	53.11	20.75	21.51	Serum	Fast	—	$P = 0.605$
Nan Mu, 2010 b AD M	81	81	—	—	—	12	32	17.38	14.89	20.75	21.51	Serum	Fast	—	$P = 0.605$
Nan Mu, 2010 c AD H	81	81	—	—	—	9	32	9.11	6.03	20.75	21.51	Serum	Fast	—	$P = 0.605$
Yan-Wu, 2008 a VD L	62	62	—	—	—	35	15	12.89	4.52	10.01	4.15	—	Fast	—	$P < 0.05$ H
Yan-Wu, 2008 b VD M	62	62	—	—	—	15	15	13.13	5.13	10.01	4.15	—	Fast	—	$P < 0.01$ H
Yan-Wu, 2008 c VD H	62	62	—	—	—	11	15	15.32	5.31	10.01	4.15	—	Fast	—	$P < 0.01$ H
Hong-li Li, 2013 AD	74	74	—	56	69	55	70	5.75	4.23	3.71	1.87	Serum	Fast	—	$P < 0.05$ H

Note. Ex: experimental group; HC: healthy control group; HCs: healthy control subjects; Edu: average years of education of all participants; state: sampling time; drug: participants received or did not receive medication interventions during the course of the study; AD: Alzheimer's disease; VD: vascular dementia; multi: nonpsychotic dementia caused by multiple diseases; MCI: mild cognitive impairment; L/M/H: different severities (light/mild, middle, and heavy) of nonpsychotic dementia, respectively; MVCI: mild cognitive impairment caused by vascular disease; H: high insulin levels in patients in the experimental group; L: low insulin levels in patients in the experimental group. *This study included a comparison of log values, and although the P value was <0.05, the actual analysis showed that insulin levels were not associated with events in nonpsychotic dementia.

Table 3: Baseline characteristics of the subjects (abnormal insulin levels and HCs).

Names (events/MMSEs)	Age		Edu	Sex		Number		Ex		HC		P value
	Ex	HC		Men	Women	Ex	HC	Mean Events	s.d.	Mean Events	s.d.	
Wen-qing Xia, 2016	59.5	56.2	10.3	32	38	38	32	28.8	1.1	29.1	1.2	$P < 0.001$ H
Chin-Chou Huang, 2014	79	79	—	73941	68803	71433	71311	8572		4992		$P < 0.001$ H
Rosebud O. Roberts, 2014	80	79	14	423	326	154	595	—	—	—	—	$P = 0.914$
Mkaya Mwamburi, 2016 a	75	80	12	—	—	70	67	25.3	3.4	25.4	4.2	$P = 0.914$
Mkaya Mwamburi, 2016 b	75	80	12	—	—	67	67	25.1	3.6	25.4	4.2	$P = 0.914$
Mkaya Mwamburi, 2016 c	75	80	12	—	—	83	67	25.4	3.2	25.4	4.2	$P > 0.05$
Heather Kenna, 2013	59	57	16	—	—	10	10	28.9	0.9	29.5	1.0	$P < 0.001$ H
Yen-Chun Fan, 2017	53	53	—	27360	24220	10316	41246	413		825		$P < 0.05$ H
Laura D. Baker, 2011	74	74	—	—	—	12	11	—	3.3	—	1.5	$P < 0.05$ H
M.S. Beeri, 2008	—	—	—	111	137	124	124	—	—	—	—	$P < 0.05$ H
Hannah Bruehl, 2009	59	60	15	42	46	41	47	—	—	—	—	—— H
Xiao-bing Zhou, 2012	73	73	—	252	280	162	370	81		66		$P < 0.05$ H
Qiong-yu Zhang, 2012	62	62	9	—	—	81	103	25.34	4.72	23.42	5.50	$P < 0.05$ H
Xiao-hong Zhao, 2009	65	65	—	—	—	31	71	17.46	9.51	10.19	6.09	$P < 0.001$ H
Jun-yi Wu, 2013	71	71	—	93	48	60	81	38		25		$P < 0.05$
Sheng Huang, 2015	65	65	—	49	51	58	42	41		18		$P < 0.05$
Jill K. Morris, 2014	76	74	16	165	99	97	167	—		—		$P = 0.009$ H

Note. Ex: experimental group; HC: healthy control group; HCs: healthy control subjects; Edu: average years of education of all participants; H: high insulin levels in patients in the experimental group; L: low insulin levels in patients in the experimental group.

between-study moderators would result in differences in the true ESs [97]. We excluded one study at a time to determine whether the results were unduly secondary to a particular study. Data regarding the average age and gender distribution of the patients and the classification and severity of cases of nonpsychotic dementia (i.e., MMSE) were also extracted.

Significant differences in heterogeneity across studies were assessed using Cochran's Q test [98], and statistical significance was set at $P < 0.1$. Using these parameters, we found that there was between-study heterogeneity. Inconsistencies across studies were identified using the I^2 index, which evaluates the impact of heterogeneity. I^2 values of 0.25, 0.50, and 0.75 indicate small, moderate, and high levels of heterogeneity, respectively. We then performed unrestricted maximum-likelihood random-effects metaregressions of the ESs [99] to determine whether covariates, including age, gender distribution (i.e., the proportion of males) and MMSE scores, represented moderators that influenced the ESs. We then performed unrestricted maximum-likelihood random-effects metaregressions of the ESs.

Funnel plots were generated by plotting the ESs against the precision (inverse of the standard error) of each study and used to visually inspect the studies for publication bias. The significance of any observed publication bias was determined using Egger's test [100], which assesses the degree of asymmetry in funnel plots. The classic fail-safe N method [101], which is an analysis that results in the number of missing (unpublished) studies that would increase the observed P value to >0.05, was also used to investigate publication bias. Statistical significance was set at a P value < 0.05 unless otherwise indicated. P values < 0.1 were reported as trends.

3. Results

3.1. Included Studies. In total, 50 high-quality studies (5–9 points) were included in this analysis. These included 206207 participants, and 77 sets of data were summarized for the subsequent analysis. The results were divided into the following three areas according to differences in study objectives: (1) the relationship between insulin levels in the CSF and the risk of nonpsychotic dementia; (2) variability in cognitive function scores (i.e., MMSE scores) and insulin levels in the peripheral blood; and (3) differences in insulin levels between nonpsychotic dementia and nondementia patients (assuming that high insulin levels and nonpsychotic dementia are positively correlated).

3.2. Main Associations between CSF Insulin Levels and Nonpsychotic Dementia. First, we compared the insulin levels (mU/L) in the CSF between patients with nonpsychotic dementia and HCs. Eight sets of data were extracted from 4 studies involving a total of 300 individuals. A random-effects meta-analysis was performed, and the results showed that the nonpsychotic dementia patients had significantly lower CSF insulin levels than were observed in the HCs (Hedges' $g = 1.196$, 95% CI = 0.238 to 2.514, and $P = 0.014$; Figure 2). A sensitivity analysis indicated that our results were significantly influenced by all studies (Additional File 1). In addition, significant heterogeneity

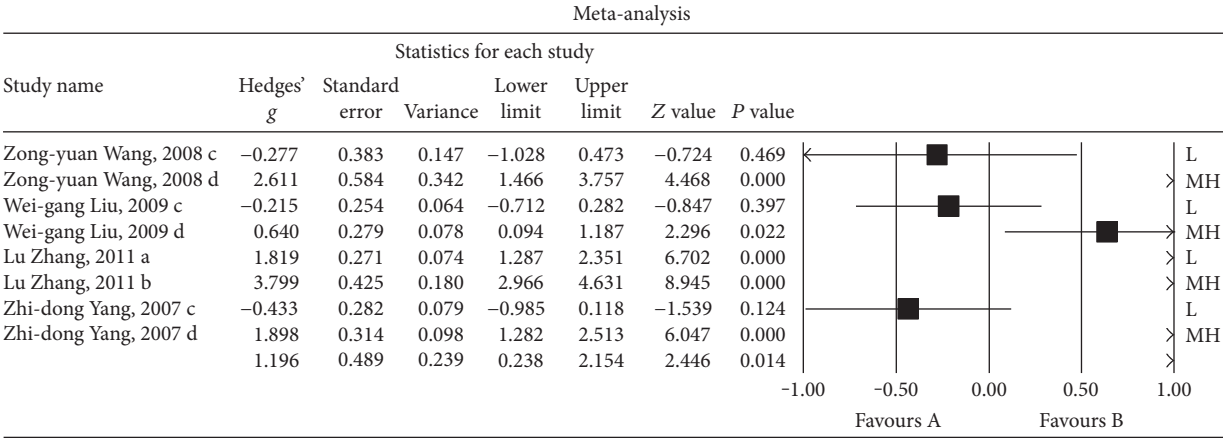

Figure 2: Forest plot of the random-effects meta-analysis of differences in CSF insulin levels between nonpsychotic dementia patients and healthy controls (HC). In all, 8 sets of data encompassing a total of 300 individuals were included. The sizes of the squares are proportional to study weight. CI, confidence interval.

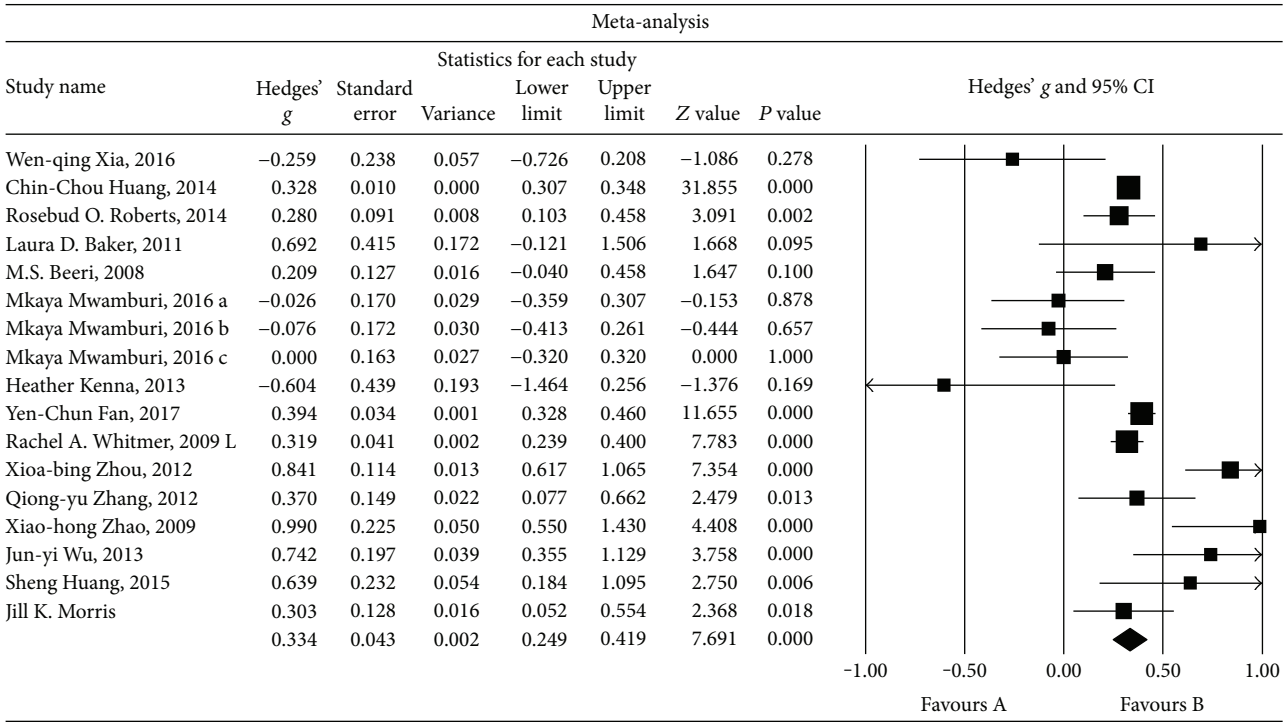

Figure 3: Forest plot of the random-effects meta-analysis of differences in MMSE scores between abnormal insulin levels and HC subjects. In all, 17 sets of data encompassing a total of 197114 individuals were included. The sizes of the squares are proportional to study weight. CI, confidence interval.

was observed among the studies in this meta-analysis ($Q = 128.753$, d.f. = 7, $I^2 = 94.563$, and $P = 0.000$).

3.3. Main Associations between MMSE Scores and Abnormal Insulin Levels in the Peripheral Blood. Second, we compared the MMSE scores and the incidence of nonpsychotic dementia between patients with abnormal levels of insulin and HCs. Sixteen sets of data were extracted from 15 studies involving a total of 197114 individuals. A random-effects meta-analysis was performed, and the results showed that high insulin levels were associated with a higher risk of nonpsychotic dementia than was observed in the HCs (Hedges' $g = 0.334$, 95% CI = 0.249 to 0.419, and $P = 0.000$; Figure 3). A sensitivity analysis indicated that our results were not unduly influenced by any particular study (Additional File 2). Furthermore, high heterogeneity was observed among the studies in this meta-analysis ($Q = 65.130$, d.f. = 16, $I^2 = 75.434$, and $P = 0.000$).

3.4. Main Associations between Insulin Levels and Nonpsychotic Dementia. Third, we compared the levels of insulin (mU/L) in the peripheral blood between patients with

Meta-analysis									
		Statistics for each study							
Study name	Subgroup within study	Hedges' *g*	Standard error	Variance	Lower limit	Upper limit	*Z* value	*P* value	Hedges' *g* and 95% CI
Si-ling Liu, 2011	AD	0.457	0.277	0.077	−0.085	1.000	1.654	0.098	
Qin-yun Li, 2015	AD	1.040	0.136	0.018	0.774	1.305	7.670	0.000	
Zong-yuan Wang, 2008 a	AD	0.207	0.382	0.146	−0.541	0.956	0.543	0.587	
Zong-yuan Wang, 2008 b	AD	0.808	0.441	0.195	−0.057	1.673	1.830	0.067	
Abimbola .A.Akintola, 2015	Multi	−0.319	0.176	0.031	−0.664	0.025	−1.816	0.069	
Angela J .Hanson, 2016	AD	0.359	0.116	0.013	0.132	0.587	3.093	0.002	
J.K. Morris, 2016	AD	0.864	0.321	0.103	0.236	1.493	2.696	0.007	
G.Stennis Watson, 2009	AD	−0.149	0.332	0.110	−0.800	0.501	−0.450	0.653	
Robert Krikorian, 2012	MCI	−0.402	0.407	0.165	−1.199	0.395	−0.988	0.323	
E.Rönnemaa, B. Zethelius, and J. Sundelöf, 2009	Multi	0.124	0.071	0.005	−0.015	0.264	1.751	0.080	
Galit. Weinstein, 2015	Multi	0.126	0.070	0.005	−0.011	0.264	1.799	0.072	
Jeffrey M. Burns, 2012	AD	−0.240	0.192	0.037	−0.617	0.137	−1.248	0.212	
Auriel A. Willette, 2015 a	MCI	−0.065	0.208	0.043	−0.473	0.343	−0.311	0.756	
Auriel A.Willette, 2015 b	AD	−0.271	0.234	0.055	−0.728	0.187	−1.158	0.247	
Amber S.Watts, 2013	AD	−0.549	0.167	0.028	−0.876	−0.223	−3.296	0.001	
Josh D. oolley, 2014 a	AD	0.808	0.344	0.119	0.133	1.483	2.347	0.019	
Josh D.Woolley, 2014 b	bvFTD	0.544	0.328	0.108	−0.099	1.187	1.658	0.097	
Xiao-hong Sun, 2010	AD	0.650	0.216	0.047	0.227	1.073	3.013	0.003	
Wei-gang Liu, 2009 a	AD	0.463	0.217	0.047	0.038	0.887	2.136	0.033	
Wei-gang Liu, 2009 b	AD	0.481	0.237	0.056	0.016	0.946	2.027	0.043	
Gui-qing Chen, 2015	AD	0.497	0.153	0.024	0.196	0.797	3.237	0.001	
Zhi-juan Wang, 2014 a	AD	−0.204	0.285	0.081	−0.762	0.355	−0.715	0.474	
Zhi-juan Wang, 2014 b	VD	−0.217	0.285	0.081	−0.776	0.341	−0.763	0.446	
Jun-shi Zhang, 2016	AD	1.047	0.228	0.052	0.600	1.494	4.590	0.000	
Jin-geng Li, 2013 a	AD	0.286	0.295	0.087	−0.292	0.863	0.969	0.332	
Jin-geng Li, 2013 b	AD	0.198	0.285	0.081	−0.360	0.757	0.697	0.486	
Jin-geng Li, 2013 c	AD	0.197	0.299	0.090	−0.390	0.783	0.657	0.511	
Zhi-dong Yang, 2007 a	AD	1.089	0.298	0.089	0.504	1.673	3.652	0.000	
Zhi-dong Yang, 2007 b	AD	2.186	0.330	0.109	1.540	2.832	6.632	0.000	
Hong-mei Yue, 2014 a	MCI	5.406	0.313	0.098	4.793	6.019	17.294	0.000	
Hong-mei Yue, 2014 b	AD	1.609	0.183	0.034	1.250	1.968	8.792	0.000	
Hong-mei Yue, 2014 c	AD	9.905	0.599	0.358	8.732	11.078	16.549	0.000	
Hong-mei Yue, 2014 d	AD	14.217	0.980	0.961	12.296	16.138	14.505	0.000	
Liang-mi Li, 2015 a	AD	−0.309	0.164	0.027	−0.630	0.012	−1.886	0.059	
Liang-mi Li, 2015 b	VD	−0.349	0.169	0.029	−0.681	−0.017	−2.062	0.039	
Qing-chun Xia, 2015 a	AD	0.616	0.253	0.064	0.119	1.113	2.431	0.015	
Qing-chun Xia, 2015 b	AD	0.956	0.279	0.078	0.408	1.503	3.423	0.001	
Ran Song, 2015	VD	2.592	0.293	0.086	2.017	3.167	8.836	0.000	
Yu-mei Yang, 2009	MCI	0.509	0.164	0.027	0.186	0.831	3.094	0.002	
Xiao-lan Liu, 2008	VD	−0.441	0.224	0.050	−0.880	−0.001	−1.967	0.049	
Rong-wei Zhang, 2008 a	VD MCI	2.344	0.306	0.094	1.743	2.944	7.649	0.000	
Rong-wei Zhang, 2008 b	VD	3.142	0.397	0.157	2.364	3.919	7.917	0.000	
Bin-bin Zang, 2011	Multi	1.051	0.272	0.074	0.517	1.585	3.859	0.000	
Zhi-juan Wang, 2014 c	AD	−0.090	0.205	0.042	−0.491	0.312	−0.438	0.661	
Hong-shan Pan, 2016	AD	−0.358	0.211	0.044	−0.771	0.055	−1.700	0.089	
Nan Mu, 2010 a	AD	0.136	0.323	0.105	−0.498	0.770	0.420	0.674	
Nan Mu, 2010 b	AD	−0.166	0.333	0.111	−0.818	0.487	−0.497	0.619	
Nan Mu, 2010 c	AD	−0.589	0.376	0.141	−1.326	0.147	−1.569	0.117	
Yan-Wu, 2008 a	VD	0.642	0.310	0.096	0.034	1.251	2.068	0.039	
Yan-Wu, 2008 b	VD	0.651	0.365	0.133	0.065	1.366	1.782	0.075	
Yan-Wu, 2008 c	VD	1.101	0.414	0.171	0.291	1.912	2.663	0.008	
Hong-li Li, 2013	AD	0.647	0.184	0.034	0.287	1.007	3.523	0.000	
		0.853	0.140	0.019	0.579	1.127	6.110	0.000	

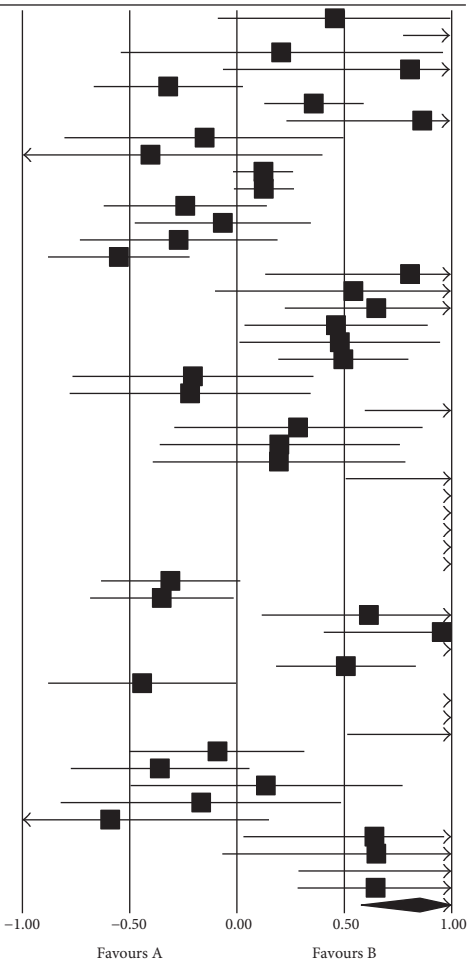

Figure 4: Forest plot of the random-effects meta-analysis of differences in blood insulin concentrations between nonpsychotic dementia patients and HCs. In all, 52 sets of data encompassing a total of 8931 individuals were included. The sizes of the squares are proportional to study weight. CI, confidence interval.

nonpsychotic dementia and HCs. Fifty-two sets of data were extracted from 36 studies involving a total of 8931 individuals. A random-effects meta-analysis was performed, and the results showed that the nonpsychotic dementia patients had significantly higher insulin levels than were observed in the HCs (Hedges' $g = 0.853$, 95% CI = 0.579 to 1.127, and $P = 0.000$; Figure 4). A sensitivity analysis indicated that our results were not unduly influenced by any particular study (Additional File 3). However, significant heterogeneity was observed among the studies in this meta-analysis ($Q = 1184.942$, d.f. = 51, $I^2 = 95.696$, and $P = 0.000$).

3.5. Investigation of Heterogeneity. Fourth, to identify the potential sources of the heterogeneity observed in this meta-analysis, we performed subgroup analyses primarily by considering the sources of the samples (i.e., serum or plasma) and the reported medications used in the patients. We then performed subgroup analyses according to the class of the samples (i.e., VD or AD) and the degree of nonpsychotic dementia in the patients.

The subgroup analysis showed that compared with the levels observed in the HCs, serum insulin levels were significantly higher in the patients with nonpsychotic dementia (25 sets of data were extracted from 17 studies; Hedges' $g = 1.482$, 95% CI = 0.909 to 2.056, and $P = 0.000$), and the same trend was observed in the plasma (13 sets of data were extracted from 9 studies; Hedges' $g = 0.445$, 95% CI = 0.154 to 0.736, and $P = 0.003$). Compared with the plasma group, the serum group had significantly greater ESs in the nonpsychotic dementia patients with higher insulin levels. High levels of heterogeneity were observed among studies that included serum ($Q = 1011.719$, d.f. = 25, $I^2 = 97.529$, and $P = 0.000$) or plasma ($Q = 79.543$, d.f. = 12, $I^2 = 84.914$, and $P = 0.000$) insulin levels. Subgroup analyses of studies involved patients who did not take any drugs, who took drugs without effect on glucose and lipid metabolism, and who are on drug withdrawal that lasted longer than

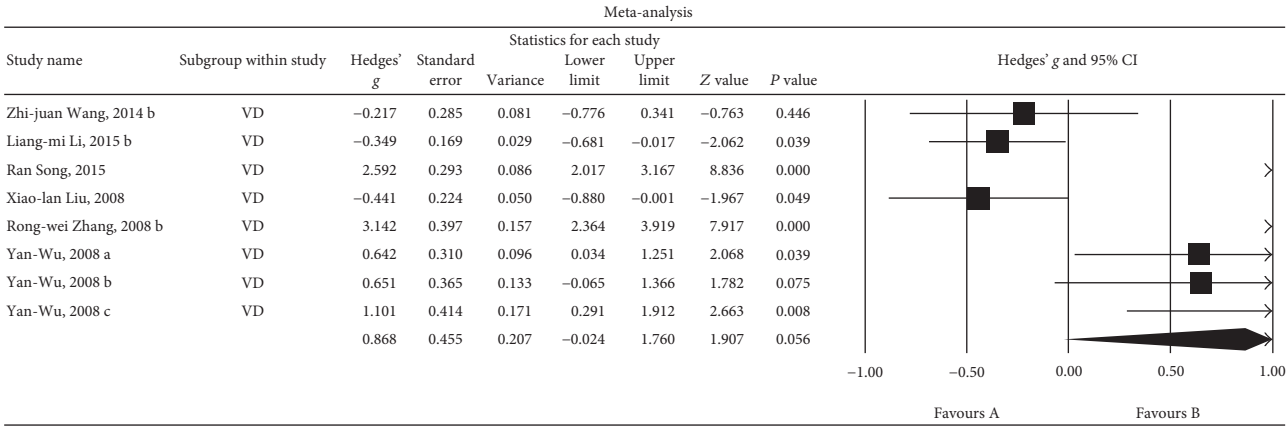

Figure 5: Forest plot of the random-effects meta-analysis of differences in blood insulin concentrations between VD patients and HC subjects. In all, 8 sets of data encompassing a total of 488 individuals were included. The sizes of the squares are proportional to study weight. CI, confidence interval.

2 weeks. The subjects were then grouped, and 10 sets of data were extracted from 8 studies involving a total of 731 individuals. A random-effects meta-analysis showed that insulin levels were not significantly different between the nonpsychotic dementia patients and HCs (Hedges' $g = 0.194$, 95% CI = −0.251 to 0.640, and $P = 0.393$). High levels of heterogeneity were also found ($Q = 76.093$, d.f. = 9, $I^2 = 88.172$, and $P = 0.000$).

3.6. Subgroup Analyses

3.6.1. Associations between Insulin Levels and the VD Group. Eight sets of data were extracted from 6 studies involving a total of 488 individuals. A random-effects meta-analysis was performed, and the results showed that the risk of VD was higher in patients with high insulin levels than in the HCs (Hedges' $g = 0.868$, 95% CI = −0.024 to 1.760, and $P = 0.056$; Figure 5). A sensitivity analysis indicated that two studies could have influenced this outcome (Additional File 4). This was not surprising because the P values of the meta-analysis outcomes were only slightly higher than 0.05. Significant heterogeneity was observed among the studies in this meta-analysis ($Q = 145.849$, d.f. = 8, $I^2 = 95.201$, and $P = 0.000$).

3.6.2. Associations between Insulin Levels and the AD Group. Thirty-four sets of data were extracted from 24 studies involving a total of 8407 individuals. A random-effects meta-analysis was performed, and the results showed that the nonpsychotic dementia patients had significantly higher insulin levels than were observed in the HCs (Hedges' $g = 0.852$, 95% CI = 0.494 to 1.209, and $P = 0.000$; Figure 6). A sensitivity analysis indicated that these results were not unduly influenced by any particular study (Additional File 5). However, high levels of heterogeneity among the studies were observed in this meta-analysis ($Q = 678.926$, d.f. = 33, $I^2 = 95.139$, and $P = 0.000$).

Fewer than 5 studies focused on the relationship between abnormal insulin levels and nonpsychotic dementia types other than AD and VD. Hence, we compared only the relationships between abnormal insulin levels and AD or VD because these two subgroups showed high heterogeneity. Thus, we next sought to determine whether there are differences in blood insulin levels between HCs and patients with MCI, mild (or light) nonpsychotic dementia (L, MMSE scores ≥ 16) and moderate or heavy nonpsychotic dementia (MH, MMSE scores < 16).

3.6.3. Associations between Insulin Levels and MCI. Five sets of data were extracted from 5 studies involving a total of 4653 individuals. A random-effects meta-analysis was performed, and the results showed that there were no significant differences in blood insulin levels between the MCI and HC groups (Hedges' $g = 1.557$, 95% CI = −0.253 to 3.367, and $P = 0.092$; Figure 7). A sensitivity analysis was not performed because the number of studies was too small. However, we identified significant heterogeneity among the studies ($Q = 264.128$, $I^2 = 98.486$, and $P < 0.001$).

3.6.4. Associations between Insulin Levels and Patients with Mild (or Light) Nonpsychotic Dementia. Eight sets of data were extracted from 8 studies involving a total of 543 individuals. A random-effects meta-analysis was performed, and the results showed that mild nonpsychotic dementia patients had significantly higher insulin levels than were observed in the HCs (Hedges' $g = 0.520$, 95% CI = 0.284 to 0.757, and $P = 0.000$; Figure 7). A sensitivity analysis indicated that these results were not unduly influenced by any particular study (Additional File 6). Furthermore, low heterogeneity was observed among the studies in this meta-analysis ($Q = 11.531$, d.f. = 7, $I^2 = 39.293$, and $P = 0.117$), demonstrating that the differences among the groups made a negligible contribution to this heterogeneity.

3.6.5. Associations between Insulin Levels and Patients with Moderate or Heavy Nonpsychotic Dementia. Twelve sets of data were extracted from 8 studies involving a total of 610 individuals. A random-effects meta-analysis was performed, and the results showed that the middle and heavy

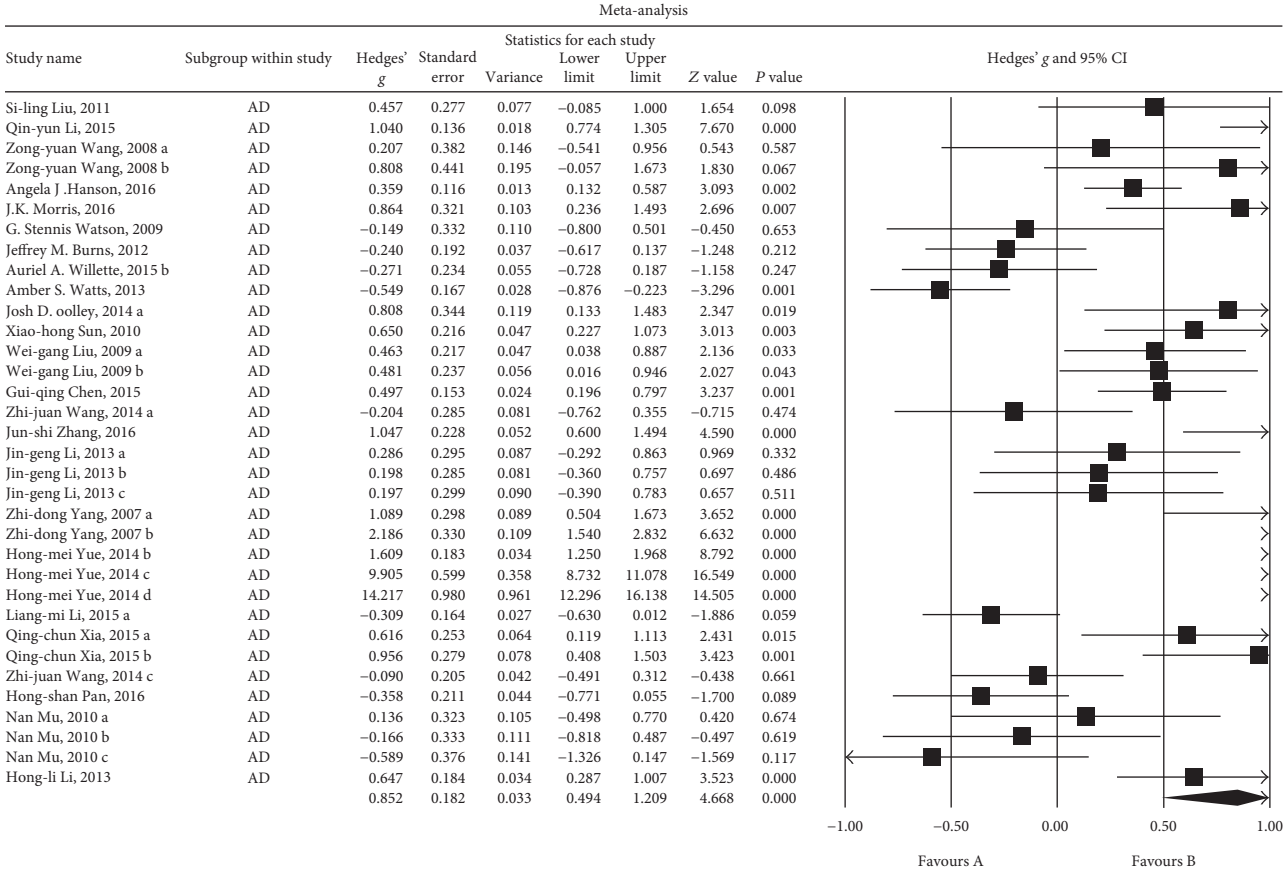

Figure 6: Forest plot of the random-effects meta-analysis of differences in blood insulin concentrations between AD patients and HC subjects. In all, 34 sets of data encompassing a total of 8407 individuals were included. The sizes of the squares are proportional to study weight. CI, confidence interval.

nonpsychotic dementia patients had significantly higher insulin levels than were observed in the HCs (Hedges' $g = 2.379$, 95% CI = 1.007 to 3.752, and $P = 0.001$; Figure 7). A sensitivity analysis indicated that the results were not unduly influenced by any particular study (Additional File 7). However, significant heterogeneity was observed among the studies in this meta-analysis ($Q = 531.782$, d.f. = 11, $I^2 = 97.931$, and $P = 0.000$).

The results of the three subgroup analyses demonstrated that the high heterogeneity observed for increased insulin levels in the peripheral blood in patients with nonpsychotic dementia may have been caused by the severity of the dementia as follows: the greater the severity of nonpsychotic dementia, the higher the ESs of peripheral blood insulin levels. Compared with those of the HC group, the insulin levels in the MCI group were not correlated with the MCI.

In a series of metaregression analyses, we assessed whether gender or continuous variables, such as age, could explain the observed between-study differences. Gender was found to have a moderating effect ($P = 0.29$), but age did not significantly contribute to heterogeneity ($P < 0.05$).

Overall, our results indicated that the significant heterogeneity observed in the patients with increased insulin and nonpsychotic dementia could have been caused by a variety of factors, such as gender, sampling differences, and the severity of nonpsychotic dementia.

3.7. Publication Bias. In the abnormal insulin group, no significant publication bias was detected among the studies in a visual inspection of funnel plots (Additional File 8). These results were confirmed in Egger's tests ($t = 0.007$, d.f. = 15, and $P = 0.497$). Moreover, the nonpsychotic dementia group and AD group showed slight publication biases and had the following Egger's test values: for insulin, $t = 3.26$, d.f. = 50, and $P = 0.001$ (Additional File 9); and for AD, $t = 2.399$, d.f. = 32, and $P = 0.011$ (Additional File 10). Because the ESs of small sample studies estimate a large amount of variation, the appearance of extreme ES values is more likely to emerge in small sample studies than in large sample studies. This publication bias was not statistically significant, and we therefore applied Duval and Tweedie's trim and fill method in further analyses.

The classic fail-safe N was used to assess publication bias, and the results revealed that 4805 missing studies would be required for insulin and 1809 missing studies would be required for AD to achieve P values of >0.05. These results support the notion that the observed publication bias was unlikely to have caused the positive results of our meta-analysis.

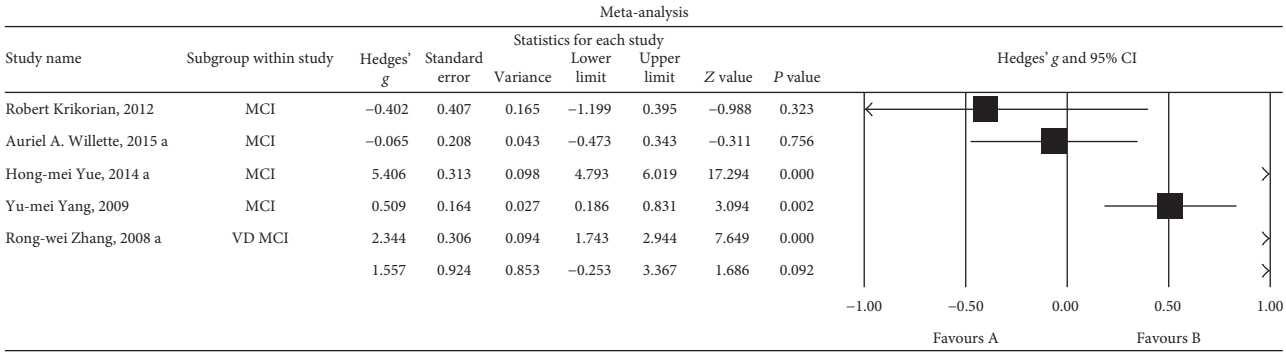

(a)

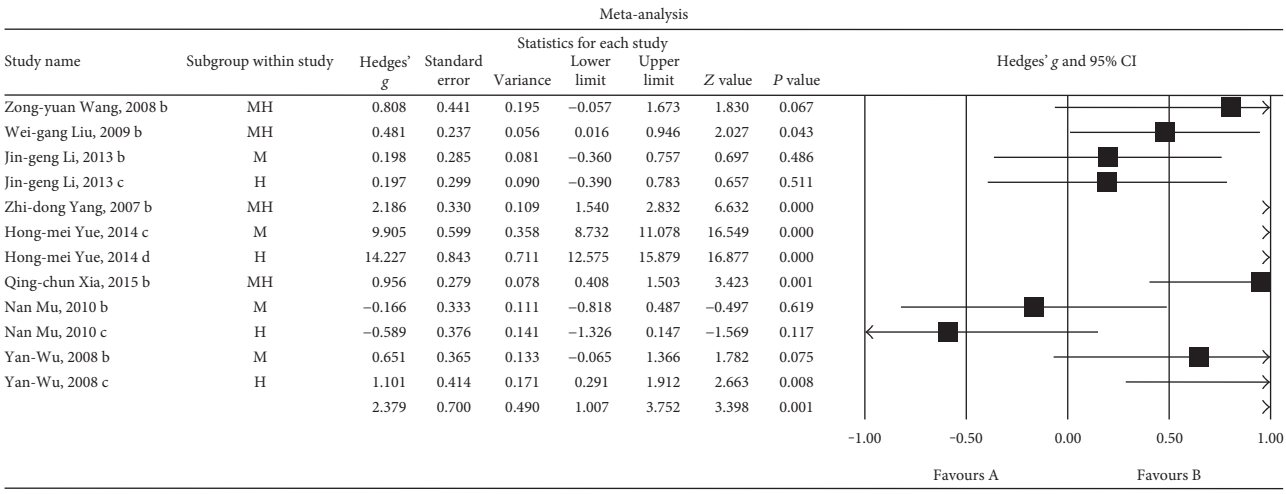

(b)

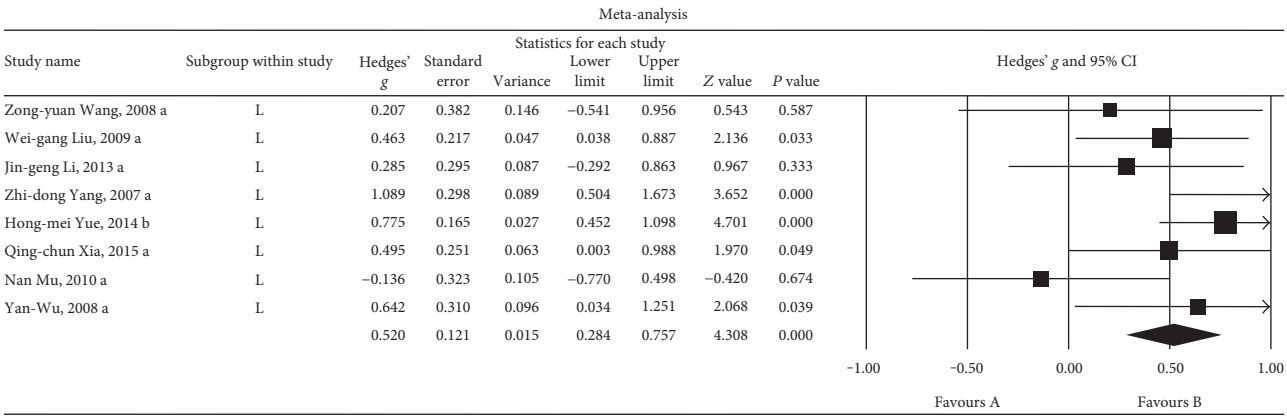

(c)

Figure 7: Forest plot of the random-effects meta-analysis of differences in blood insulin concentrations between patients with different severities of dementia and HC subjects. These 3 pictures in (a), (b), and (c) represent a comparison of insulin levels between HC subjects and MCI, mild (L), and moderate to severe (MH) dementia patients, respectively.

4. Discussion

Many studies have focused on the changes that occur in the Pi3k-Akt insulin signaling pathway in nonpsychotic dementia patients. The Pi3k-Akt insulin signaling pathway is an important pathway in insulin metabolism and is also involved in growth and development, metabolism, and vital cognitive activities. Therefore, it is important to determine whether insulin plays a specific role in nonpsychotic dementia. Whether circulating levels of insulin are altered in nonpsychotic dementia patients has been controversial for a long time. Hence, the significance of insulin levels to the etiology of nonpsychotic dementia etiology was not fully known. The results of this study provide strong clinical evidence supporting the notion that nonpsychotic dementia is associated with increased levels of circulating

insulin and decreased levels of insulin in the CSF. These results provide new insights into a potential molecular pathway that confers vulnerability to the development of nonpsychotic dementia. A strength of this study is that it is based on a large amount of data and a sufficient number of studies related to nonpsychotic dementia.

We explored the relationship between insulin levels and the occurrence of nonpsychotic dementia from three different perspectives. Our results show that CSF insulin levels are lower in patients with nonpsychotic dementia than in HCs, while insulin levels in the peripheral blood may be higher. Additionally, high insulin levels in the peripheral blood were associated with lower scores in cognitive functions. Because the number of studies that included a CSF group, a VD group, an MCI patient group, an L group, and an MH group was small, our results only reveal that there is a correlation between insulin levels and nonpsychotic dementia in these groups. The results suggest that insulin levels are higher in the peripheral blood in VD, AD, L, and MH patients while CSF insulin levels are lower in nonpsychotic dementia patients. The ES was higher in the VD group than in the AD group and higher in the MH group than in the L group.

Our results show that there was no difference in insulin levels between MCI patients and HCs. Eight sets of data obtained from 4 studies support the finding that there is a relationship between CSF insulin levels and the severity of nonpsychotic dementia. Because the number of enrolled patients was small, the present results show that CSF insulin levels are lower in patients with severe nonpsychotic dementia, and there were no significant differences between MCI patients and HCs. Moreover, when the effects of drugs on insulin metabolism were excluded, a subgroup analysis showed that there was no correlation between nonpsychotic dementia and insulin levels. Therefore, the following two possibilities are considered. First, because MMSE scores were significantly lower in the high insulin subjects than in the HC group, the fact that there was no correlation may be related to the small sample size. Hence, as the study size increased, the trend toward an increase in serum insulin levels in the MCI patients might reach significance, and insulin levels are more likely to vary with the severity of the nonpsychotic dementia. Second, because the severity of nonpsychotic dementia increased with the ages of the affected patients, insulin levels may simply increase with age and may not be a key factor in the pathology of nonpsychotic dementia.

Several studies [44–46] have described insulin levels and MMSE scores in nonpsychotic dementia patients without diabetes, type 2 diabetes patients without dementia, and patients with nonpsychotic dementia and type 2 diabetes, and these studies have reported that there are no significant differences in the ages or genders of these patients. Insulin levels increased in the nonpsychotic dementia patients, and cognitive function scores decreased in subjects with high insulin levels. Further investigations of insulin levels in MCI patients are required to confirm these results.

In this meta-analysis, we found various levels of between-study heterogeneity in the outcomes. Although we attempted to adjust for potential confounders, none of the theoretically relevant categorical or continuous variables that were tested explained the observed heterogeneity. A subgroup analysis showed that serum insulin levels (as opposed to plasma levels) were significantly higher in nonpsychotic dementia patients than in HC subjects and that VD insulin levels (as opposed to AD levels) were significantly higher in nonpsychotic dementia patients than in HC subjects. However, the high level of between-study heterogeneity was not lower in these subgroup analyses. MH insulin levels (but not L levels) were significantly higher in nonpsychotic dementia patients than in HC subjects, and low heterogeneity was found in the L group analysis. The high level of between-study heterogeneity was not reduced in the MH and drug intervention elimination groups. This high level of between-study heterogeneity may have been caused by the differences in the samples (i.e., according to gender, age, or sample type), the type of nonpsychotic dementia, the degree of nonpsychotic dementia, or the drug intervention. In addition, hunger, cold, exogenous diet stimulation, endocrine diseases, and the selection of inspection methods and reagents could potentially have caused an abnormal secretion of insulin. Hence, potential confounders that could contribute to the observed between-study heterogeneity were present in a variety of the analyzed studies and may have been related to patient conditions during sample extraction. Because insulin levels that are determined using blood samples can be affected by handling time and the state of the research subjects, studies that include patients who provide samples while on an empty stomach and who are not affected by other endocrine factors may be required to further investigate whether these factors contributed to the variance observed among the studies in this analysis.

5. Conclusions

Overall, CSF insulin levels were lower in nonpsychotic dementia patients (enrolled sample number < 10, more experimental data are needed to support this finding). The high insulin subjects had significantly lower MMSEs and nonpsychotic dementia events than were observed in the HCs, and blood insulin levels were significantly higher in nonpsychotic dementia patients than in HCs. These results indicate that insulin levels are an important indicator that may be useful in clinical diagnoses of nonpsychotic dementia.

Abbreviations

Aβ42:	Beta-amyloid 42
AD:	Alzheimer's disease
APP:	Amyloid precursor protein
CSF:	Cerebrospinal fluid
ESs:	Effect sizes
HC:	Healthy control
HCs:	Healthy control subjects
L:	Light/mild
MH:	Middle and heavy
MCI:	Mild cognitive impairment
MMSE:	Mini-Mental State Examination
NOS:	Newcastle-Ottawa Scale

PRISMA: Reporting Items for Systematic Reviews and Meta-Analysis
s.d.: Standard deviation
VD: Vascular dementia
95% CI: 95% confidence interval.

Additional Points

Availability of Data and Material. The datasets supporting the conclusions of this article are included within the article and its additional files.

Disclosure

The funders had no role in the study design, analysis, decision to publish, or preparation of the manuscript.

Conflicts of Interest

The authors declare that there is no conflict of interest regarding the publication of this article.

Authors' Contributions

Jia-xu Chen and Qiu-xia Pan raised the idea of this study. Qiu-xia Pan and Xiao-juan Li contributed equally as first authors of this manuscript and were the two main reviewers of this study. Fang-fang Wang and Ya-jing Hou contributed to the data collection. You-ming Jiang provided guidance regarding the methodology. Yue-yun Liu took part in the data selection and extraction. Zhi-yi Yan participated in the data extraction. Qiu-xia Pan, Qing-lai Bian, and Wen-qi Qiu cocompleted the primary draft. All authors contributed to the design of this meta-analysis and played a substantial role in the manuscript redaction. All authors approved the final version of this article.

Acknowledgments

The authors thank Yao-wen Zhang for the very helpful and constructive suggestions related to data extraction during this study. This work was funded by the National Natural Science Foundation of China (Grant nos. 81473597 and 81630104), the Beijing Natural Sciences Foundation (Grant no. 7152093), and the 111 Project (no. B07007).

Supplementary Materials

Supplementary 1. Sensitivity analysis of differences in insulin levels in the CSF between nonpsychotic dementia patients and HC subjects.

Supplementary 2. Sensitivity analysis of the random-effects meta-analysis of differences in MMSE scores between patients with abnormal insulin levels and HC subjects.

Supplementary 3. Sensitivity analysis of differences in blood insulin levels between nonpsychotic dementia patients and HC subjects.

Supplementary 4. Sensitivity analysis of differences in blood insulin levels between vascular dementia (VD) patients and HC subjects.

Supplementary 5. Sensitivity analysis of differences in blood insulin levels between AD patients and HC subjects.

Supplementary 6. Sensitivity analysis of differences in insulin levels between L (light/mild) nonpsychotic dementia patients and HC subjects.

Supplementary 7. Sensitivity analysis of differences in insulin levels between MH (moderate to heavy) nonpsychotic dementia patients and HC subjects.

Supplementary 8. Publication bias in MMSE scores between patients with abnormal insulin levels and HC subjects.

Supplementary 9. Publication bias in insulin levels between nonpsychotic dementia patients and HC subjects.

Supplementary 10. Publication bias in insulin levels between AD patients and HC subjects.

Supplementary 11. PRISMA 2009 checklist.

Supplementary 12. PRISMA 2009 flow diagram.

References

[1] C. U. Onyike, "Psychiatric aspects of dementia," *CONTINUUM: Lifelong Learning in Neurology*, vol. 22, no. 2, pp. 600–614, 2016.

[2] H. Umegaki, T. Kawamura, T. Umemura, and N. Kawano, "Factors associated with cognitive decline in older adults with type 2 diabetes mellitus during a 6-year observation," *Geriatrics & Gerontology International*, vol. 15, no. 3, pp. 302–310, 2015.

[3] Z. Chen, Y. Y. Xu, R. Wu et al., "Impaired learning and memory in rats induced by a high-fat diet: involvement with the imbalance of nesfatin-1 abundance and copine 6 expression," *Journal of Neuroendocrinology*, vol. 29, no. 4, 2017.

[4] A. L. Kauffman, J. M. Ashraf, M. R. Corces-Zimmerman, J. N. Landis, and C. T. Murphy, "Insulin signaling and dietary restriction differentially influence the decline of learning and memory with age," *PLoS Biology*, vol. 8, no. 5, article e1000372, 2010.

[5] Q. C. Li, G. I. Wand, B. Y. Li, H. Sun, and N. C. Jiang, "The effect of insulin on the spatial learning and memory abilities of the Alzheimer's disease model rats," *Zhongguo Ying Yong Sheng Li Xue Za Zhi*, vol. 24, no. 4, pp. 494–498, 2008.

[6] J. Q. Wang, J. Yin, Y. F. Song et al., "Brain aging and AD-like pathology in streptozotocin-induced diabetic rats," *Journal of Diabetes Research*, vol. 2014, Article ID 796840, 12 pages, 2014.

[7] A. M. Dorrance, N. Matin, and P. W. Pires, "The effects of obesity on the cerebral vasculature," *Current Vascular Pharmacology*, vol. 12, no. 3, pp. 462–472, 2014.

[8] J. M. Burns, R. A. Honea, E. D. Vidoni, L. J. Hutfles, W. M. Brooks, and R. H. Swerdlow, "Insulin is differentially related to cognitive decline and atrophy in Alzheimer's disease and

aging," *Biochimica et Biophysica Acta (BBA) - Molecular Basis of Disease*, vol. 1822, no. 3, pp. 333–339, 2012.

[9] A. M. Dorrance, N. Matin, and P. W. Pires, "The effects of obesity on the cerebral vasculature," *Current Vascular Pharmacology*, vol. 12, no. 3, pp. 462–472, 2014.

[10] A. M. Dorrance, N. C. Rupp, and E. F. Nogueira, "Mineralocorticoid receptor activation causes cerebral vessel remodeling and exacerbates the damage caused by cerebral ischemia," *Hypertension*, vol. 47, no. 3, pp. 590–595, 2006.

[11] S. Craft, L. D. Baker, T. J. Montine et al., "Intranasal insulin therapy for Alzheimer disease and amnestic mild cognitive impairment: a pilot clinical trial," *Archives of Neurology*, vol. 69, no. 1, pp. 29–38, 2012.

[12] R. O. Roberts, Y. E. Geda, D. S. Knopman et al., "Association of duration and severity of diabetes mellitus with mild cognitive impairment," *Archives of Neurology*, vol. 65, no. 8, pp. 1066–1073, 2008.

[13] J. Y. Jeon, S. R. Kim, H. J. Kim et al., "Risk factors of severe hypoglycemia requiring medical assistance and neurological sequelae in patients with diabetes: a case-control study," *Medicine*, vol. 95, no. 47, article e5365, 2016.

[14] H. Kenna, F. Hoeft, R. Kelley et al., "Fasting plasma insulin and the default mode network in women at risk for Alzheimer's disease," *Neurobiology of Aging*, vol. 34, no. 3, pp. 641–649, 2013.

[15] M. Mwamburi and W. Q. Qiu, "Different associations of premorbid intelligence *vs*. current cognition with BMI, insulin and diabetes in the homebound elderly," *Integrative Molecular Medicine*, vol. 3, no. 3, pp. 547–552, 2016.

[16] A. Liberati, D. G. Altman, J. Tetzlaff et al., "The PRISMA statement for reporting systematic reviews and meta-analyses of studies that evaluate health care interventions: explanation and elaboration," *Journal of Clinical Epidemiology*, vol. 62, no. 10, pp. e1–e34, 2009.

[17] R. L. Ownby, E. Crocco, A. Acevedo, V. John, and D. Loewenstein, "Depression and risk for Alzheimer disease: systematic review, meta-analysis, and metaregression analysis," *Archives of General Psychiatry*, vol. 63, no. 5, pp. 530–538, 2006.

[18] L. Chen, *The Level of Risk Factors for Cognitive Impairment in Insulin Resistance and Diabetes Rat Brain, [M.Sc. Thesis]*, Hebei Medical University, 2009.

[19] Q. H. Fang, *Risk Factors of Mild Cognitive Impairment in Type 2 Diabetes, [M.Sc. Thesis]*, Anhui Medical University, 2014.

[20] D. H. Liu, *Resting-State Functional MRI Study on the Cognitive Impairment in Type 2 Diabetes Mellitus, [M.Sc. Thesis]*, Third Military Medical University, 2015.

[21] J. K. Liu, *The Research of mTOR and Tau Phosphorylated Protein in Hippocampus Tissue of Type 2 Diabetes and Alzheimer's Disease Rats, [M.Sc. Thesis]*, Nanchang University, 2012.

[22] Y. F. Mao, *The Function and Mechanism of Intranasal Insulin on Alzheimer's Disease*, Dr. Dissertation, Zhejiang University, 2016.

[23] W. Shen, *Resting-State Functional Magnetic Resonance Imaging and Neurocognitive Function in Type 2 Diabetes Mellitus, [M.Sc. Thesis]*, Southern Medical University, 2014.

[24] Y. Wang, *Relationship between Cognitive Dysfunction and Vascular Complications in Patients with Type 2 Diabetes Mellitus, [M.Sc. Thesis]*, Shandong University, 2015.

[25] H. Xiong, L. Ding, W. JJ et al., "Effect the impact of insulin on learning and memory of Alzheimer-like mice and its mechanism," *Tianjin Medical Journal*, vol. 41, no. 04, pp. 337–340, 2013.

[26] Y. Y. Xiong, *Prevalence and Risk Factors for Dementia in Diabetics: A Community-Based Case-Control Study [M.Sc. Thesis]*, Fudan University, 2008.

[27] H. Y. Yu, Q. S. Wang, P. Li, and B. X. Yang, "The placebo-controlled study of type 2 diabetes patients with mild cognitive impairment," *Chinese Journal of Gerontology*, vol. 21, pp. 4087–4089, 2011.

[28] T. R. Bomfim, L. Forny-Germano, L. B. Sathler et al., "An anti-diabetes agent protects the mouse brain from defective insulin signaling caused by Alzheimer's disease-associated Aβ oligomers," *The Journal of Clinical Investigation*, vol. 122, no. 4, pp. 1339–1353, 2012.

[29] D. A. Costello, M. Claret, H. Al-Qassab et al., "Brain deletion of insulin receptor substrate 2 disrupts hippocampal synaptic plasticity and metaplasticity," *PLoS One*, vol. 7, no. 2, article e31124, 2012.

[30] M. Hokama, S. Oka, J. Leon et al., "Altered expression of diabetes-related genes in Alzheimer's disease brains: the Hisayama study," *Cerebral Cortex*, vol. 24, no. 9, pp. 2476–2488, 2014.

[31] S. M. Hoscheidt, E. J. Starks, J. M. Oh et al., "Insulin resistance is associated with increased levels of cerebrospinal fluid biomarkers of Alzheimer's disease and reduced memory function in at-risk healthy middle-aged adults," *Journal of Alzheimer's Disease*, vol. 52, no. 4, pp. 1373–1383, 2016.

[32] S. Maimaiti, K. L. Anderson, C. DeMoll et al., "Intranasal insulin improves age-related cognitive deficits and reverses electrophysiological correlates of brain aging," *The Journals of Gerontology Series A: Biological Sciences and Medical Sciences*, vol. 71, no. 1, pp. 30–39, 2016.

[33] T. M. van Himbergen, A. S. Beiser, M. Ai et al., "Biomarkers for insulin resistance and inflammation and the risk for all-cause dementia and Alzheimer disease: results from the Framingham Heart Study," *Archives of Neurology*, vol. 69, no. 5, pp. 594–600, 2012.

[34] W. L. Xu, N. L. Pedersen, L. Keller et al., "*HHEX_23* AA genotype exacerbates effect of diabetes on dementia and Alzheimer disease: a population-based longitudinal study," *PLoS Medicine*, vol. 12, no. 7, article e1001853, 2015.

[35] X. J. Han, P. Yan, L. Wang, L. Cong, and Y. F. Du, "A preliminary study on the changes of insulin signaling pathway in Alzheimer disease," in *National Symposium on Senile Dementia and Related Diseases*, vol. 2013, pp. 74-75, Chinese Pharmacological Society, Nanjing, China, 2013.

[36] Y. Z. Rong, Y. J. Xie, X. M. Chen, and B. R. Zhou, "Analysis of the correlation among insulin resistance ApoE gene polymorphism and mild cognitive impairment," *Hebei Medicine*, vol. 19, no. 11, pp. 1604–1607, 2013.

[37] A. Ernst, A. N. Sharma, K. M. Elased, P. C. Guest, H. Rahmoune, and S. Bahn, "Diabetic *db*/*db* mice exhibit central nervous system and peripheral molecular alterations as seen in neurological disorders," *Translational Psychiatry*, vol. 3, article e263, 2013.

[38] A. Jayaraman, D. Lent-Schochet, and C. J. Pike, "Diet-induced obesity and low testosterone increase neuroinflammation and impair neural function," *Journal of Neuroinflammation*, vol. 11, p. 162, 2014.

[39] S. D. Ostergaard, S. Mukherjee, S. J. Sharp et al., "Associations between potentially modifiable risk factors and Alzheimer disease: a Mendelian randomization study," *PLoS Medicine*, vol. 12, no. 6, article e1001841, 2015.

[40] J. J. He, Y. Z. Zhang, and X. F. Zhang, "The relationship of cognitive dysfunction in elderly diabetic patients with insulin resistance and care analysis," *China Modern Doctor*, vol. 52, no. 28, pp. 138–140, 2014.

[41] Q. C. Li, G. L. Wang, B. Y. Li, H. Sun, and N. C. Jiang, "Effects of insulin on spatial learning and memory in AD rats," *Chinese Journal of Applied Physiology*, vol. 24, no. 04, pp. 494–498, 2008.

[42] Y. Yang, D. L. Ma, Y. P. Wang, T. Jiang, S. H. Hu, and X. F. Yu, "Intranasal insulin treatment ameliorates Alzheimer disease-like changes in hippocampus in a rat model of type 2 diabetes," *Chinese Journal of Pathophysiology*, vol. 29, no. 01, pp. 56–61, 2013.

[43] T. Kawamura, T. Umemura, and N. Hotta, "Cognitive impairment in diabetic patients: can diabetic control prevent cognitive decline?," *Journal of Diabetes Investigation*, vol. 3, no. 5, pp. 413–423, 2012.

[44] L. J. Cao, "Relationship between cognitive dysfunction and insulin resistance in elderly patients with diabetes mellitus and nursing care," *Nurses Training*, vol. 28, no. 03, pp. 266-267, 2013.

[45] J. Dong, "Relationship between cognitive dysfunction and insulin resistance in elderly patients with diabetes mellitus and nursing care," *World Latest Medicine Information*, vol. 15, no. 105, pp. 303–306, 2015.

[46] M. Li, L. Ma, Y. Fan, Z. Q. Song, and J. Li, "Effect of insulin on patients with type 2 diabetes mellitus complicated with mild cognitive impairment," *Cardiovascular Disease Journal of of integrated Traditional Chinese and Western Medicine*, vol. 14, no. 20, pp. 2417–20, 2016.

[47] N. Mu, S. C. Xu, Q. Chang, D. P. Rao, J. P. Chen, and C. Ma, "Serum lipids, insulin metabolism and 311 gene polymorphism of paraoxonase-2 in patients with different subtypes of Alzheimer's disease," *Chinese Journal of Gerontology*, vol. 34, pp. 5346–5348, 2014.

[48] Z. Shen and Y. Lin, "Significance of fasting serum insulin and C peptide in patients with Alzheimer's disease," *Chinese Journal of Clinical Healthcare*, vol. 15, no. 01, pp. 61-62, 2012.

[49] L. Su, Q. W. Zhang, W. Li et al., "Effect of course on cognitive function and related risk factors in elderly patients with type 2 diabetes mellitus," *Chinese Journal of Geriatric Heart BrainVessel Diseases*, vol. 17, no. 10, pp. 1071–1075, 2015.

[50] L. Y. Tang and W. Tang, "Effect of blood glucose fluctuation on the treatment of senile dementia," *The Word Clinical Medicine*, vol. 9, no. 7, pp. 67-68, 2015.

[51] Q. Tao, "The risk factors of senile patients with type II diabetes," *Modern Hospital*, vol. 15, no. 03, pp. 152-153, 2015.

[52] Q. H. Zhang and Y. F. Du, "Study on the relationship between cognitive impairment and serum levels of TNF-α and IL-6 in middle-aged and elderly patients with type 2 diabetes mellitus," in *National Symposium on Senile Dementia and Related Diseases*, vol. 2013, pp. 67-68, Nanjing: Chinese Pharmacological Society, Nanjing, China, 2013.

[53] M. W. Akhtar, S. Sanz-Blasco, N. Dolatabadi et al., "Elevated glucose and oligomeric β-amyloid disrupt synapses via a common pathway of aberrant protein S-nitrosylation," *Nature Communications*, vol. 7, p. 10242, 2016.

[54] A. M. Barron, E. R. Rosario, R. Elteriefi, and C. J. Pike, "Sex-specific effects of high fat diet on indices of metabolic syndrome in 3xTg-AD mice: implications for Alzheimer's disease," *PLoS One*, vol. 8, no. 10, article e78554, 2013.

[55] L. Devi, M. J. Alldred, S. D. Ginsberg, and M. Ohno, "Mechanisms underlying insulin deficiency-induced acceleration of β-amyloidosis in a mouse model of Alzheimer's disease," *PLoS One*, vol. 7, no. 3, article e32792, 2012.

[56] Y. D. Ke, F. Delerue, A. Gladbach, J. Gotz, and L. M. Ittner, "Experimental diabetes mellitus exacerbates tau pathology in a transgenic mouse model of Alzheimer's disease," *PLoS One*, vol. 4, no. 11, article e7917, 2009.

[57] J. J. Ramos-Rodriguez, S. Molina-Gil, O. Ortiz-Barajas et al., "Central proliferation and neurogenesis is impaired in type 2 diabetes and prediabetes animal models," *PLoS One*, vol. 9, no. 2, article e89229, 2014.

[58] P. Serbedzija, J. E. Madl, and D. N. Ishii, "Insulin and IGF-I prevent brain atrophy and DNA loss in diabetes," *Brain Research*, vol. 1303, pp. 179–194, 2009.

[59] K. Talbot, H. Y. Wang, H. Kazi et al., "Demonstrated brain insulin resistance in Alzheimer's disease patients is associated with IGF-1 resistance, IRS-1 dysregulation, and cognitive decline," *The Journal of Clinical Investigation*, vol. 122, no. 4, pp. 1316–1338, 2012.

[60] H. Y. Mu, "Comparative analysis of insulin resistance in patients with Alzheimer's disease and type 2 diabetes mellitus," in *The 4th National Symposium on Dementia and Cognitive Impairment and Senior Speeches*, vol. 2015, p. 173, Beijing: Chinese Medical Association, Beijing, China, 2015.

[61] C. G. Jolivalt, R. Hurford, C. A. Lee, W. Dumaop, E. Rockenstein, and E. Masliah, "Type 1 diabetes exaggerates features of Alzheimer's disease in APP transgenic mice," *Experimental Neurology*, vol. 223, no. 2, article 19931251, pp. 422–431, 2010.

[62] Y. F. Mao, Z. Guo, T. Zheng et al., "Intranasal insulin alleviates cognitive deficits and amyloid pathology in young adult APPswe/PS1dE9 mice," *Aging Cell*, vol. 15, no. 5, pp. 893–902, 2016.

[63] M. Solas, B. Aisa, M. C. Mugueta, R. J. Del, R. M. Tordera, and M. J. Ramirez, "Interactions between age, stress and insulin on cognition: implications for Alzheimer's disease," *Neuropsychopharmacology*, vol. 35, no. 8, pp. 1664–1673, 2010.

[64] M. Chen, P. Y. Shan, A. F. Liu, L. Ma, and X. L. Yu, "Plasma fasting glucose, fasting insulin and insulin degrading enzyme in Alzheimer's disease," *Journal of Shandong University (Health Sciences)*, vol. 50, no. 03, pp. 75–78, 2012.

[65] R. Y. Huang, J. J. Ren, H. Y. Han, and M. N. Tang, "The correlation between metabolic syndrome and Alzheimer's disease research," *Journal of Psychiatry*, vol. 26, no. 03, pp. 175–177, 2013.

[66] G. X. Wang, "Correlation analysis of insulin resistance and cognitive impairment," *China Practical Medicine*, vol. 6, no. 26, pp. 38-39, 2011.

[67] H. M. Kim, J. M. Seong, and J. Kim, "Risk of hospitalization for hypoglycemia among older Korean people with diabetes mellitus: interactions between treatment modalities and comorbidities," *Medicine*, vol. 95, no. 42, article e5016, 2016.

[68] N. L. Rasgon, H. A. Kenna, T. E. Wroolie et al., "Insulin resistance and hippocampal volume in women at risk for

Alzheimer's disease," *Neurobiology of Aging*, vol. 32, no. 11, pp. 1942–1948, 2011.

[69] E. M. Schrijvers, J. C. Witteman, E. J. Sijbrands, A. Hofman, P. J. Koudstaal, and M. M. Breteler, "Insulin metabolism and the risk of Alzheimer disease: the Rotterdam study," *Neurology*, vol. 75, no. 22, pp. 1982–1987, 2010.

[70] Z. S. Tan, A. S. Beiser, C. S. Fox et al., "Association of metabolic dysregulation with volumetric brain magnetic resonance imaging and cognitive markers of subclinical brain aging in middle-aged adults: the Framingham Offspring Study," *Diabetes Care*, vol. 34, no. 8, pp. 1766–1770, 2011.

[71] M. K. Townsend, O. I. Okereke, W. Xia, T. Yang, D. J. Selkoe, and F. Grodstein, "Relation between insulin, insulin-related factors, and plasma amyloid beta peptide levels at midlife in a population-based study," *Alzheimer Disease and Associated Disorders*, vol. 26, no. 1, pp. 50–54, 2012.

[72] M. van Oijen, O. I. Okereke, J. H. Kang et al., "Fasting insulin levels and cognitive decline in older women without diabetes," *Neuroepidemiology*, vol. 30, no. 3, pp. 174–179, 2008.

[73] A. A. Willette, S. C. Johnson, A. C. Birdsill et al., "Insulin resistance predicts brain amyloid deposition in late middle-aged adults," *Alzheimers Dement*, vol. 11, no. 5, pp. 504–510, 2015.

[74] T. T. Huang, "Effects of insulin resistance on cognitive impairment in patients with Parkinson's disease," *Journal of Bethune Medical Science*, vol. 13, no. 02, pp. 129-130, 2015.

[75] M. Chen, *Relationship of Metabolism Related Factors and Alzheimer's Disease [M.Sc. Thesis]*, Shandong University, 2012.

[76] Z. S. Deng, *Activity of Cholinesterase and Expression of ChAT, Aβof Brain Tissue in Type-2 Diabetic Rat [M.Sc. Thesis]*, Shanxi Medical University, 2008.

[77] W. G. Liu, R. H. Liu, L. Li et al., "Study of CSF levels of glucose, true insulin, $A\beta_{40}$ and $A\beta_{42}$ in patients with Alzheimer's disease," *Journal of Brain and Nervous Diseases*, vol. 17, no. 06, pp. 434–436, 2009.

[78] W. G. Liu, R. Z. Tian, Y. Q. Feng et al., "Level of fasting plasma glucose, true insulin, C-peptide and amyloid Beta-protein in patients with Alzheimer disease," *Chinese Rehabilitation Theory and Practice*, vol. 13, no. 07, pp. 645-646, 2007.

[79] Y. Q. Ma, *Study on the Relationship between PI3K/PKB/mTOR/S6K1 Signaling Pathway and Type 2 Diabetes Mellitus and Alzheimer's Disease*, Dr. Dissertation, Nanchang University, 2013.

[80] L. Zhang, Y. Fang, Y. J. Lian, J. K. Wang, Y. K. Zheng, and Z. Y. Luo, "Study on relationship between the insulin resistant with the concentration of tau protein and β-amyloid protein in cerebrospinal fluid of patients with mild cognitive impairment," *Modern Preventive Medicine*, vol. 38, no. 09, pp. 1774-1775, 2011.

[81] X. H. Zhao, Y. M. Yang, J. Bao, X. Wang, Y. Y. Zhang, and Q. Zhao, "Clinical study on relationship between metabolic syndrome and mild cognitive impairment," *Journal of Kunming Medical University*, vol. 05, pp. 82–86, 2012.

[82] E. Grunblatt, J. Bartl, D. I. Iuhos et al., "Characterization of cognitive deficits in spontaneously hypertensive rats, accompanied by brain insulin receptor dysfunction," *Journal of Molecular Psychiatry*, vol. 3, no. 1, p. 6, 2015.

[83] W. J. Katon, E. H. Lin, L. H. Williams et al., "Comorbid depression is associated with an increased risk of dementia diagnosis in patients with diabetes: a prospective cohort study," *Journal of General Internal Medicine*, vol. 25, no. 5, pp. 423–429, 2010.

[84] L. Ma, M. Feng, Y. Qian et al., "Insulin resistance is an important risk factor for cognitive impairment in elderly patients with primary hypertension," *Yonsei Medical Journal*, vol. 56, no. 1, pp. 89–94, 2015.

[85] M. D. Sullivan, W. J. Katon, L. C. Lovato et al., "Association of depression with accelerated cognitive decline among patients with type 2 diabetes in the ACCORD-MIND trial," *JAMA Psychiatry*, vol. 70, no. 10, pp. 1041–1047, 2013.

[86] B. Y. Ding, *The Incidence and Related Risk Factors of Vascular Cognitive Impairment Not Dementia in Inpatients with Diabetes Mellitus Type 2 and Acute Cerebral Infarction, [M.Sc. Thesis]*, Dalian Medical University, 2015.

[87] J. Hou, *The Study for the Change of CMBs-Related Memory Function and Resting-State Brain Function in T2DM with CMBs, [M.Sc. Thesis]*, Central South University, 2014.

[88] C. H. Shao, K. Li, and X. B. Cao, "Hypertension and related risk factors of vascular dementia," *Chinese Focus Journal*, vol. 27, no. 01, pp. 13–15, 2012.

[89] X. Zhang, *The Control of Glycated Hemoglobin Level and the Use of Insulin Affect the Cognitive Function in Type2 Diabetes, [M.Sc. Thesis]*, Third Military Medical University, 2014.

[90] X. Liu, Y. N. Zhang, L. H. Jiang, and W. Li, "Abnormal expression of insulin receptor and insulin-like growth factor I receptor in hippocampus of Alzheimer's disease," *Chinese Journal of Gerontology*, vol. 07, pp. 1191–1194, 2011.

[91] Y. Ma, D. Wu, W. Zhang, J. Liu, S. Chen, and B. Hua, "Investigation of PI3K/PKB/mTOR/S6K1 signaling pathway in relationship of type 2 diabetes and Alzheimer's disease," *International Journal of Clinical and Experimental Medicine*, vol. 8, no. 10, pp. 18581–18590, 2015.

[92] Z. S. Deng, S. L. Zhang, Y. Zhang, Y. Chen, and X. J. Yang, "The study of expression of β-amyloid of serum and brain tissue in type-2 diabetic rat," *Journal of Practical Medical Techniques*, vol. 15, no. 12, pp. 1503–1505, 2008.

[93] X. Gao, D. Zhao, H. J. Cui, and F. Y. Li, "Study on expression of $A\beta$ in serum and brain tissues in rats with type 2 diabetes mellitus and its relationship with Alzheimer's disease," *Hebei Medical Journal*, vol. 34, no. 22, pp. 3386-3387, 2012.

[94] A. H. Lv, S. K. Zhu, and X. M. Zhang, "Effect of insulin resistance on the expression of $A\beta$ protein in hippocampus of rats and the change of cognitive behavior," *Chinese Journal of Practical Nervous Diseases*, vol. 14, no. 21, pp. 40-41, 2011.

[95] S. H. Yuan, S. Z. Gao, X. P. Liu et al., "The change of cognition function in insulin resistance rats and its brain tissues with Alzheimer-like disease," *Stroke and Neurological Disorders*, vol. 17, no. 03, pp. 139–143, 2010.

[96] X. J. Zhang, S. S. Yang, M. X. Zhang, and Y. Yang, "Common pathogenesis of type 2 diabetes and Alzheimer's disease: a potential mechanism," *Chinese Journal of Pathophysiology*, vol. 26, no. 06, pp. 1107–1114, 2010.

[97] D. Baumeister, R. Akhtar, S. Ciufolini, C. M. Pariante, and V. Mondelli, "Childhood trauma and adulthood inflammation: a meta-analysis of peripheral C-reactive protein, interleukin-6 and tumour necrosis factor-α," *Molecular Psychiatry*, vol. 21, no. 5, pp. 642–649, 2016.

[98] J. Bowden, J. F. Tierney, A. J. Copas, and S. Burdett, "Quantifying, displaying and accounting for heterogeneity in the

meta-analysis of RCTs using standard and generalised Q statistics," *BMC Medical Research Methodology*, vol. 11, p. 41, 2011.

[99] A. Masi, D. S. Quintana, N. Glozier, A. R. Lloyd, I. B. Hickie, and A. J. Guastella, "Cytokine aberrations in autism spectrum disorder: a systematic review and meta-analysis," *Molecular Psychiatry*, vol. 20, no. 4, pp. 440–446, 2015.

[100] P. Langhorne, "Bias in meta-analysis detected by a simple, graphical test. Bias in meta-analysis detected by a simple, graphical test. Prospectively identified trials could be used for comparison with meta-analyses," *BMJ*, vol. 316, no. 7129, article 9492689, p. 471, 1998.

[101] K. L. Soeken and A. Sripusanapan, "Assessing publication bias in meta-analysis," *Nursing Research*, vol. 52, no. 1, pp. 57–60, 2003.